Office of Environmental Management – Grand Junction

MOAB UTAH UMTRA

UMTRA Project

Revised Remedial Action Plan and Site Design for Stabilization of Moab Title I Uranium Mill Tailings at the Crescent Junction, Utah, Disposal Site

Attachment 2: Geology

June 2007

U.S. Department of Energy

Office of Environmental Management

Work Performed Under DOE Contract No. DE–AC01–02GJ79491
for the U.S. Department of Energy Office of Environmental Management.
Approved for public release; distribution is unlimited.

Remedial Action Plan and Site Design for Stabilization of Moab Title I Uranium Mill Tailings at the Crescent Junction, Utah , Disposal Site

Attachment 2: Geology

Work performed under DOE Contract No. DE–AC01–02GJ79491
for the U.S. Department of Energy Office of Environmental Management.
Approved for public release; distribution is unlimited.

Calculation Cross-Reference Guide

Location	Calculation Number	Calculation Title
Attachment 1: Disposal Cell Design Specifications		
Appendix A	MOA-02-08-2006-5-19-01	Freeze/Thaw Layer Design
Appendix B	MOA-02-08-2006-5-13-01	Radon Barrier Design Remedial Action Plan
Appendix C	MOA-02-05-2007-5-17-02	Slope Stability of Crescent Junction Disposal Cell
Appendix D	MOA-02-05-2007-3-16-01	Settlement, Cracking, and Liquefaction Analysis
Appendix E	MOA-02-09-2005-2-08-01	Site Drainage – Hydrology Parameters
Appendix F	MOA-02-06-2006-5-08-00	Crescent Junction Site Hydrology Report
Appendix G	MOA-02-04-2007-5-25-02	Diversion Channel Design, North Side Disposal Cell
Appendix H	MOA-02-08-2006-6-01-00	Erosional Protection of Disposal Cell Cover
Appendix I	MOA-01-06-2006-5-02-01	Volume Calculation for the Moab Tailings Pile
Appendix J	MOA-02-08-2006-5-03-00	Weight/Volume Calculation for the Moab Tailings Pile
Appendix K	MOA-01-08-2006-5-14-00	*Average Radium-226 Concentrations for the Moab Tailings Pile*
Attachment 2: Geology		
Appendix A	MOA-02-04-2007-1-05-01	Site and Regional Geology – Results of Literature Research
Appendix B	MOA-02-04-2007-1-01-01	Surficial and Bedrock Geology of the Crescent Junction Disposal Site
Appendix C	MOA-02-04-2007-1-06-01	Site and Regional Geomorphology – Results of Literature Research
Appendix D	MOA-02-04-2007-1-07-01	Site and Regional Geomorphology – Results of Site Investigations
Appendix E	MOA-02-04-2007-1-08-01	Site and Regional Seismicity – Results of Literature Research
Appendix F	MOA-02-04-2007-1-09-02	Site and Regional Seismicity – Results of Maximum Credible Earthquake Estimation and Peak Horizontal Acceleration
Appendix G	MOA-02-04-2007-1-02-01	Photogeologic Interpretation
Attachment 3: Ground Water Hydrology		
Appendix A	MOA-02-02-2006-2-07-00	Saturated Hydraulic Conductivity Determination of Weathered Mancos Shale
Appendix B	MOA-02-03-2006-2-10-00	Field Permeability "Bail" Testing
Appendix C	MOA-02-03-2006-2-06-00	Field Permeability "Packer" Testing
Appendix D	MOA-02-04-2006-2-03-00	Hydrologic Characterization – Ground Water Pumping Records
Appendix E	MOA-02-05-2006-2-13-00	Hydrologic Characterization – Vertical Travel Time to Uppermost (Dakota) Aquifer
Appendix F	MOA-02-02-2007-3-01-00	Geochemical Characterization – Radiocarbon Age Determinations for Ground Water Samples Obtained From Wells 0203 and 0208
Appendix G	MOA-02-06-2007-2-14-00	Hydrologic Characterization – Lateral Spreading of Leachate
Attachment 4: Water Resources Protection		
Appendix A	MOA-02-06-2006-5-24-00	Material Placement in the Disposal Cell
Appendix B	MOA-02-06-2006-3-05-00	Geochemical Attenuation and Performance Assessment Modeling
Attachment 5: Field and Laboratory Results, Volume I		
Appendix A	MOA-02-03-2006-1-03-00	Corehole Logs for the Crescent Junction Site
Appendix B	MOA-02-03-2006-1-11-00	Borehole Logs for the Crescent Junction Site
Appendix C	MOA-02-03-2006-1-04-00	Geophysical Logs for the Crescent Junction Site
Appendix D	MOA-02-03-2006-1-10-00	*Test Pit Logs for the Crescent Junction Site*
Appendix E	MOA-02-03-2006-4-01-00	Geotechnical Properties of Native Materials
Appendix F	MOA-01-06-2006-5-22-00	Cone Penetration Tests for the Moab Processing Site
Appendix G	MOA-02-05-2006-4-07-00	Seismic Rippability Investigation for the Crescent Junction Site
Appendix H	MOA-02-03-2007-3-04-01	Background Ground Water Quality for the Crescent Junction Site
Appendix I	MOA-01-08-2006-4-08-00	Boring and Test Pit Logs for the Moab Processing Site
Appendix J	MOA-01-08-2006-4-09-01	Geotechnical Laboratory Testing Results for the Moab Processing Site
Appendix K	MOA-02-04-2007-4-03-01	Supplemental Geotechnical Properties of Native Materials
Attachment 5: Field and Laboratory Results, Volume II		
Appendix L	MOA-02-08-2006-1-06-00	Compilation of Geologic and Geophysical Logs
Appendix M	N/A	Radiological Assessment for Non-Pile Areas of the Moab Project Site
Appendix N	MOA-02-05-2007-4-04-00	Supplemental Geotechnical Properties of Tailings Materials from the Moab Processing Site

Attachment 2
Table of Contents

U.S. Department of Energy—Grand Junction, Colorado

Calculation Cover Sheet

Calc. No.: MOA-02-04-2007-1-05-01 **Doc. No.:** X0113800	**Discipline:** Geologic and Geophysical Properties	**No. of Sheets:** 20

Location: Attachment 2, Appendix A

Project: Moab Project

Site: Crescent Junction Disposal Site

Feature: Site and Regional Geology – Results of Literature Research

Sources of Data:

Published reports and maps – see list of references at end of calculation set.

Purpose of Revision:

Revision is being issued to include information collected from additional references on geologic features and mineral resources. These references were acquired during site characterization activities in late 2005 and early 2006 and in response to U.S. Nuclear Regulatory Commission questions on certain geologic aspects in 2006.

Sources of Formulae and References:

See list of references at end of calculation set.

Preliminary Calc. ☐ **Final Calc.** ☒ **Supersedes Calc. No. MOA-02-08-2005-1-05-00**

Author:	Craig Goodknight 31 May 07 Name Date	**Checked by:**	31 May 07 Name Date
			Craig Goodknight 31 May 07 Name Date
Approved by:	Kent Kruse 5/31/07 Name Date		Mark Kautsky 5-31-07 Name Date
	Joseph h. Reed 31 May 07		MAY 31, 07 Name Date

No text for this page

Problem Statement:

Determination of the suitability of the Crescent Junction Disposal Site as the repository for the Moab uranium mill tailings material, and development of the Site and Regional Geology sections of the Remedial Action Plan and Site Design for Stabilization of the Title I Uranium Mill Tailings at the Crescent Junction, Utah, Disposal Site (RAP) require a thorough review of available literature that applies to the Crescent Junction Site. The compiled list of references is presented at the end of this calculation set and relevant information is summarized below.

This calculation set was initially prepared in August 2005 during the early stages of characterization of the Crescent Junction Site. Additional references and information collected during site characterization activities in late 2005 and early 2006 have made revision of this calculation set necessary. This revised calculation set is a general summary of geologic conditions at the site based on literature research. Information from this calculation is incorporated into Attachment 2 (Geology) of the RAP and summarized in the appropriate sections of the Remedial Action Selection (RAS) Report for the Moab Site.

Method of Solution:

Literature sources were identified using a combination of published reports and maps that were developed during the Crescent Junction Site-selection process, online (Internet-based) resources, and relevant literature citations from the other Uranium Mill Tailings Radiation Control Act (UMTRCA) Sites.

Assumptions:

It is assumed that the literature sources are reliable and representative of the current understanding of the geology of the region.

Calculation:

None required.

Discussion:

Physiographic Setting

The Crescent Junction Disposal Site in Grand County of east-central Utah is approximately 20 miles (mi) east of the town of Green River and 30 mi north-northwest of the town of Moab (Figure 1) in the north-central part of the Crescent Junction 7.5-minute topographic quadrangle. The site is in the north part of the Canyon Lands section, situated in the north part of the Colorado Plateau physiographic province (Figure 2, upper half). Further physiographic subdivisions recognized in the state of Utah (Stokes 1977) place the site in the Mancos Shale Lowland (Figure 2, lower half). Characteristics of the Canyon Lands section include deeply incised drainages, isolated mesas, gently dipping bedrock, and anticlines formed by salt intrusion that have been breached in places by erosion to form anticlinal valleys.

Immediately north of the site, the erosional escarpment of the Book Cliffs rises up 700 to 800 feet (ft) to elevations of between 5,800 and 5,900 ft. The Book Cliffs are the southern boundary of the Uinta Basin section of the Colorado Plateau province (Figure 2, upper half). The Uinta Basin section is a rugged, intricately dissected plateau bounded on the south by sets of cliffs (one of which is the Book Cliffs) that are highly irregular, with many salients and canyons (reentrants).

As shown on the Crescent Junction 7.5- and 15-minute topographic quadrangles, the site is centered about 1.5 mi northeast of the abandoned community of Crescent Junction on what is known as Crescent Flat. This "flat" slopes gently to the south for approximately 2 mi, from the base of the Book Cliffs at the north at an elevation of approximately 5,100 ft to Interstate Highway 70 (I-70) at the south at an elevation of approximately 4,900 ft.

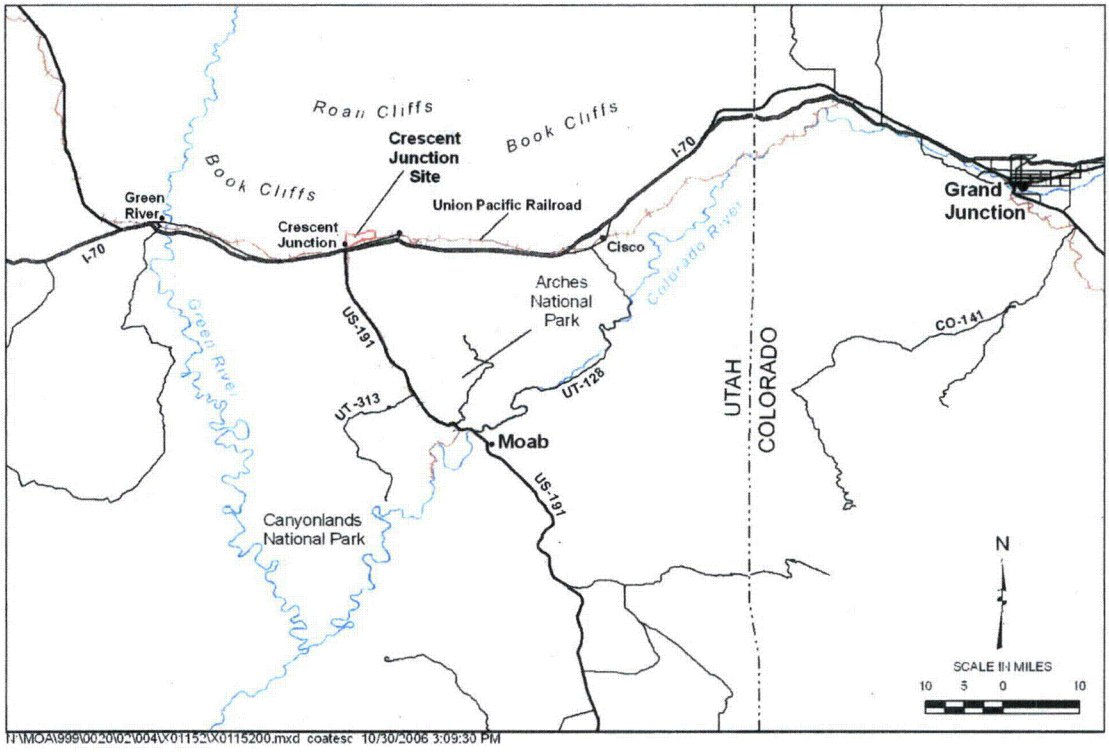

Figure 1. Location of the Crescent Junction, Utah, Site

General Geology

A temporary withdrawal area of approximately 2,300 acres of public (U.S. Bureau of Land Management [BLM]) land was established for the U.S. Department of Energy (DOE) to accommodate construction of a disposal cell and a buffer zone. This area—referred to as the site area or withdrawal area in this calculation—shown by a red rectangle in the small-scale map in Figure 3, includes parts of Sections 22 through 27 in T21S, R19E. Within the withdrawal area is the disposal cell footprint area of only approximately 250 acres in parts of Sections 22, 23, 26, and 27. Both of these areas are shown in the large-scale map in Figure 4.

Small-scale geologic maps that cover the site area include the 1:62,500-scale geologic map of the Salt Valley area (Woodward-Clyde Consultants 1984), the 1:100,000-scale Moab and eastern part of the San Rafael Desert 30-minute × 60-minute quadrangles geologic map (Doelling 2001 and 2002), and the 1:250,000-scale geologic map of the Moab 1-degree × 2-degree quadrangle (Williams 1964). Other small-scale geologic maps that cover areas near the site include the geologic map at a scale of 1:50,000 of parts of Crescent Junction and Floy Canyon 15-minute quadrangles (Gualtieri 1982), which covers an area just north of the site, and a geologic map for the 1:100,000-scale Westwater 30-minute × 60-minute quadrangle (Gualtieri 1988), which covers the large area just north of the Moab 30-minute × 60-minute quadrangle.

A large (1:24,000)-scale geologic map has not been published for the Crescent Junction 7.5-minute quadrangle. Geologic maps published for 7.5-minute quadrangles adjacent to the Crescent Junction quadrangle include Hatch Mesa (Chitwood 1994) to the west, Dee Pass (Moab-5) (Dettermann 1955) to the southwest, Valley City (Doelling 1997) to the south, and Sego Canyon (Willis 1986) to the northeast. A soils map published for the Crescent Junction 7.5-minute quadrangle is included as sheet number 35 in the Soil Survey of Grand County, Central Part (Hansen 1989).

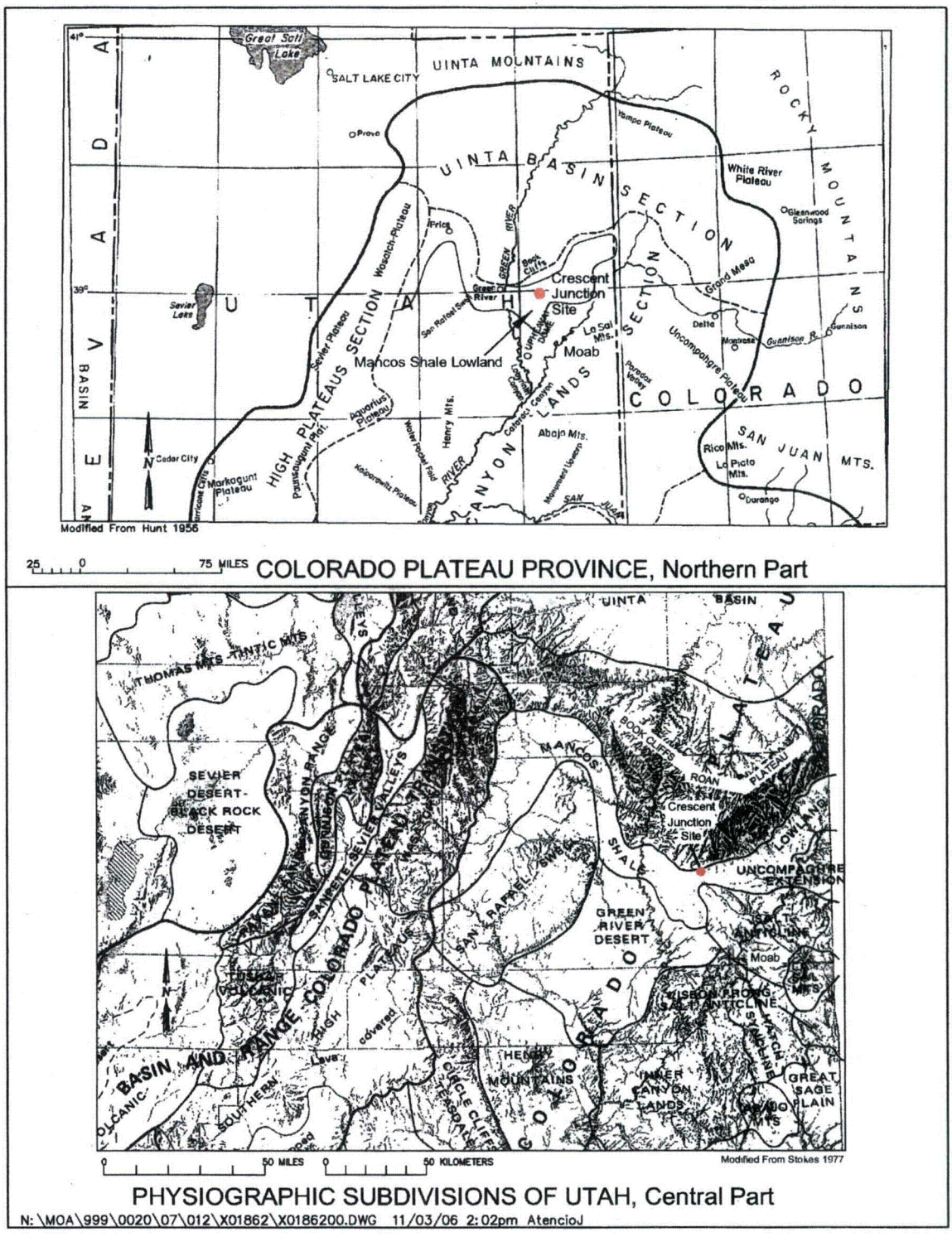

Figure 2. Physiographic Setting of the Crescent Junction Site

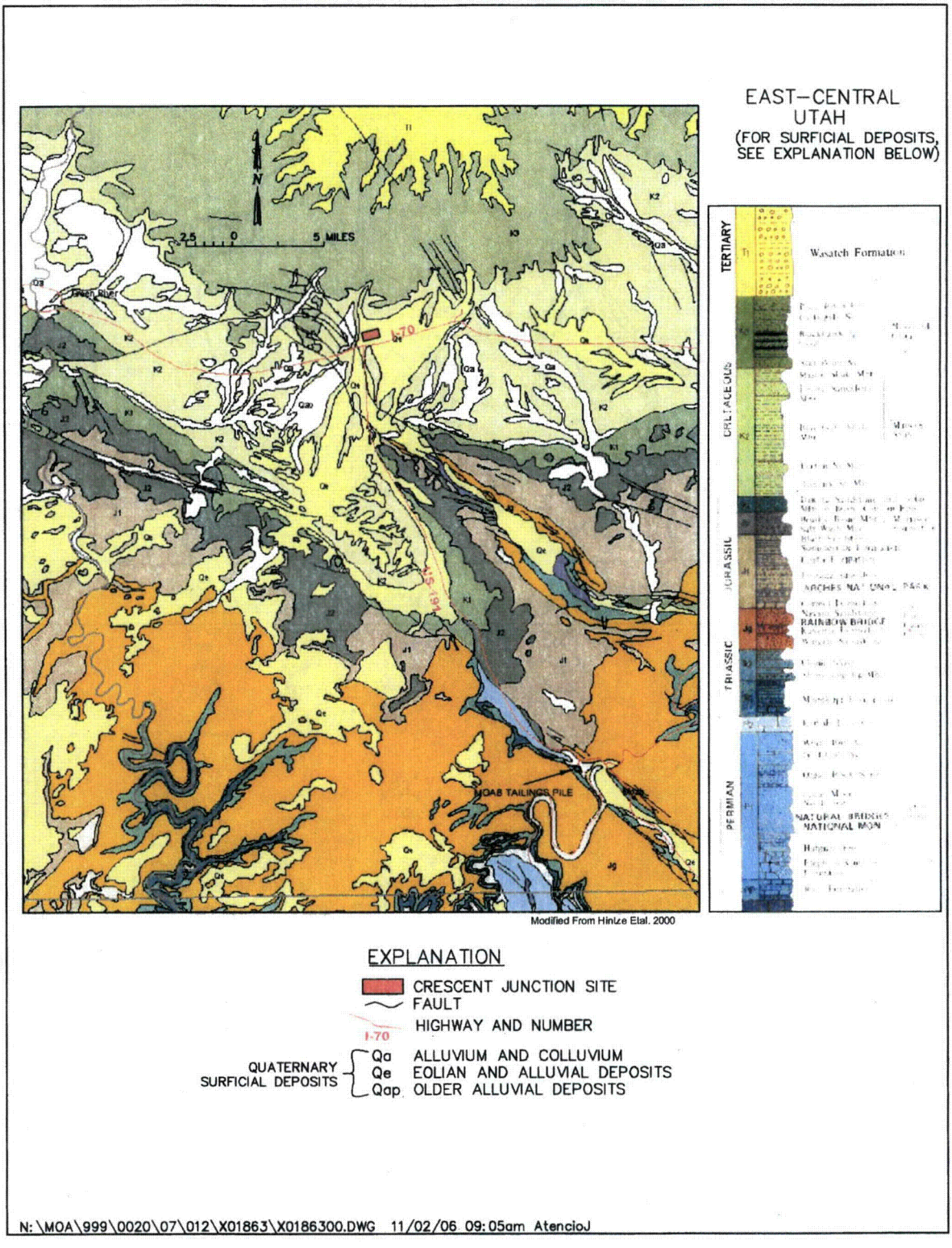

Figure 3. Regional Geology of the Crescent Junction Site

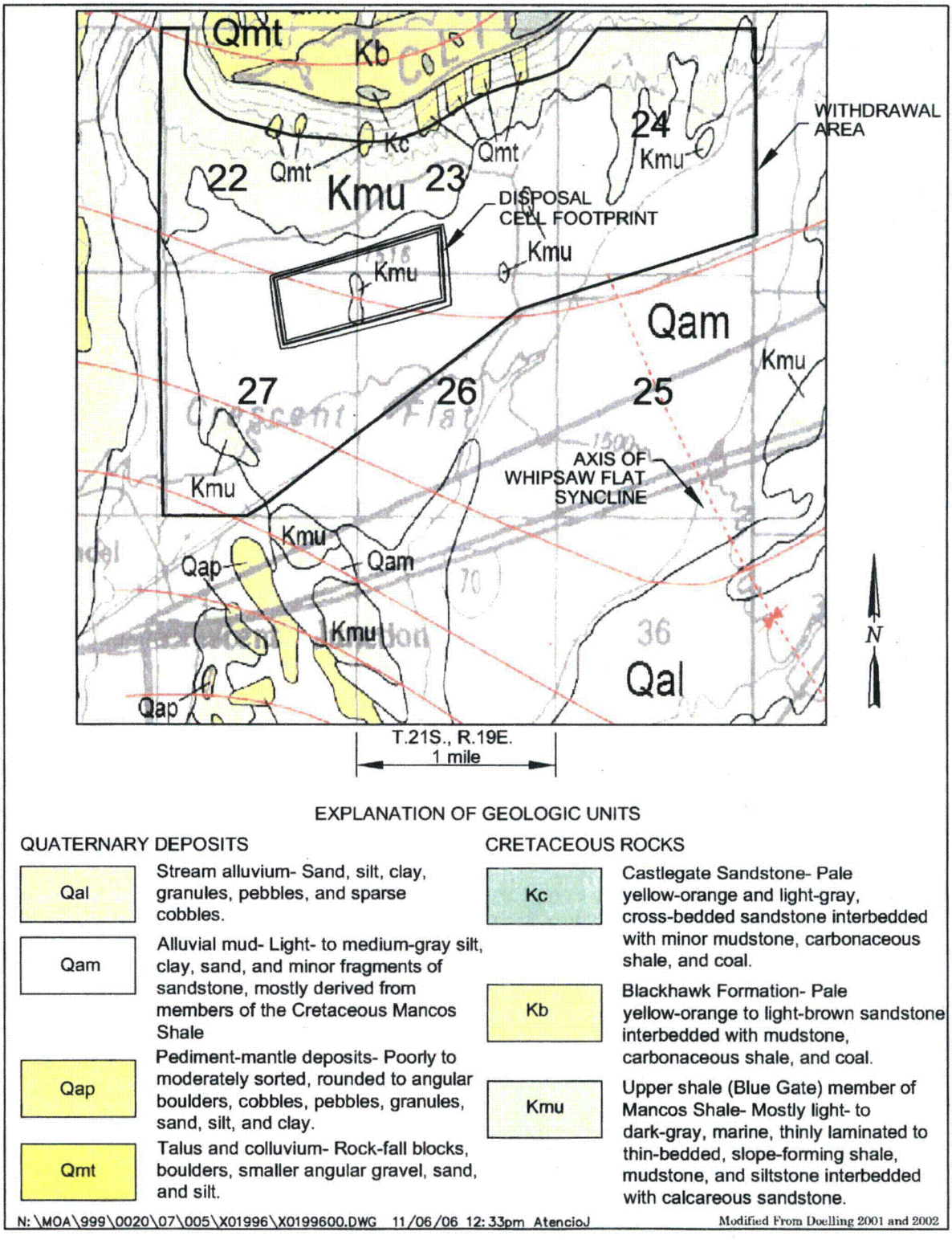

Figure 4. Geologic Map of the Crescent Junction Site

Stratigraphic Setting

The regional geologic setting of the Crescent Junction Site is shown in the geologic map of east-central Utah in Figure 3. A more detailed geologic map of the Crescent Junction Site and immediately adjacent area is shown in Figure 4.

Bedrock in the Mancos Shale Lowland is covered in many places by unconsolidated Quaternary material that includes alluvial mud, stream alluvium, pediment-mantle deposits, and talus and colluvium (Figure 3 and Figure 4). The gray alluvial mud of Holocene and late Pleistocene age is less than 30 ft thick, fills swales on the Mancos Shale bedrock surface, and consists of silt, clay, sand, and minor fragments of sandstone. Stream alluvium is less than 30 ft thick, occurs in and adjacent to active stream courses, and consists of a wide range of particle sizes from silt and sand up to sparse cobbles and boulders. Near the Crescent Junction Site, these alluvial deposits occur in and along Crescent Wash and were derived from the Book and Roan Cliffs up to 10 mi to the north.

Pediment-mantle deposits are of Pleistocene age and less than 100 ft thick, cover Mancos Shale bedrock surfaces between drainages as much as 400 ft above local base level, and consist of a wide range of particle sizes from silt and sand up to cobbles and boulders. These deposits nearest the Crescent Junction Site cap the low mesas west of and about 100 ft higher than Crescent Wash.

Talus and colluvium deposits of Holocene and late Pleistocene age are less than 15 ft thick, occur on slopes below cliffs and steep slopes, and consist of material from silt size up to boulders and large rock-fall blocks. These deposits near the site occur along the south-facing slopes of the Book Cliffs and as landslides on north aspects of the Book Cliffs.

An estimated 4,000-ft thickness of continental sedimentary rocks from Triassic (Moenkopi Formation) to Early Cretaceous (Dakota Sandstone) age underlie the site area. This sequence is overlain by the predominantly marine sediments of the Mancos Shale, which in turn is overlain by the Mesaverde Group of Late Cretaceous age. The formations representing these intervals are shown in the columnar stratigraphic section for the site area in Figure 5. Also shown in Figure 5 is the stratigraphic position of the Crescent Junction Site area in the upper one-third of the Mancos Shale.

A 5- to 10-mile-wide swath of outcrop of Mancos Shale of Late Cretaceous age corresponds to the Mancos Shale Lowland where the Crescent Junction Site is located. Rocks in the Lowland area of the site dip generally northward at low angles of less than 10 degrees toward the Uinta Basin. Local variation in this dip of bedrock is mainly due to northwest-striking anticlines and synclines. These structures also affect the width of outcrop of the Mancos Shale; synclines widen the outcrop and anticlines narrow the outcrop (Figure 3).

Most of the Mancos Shale, which is nearly 4,000 ft thick in this region, was deposited in an open-marine environment in the Cretaceous Western Interior Seaway. The Mancos Shale consists of thickly bedded, calcareous mudstone (Chitwood 1994), with thinly bedded siltstone, fine-grained sandstone, and bentonite interbeds widely spaced within the mudstone. In the upper part of the Mancos Shale, a sandy interval from several hundred to approximately 1,000 ft thick that represents some nearshore deposits is designated as the Prairie Canyon Member (Cole et al. 1997). The site area is at the approximate stratigraphic level of this member. Above and below the Prairie Canyon Member are the more typical deposits of the Mancos Shale—thick shale and mudstone designated as the Blue Gate Member. Approximately 2,000 ft of the Blue Gate Member underlie the Prairie Canyon Member in the site area. Members of the Mancos Shale below the Blue Gate Member are the Ferron Sandstone Member, which is about 60 ft thick and contains two fine- to medium-grained sandstone beds, underlain by the Tununk Shale Member, which is about 250 to 350 ft thick and consists mainly of shale and mudstone—typical for Mancos Shale.

The upper part of the Blue Gate Member just north of the site area is about 700 to 800 ft thick and forms the steep slopes of the lower part of the Book Cliffs. Gradual regression of the Cretaceous Western Interior Seaway to the east is marked by the Blackhawk Formation, which consists of littoral sandstone overlain by lagoonal deposits with some thin coal beds. Sandstone of the Blackhawk Formation, the lowest unit of the Mesaverde Group, forms the resistant cliff cap at the top of the Book Cliffs just north of the site area. Overlying the Blackhawk Formation, the Castlegate Sandstone is a delta plain deposit

composed mainly of sandstone with interbeds of siltstone, shale, and thin coal beds. The resistant sandstone of the Castlegate Sandstone may form a second cliff on top of the Blackhawk Formation or it may form a cliff some distance downdip to the north above the Blackhawk Formation. An abrupt transgression of the Cretaceous Western Interior Seaway returning to the area is marked by the Buck Tongue of Mancos Shale, the uppermost member that has much of the same character as the Blue Gate Member. Overlying the Buck Tongue of Mancos Shale, the Sego Sandstone of the Mesaverde Group represents the gradual (and final) regression of the Cretaceous Western Interior Seaway and a return to coastal and deltaic conditions. Above the Sego Sandstone are additional units of the Mesaverde Group—the Neslen Formation that contains the major coal beds in the Book Cliffs area and the overlying thick fluvial sandstone and siltstone beds of the Farrer Formation.

The Dakota Sandstone of Early Cretaceous age underlies the Mancos Shale and consists of sandstone, conglomeratic sandstone, and shale that were deposited on a broad coastal plain in front of the advancing Cretaceous Western Interior Seaway (Doelling 1997). This formation is probably 50 to 100 ft thick in the site area and is likely the shallowest bedrock unit containing a small amount of ground water. The Cedar Mountain Formation, also of Early Cretaceous age, underlies the Dakota Sandstone, is probably 100 to 200 ft thick, consists of several sandstone and conglomeratic sandstone beds interbedded with thickly bedded mudstone, and is a swampy floodplain deposit. A small amount of ground water is also likely present in the sandstone and conglomeratic sandstone beds of the Cedar Mountain Formation, as noted in Hurlow and Bishop (2003, Table 2). Together, the Dakota Sandstone and Cedar Mountain Formation are considered the first aquifer (Figure 5) beneath the Crescent Junction Site.

The Morrison Formation of Late Jurassic age underlies the Cedar Mountain Formation and consists of three members, in descending order: the Brushy Basin Member, Salt Wash Member, and Tidwell Member. Approximately 75 percent of the Brushy Basin Member is silty and clayey mudstone; the remainder consists of muddy sandstone and lenses of conglomeratic sandstone. The Salt Wash Member is composed mainly of lenticular sandstone and siltstone and represents ancient river channels. The Tidwell Member is thin and consists mostly of limy, silty, fine-grained sandstone and siltstone. Small amounts of ground water are likely present in the Brushy Basin Member and Salt Wash Member (Hurlow and Bishop 2003, Table 2). Red siltstone and sandstone beds that were formerly designated as the Summerville Formation in this area have been reassigned to the Tidwell Member and to the uppermost Curtis Formation (Doelling et al. 2002).

Middle Jurassic rocks of the San Rafael Group are represented by the three formations, in descending order, Curtis Formation, Entrada Sandstone, and Carmel Formation (Figure 5). The Moab Member of the Curtis Formation consists of crossbedded, fine- to medium-grained eolian sandstone that likely is the shallowest occurrence of abundant ground water (Hurlow and Bishop 2003, Table 2). Also likely to contain abundant ground water is the Slick Rock Member of Entrada Sandstone, a thick, eolian sandstone. The Dewey Bridge Member of the Carmel Formation is a tidal flat deposit of red, silty sandstone.

Lower Jurassic rocks of the Glen Canyon Group are represented by the three formations, in descending order, Navajo Sandstone, Kayenta Formation, and Wingate Sandstone (Figure 5). Abundant ground water is expected to occur in the thick eolian sandstones of the Navajo Sandstone and Wingate Sandstone (Hurlow and Bishop 2003, Table 2). The Kayenta Formation, composed mainly of stream-deposited sandstone is less likely to contain significant ground water. Triassic rocks represented by the Chinle Formation (fluvial sandstone and siltstone) and Moenkopi Formation (mudflat and shallow marine siltstone and sandstone) are unlikely to contain significant ground water.

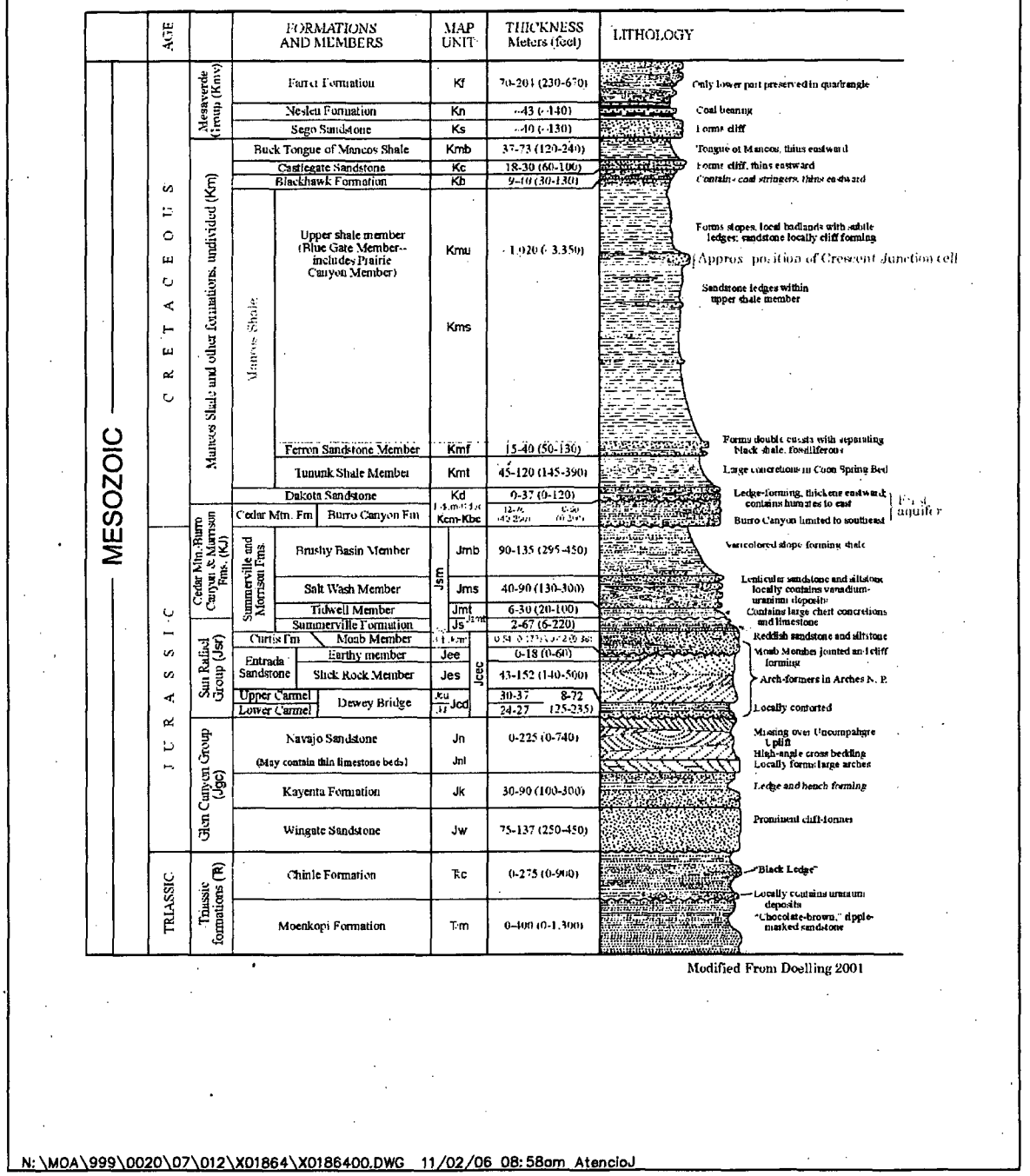

Modified From Doelling 2001

N:\MOA\999\0020\07\012\X01864\X0186400.DWG 11/02/06 08:58am AtencioJ

Figure 5. Columnar Stratigraphic Section of Mesozoic Rocks in the Crescent Junction Site Area

Structural Setting

The regional structural geologic setting of the Crescent Junction Site is shown in Figure 6. The site is near the south edge of the Uinta Basin and in the northwestern part of the ancestral Paradox Basin, where thick salt was deposited in Pennsylvanian time. The younger Uinta Basin actually overlaps part of the northern Paradox Basin (Figure 6). Soon after the salt was deposited and buried, geostatic load caused the salt to behave plastically and flow toward northwest-striking faults in the basin floor, where it became thick and formed northwest-striking, elongated salt diapirs. Basins called rim synclines formed between the salt diapirs. Regional compression during the Laramide orogeny (Late Cretaceous to Paleogene time) accentuated these structures to form broad northwest-striking anticlines and synclines. The northern part of the Paradox Basin where these anticlines and synclines formed as a result of thick salt accumulation is referred to as the Paradox Fold and Fault Belt (Figure 6).

The anticlines in the Fold and Fault Belt are salt-cored; the Salt Valley and Thompson Anticlines southwest and northeast of the site, respectively, are examples of these structures. Separating these two anticlines is the broad and subtle Whipsaw Flat Syncline, where the Crescent Junction Site is located (Figure 4 and Figure 6). The Whipsaw Flat Syncline, named by Woodward-Clyde Consultants (1984, Figure 5-2), had previously been referred to as the Crescent Wash Syncline (Young 1983, Plate 1). In the immediate site area, Mancos Shale bedrock dips 5 to 10 degrees or less to the north-northeast away from the Salt Valley Anticline and toward the axis of the Whipsaw Flat Syncline.

Broad uplift of the Colorado Plateau in Neogene time and the resulting erosion allowed ground water to reach the upper parts of the salt diapirs through fractures and joints in the anticlines. The resulting dissolution of the salt during Neogene and Quaternary time (and continuing at the present time) caused collapse, tilting, faulting, and subsidence of overlying strata along and near the axes of the salt-cored anticlines. The amount of ground water available for dissolution has determined the degree of breaching of the salt-cored anticlines. Approximately 7 mi south of the site, the crest of the Salt Valley Anticline has collapsed to form a valley (Figure 6); whereas, 1 to 2 mi west of the site, the crest of the Salt Valley Anticline is expressed by graben faulting and tilted beds that signify incipient collapse. These faults are exposed in only a few places, but reportedly have as much as 1,000 ft of displacement (Fisher 1936), as determined by oil test wells drilled in the area in the 1920s and 1930s. The Thompson Anticline northeast of the site displays some minor graben and normal faults that are expressions of incipient collapse.

Based on subsurface formation contacts found in two early oil test holes drilled in the 1920s, a northwest-striking normal fault was inferred in the southwest corner of the withdrawal area in the SW¼ of Section 27. This fault was first shown in a map prepared in September-October 1924 (Harrison 1927, Figure 9), and Fisher (1936) later described the fault as a "minor dip fault with 100 ft of downthrow to the south". No surface expression of this fault has been noted on geologic maps by Woodward-Clyde Consultants (1984) or Doelling (2001). Information about the two test holes from the State of Utah, Department of Water Resources, is sparse and vague, but shows the Crescent Oil Syndicate No. 1 well (API No. 43-019-11525) drilled to 2,171 ft by Crescent Drilling Company in the SW¼ of Section 27, and the McCarthy No. 1 well (API No. 43-019-20369) drilled to 2,200 ft by Western States Development in the NW¼ of Section 34. The difference in depth to the top of the Dakota Sandstone in these two holes apparently was the basis for inferring the existence of a fault.

A drill hole is shown in the SW¼ of Section 27 on the 7.5-minute Crescent Junction topographic quadrangle; however, no drill hole is shown in the NW¼ of Section 34. A field check was made to determine if a drill hole is present in the NW¼ of Section 34 and if there is any surface evidence for a northeast-striking fault between the old test holes. Results of this field check are included in the "Surficial and Bedrock Geology of the Crescent Junction Disposal Site" calculation (RAP Attachment 2, Appendix B, page 13, Structural Features and Weathered Bedrock).

Lineaments and geologic structures at the site and surrounding region noted by Friedman and Simpson (1980) and Friedman et al. (1994) from Landsat satellite images coincide with most of the known geologic structures. None of the lineaments identified in the northern Paradox Basin cross the Crescent Junction Site or withdrawal area.

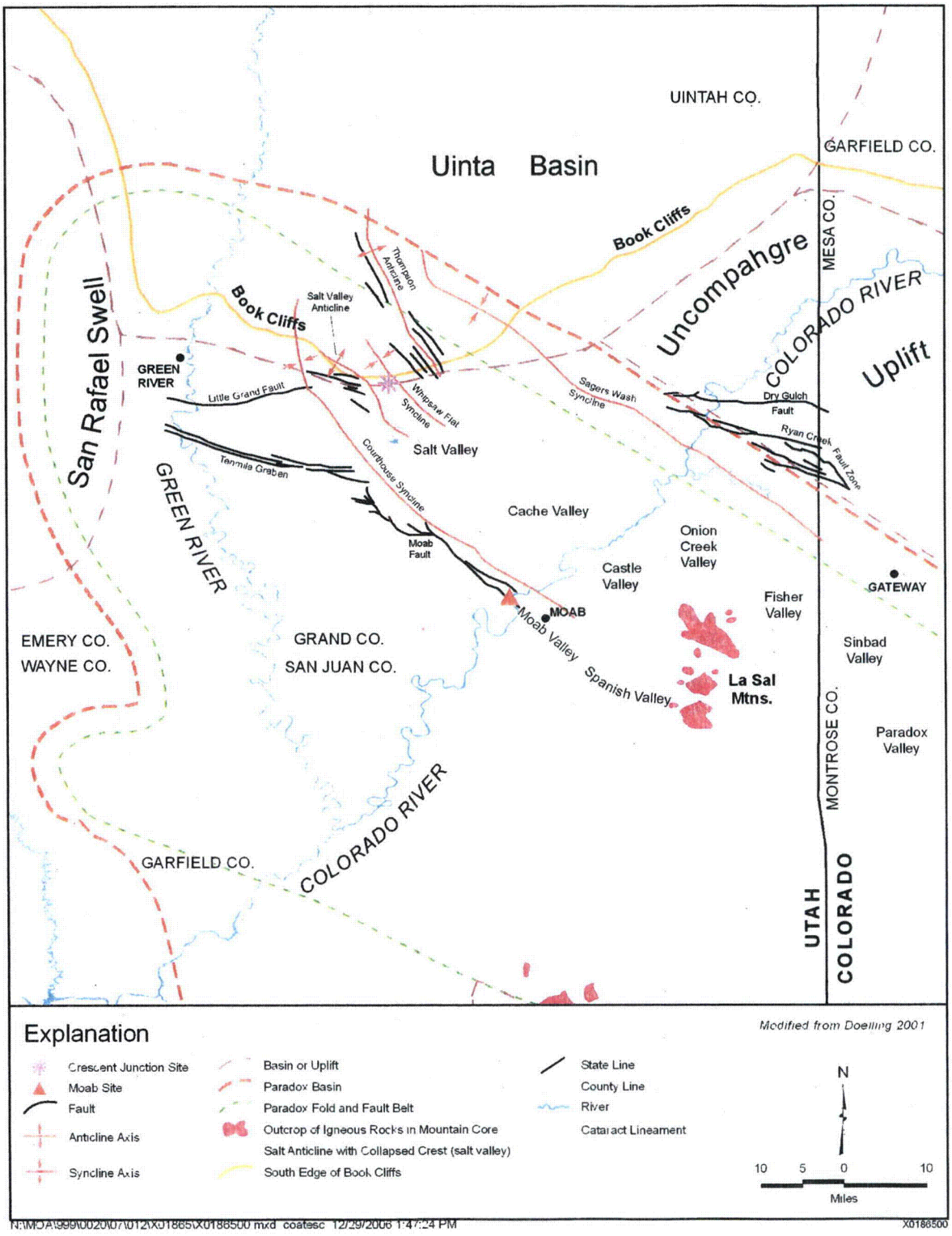

Figure 6. Regional Structural Setting of the Crescent Junction Site Area

Resource Development

Geologic resources at the Crescent Junction Site area and nearby region include oil and gas, potash and salt, coal, uranium and vanadium, copper and silver, gold, and sand and gravel. These resources are evaluated for their potential to occur in the immediate site (withdrawal) area and the effect (if any) of the existence of the disposal cell on possible recovery of these resources. Two reports prepared by the BLM give the occurrence and development potential of these resources: the first is the Mineral Potential Report for the Moab Planning Area (north part of the Moab BLM District) (Tabet 2005), and the second is the Mineral Report on the DOE Proposed Disposal Site (Bain 2005) that encompasses the withdrawal area. These BLM reports obtained much information on geologic resources from two earlier reports that were prepared as part of DOE's evaluation of salt in the Paradox Basin area for permanent disposal of high-level nuclear waste. These earlier reports include a mineral resource inventory of the Paradox salt basin (Merrell 1979) and a geologic characterization of the Salt Valley area of the Paradox Basin (Woodward-Clyde Consultants 1984).

Oil and Gas

No significant oil and gas resources have been found in the withdrawal area or within 2 mi of it. However, all of the BLM withdrawal area is currently leased for oil and gas, and several oil and gas test holes have been drilled recently in the nearby areas to the south and southwest of the withdrawal area.

As part of the United States Geological Survey (USGS) assessment of the country's oil and gas resources, they defined four oil and gas plays in the Uinta-Piceance and Paradox Basins that may occur in the Crescent Junction Site area. These plays include: 1) Buried Fault Block, 2) Fractured Interbed, 3) Salt Anticline Flank, and 4) Cretaceous Dakota to Triassic. The only nearby field that is an example of one of these plays is the Blaze Canyon (production mainly from the Navajo Sandstone), which exemplifies the Cretaceous Dakota to Triassic play. In the Mineral Potential Report for the BLM Moab Planning Area (Tabet 2005), the occurrence and development potential for the four plays listed above is classified as high for the Crescent Junction Site area.

Only one old oil test hole (the Crescent Oil Syndicate No. 1, mentioned above) has been drilled in the withdrawal area (southwest corner). Drilled just south of the withdrawal area in Section 34 a few years later, the McCarthy No. 1 oil test hole (mentioned above) drill log reported water in shale at a depth of 70 ft and "gas that blew rocks over the top of the mast" at a depth of 121 ft. Both of these old test holes were dry and were plugged and abandoned. No other shallow test holes for oil in nearby areas reported gas; however, the occurrence of gas in thick marine shale is not unusual.

Several small oil fields, now inactive or abandoned, have been found within 5 mi of the Crescent Junction disposal cell. The inactive Blaze Canyon field, about 4 mi west-northwest of the disposal cell, has produced mainly oil (about 40,000 barrels) and some gas (about 4,500 million cubic feet) mostly from the Navajo Sandstone and some from the Morrison Formation (Chitwood 1994). The abandoned Crescent Junction oil field about 4 mi south-southwest of the disposal cell produced a small amount of oil from the Morrison Formation. As shown on the Oil and Gas Fields Map of Utah (Chidsey et al. 2004), the wildcat oil field is about 2 mi southwest of the disposal cell in Section 32 and has produced from the Kayenta Formation and Wingate Sandstone. The field is very small and is composed of one well (State 1-32) drilled by MSC Exploration, LP, in 2002. The Utah Division of Oil, Gas and Mining oil and gas information website indicates, however, that the well has produced 198 barrels of oil from the Navajo Sandstone, and the well was plugged in 2006.

Two oil and gas test holes recently drilled by MSC Exploration, LP, just south of the Crescent Junction Site withdrawal area include the State MSC 35-1 drilled in 2004 and 2005 to a depth of 10,980 ft and the Federal MSC 26-1 drilled in 2005 to a similar (but undisclosed) depth. Both holes are listed in the state oil and gas information website as shut-in gas wells. The depth of these test holes is greater than would be expected for exploration for the Cretaceous Dakota to Triassic play; instead, these holes were likely exploring for the three other deeper plays in rocks of Devonian to Pennsylvanian age.

Four oil test holes have been drilled recently about 2 mi west–southwest of the disposal cell area in the faulted and structurally complex incipient collapse area of the northwest extension of the Salt Valley Anticline. Three of the oil test holes were in Section 32. The MSC Exploration, LP, State 1-32 well noted above was drilled to a depth of 4,630 ft, and its oil production from the Navajo Sandstone indicates exploration for the Cretaceous Dakota to Triassic play, similar to that of the Blaze Canyon field to the north. MSC Exploration, LP, drilled the State 21-19(32-16D) well in 2003 just south of I-70 to a depth of 4,054 ft; the state oil and gas information website lists this as a temporarily abandoned oil well. The third well in Section 32, Tidewater State 32-3, was drilled to a depth of 4,505 ft in the Navajo Sandstone in 2006 by Samson Resources Company about 0.5 mi north of the State 1-32 well; the state oil and gas information website lists this as a shut-in oil well.

The fourth oil test, the Tidewater Cactus Rose Federal 29-44-2119, was drilled in the SE¼ SE¼ of Section 29 to a depth of approximately 4,400 ft in late 2006 and early 2007. No completion information is available for this test hole, whose target was the Navajo Sandstone. Another test hole is planned and permitted in the SW¼ of Section 29, the Tidewater Federal 29-24-2119, which may be drilled in 2007.

According to the Mineral Report by the BLM on the DOE Proposed Disposal Site (Bain 2005), the entire withdrawal area is currently leased for oil and gas by Tidewater Oil and Gas Company of Denver, Colorado, which reportedly was recently acquired by Samson Resources Company. The lessee has notified the BLM that development of the disposal site would negatively affect their exploration for what they consider as a major oil and gas play. Exploration for oil and gas would not be prohibited for these pre-existing leases in the withdrawal area during construction of the disposal cell (approximately 250 acres) and associated support infrastructure. For the approximately 10 percent of the withdrawal area to be occupied by the disposal cell, directional drilling could be used to explore for oil and gas resources directly beneath the cell. Therefore, exploration and development of oil and gas resources should not be adversely affected by the construction and operation of the disposal cell.

If oil and/or gas resources were discovered and produced from beneath the disposal cell area, the occurrence of surface subsidence would be very unlikely. If these resources occur, they are probably at depths of between 4,000 and 11,000 ft, and they would fill void (pore) space in the rock (intergranular space in sandstone) that typically amounts to as much as 20 to 25 percent of the volume of the rock. Production of oil and/or gas usually recovers only 30 to 50 percent of the resource, resulting in removal of only up to 10 percent of the rock volume. The removal of this small volume from a deeply buried sandstone that is grain-supported makes it extremely unlikely that any subsidence would occur or be transmitted to the surface; no surface subsidence has been reported in association with numerous oil and gas fields in east-central Utah (Tabet 2007).

Potash and Salt

Potash and salt resources are known in the Paradox Formation of Pennsylvanian age in the Paradox Fold and Fault Belt; however, no exploration or development for these resources has occurred in or immediately adjacent to the site area. Some exploration for potash and salt resources occurred from the 1920s to the 1960s near the site area, in an area of potash leases several miles south of Crescent Junction. Potash and an associated salt, carnallite, which contains magnesium, were discovered by drilling as early as 1924. During World War II, additional exploration of the salt for the strategic commodity, magnesium, was conducted about 2.5 mi south–southwest of the disposal cell area with the drilling of the Thompson magnesium well (Severy at al. 1949). Potash and other salt minerals in this explored area occurs in deformed beds that have undergone diapiric movement along the axis of the Salt Valley Anticline.

Thick beds of salt were deposited in the ancestral Paradox salt basin as part of the saline facies of the Paradox Formation. The saline facies consists of partial and complete evaporate cycles and intervening clastic rocks that include black shale with a significant amount of organic carbon (Bain 2005). A typical evaporitic cycle may include halite (sodium chloride), with or without the potash salts sylvite (potassium chloride) and carnallite (hydrated potassium magnesium chloride), anhydrite, gypsum, and silty dolomite. Potash is one of the last salts to precipitate during brine formation, so it is typically present near the top of each evaporate cycle.

Most favorable targets for exploitable potash deposits are in non-diapiric salt anticlines because they have thickened salt cores where potash beds are shallow and their continuity has not been destroyed by

flowage (Tabet 2005). The Salt Valley Anticline just west of the site has characteristics of diapiric salt movement; therefore, its favorability for occurrence of exploitable potash deposits is low. In the Mineral Potential Report for the BLM Moab Planning Area (Tabet 2005), the occurrence potential for potash and salt deposits in the Crescent Junction Site area is shown as moderate, but the development potential is shown as low. The favorability even for the occurrence of potash and salt deposits may be very low because most of the withdrawal area (particularly Section 27 and most of Sections 22 and 26) is shown to be in an area of the Paradox Formation that is lacking salt as a result of salt flowage toward the Salt Valley Anticline; this interpretation was made from deep Paleozoic oil test holes and extensive seismic data that characterized stratigraphic relationships in the northern part of the Paradox Basin (Frahme and Vaughn 1983, Figure 7). From this, the probability is very low that potash and other salt mineral resources occur in the site area, and exploration for them would not be adversely affected by the small area occupied by the disposal cell.

Coal

Coal occurs in the Castlegate Sandstone and Neslen Formation, both in the Mesaverde Group, in the Book Cliffs just north of the Crescent Junction Site area. This resource has no potential for occurrence at the site, however, because rocks of the Mesaverde Group are stratigraphically younger than rocks at the site.

Uranium and Vanadium

Uranium and vanadium deposits are in scattered locations in east-central Utah in the Morrison Formation of Jurassic age and the Chinle Formation of Triassic age. Deposits nearest the site are in the Morrison Formation where it crops out about 6 mi south of the site in the Klondike Ridge-Courthouse Wash mining area (Tabet 2005). At the site area, the Morrison and Chinle Formations are 3,000 to 4,000 ft, respectively, below the surface. No potential for occurrence of these resources is shown for the site area in the Mineral Potential Report by Tabet (2005). In the extremely unlikely event that exploration found uranium-vanadium deposits beneath the site area, mining (by underground or solution methods) would not be economically feasible (even with the presently elevated prices) because of the great depth of the host formations.

Copper and Silver

Copper (and silver as a minor constituent) deposits occur in the Morrison Formation along faults on the southwest flank of the Salt Valley Anticline about 8 mi south-southeast of the site area. The Morrison Formation is at least 3,000 ft below the surface at the site. No potential for occurrence of copper is shown for the site area in the Mineral Potential Report by Tabet (2005). Exploration for copper deposits in the site area, even with the recently elevated price for copper, would not be economically feasible because of the great depth of the host formation.

Gold

High concentrations of gold in Mancos Shale have been rumored to occur for many years. As recently as the 1980s when the price for gold reached record high levels, mining claims for gold were staked over large parts of the Mancos Shale outcrop area in eastern Utah and western Colorado. As a marine-deposited, organic-rich black shale, the Mancos Shale is naturally enriched in metals such as uranium, copper, silver, vanadium, mercury, arsenic, and gold. These metals likely originated in volcanic ash (since altered to bentonite), which was deposited during the long accumulation of sea-bottom sediment forming the Mancos Shale. To evaluate the occurrence of anomalously high concentrations of some of these metals, an area of exposed Mancos Shale generally between Salt Valley and the Book Cliffs (including the site area) was sampled by Marlatt (1991) and analyzed for gold, silver, and copper. Gold content of the samples ranged from 30 to 100 parts per billion, which is about 10 times the background concentration for gold in shale. Marlatt (1991) concluded that the high gold concentrations in Mancos Shale indicated that gold had migrated and had been reconcentrated by diagenetic fluids, but that it was unlikely that conditions necessary to form ore bodies (permeable, reactive host zones in the Mancos Shale) were ever present. Gold concentrations indicated in the Mancos Shale are much too low to warrant economic extraction (gold content would generally have to be more than 1 part per million), even with the recent rise in the price of gold.

Sand and Gravel

Sand and gravel resources do not occur in the withdrawal area; therefore, construction and operation of the Crescent Junction disposal cell would not affect these resources. The BLM Mineral Potential Report (Tabet 2005, Map 18b) shows a high development potential for sand and gravel in the site area. This was based on the small-scale state of Utah geologic map by Hintze et al. (2000), which shows eolian sand covering much of the Crescent Flat area. More recent and larger scale mapping by Doelling (2001) shows correctly that Crescent Flat is covered instead by fine-grained alluvial mud derived from Mancos Shale. The nearest potential sand and gravel deposits are west of Crescent Wash approximately 0.5 mi west of the withdrawal area in Section 28 and a similar distance to the south in Section 34. These deposits are shown by McDonald (1999) and are mapped by Doelling (2001) as Mancos Shale pediment-mantling material deposited by ancestral Crescent Wash drainages.

Geologic Hazards

Landslides, situated mainly on northerly-facing slopes of the Blackhawk Formation/Castlegate Sandstone escarpment of the Book Cliffs, occur just north of the withdrawal area. Harty (1993) mapped two deep-seated landslides classified as earth slumps—the larger of the two slides is on a north-facing slope in the south side of an area known as "Horse Heaven" behind the Book Cliffs; and the smaller slide is on a northeast-facing slope of the Book Cliffs in the south-central part of Section 13. Both landslides are just north of the withdrawal area. More recent mapping by Doelling (2001) shows these two landslides as "Qmt" and also shows by the same symbol several small remnants of ancestral landslides along the south face of the Book Cliffs along the north edge of the withdrawal area (Figure 4). Other than along the north edge of the withdrawal area on the lower flanks of the Book Cliffs, slopes in the rest of the withdrawal area are low, resulting in no potential for landslides.

Swelling clay in the Mancos Shale poses a potential geologic hazard at the site. Swelling is caused by the presence in Mancos Shale of the clay mineral, montmorillonite, which originated from volcanic ash that was altered after it fell into the Western Interior Seaway (Tourtelot 1974). Fresh and slightly weathered Mancos Shale swells considerably when wetted—a 25 to 58 percent volume increase was noted by Schumm (1964) in free swell tests. Mulvey (1992) documented the expansive-soil problems associated with Mancos Shale in Utah with examples of damaged buildings in Green River and heaving concrete slabs at the Moab airport (Canyonlands Field). Frequent maintenance (resurfacing) has been required for I-70, which passes just south of the disposal site, in sections of the highway that are on Mancos Shale.

Because of these swelling conditions, no rigid (concrete) pavement can be used for I-70 on the Mancos Shale; flexible (asphaltic) pavement is required (Gay 2007). If no permanent concrete-slab structures and no paved roads are planned for the disposal site, the swelling clay in the Mancos Shale should not pose a geologic hazard.

The site area has a moderate to high radon-hazard potential for occurrence of indoor radon based on the geologic factors of uranium concentration, soil permeability, and ground water depth (Black 1993). The moderate to high rating is created by the relatively high concentration of uranium in the Mancos Shale, the relatively high soil permeability caused by shrinking and swelling of the Mancos Shale-derived soil, and the relatively deep ground water depths (shallow ground water retards radon migration). No permanent structures are planned for the disposal site; therefore, high indoor radon concentration will not be a problem.

Conclusion and Recommendations:

Based on evaluation of the results of the literature research, the Crescent Junction Site is apparently suitable for disposal of the Moab uranium mill tailings and contaminated material. Potential geologic hazards appear to be limited to swelling clay, and this would not pose a hazard if no permanent concrete-slab structures or paved roads are constructed at the disposal site. Although faults occur within several miles of the withdrawal area, they do not appear to have displaced Quaternary surficial deposits. This indicates that significant offset occurred prior to the Quaternary Period, and it is thought that the faults represent adjustments by slow subsidence to dissolution of deeply buried, thick salt deposits in the north part of the Paradox Basin. Recovery of oil and gas, which are the geologic resources that have the

highest potential for development, would not be precluded by use of the area as a disposal cell. Any petroleum resources could be explored and recovered (if present) by directional drilling.

Computer Source:

Not applicable.

References

Bain, Frank, 2005. *Mineral Report on Department of Energy Proposed Site,* prepared for DOE/EIS 0355D by the U.S. Bureau of Land Management, Moab, Utah, District Office, December.

Black, B.D., 1993. *The Radon-Hazard-Potential Map of Utah*, Utah Geological Survey Map 149, scale 1:1,000,000.

Chidsey, T.C. Jr., S. Wakefield, B.G. Hill, and M. Hebertson, 2004. *Oil and Gas Fields Map of Utah*, Utah Geological Survey Map 203DM, CD-ROM, scale 1:700,000.

Chitwood, J.P., 1994. *Provisional Geologic Map of the Hatch Mesa Quadrangle, Grand County, Utah*, Utah Geological Survey Map 152, scale 1:24,000.

Cole, R.D., R.G. Young, and G.C. Willis, 1997. *The Prairie Canyon Member, a New Unit of the Upper Cretaceous Mancos Shale, West-Central Colorado and East-Central Utah*, Utah Geological Survey Miscellaneous Publication 97-4.

Detterman, J.S., 1955. *Photogeologic Map of the Moab-5 Quadrangle, Grand County, Utah*, Utah Geological Survey Miscellaneous Investigations Map I-57, scale 1:24,000.

Doelling, H.H., 1997. *Interim Geologic Map of the Valley City Quadrangle, Grand County, Utah,* Utah Geological Survey Open-File Report 351, scale 1:24,000.

Doelling, H.H., 2001. *Geologic Map of the Moab and Eastern Part of the San Rafael Desert 30' × 60' Quadrangles, Grand and Emery Counties, Utah, and Mesa County, Colorado*, Utah Geological Survey Map 180, scale 1:100,000.

Doelling, H.H., 2002. *Geologic Map of the Moab and Eastern Part of the San Rafael Desert 30' × 60' Quadrangles, Grand and Emery Counties, Utah, and Mesa County, Colorado,* Utah Geological Survey Map 180DM, CD-ROM, scale 1:100,000.

Doelling, H.H., M.L. Ross, and W.E. Mulvey, 2002. *Geologic Map of the Moab 7.5' Quadrangle, Grand County, Utah,* Utah Geological Survey Map 181, scale 1:24,000.

Fisher, D.J., 1936. *Book Cliffs Coal Field in Emery and Grand Counties, Utah*, U.S. Geological Survey Bulletin 852, scale 1:62,500.

Frahme, C.W., and E.B. Vaughn, 1983. "Paleozoic Geology and Seismic Stratigraphy of the Northern Uncompahgre Front, Grand County, Utah," in Lowell, J.D., editor, *Rocky Mountain Foreland Basins and Uplifts*, Rocky Mountain Association of Geologists 1983 Symposium Guidebook, pp. 201–211.

Friedman, J.D., J.E. Case, and S.L. Simpson, 1994. *Tectonic Trends of the Northern Part of the Paradox Basin, Southeastern Utah and Southwestern Colorado, as Derived from Landsat Multispectral Scanner Imaging and Geophysical and Geologic Mapping*, U.S. Geological Survey Bulletin 2000-C.

Friedman, J.D., and S.L. Simpson, 1980. *Lineaments and Geologic Structure of the Northern Paradox Basin, Colorado and Utah*, U.S. Geological Survey Miscellaneous Field Studies Map MF-1221, scale 1:250,000.

Gay, Larry, 2007. Personal communication, C. Goodknight, Senior Geologist, S.M. Stoller Corporation, telephone conversation with L. Gay, Materials Engineer, Utah Department of Transportation, January.

Gualtieri, J.L., 1982. *Geologic Map of Parts of Crescent Junction and Floy Canyon Quadrangles, Utah, Showing Coal Zones and Adjacent Rocks,* U.S. Geological Survey Open-File Report 82-584, scale 1:50,000.

Gualtieri, J.L., 1988. *Geologic Map of the Westwater 30' × 60' Quadrangle, Grand and Uintah Counties, Utah, and Garfield and Mesa Counties, Colorado*, U.S. Geological Survey Miscellaneous Investigations Series Map I-1765, scale 1:100,000.

Hanson, D.T., 1989. *Soil Survey of Grand County, Utah, Central Part*, U.S. Department of Agriculture, Soil Conservation Service, 60 sheets, scale 1:24,000.

Harrison, T.S., 1927. *Colorado-Utah Salt Domes*, American Association of Petroleum Geologists Bulletin, 11(2) pp. 111–133.

Harty, K.M., 1993. *Landslide Map of the Moab 30' × 60' Quadrangle, Utah,* Utah Geological Survey Open-File Report 276, scale 1:100,000.

Hintze, L.F., G.C. Willis, D.Y.M. Laes, D.A. Sprinkel, and K.D. Brown, 2000. *Digital Geologic Map of Utah,* Utah Geological Survey Map 179DM, CD-ROM, scale 1:500,000.

Hunt, C.B., 1956. *Cenozoic Geology of the Colorado Plateau*, Utah Geological Survey Professional Paper 279.

Hurlow, H.A., and C.E. Bishop, 2003. *Recharge Areas and Geologic Controls for the Courthouse-Sevenmile Spring System, Western Arches National Park, Grand County, Utah*, Utah Geological Survey Special Study 108.

Marlatt, Gordon, 1991. *Gold Occurrence in the Cretaceous Mancos Shale, Eastern Utah*, Utah Geological and Mineral Survey Contract Report 91-5.

McDonald, G.N., 1999. *Known and Potential Sand, Gravel, and Crushed Stone Resources in Grand County, Utah*, Utah Geological Survey Open-File Report 369.

Merrell, H.W., 1979. *Mineral Resource Inventory of the Paradox Salt Basin, Utah and Colorado*, prepared in conjunction with the staff of Utah Geological and Mineral Survey, Report of Investigation No. 143, October.

Mulvey, W.E., 1992. *Soil and Rock Causing Engineering Geologic Problems in Utah*, Utah Geological Survey Special Study 80, scale 1:500,000.

Schumm, S.A., 1964. "Seasonal Variations of Erosion Rates and Processes on Hillslopes in Western Colorado," *Zeitschrift für Geomorphologie,* Vol. 5, pp. 215–238.

Severy, C.L., M.H. Klein, and P.T. Allsman, 1949. *Investigations of the Thompson Magnesium Well, Grand County, Utah*, U.S. Bureau of Mines Report of Investigations RI–4496.

Stokes, W.L., 1977. "Subdivisions of the Major Physiographic Provinces in Utah," *Utah Geology,* Utah Geological and Mineral Survey, 4(1) pp. 1–17.

Tabet, D.E., 2005. *Mineral Potential Report for the Moab Planning Area,* prepared by the Utah Geological Survey, Energy and Minerals Division, for the Moab, Utah, Field Office of the U.S. Bureau of Land Management.

Tabet, D.E., 2007. Personal communication, C. Goodknight, Senior Geologist, S.M. Stoller Corporation, telephone conversation with D.E. Tabet, Geologic Manager, Energy and Minerals Program, Utah Geological Survey, January.

Tourtelot, H.A., 1974. *Geologic Origin and Distribution of Swelling Clays*, Association of Engineering Geologists Bulletin, XI(4) pp. 259–275.

Williams, P.L., compiler, 1964. *Geology, Structure, and Uranium Deposits of the Moab Quadrangle, Colorado and Utah,* U.S. Geological Survey Miscellaneous Geologic Investigations Map I-360, scale 1:250,000.

Willis, G.C., 1986. *Provisional Geologic Map of the Sego Canyon Quadrangle, Grand County, Utah,* Utah Geological and Mineral Survey Map 89, scale 1:24,000.

Woodward-Clyde Consultants, 1984. "Geologic Characterization Report for the Paradox Basin Study Region, Utah Study Areas, Volume VI, Salt Valley," unpublished report ONWI-290, prepared for the Office of Nuclear Waste Isolation, Battelle Memorial Institute, Columbus, Ohio, Salt Valley area geologic map, scale 1:62,500.

Young, R.G., 1983. "Petroleum in Northeastern Grand County, Utah," in Averett, W.R., editor, *Northeastern Paradox Basin – Uncompahgre Uplift*, Grand Junction Geological Society 1983 Field Trip Guidebook, pp. 1–6.

End of current text

U.S. Department of Energy—Grand Junction, Colorado

Calculation Cover Sheet

Calc. No.: MOA-02-04-2007-1-01-01 **Discipline:** Geology **No. of Sheets:** 18
Doc. No.: X0153800

Location: Attachment 2, Appendix B

Project: Moab UMTRA Project

Site: Crescent Junction Disposal Site

Feature: Surficial and Bedrock Geology of the Crescent Junction Disposal Site

Sources of Data:

Geologic mapping of the Crescent Junction Disposal Site area.

Geologic literature research for a 30-mile radius of the disposal site area.

Lithologic logs for boreholes and test pits emplaced at the disposal site area from August to December 2005.

Purpose of Revision:

Revision of this calculation set became necessary because the size and orientation of the disposal cell footprint changed and some additional references and information were included as a result of responses to U.S. Nuclear Regulatory Commission (NRC) review questions.

Sources of Formulae and References:

See list of references at end of calculation set.

Preliminary Calc. ☐ **Final Calc.** ☒ **Supersedes Calc. No.** MOA-02-03-2006-1-01-00

Author: Craig Goodknight 31 May 07
Name Date

Checked by: J C Summers 5/31/07
Name Date

31 May 07
Name Date

Approved by: Kent Kruys 5/31/07
Name Date

Craig Goodknight 31 May 07
Name Date

Reviewed by: Mark Kautsky 5-31-07

MAY 31, 07
Name Date

No text for this page

Problem Statement:

Preliminary site selection performed jointly by the U.S. Department of Energy (DOE) and the Contractor has identified a 2,300-acre withdrawal area in the Crescent Flat area just northeast of Crescent Junction, Utah, as a possible site for a final disposal cell for the Moab uranium mill tailings. The proposed disposal cell would cover approximately 250 acres. Based on the preliminary site-selection process, the suitability of the Crescent Junction Disposal Site is being evaluated from several technical aspects, including geomorphic, geologic, hydrologic, seismic, geochemical, and geotechnical. The objective of this calculation set is to discuss the surface and bedrock geology of the site and provide the geologic map, cross sections, and bedrock contour map that were generated during the investigation.

This calculation set was initially prepared in March 2006 and included results of geologic characterization conducted at the Crescent Junction Site. Revision of this calculation set became necessary because the size and orientation of the disposal cell footprint changed and some additional references and information were included as a result of responses to U.S. Nuclear Regulatory Commission (NRC) review questions.

Information from this revised calculation was incorporated into Attachment 2 (Geology) of the Remedial Action Plan and Site Design for Stabilization of Moab Title I Uranium Mill Tailings at the Crescent Junction, Utah, Site (RAP), and summarized in the appropriate sections of the Remedial Action Selection (RAS) report for the Moab Site.

Method of Solution:

Surface geologic features were identified by aerial photography and field observation mapping. A geologic map of the site area (Plate 1) was prepared that shows these features. Subsurface features of the Quaternary material and bedrock were identified from lithologic logging at test pits and from core retrieved from coreholes and geotechnical boreholes (see RAP Attachment 5). Cross sections across the site area (Plate 2) were prepared from the borehole lithologic logs that show bedrock features. A bedrock (top of weathered Mancos Shale) contour map for the site area (Plate 3) was prepared from the borehole and test pit lithologic logs and mapped surface outcrops. Review of geologic literature for the region provided the stratigraphic framework for the surface and subsurface features identified in the site area.

Assumptions:

Not applicable

Calculation:

Not applicable – see discussion of information in next section.

Discussion:

Maps of Site Area

A geologic map (Plate 1) and bedrock contour map (Plate 3) were prepared for the Crescent Junction Site area, which covers about 2 square miles (mi). For this calculation, the site area is synonymous with the (geologically) mapped area.

Geologic Map

The geologic map of the site area was prepared during field work, mainly in September and October 2005. The mapped area includes the proposed disposal cell footprint and the larger area covered by characterization boreholes (coreholes and geotechnical boreholes) and test pits. Mapping was done on a base map with a 2-foot (ft) topographic contour interval at a scale of 1:4,800 (1 inch = 400 ft). Contacts of the few and scattered bedrock outcrops of Mancos Shale of Late Cretaceous age in the area are shown on the map. At these bedrock outcrops, a Brunton compass was used to measure strike and dip of bedding and strike of vertical joints in the few places these features could be observed. Contacts between several types of unconsolidated surficial material of Quaternary age are shown on the map;

these contacts are subtle and gradational and are not as evident or as sharp as the contacts between bedrock units. Descriptions of the mapped units of Quaternary age and the mapped units in the Mancos Shale are in the following subsections. Also shown on the geologic map are lines for five cross sections (Plate 2) connecting the coreholes and geotechnical boreholes included in each cross section.

Bedrock Contour Map

A contour map of the top of bedrock topography is shown in Plate 3 at the same scale as the geologic map. The bedrock topography shows two subtle ridges that strike north-northwest. One ridge extends through the west part of the proposed disposal cell and one is through the east-central part. Both bedrock ridges coincide with subtle surface ridges in the proposed disposal cell area. In addition, the east-central bedrock ridge appears to be a southward continuation of the surface ridge north of what is referred to as the 3 ponds area. The 3 ponds (Plate 1) contain ephemeral water and were constructed by the U.S. Bureau of Land Management as a source of water for cattle grazing in the area. Local relief of as much as 20 ft occurs on the bedrock surface, as shown in the east end of the mapped area where bedrock in test pit 0156 is 20 ft lower than bedrock exposed on a nearby subtle ridge to the southwest. Occurrences of similar local bedrock relief are likely present in the proposed disposal cell area.

Surficial Geology — Quaternary Material

Unconsolidated Quaternary material covers approximately 98 percent of the mapped area. This material covers Mancos Shale bedrock and reaches a thickness of nearly 25 ft. Five types of Quaternary material were mapped—the most significant from areal and volume perspectives are alluvial-mud (mixed silt and clay) deposits. Material along active sheet wash flow paths and litter from the Book Cliffs that mantles the alluvial mud are two other mapped units that are related to the alluvial mud. The two other Quaternary units mapped are sandy alluvium and pediment-mantling litter. Both of these are in the southwest and west parts of the mapped area and represent alluvial deposits from the Crescent Wash drainage system that has transported sandy material southward from the Book and Roan Cliffs, which are composed of rocks of Late Cretaceous and Paleogene ages, respectively.

Alluvial Mud Deposits

Gray mud, silt, and clay cover most of the surface of the site area at distances of more than 0.5 mi south of the base of the Book Cliffs. This material is mostly of alluvial and colluvial origins, derived from sheet wash erosion from the lower slopes of the Book Cliffs where Mancos Shale is exposed in a badlands setting. Some of the material is residual and forms from weathering of muddy outcrops of Mancos Shale. Alluvial-mud deposits covering Mancos Shale are mapped by Doelling (2001) who described these deposits in the site area and to the south in the Valley City quadrangle (Doelling 1997).

Surface expression of the alluvial mud is mostly in the form of silt to clayey silt and was described in the field as ML, in the Unified Soil Classification System (USCS). This fine-grained material is typically light brownish gray (10YR 6/2), highly calcareous, and represents successive sheet wash deposits. Laboratory test results of this material sampled from geotechnical boreholes indicates a high clay (CL in the USCS) content.

Below the surface, most of the alluvial mud is fine-grained, but discontinuous layers of coarser grained material of eolian and channel-fill origin are also present around the site area. Material of eolian origin was found in several boreholes and test pits (see lithologic logs of test pits 0151 and 0153 in RAP Attachment 5). Eolian material is typically sandy silt (ML in the USCS), light brown (7.5YR 6/4), 1 to 3 ft thick, and at depths of 6 to 12 ft. The brown eolian material exposed in test pit 0151 is shown in Figure 1. The sporadic occurrence of this material, not in a continuous layer, indicates it was removed by erosion and reworked after its deposition, which was probably in a dry period during mid-Holocene time.

Coarser grained, sand to gravel, and small boulder-sized material occurs also in sporadic, discontinuous layers and lenses in the alluvium. Several of the coreholes and geotechnical boreholes around the site area penetrated gravelly sand (SW in the USCS) layers that contained shale and sandstone fragments. Some of this deeper material has been cemented by calcite. The gravelly sand material represents alluvial detritus deposited in small channels similar to the litter deposits on the surface in the north part of the site area closer to the base of the Book Cliffs. Material as large as small boulders also is present in a few locations—notably exposed in test pit 0156. Here, small boulders up to 2 ft in diameter fill an alluvial

channel cut into Mancos Shale bedrock at a depth of approximately 20 ft. Mancos Shale is exposed in the bottom of test pit 0156 in Figure 2. Sandstone bedrock is at the surface (Plate 1) only about 200 ft to the southwest of this coarse bouldery material. This relief of at least 20 ft on the bedrock surface in a short distance and the coarse bouldery deposits indicates a former channel about 800 ft east of the disposal cell footprint where coarse material was transported southward from the ancestral Book Cliffs (Plate 2, cross section E-E', and Plate 3). No indication of ground water was found in this channel. Other former channels or swales on the top of bedrock similar to this one exposed at test pit 0156 may occur westward across the site area.

Figure 1. View of brown eolian material exposed at a depth of 7 ft in test pit 0151.

Figure 2. Test pit 0156. Alluvial-mud deposits are approximately 20 ft thick, and Mancos Shale is at bottom of pit. White 5-gallon buckets and shovel provide scale.

Alluvial mud in the site area has been deposited over Mancos Shale bedrock in a long-term process of successive sheet wash episodes during much of Quaternary time. The thickest accumulation of alluvial mud is in subtle bedrock lows between several north-northwest striking bedrock ridges that cross the site area (Plate 3). The thickest alluvial mud accumulations of about 23 ft were found in geotechnical boreholes 0014 and 0025, north of the west part of the proposed disposal cell. A thick accumulation is also in the east part of the proposed disposal cell where 22 ft of alluvial mud was found in corehole 0208, and a similar thickness was found in corehole 0209 just inside the southeast corner of the proposed disposal cell. The average thickness of alluvial mud at the proposed disposal cell is 10 to 12 ft. Alluvial mud thickness overlying the two bedrock ridges in the west and east-central parts of the proposed disposal cell is less than 10 ft. Between these ridges, the thickness is from 10 to 20 ft, and along the east side of the eastern ridge, the thickness is from 10 to 22 ft.

Material along Active Sheet Wash Flow Paths

Several paths along which the sheet wash process is active are shown on the geologic map (Plate 1). These paths are visible in the high-altitude vertical aerial photos by their drab-gray color and are shown in Plate 1 of the "Photogeologic Interpretation" calculation set (RAP Attachment 2, Appendix G). Vegetation is generally absent from the paths, and recently-deposited gray mud covers most of the surface. Some small fragments of sandstone transported from the flanks and base of the Book Cliffs may be scattered on the surface of the paths.

The active sheet wash paths are generally in the north part of the site area within about 0.5 mi of the base of the Book Cliffs. The north ends of these paths typically merge into gullies that drain away from the base of the Book Cliffs (Plate 1). Four paths enter or cross the proposed disposal cell footprint. Of these, the most prominent path is the one that extends south-southeastward across the east part of the disposal cell footprint to the Union Pacific Railroad from the drainage just west of the 3 ponds area (Plate 1 and Figure 3). Material transported down this drainage is deposited along the path as the gradient decreases southward from about 3 to 4 degrees to about 2 degrees across the disposal cell footprint.

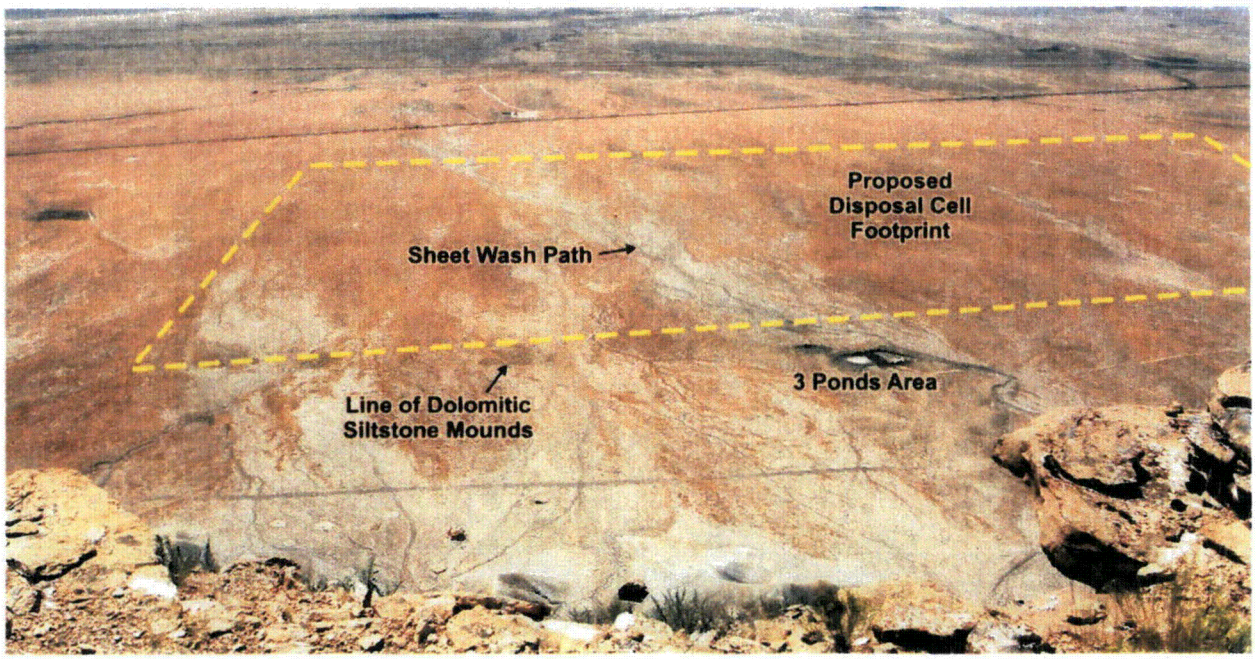

Figure 3. View south from top of Book Cliffs of the disposal cell footprint, the sheet wash path extending south-southeast from the 3 ponds area, and the east-trending line of dolomitic siltstone mounds.

Flows along the sheet wash paths are infrequent, but represent the main process by which alluvial mud has been slowly deposited over bedrock at the site area. One episode of active sheet wash flow was witnessed in late September 2005 during site characterization drilling. Flows occurred in several sheet wash paths (Figure 4) immediately following a high-intensity rain and hail event during which at least 0.5 inch of precipitation fell in less than 30 minutes. It is estimated that events of this magnitude typically occur about once per year.

Two or three high-intensity rainfall events affected the site area and much of eastern Utah in the early and middle parts of October 2006. Rainfall from these events totaled an estimated 4 to 5 inches and occurred as moderate intensity rains over durations of several hours to as much as one day. The amount of these rains, produced from plumes of moisture from dying hurricanes in the eastern Pacific Ocean-Gulf of California area, was unusual; an early-fall event of this magnitude had not occurred since the early 1970s. Significant flows occurred in the sheet wash areas resulting from these events. In several sheet wash areas crossed by the access road north of the disposal cell, up to a 6-inch thickness of alluvial mud had been deposited.

Figure 4. View east of active sheet wash flowing over site access road just north of geotechnical borehole 0025, September 21, 2005.

Litter from Book Cliffs that Mantles Alluvial Mud and Mancos Shale

Mancos Shale and alluvial mud are increasingly covered from south to north across the mapped area by what is referred to as litter that is composed mainly of sandstone fragments ranging from one inch to as much as 3 ft in diameter. North of the mapped area and closer to the base of the Book Cliffs, sandstone boulders are as large as several tens of feet in diameter. The smaller sandstone fragments in the mapped area are derived from the top of the Book Cliffs and consist of tan, friable, subrounded fragments and chunks of fine-grained sandstone of the Blackhawk Formation and slabs of rusty-colored, brittle, well-cemented, fine-grained dolomitic sandstone of the Castlegate Sandstone. The surface areas covered by the litter contain some dark-colored biological soil crust, dominated by cyanobacteria, that favors plant growth and supports scattered prickly pear cactus.

Northward from the proposed disposal cell to the base of the Book Cliffs (nearer to the source of the sandstone), the sandstone litter covers most of the surface. Southward through the proposed disposal cell, the litter is present only in narrow strips that generally correspond to subtle, north-northwest striking ridges (Plate 1). The litter-covered low ridges also correspond, in most places in the proposed disposal cell area, to subtle bedrock ridges, as shown in Plate 3. The litter in the proposed disposal cell area represents residual sandstone material that was deposited as rock falls along the base of the Book Cliffs during erosion of the supporting Mancos Shale. This residual rockfall material has not yet been eroded away or has not been covered by sheet wash material during the accumulation of the alluvial-mud deposits.

Sandy Alluvium

Alluvium from an earlier Crescent Wash drainage system occurs in low ridges along the southwest edge of the mapped area. This material consists mainly of silty sand, and the sand is mostly fine- to very fine-grained. The sandy character of this alluvium is different from the Mancos Shale-derived alluvial mud and reflects the dominantly sandstone lithology in the Book and Roan Cliffs area drained by the Crescent Wash system. A few sandstone chunks (rarely as large as boulders) and chert pebbles occur in the alluvium; these are representative of the Mesaverde Group sandstones and Paleogene sandstones with chert that are in the Crescent Wash drainage. The sandy alluvial ridges also support more vegetation than the alluvial mud flats.

Evidence of former courses of Crescent Wash is expressed in the sandy alluvium as arcuate topographic lows near the west-central edge of Section 27 (Plate 1). These former stream courses were as much as 1,000 ft east of the present wash. Sandy alluvium is absent immediately east of the large incised meander of Crescent Wash near the northwest corner of Section 27. This indicates that no former Crescent Wash course has been east of the present wash course at the large meander.

Pediment-Mantling Litter

Several small areas along the west and southwest edges of the mapped area are covered by a distinctive, resistant, gravelly material that veneers alluvial mud, sandy alluvium, or Mancos Shale outcrops. Pebbles in this gravelly material consist of brown sandstone and resistant white quartzite and distinctive, exotic, black chert (up to 2 inches in diameter). The pebbles are loose and scattered and "litter" the surface.

These deposits represent the erosion-resistant lag material from former pediment-mantling deposits laid down by the ancestral Crescent Wash drainage system. The pediment-mantling deposits are no longer preserved in place in the mapped area. These deposits are preserved in place about 0.5 mi west of the mapped area where they cap a low mesa at an elevation about 100 ft above Crescent Wash and are mapped as pediment-mantle deposits by Doelling (2001). These in-place deposits contain the same type of resistant pebbles found as lag (or litter) in the mapped area. The distinctive, exotic, black chert and vari-colored quartzite pebbles in the pediment-mantle deposits are a constituent of a conglomerate in the Dark Canyon Sequence of the Wasatch Formation of early Paleocene age that crops out in the Roan Cliffs about 6 to 8 mi north up the Crescent Wash drainage (Franczyk et al. 1990). The occurrence of this pediment-mantling deposit whose matrix contains Stage II carbonate development about 100 ft above current drainages probably correlates to similar cemented deposits on Mancos Shale pediments mapped by Willis (1994) in the Harley Dome area about 35 mi to the east-northeast. Those deposits were estimated by Willis (1994) to be 100,000 to 200,000 years old based on their height (50 to 110 ft) above current drainages and their carbonate development (Stage II).

At the southwest end of the mapped area, several areas of pediment-mantling litter lie on the sides of a low hill where weathered Mancos Shale is poorly exposed (Plate 1). This hill is likely an erosional remnant of a Mancos Shale pediment surface east of the current Crescent Wash that was capped by the pediment-mantle deposits about 100,000 to 200,000 years ago (late to middle Pleistocene age) emplaced by the ancestral Crescent Wash system. The other scattered small deposits of pediment-mantling litter (mainly in the area near corehole 0202) are evidence of the former extent of this pediment.

Bedrock Geology – Cretaceous Mancos Shale

The mapped site area is underlain by the Mancos Shale of Late Cretaceous age that dips gently northward. The shale forms a broad, east-trending belt immediately south of the Book Cliffs. Topographically, the shale forms a badlands that is the lower or buttressing part of the Book Cliffs and the wide expanse of lowlands, or "flats", extending several miles to the south (Fisher et al. 1960).

Total thickness of the Mancos Shale, which generally represents the open-marine mudstones deposited in the Cretaceous Western Interior Seaway, is approximately 3,500 ft if measured from the top of the Book Cliffs just north of the site area. Most of the Mancos Shale is a monotonously uniform drab or bluish gray shale; however, in the site area, which is in the upper third of the formation, an anomalously sandy interval represents a period of near-shore deposition. This sandy interval was earlier recognized as the "Mancos B" (zone or horizon) because of its natural gas-producing characteristics on the Douglas Creek arch near the Utah-Colorado border (Kellogg 1977). More recent stratigraphic studies have identified the nearshore facies of this sandy interval and formalized this unit and renamed it the Prairie Canyon Member (Cole et al. 1997). Some facies of the Prairie Canyon Member, as identified by Hampson et al. (1999) as fluvial-dominated delta front deposits, occur in the north part of the mapped area. These delta-front deposits, therefore, are mapped as representing the Prairie Canyon Member in the site area. From the sandy (generally very fine-grained) nature of this member as exposed in a few outcrops, seen in several coreholes and test pits, and expressed as a marked reduction in the gamma ray geophysical log response from coreholes, the thickness of the Prairie Canyon Member in the mapped area is approximately 150 to 200 ft. As much as 150 ft of the Prairie Canyon Member is beneath the north edge of the proposed disposal cell.

Underlying and overlying the sandy interval of the Prairie Canyon is the Blue Gate Member of the Mancos Shale. The Blue Gate Member consists mainly of open-marine mudstone and shale, with a few thin siltstone layers. In the site area, the Blue Gate Member is divided into lower and upper parts to accommodate the Prairie Canyon Member. Outcrops of both lower and upper parts of the Blue Gate Member are rare—only one of each was found in the mapped area (Plate 1). A thickness of approximately 2,000 ft of lower Blue Gate Member is in the site area. Below the Blue Gate Member are the lowermost members of the Mancos Shale, the Ferron Sandstone Member underlain by the Tununk Shale Member, that combine for an approximate 300 to 400 ft thickness. It is therefore estimated that approximately 2,400 ft of Mancos Shale underlies the center of the proposed disposal cell; this includes all of the lower Blue Gate Member, the Ferron Sandstone Member, and the Tununk Shale Member.

This thickness estimate of Mancos Shale beneath the disposal cell is supported by a depth of 2,360 ft to the top of the Dakota Sandstone reported from the Federal MSC 26-1 test hole drilled about 1,750 ft south of the disposal cell footprint (Plate 1). This depth pick was from a geophysical log of the MSC 26-1 hole, provided to a depth of 2,400 ft by Tidewater Oil and Gas Company.

The upper Blue Gate Member, above the Prairie Canyon Member, is approximately 700 to 800 ft thick. It is overlain by the Blackhawk Formation, the lowermost unit of the Mesaverde Group, which forms the sandstone crest of the Book Cliffs immediately north of the site area.

A generalized stratigraphic section of the mapped site area is shown in Figure 5. Characteristics of each member of Mancos Shale as seen in outcrops and in borehole core are discussed in the following subsections, in chronologic order from oldest to youngest. Detailed lithologic descriptions of bedrock from the 10 deep (300 ft) coreholes are in Attachment 5 of the RAP. Five cross sections (Plate 2) across the site show the lithologic position of the Prairie Canyon Member in the subsurface. The bedrock contour map (Plate 3) shows subtle ridges and other variations in the bedrock topography.

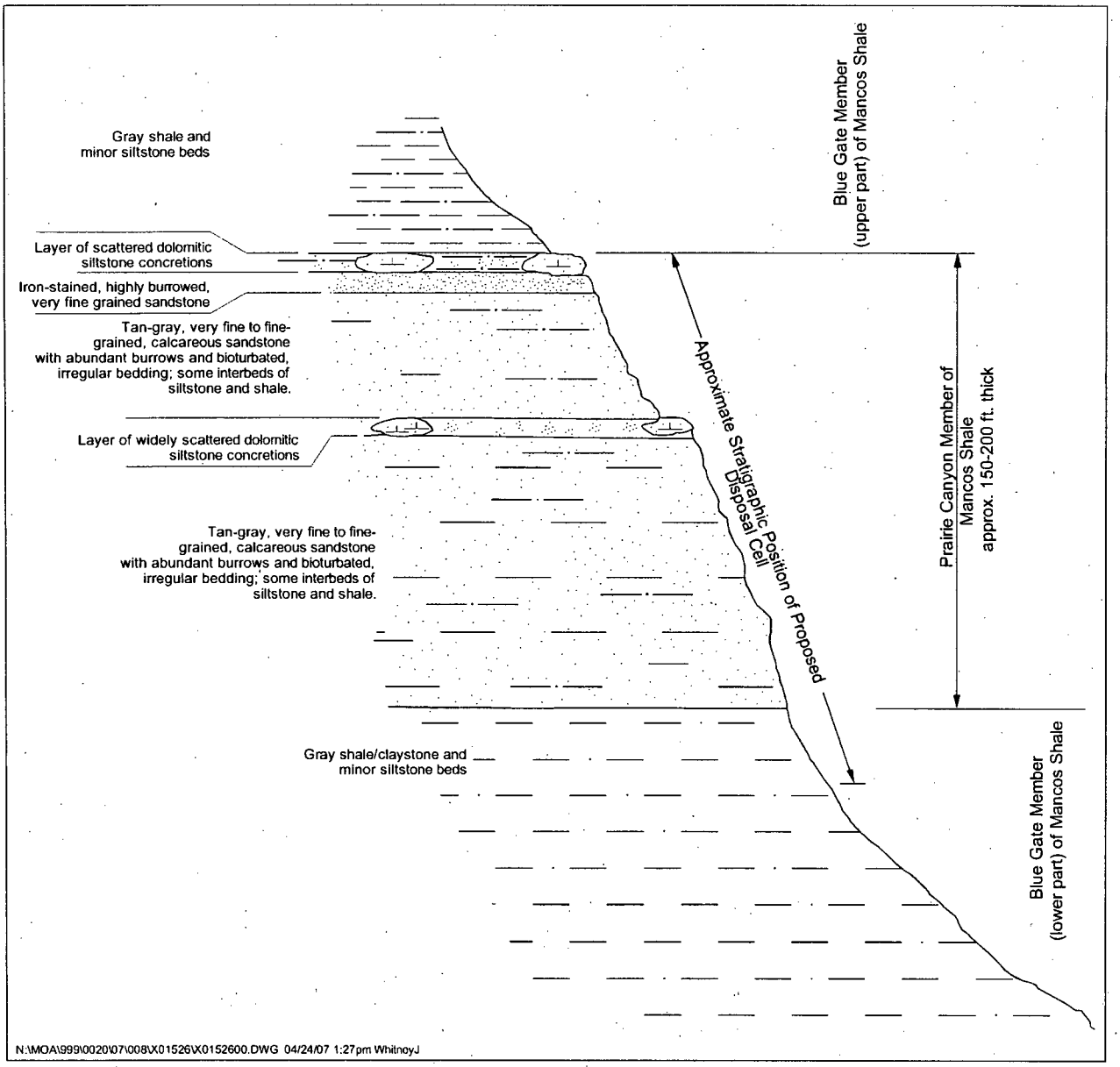

Figure 5. Generalized stratigraphic section of the Crescent Junction, Utah, Site area.

Lower Blue Gate Member

The lower part of the Blue Gate Member does not crop out on or immediately around the proposed disposal cell; however, the unit is in the subsurface, and the bottoms of all 10 of the coreholes were in the upper part of the unit. The unit crops out in poor exposures in one place in the southwest edge of the mapped area on a low hill that is an eroded remnant of a pediment surface (Plate 1). Here, the exposures are mainly gray shale and minor, thin, lenticular beds of light gray to brown-orange (limonitic) siltstone that contains small tracks and other trace fossils.

Bedrock penetrated by four of the coreholes (0202, 0205, 0207, and 0209) consisted solely of the lower Blue Gate Member. Also, one packer test hole (0212) was cored solely in the lower Blue Gate Member, and the bottom of test pit 0154 was in the lower Blue Gate Member. The other coreholes passed through part of the Prairie Canyon Member before reaching total depth in the lower Blue Gate Member.

The lower Blue Gate Member penetrated by the coreholes is mostly medium gray (N5), calcareous, silty claystone, and is fissile in some places. Several thin zones have a small percentage (less than 20 percent) of bioturbated bedding of siltstone or very fine-grained sandstone that is lighter colored, very light gray (N8). Fine, black carbonaceous material and framboidal pyrite (plated on fossils in places) are in trace amounts. Large fossils in the core consist mainly of coiled and flattened cephalopods and pelecypods. Curious dense masses up to 2 inches in diameter of white, highly calcareous (porcelaneous-appearing) material are rarely in the deeper part of the lower Blue Gate Member (more than 150 ft below the upper contact). Small beads (up to 0.05 inch diameter) of amber or resin are in trace amounts in various depths in most coreholes into the lower Blue Gate Member. Below a depth of 100 ft into this bedrock, no natural fractures were noted and no evidence was seen of water movement (interior of broken core was dry).

The top of the lower Blue Gate Member is generally in the space of several ft where bioturbated bedding and associated very fine-grained sandstone increases to about 30 percent. This change is best seen in the geophysical logs as a marked reduction in gamma ray response. In the five coreholes that were geophysically logged, the depth of the contact of the lower Blue Gate Member and Prairie Canyon Member is picked as follows: 0203 – 117 ft, 0204 – 52 ft, 0206 – 107 ft, 0208 – 112 ft, and 0210 – 139 ft. In corehole 0201, which was not geophysically logged, the contact is placed where the amount of bioturbation increases very rapidly at a depth of approximately 157 ft. The contact of the Prairie Canyon Member and top of the lower Blue Gate Member is shown in Plate 2 in the north-south cross sections A-A', B-B', and C-C', and more along strike in the west-east cross section D-D'.

Prairie Canyon Member

Several outcrops of very fine-grained sandstone of the Prairie Canyon Member are in the proposed disposal cell area (Plate 1). Additional small outcrop areas of sandstone are east and north of the proposed disposal cell. A band of scattered small outcrops of dolomitic siltstone concretions (several of which are at the northeast corner of the disposal cell footprint) also is across the north part of the site area, marking the top of the Prairie Canyon Member. Three lithologic facies were selected for mapping (Plate 1) to show the variation of this member in the site area. The lower and thickest unit is a tan, burrowed sandstone. A thin, distinctive, rusty brown, burrowed sandstone unit is just below the uppermost dolomitic siltstone concretions. A belt of discontinuous, large, resistant, dolomitic siltstone concretions is approximately 50 ft stratigraphically (Figure 5) below the top band of concretions. Each of these facies is described in the following subsections, and they are similar in many characteristics to those described by Hampson et al. (1999) in this part of the outcrop belt of the Prairie Canyon Member.

Tan, Burrowed Sandstone

This facies is exposed in the proposed disposal cell area on a subtle, north-striking ridge approximately along the section line between Sections 26 and 27 (Plate 1). Here, the light gray to tan sandstone is fine- to very fine-grained, calcareous, burrowed, and is exposed in lenticular to slabby beds about 1 inch thick.

This fine- to very fine-grained, burrowed sandstone subcrops under approximately the northern 85 percent of the proposed disposal cell area. This estimated subcrop of the base of the Prairie Canyon Member shown in Plate 1 is based on scattered outcrops of the tan and gray sandstone in the proposed disposal cell area and along strike just to the east in a low ridge near test pit 0156. Also, several geotechnical boreholes (0085 and 0087) found sandstone bedrock at their total depths.

The sandstone crops out stratigraphically higher in scattered locations north of the proposed disposal cell and in the northeast part of the cell footprint. The largest outcrop is an area more than 500 ft long in the northeast part of the disposal cell footprint along the west side of a low ridge extending south-southeast from the area of the 3 ponds (Plate 1). In this outcrop area, the slabby sandstone is tan, fine-grained, calcareous, slightly friable, bioturbated, with abundant sole marks and burrows. Two other larger outcrops of sandstone outcrops are along strike to the west—from corehole 0201, one is about 1,300 ft to the west, and one is just to the south. Eastward along strike, additional sandstone outcrops are to the northwest and northeast of corehole 0210. These scattered outcrops are mainly on the south side of a band of low mounds formed (capped) by resistant, large, dolomitic siltstone concretions, an upper facies of the Prairie Canyon Member.

Core from the several holes through the Prairie Canyon Member show that most of the rock is medium gray (N5) silty claystone to clayey siltstone, and 10 to 30 percent of the rock is very light gray (N8), very fine-grained sandstone. The sandstone is bioturbated, wavy bedded, and contains traces of framboidal pyrite, fine carbonaceous (plant fragment?) material, and pelecypod and cephalopod imprints. The percentage of sandstone (up to 30 percent) shown in the core is more of a true account of the stratigraphy of this member, rather than reliance on the surface outcrops, which tend to be of the more resistant sandstone. Coreholes in the mapped area that penetrated part of the Prairie Canyon Member sandstones are 0201 (penetrated nearly all of the Prairie Canyon Member), 0204, 0206, 0208, and 0210. Lithologic logs from coreholes 0201, 0208, and 0210 contain the most detailed description of the lithology. Below a depth of about 80 ft into this bedrock, no natural fractures were noted and no evidence was seen of water movement (interior of broken core was dry).

Rusty Brown, Burrowed Sandstone

This thin, distinctive facies crops out in scattered locations along an east-trending belt across the north part of the mapped area (Plate 1). The unit is only about 3 ft thick and typically lies just below the large dolomitic siltstone concretions that form the northernmost line of low mounds. The facies consists of dense, resistant, rusty brown, very fine- to fine-grained sandstone that contains large burrows up to 1.5 inches in diameter, and abundant trace fossils and casts. Intense and diverse bioturbation is characteristic of this facies. The unit was not seen in all of the northernmost dolomitic siltstone concretion mounds, possibly because of cover or poor outcrops.

Dolomitic Siltstone Concretion

This facies, the best exposed in the mapped area, is in two east-trending bands of low, scattered mounds up to 15 ft high in the north part of the mapped area just north of and at the northeast corner of the proposed disposal cell. Each mound is capped by one or more large concretions of dolomitic siltstone. The lower band, represented by several widely scattered mounds, is stratigraphically about 50 ft below the upper band. The dolomitic concretion-capped mound just west of corehole 0210 is the best example of this lower band (Plate 1).

The upper band contains more numerous mounds in the mapped area and consists of 10 to 15 scattered mounds. The top of these mounds represents the top of the Prairie Canyon Member in the mapped area, as shown in Plate 1. This contact of the top of the Prairie Canyon and base of the upper Blue Gate Member marks a delta-front abandonment and marine-flooding surface followed by deposition of marine shales of the upper Blue Gate Member (Cole et al. 1997).

Concretions are hard, dense, brittle, up to 5 ft thick, and are composed of dolomitic siltstone; some contain calcite crystals and masses. Dolomitic siltstone on fresh surfaces is medium gray (N5) and weathered surfaces are grayish orange (10YR 7/4). Bedding is wavy, flaser (flame or streak)-shaped, and interrupted in places by burrowing. The concretion-capped mounds (Figure 6) vary in diameter from 20 or 30 ft to the large mound about 200 ft in exposed diameter just southwest of corehole 0201. The top of the resistant concretion mounds forms a north-dipping cuesta-like surface where the dip of the Mancos Shale could be measured in several places (Plate 1) at approximately 5 to 6 degrees. This dip is similar to other northward dips measured just north of the mapped area—3 degrees at the top of the Book Cliffs (Williams 1964), and dips of 4 and 5 degrees (Doelling 2001). Vertical joints, some coated with limonite, form in the brittle dolomitic siltstone. These joints were measured in several locations (Plate 1). The principal joint direction is approximately N10E and subsidiary directions are N50W and N85W.

As described by Hampson et al. (1999), the dolomite-cemented concretion horizon forms a stratigraphic marker that can be mapped over several kilometers or tens of kilometers. The upper band of concretions forms such a stratigraphic horizon, which is evident across the north part of the withdrawal area as seen from the top of the Book Cliffs. Figure 3 shows a part of this linear band of concretionary mounds that extends eastward about ¾ mi from just west of the 3 ponds area. The upper band of concretions in the site area can be traced from the east edge of Section 21 for about 3 mi eastward to the area of the East Branch of Kendall Wash in the east part of Section 24 (Plate 1). This band of concretions was investigated for any evidence of displacement or offset along its length. No offsets were seen, and no slickensides were noted on any of the joint surfaces, and it is concluded that the linear band represents the stratigraphic horizon marking the top of the Prairie Canyon Member in the site area.

Figure 6. View northeast of a low mound formed by the uppermost band of dolomitic siltstone concretions at the top of the Prairie Canyon Member of Mancos Shale.

Upper Blue Gate Member

The only outcrop of the upper part of the Blue Gate Member in the mapped area is north of the 3 ponds area along a steep, west-facing slope above a small drainage. Cropping out on the slope is soft, gray brown, silty shale and some interbeds of slabby, thin, tan brown, very fine-grained, burrowed sandstone. Sandstone litter and sheet wash cover most outcrops north of the mounds, which mark the top of the Prairie Canyon Member, until the steep badland slopes of exposed Upper Blue Gate Member are reached at the base of the Book Cliffs.

Structural Features and Weathered Bedrock

No faults or evidence of faults (slickensides on fracture surfaces) were found in the deep coreholes. Lithologic logs, geophysical logs, and surface outcrops verify that the dip of Mancos Shale bedrock in most of the mapped area is approximately 5 to 6 degrees to the north. This is shown in cross sections B-B' and C-C' (Plate 2). Evidence that the northward dip may be slightly less in the western part of the mapped area is from the slightly wider subcrop belt of the Prairie Canyon Member shown in Plate 1 and cross section A-A' (Plate 2).

As specified in the "Site and Regional Geology – Results of Literature Research" calculation set (RAP Attachment 2, Appendix A), a field search was made for the old oil test well (McCarthy No. 1) drilled in the 1920s in the NW¼ of Section 34 and for surface evidence of a northeast-striking fault that was inferred to be between the McCarthy No. 1 well and the Crescent Oil Syndicate No. 1 well in the SW¼ of Section 27 (Plate 1). No surface evidence was seen in the NW¼ of Section 34 for either the McCarthy No. 1 test well or the northeast-striking fault. Highway and railroad construction have disturbed much of the surface of this area and could have obliterated any trace of an old test well.

Characteristics of weathered bedrock were noted during lithologic logging of the deep coreholes. The spacing of natural bedding plane fractures was used as an approximate and subjective means of distinguishing degree of weathering of the bedrock. Closely spaced bedding plane fractures, generally 0.1 to 0.5 ft apart, were assigned a characteristic of highly to moderately weathered bedrock. The thickness of each degree of weathering varied considerably among the coreholes, with the thickness of the slightly weathered bedrock usually being slightly to much thicker than the highly to moderately

weathered bedrock. The transition from highly weathered to slightly weathered bedrock may be in a depth interval of only several ft, as shown in core from hole 0210 (Figure 7). Bedding plane fracture spacing and other characteristics for the highly to moderately weathered and slightly weathered bedrock are shown in Figure 8.

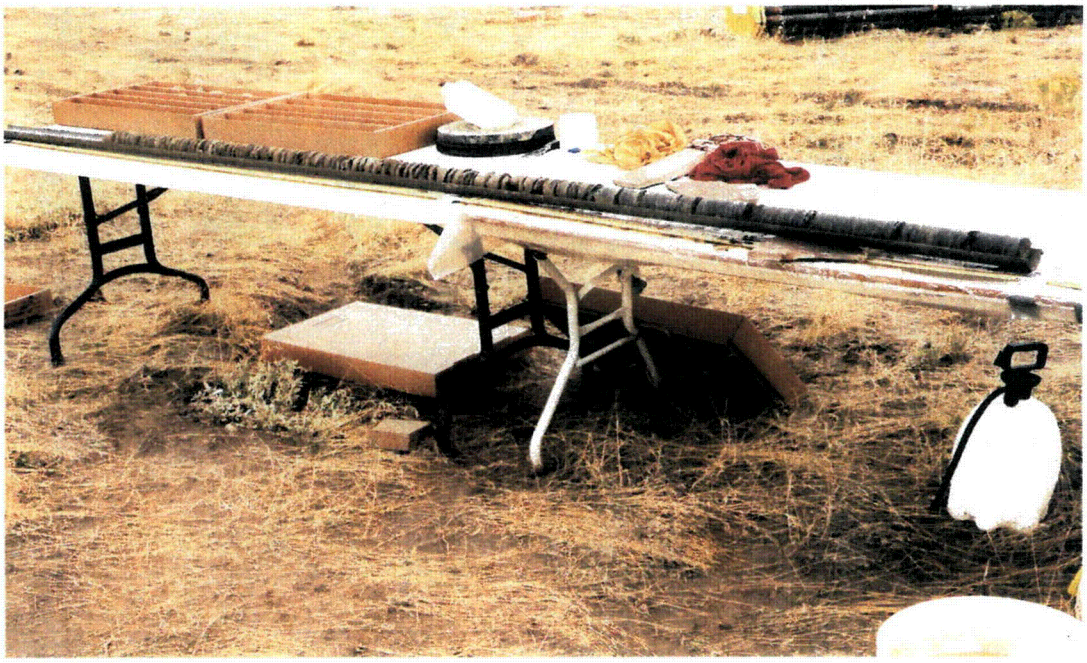

Figure 7. Core from hole 0210, from 26 (left) to 36 ft (right), showing progression in depth from highly weathered to slightly weathered bedrock in the Prairie Canyon Member.

Characteristics of weathered bedrock other than bedding plane fractures include non-bedding plane fractures and the material that fills or coats the fractures, color, rock quality designation (RQD), and the member of the Mancos Shale bedrock. High-angle to vertical (not bedding plane) fractures are numerous in the highly to moderately weathered bedrock and they are infrequent in the slightly weathered bedrock. The deepest natural fracture seen in core was from a depth of about 100 ft into the bedrock (corehole 0207), and natural fracturing was seen only to a depth of about 20 ft into bedrock in corehole 0208. Only a few natural fractures extend below a depth of 50 ft into essentially unweathered bedrock. Natural fractures, both bedding plane and non-bedding plane, are typically coated or filled with white crystalline gypsum (and possibly some calcite) in highly to moderately weathered bedrock, as seen in Figure 9. These shallow fractures and, particularly, the deeper and more infrequent fractures in the slightly weathered bedrock (and a few fractures extending deeper into essentially unweathered bedrock) may be coated (stained) with limonite (Figure 10), which indicates some past minor movement of ground water possibly during periods of higher precipitation associated with glaciation in the late Pleistocene Epoch.

Highly to moderately weathered bedrock is yellow-brown and yellow-gray—a limonitic appearance, reflecting its content of oxidized iron. Common colors of this cored material include yellowish gray (5Y 7/2), pale yellowish brown (10YR 6/2), and light olive-gray (5Y 5/2). Slightly weathered bedrock and essentially unweathered bedrock with rare fractures has more of a fresh appearance—the dominant rock types, claystone and siltstone, are mostly medium gray (N5), and the less common very fine-grained sandstone is very light gray (N8). Limonite-staining of the widely spaced bedding plane fractures and the infrequent high-angle fractures in the slightly weathered bedrock (and extending in a few places into unweathered bedrock) is most commonly dark yellowish-orange (10YR 6/6). Unweathered bedrock of the typical claystone and siltstone composition is mostly medium dark gray (N4), and the less common very fine-grained sandstone is very light gray (N8).

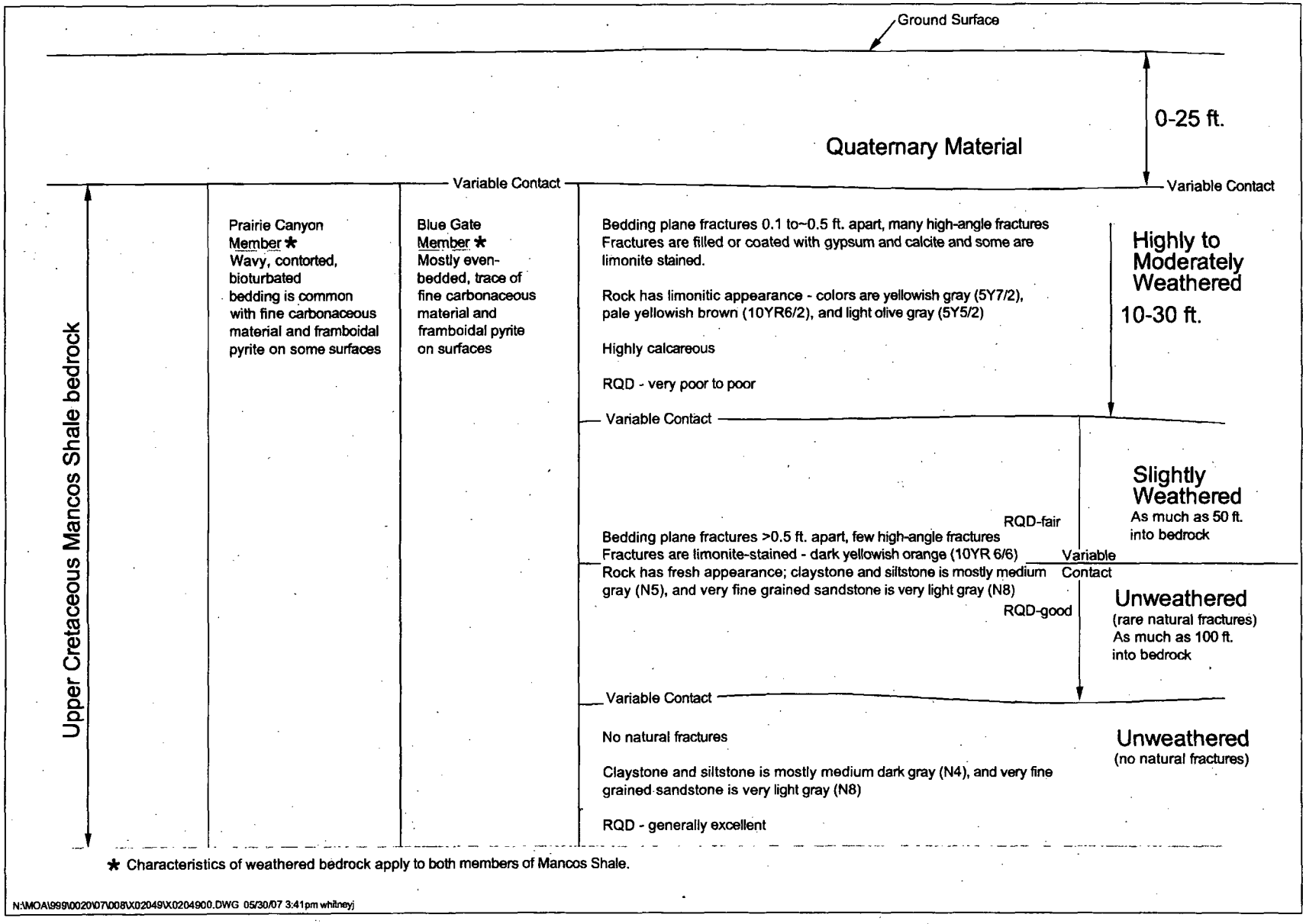

Figure 8. Characteristics of weathered Mancos Shale bedrock at the Crescent Junction Site.

Figure 9. Gypsum (white) filling a vertical fracture at 39.5- to 40-ft depth in moderately weathered lower Blue Gate Member bedrock at corehole 0209.

Figure 10. Limonite (orange) coating high-angle fracture at about a 62-ft depth in slightly weathered lower Blue Gate Member bedrock at corehole 0207.

RQD, an approximate measure of degree of fracturing, as reported in *Corehole Logs,* Appendix A of RAP Attachment 5, Vol. I, corresponds also generally to the degree of weathering in the bedrock. As shown in Figure 8, an RQD of less than 50 percent, described as very poor to poor, is assigned to highly to moderately weathered bedrock. An RQD of 50 to 75 percent, described as fair, is assigned to slightly weathered bedrock. An RQD of 75 to 90 percent, described as good, is assigned to essentially

unweathered bedrock and competent bedrock, which may have a few natural fractures. Unweathered bedrock with no natural fractures has an RQD of 90 percent or higher, described as excellent.

In addition to the above characteristics, the nature of weathered bedrock is related to which member of the Mancos Shale is represented—Prairie Canyon or Blue Gate. Weathered Prairie Canyon Member is characterized by bioturbated bedding that is wavy and contorted (Figure 11); fine carbonaceous (black) material and framboidal pyrite are along some bedding surfaces. The contorted bedding in the Prairie Canyon Member is typically expressed by the lighter-colored, very fine-grained sandstone—a constituent of up to about 30 percent of the rock. Weathered Blue Gate Member is characterized by its predominately even (parallel) beds, which also have a trace of fine carbonaceous material and framboidal pyrite on bedding surfaces.

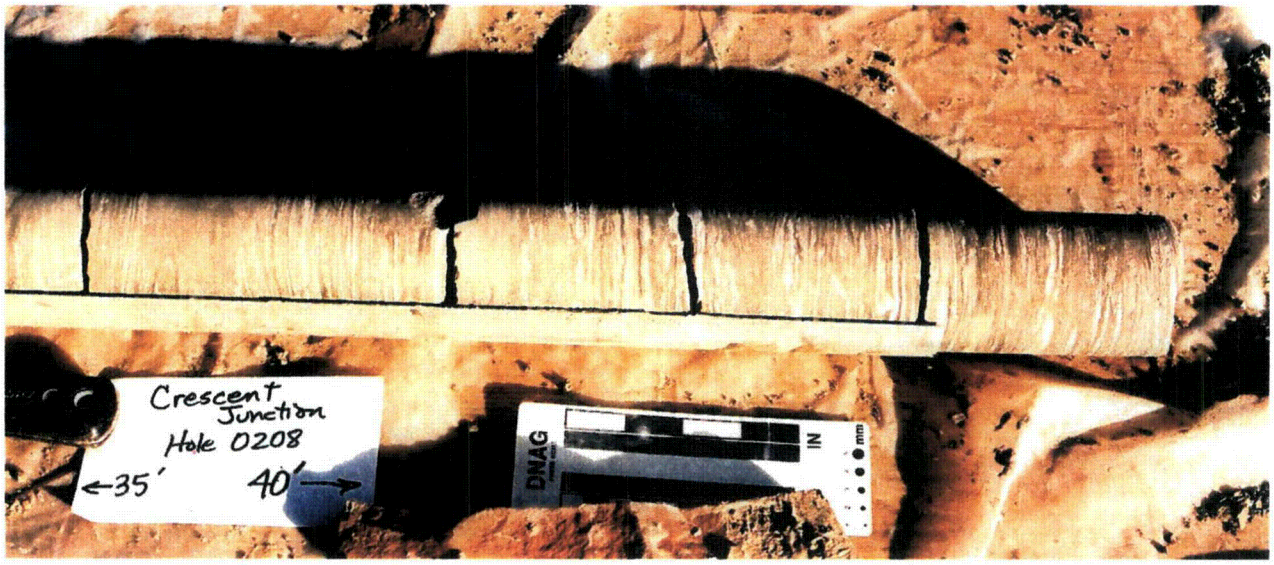

Figure 11. Bioturbated, contorted bedding in slightly weathered Prairie Canyon Member bedrock at about 38 to 40 ft depth at corehole 0208.

Conclusions

Based on interpretation of characterization of the surficial and bedrock geology of the mapped area in and around the proposed disposal cell area, the following features and characteristics of the surficial and bedrock geology of the site area favor its suitability for a disposal cell:

- Approximately 2,400 ft of Mancos Shale, represented mainly by open-marine mudstone, is beneath the center of the proposed disposal cell.
- No evidence for faults was noted in the surface or in bedrock units.
- No evidence of saturation in the bedrock was seen; core was dry when broken open.
- Natural fractures are mostly in the top 10 to 30 ft of bedrock, which has been highly to moderately weathered. Below that, slightly weathered bedrock containing fewer fractures extends to depths of as much as 50 ft into bedrock. At depths greater than 50 ft into bedrock, the rock is competent and considered unweathered with only a few natural fractures that may occur at depths of as much as 100 ft into bedrock. No natural fractures were seen deeper than 100 ft into the bedrock.
- Surficial deposits have been emplaced in a stable geologic environment mainly by a slow accumulation of material transported during infrequent heavy rainfall episodes from the base and sides of the Book Cliffs along active sheet wash paths.

Computer Source:

Not applicable.

References:

Cole, R.D., R.G. Young, and G.C. Willis, 1997. *The Prairie Canyon Member, a New Unit of the Upper Cretaceous Mancos Shale, West-Central Colorado and East-Central Utah*, Utah Geological Survey Miscellaneous Publication 97-4.

Doelling, H.H., 1997. *Interim Geologic Map of the Valley City Quadrangle, Grand County, Utah*, Utah Geological Survey Open-File Report 351, scale 1:24,000.

Doelling, H.H., 2001. *Geologic Map of the Moab and Eastern Part of the San Rafael Desert 30' x 60' Quadrangles, Grand and Emery Counties, Utah, and Mesa County, Colorado,* Utah Geological Survey Map 180, scale 1:100,000.

Fisher, D.J., C.E. Erdmann, and J.B. Reeside, Jr., 1960. *Cretaceous and Tertiary Formations of the Book Cliffs, Carbon, Emery, and Grand Counties, Utah, and Garfield and Mesa Counties, Colorado*, U.S. Geological Survey Professional Paper 332.

Franczyk, K.J., J.K. Pitman, and D.J. Nichols, 1990. *Sedimentology, Mineralogy, Palynology, and Depositional History of Some Uppermost Cretaceous and Lowermost Tertiary Rocks Along the Utah Book and Roan Cliffs East of the Green River*, U.S. Geological Survey Bulletin 1787-N.

Hampson, G.J., J.A. Howell, and S.S. Flint, 1999. "A Sedimentological and Sequence Stratigraphic Re-Interpretation of the Upper Cretaceous Prairie Canyon Member ("Mancos B") and Associated Strata, Book Cliffs Area, Utah, U.S.A.," *Journal of Sedimentary Research,* 69(2), pp. 414–433.

Kellogg, H.E., 1977. "Geology and Petroleum of the Mancos B Formation, Douglas Creek Arch Area, Colorado and Utah," in Veal, H.K., editor, *Exploration Frontiers of the Central and Southern Rockies*, Rocky Mountain Association of Geologists, pp. 167–179.

Williams, P.L., compiler, 1964. *Geology, Structure, and Uranium Deposits of the Moab Quadrangle, Colorado and Utah*, Utah Geological Survey Miscellaneous Geologic Investigations Map I-360, scale 1:250,000.

Willis, G.C., 1994. *Geologic Map of the Harley Dome Quadrangle, Grand County, Utah*, Utah Geological Survey Map 157, scale 1:24,000.

THIS PAGE IS AN OVERSIZED DRAWING OR FIGURE,

THAT CAN BE VIEWED AT THE RECORD TITLED:

DRAWING NO.: X0130400, "PLATE 1 - GEOLOGIC MAP OF BEDROCK OUTCROPS AND SURFICIAL DEPOSITS, CRESCENT JUNCTION, UT, PROPOSED REPOSITORY SITE"

WITHIN THIS PACKAGE... OR, BY SEARCHING USING THE DOCUMENT/REPORT DRAWING NO. X0130400

D-01

THIS PAGE IS AN OVERSIZED DRAWING OR FIGURE,

THAT CAN BE VIEWED AT THE RECORD TITLED:
DRAWING NO.: X01525, "PLATE 2 - GEOLOGIC CROSS SECTIONS"

WITHIN THIS PACKAGE... OR, BY SEARCHING USING THE DOCUMENT/REPORT DRAWING NO. X01525

D-02

THIS PAGE IS AN OVERSIZED DRAWING OR FIGURE,

THAT CAN BE VIEWED AT THE RECORD TITLED:
DRAWING NO.: X0153900, "PLATE 3 - BEDROCK CONTOUR MAP"

WITHIN THIS PACKAGE... OR, BY SEARCHING USING THE DOCUMENT/REPORT DRAWING NO. X0153900

D-03

U.S. Department of Energy—Grand Junction, Colorado

Calculation Cover Sheet

Calc. No.: MOA-02-04-2007-1-06-01 **Doc. No.:** X0113700	**Discipline:** Geologic and Geophysical Properties	**No. of Sheets:** 8

Location: Attachment 2, Appendix C

Project: Moab Project

Site: Crescent Junction Disposal Site

Feature: Site and Regional Geomorphology – Results of Literature Research

Sources of Data:

Published reports and maps – see list of references at end of calculation set.

Purpose of Revision:

Revision is being issued to include information collected from additional references on geomorphic features that were acquired during site characterization activities in late 2005 and early 2006.

Sources of Formulae and References:

See list of references at end of calculation set.

Preliminary Calc. ☐ **Final Calc.** ☒ **Supersedes Calc. No.** MOA-02-08-2005-1-06-00

Author: Craig Goodknight 31 May 07 (Name / Date) **Checked by:** [signature] 31 May 07 (Name / Date)

Approved by: [signature] 5/31/07 (Name / Date)

[signature] 5-31-07 (Name / Date)

[signature] 31 May 07 (Name / Date)

[signature] May 31, 07 (Name / Date)

No text for this page

Problem Statement:

Determination of the suitability of the Crescent Junction Disposal Site as the repository for the Moab uranium mill tailings material, and development of the Site and Regional Geomorphology sections of the Remedial Action Plan and Site Design for Stabilization of Moab Title I Uranium Mill Tailings at the Crescent Junction, Utah, Disposal Cell (RAP) require a thorough review of available literature that applies to the Crescent Junction Site. The compiled list of references is presented at the end of this calculation set, and relevant information is summarized below.

This calculation set was initially prepared in August 2005 during the early stages of characterization of the Crescent Junction Site. Additional references and characterization activities in late 2005 and early 2006 have made revision of the calculation set necessary. This revised calculation set is a general summary of geomorphological conditions at the site based on literature research. This information is incorporated into Attachment 2 (Geology) of the RAP and summarized in the appropriate sections of the RAP Remedial Action Selection (RAS) report for the Moab Site.

Method of Solution:

Literature sources were identified using a combination of published reports and maps that were developed during the Crescent Junction Site selection process, online (internet-based) resources, and relevant literature citations from the other Uranium Mill Tailings Radiation Control Act (UMTRCA) Sites.

Assumptions:

It is assumed that the literature sources are reliable and representative of the current understanding of the geomorphology of the region.

Calculation:

None required.

Discussion:

Geomorphic Setting

Principal geomorphic features at and near the Crescent Junction Disposal Site include a pediment surface of low relief that slopes gently southward and the Book Cliffs escarpment that borders the pediment to the north and rises abruptly 700 to 800 feet (ft) above it (Figure 1). The pediment surface on Mancos Shale, mostly covered by a veneer of alluvial and colluvial surficial deposits, extends southward from the base of the Book Cliffs for about 2 miles (mi) and is called Crescent Flat. The subtle, minor drainages on the surface over most of Crescent Flat indicate that depositional (or aggradational), rather than erosional (or degradational) processes are dominant.

Geomorphic processes in this area that may affect disposal cell performance include fluvial, mass movement, and eolian. Fluvial processes, related to the drainage system of the withdrawal area (approximately 2,300 acres) and the nearby surrounding area (Figure 1), predominate in this geomorphic setting (Woodward-Clyde Consultants 1984). Mass movement processes affect the steep slopes associated with the Book Cliffs just north of the withdrawal area. Eolian processes are apparently least significant in the site area based on the scarcity of mapped deposits (Doelling 2001). Each process and the Quaternary deposits produced or affected by that process are described in the following subsections.

Fluvial Processes

Surface water over most of the withdrawal area is drained by the ephemeral Kendall Wash system. Ephemeral Crescent Wash, just west of the withdrawal area (Figure 1), drains a large area in the Book and Roan Cliffs north of Crescent Flat. Elevated pediment surfaces west of Crescent Wash are capped by sediments from the ancestral wash. Incision and denudation rates are variable, but both provide some estimate of the long-term effect of fluvial erosion.

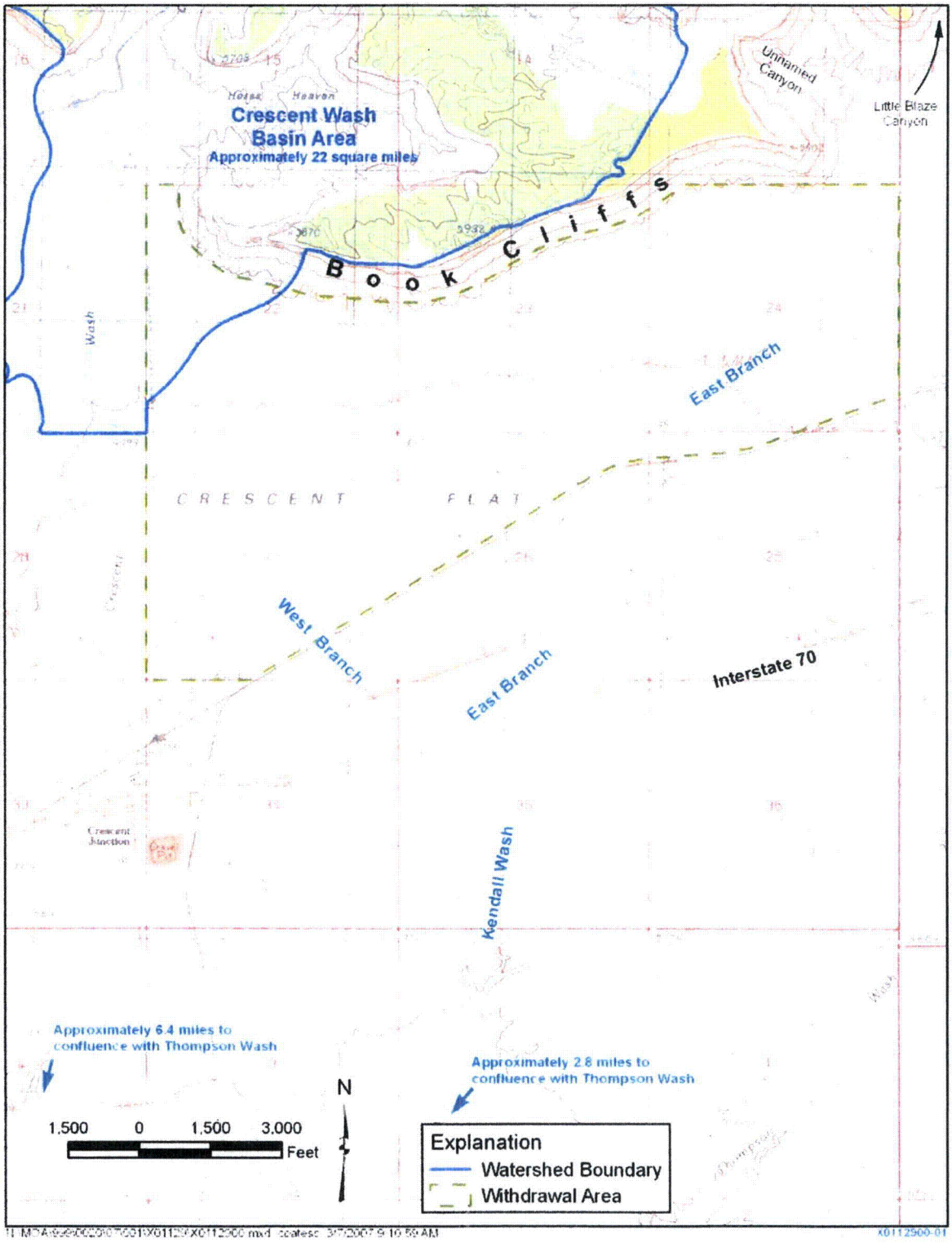

Figure 1. Topographic Map of Crescent Junction, Utah, Area Showing Geomorphic Features and Surface Water Drainages.

Subtle drainage features across most of Crescent Flat are part of the north end of the Kendall Wash system. The name "Kendall Wash" is shown on the 1:250,000-scale Moab 1° x 2° topographic quadrangle for the drainage south of Interstate 70 (I-70), about 1.5 mi east of Crescent Junction. This designation is not shown, however, in the more recent, larger-scale (1:24,000) Crescent Junction topographic quadrangle map. For this project, the name "Kendall Wash" will be used to describe the drainage systems across most of the withdrawal area. Kendall Wash forks north of I-70 into a larger channel that trends northeast and a smaller channel that trends northwest. For this project, the channels are informally designated the East Branch and the West Branch (Figure 1), respectively, of Kendall Wash. The West Branch extends only about 1 mi northwest of I-70 into the center of Section 27, and the East Branch extends 3 to 4 mi to the northeast where it heads in an unnamed canyon and Little Blaze Canyon in the Book Cliffs (Figure 1).

The drainage pattern shown by the East and West Branches of Kendall Wash and by the numerous subtle drainages that cross Crescent Flat is classified as parallel (Schumm and Chorley 1983). This drainage pattern is typically found on moderately sloping areas; Crescent Flat slopes southward at a grade of generally 2 to 3 percent. The channel of the East Branch of Kendall Wash in the east part of the withdrawal area is generally straight and incised 10 to 15 ft deep. This channel pattern is classed as a mixed-load straight channel by Schumm and Chorley (1983) that carries a small load of sand and gravel and has a sinuous thalweg (or deepest part of the channel). Also classified as a mixed-load straight channel, the West Branch is incised up to 10 ft deep and seems to be advancing headward, as evidenced by knickpoints at heads of the several tributary washes. Results of an investigation on the rate of incision advance and the implications of the advance over a long term on the disposal cell location are included in the "Site and Regional Geomorphology – Results of Site Investigations" calculation set (RAP Attachment 2, Appendix D), and the "Photogeologic Interpretation" calculation set (RAP Attachment 2, Appendix G).

Downstream from I-70, Kendall Wash joins Thompson Wash approximately 3.5 mi south of Crescent Junction. About 7.5 mi south-southwest of Crescent Junction, Crescent Wash joins Thompson Wash. After several more miles, Thompson Wash joins Tenmile Wash, which flows through Tenmile Canyon to join with Green River about 23 mi southwest of Crescent Junction.

Crescent Wash, upstream from the site, courses through Crescent Canyon and heads about 10 mi north of Crescent Flat into the Book and Roan Cliffs. Upstream from the northwest corner of Section 27, the drainage basin area of Crescent Wash is approximately 22 square mi. Incised 10 to 15 ft along much of its course just west of the withdrawal area, Crescent Wash fits into the transitional meander-braided drainage pattern of Schumm and Chorley (1983). Drainages of this pattern carry a large sediment load, with sand, gravel, and cobbles constituting a significant fraction of the total sediment. This large sediment load, with high content of coarse constituents (cobbles and boulders), is consistent with the high-relief area containing thick sandstones in the Mesaverde Group that Crescent Wash drains. During infrequent high flows, Crescent Wash is capable of significant erosion, and the possibility of its migration into the withdrawal area (particularly at a prominent incised meander near the northwest corner of Section 27) is evaluated in the "Site and Regional Geomorphology - Results of Site Investigations" calculation set (RAP Attachment 2, Appendix D.).

The pediment surface on Mancos Shale that is west of Crescent Wash is an example of the many pediments that are characteristically developed along the base of the Book Cliffs between Grand Junction, Colorado, and Price, Utah (Schumm 1980). Alluvial sand and gravel (with some material as large as cobbles and boulders) mantles and armors the pediment surface, which is elevated about 100 ft above Crescent Wash (Doelling 2001). Originally described by Rich (1935), these pediment surfaces are the result of stream capture by a process described by Schumm (1980) and Carter (1977). Streams such as Crescent Wash drain coarse sandstone-laden sediment from the Book and Roan Cliffs, and they have a steeper gradient than streams that are eroding into Mancos Shale. The lower-gradient shale stream captures the high-gradient upland stream and causes the coarse-grained sediment to be abandoned and form a pediment level. Pediment levels are west of the withdrawal area and represent ancestral courses of Crescent Wash; the effect of this process, sustained by future stream capture, on the disposal cell location is evaluated in the "Site and Regional Geomorphology - Results of Site Investigations" calculation set (RAP Attachment 2, Appendix D.).

Incision and denudation rates offer some understanding of the long-term fluvial erosion that could affect the site area. These rates vary according to the time frame considered and the geologic material being eroded. The rate of incision for the Colorado River in the Paradox Basin of southeastern Utah during Neogene time has been estimated at about 9 inches per 1,000 years (Woodward-Clyde Consultants 1982); the same reference shows, in a table (Table 3-11) of denudation rates based on recent historic data for watersheds in the Colorado Plateau, a denudation rate of 2.5 ft per 1,000 years for Crescent Wash. Other areas of recent historic high erosion rates are also in areas underlain by Mancos Shale, and the rates range from 1.5 to 7.2 ft per 1,000 years (Woodward-Clyde Consultants 1982).

Incision rates can also be measured using the Lava Creek B ash, erupted from the Yellowstone caldera about 640,000 years ago, preserved in Quaternary deposits. Using the height above modern grade of fluvial terraces containing Lava Creek B ash, the incision rate shown by Dethier (2001) for the site area is 10 to 15 centimeters (or about 4 to 6 inches) per 1,000 years.

Mass Movement Processes

Landslides, rock falls, and scarp retreat are mass movement (or wasting) processes and landforms involving downslope transport of surficial materials and bedrock blocks by gravity. These processes are associated with the Book Cliffs escarpment and its steep slopes along and just north of the north boundary of the site withdrawal area (Figure 1).

The map of landslides in the Moab 30-minute x 60-minute quadrangle (Harty 1993) shows two landslides in the Book Cliffs, just north of the withdrawal area. The larger of the two landslides is about 100 acres and is in the south part of a small tributary drainage basin to Crescent Wash known as Horse Heaven (Figure 1). The smaller landslide is less than 10 acres and is just north of the northeast end of the withdrawal area, and just north of the sandstone spire detached from the Book Cliffs that is marked as an elevation of 5,903 ft (Figure 1). Both landslides are of the deep-seated "earth slump" type and have northerly exposures (a north and northwest aspect for the larger landslide and a northeast aspect for the smaller landslide). In his geologic map of the Moab 30-minute x 60-minute quadrangle, Doelling (2001) mapped these landslides as "Qmt", talus and colluvium, and he also mapped several small areas of "Qmt" along the south-facing slope of the Book Cliffs. These small areas were field checked to determine if they are landslides, and results are included in the "Site and Regional Geomorphology – Results of Site Investigations" calculation (RAP Attachment 2, Appendix D). The landslide in the Horse Heaven area is shown in the "Soil Survey of Grand County, Central Part" (Hansen 1989). It is recognized that these landslides originated during periods of higher precipitation in the late Pleistocene and early Holocene Epochs.

Rock falls from the Mesaverde Group sandstone that caps the Book Cliffs are the dominant mechanism of scarp retreat. Pressure-release jointing parallel to the cliff face, ensuing erosion along the joints, and slow movement (rock creep) of blocks precede the sudden failure of blocks from the cliff wall (Schumm and Chorley 1966). The process of scarp retreat is described by Koons (1955), and it is generally a discontinuous process consisting of sudden rock falls separated by long periods of stability. As described by Koons (1955), the talus angle and rock slope angle was measured along the lower slopes of the Book Cliffs north of the site to determine if talus accumulation or cliff retreat are the dominant processes now occurring. Results of these measurements are included in the "Site and Regional Geomorphology – Results of Site Investigations" calculation (RAP Attachment 2, Appendix D). Also included in that calculation set is an evaluation of the rock fall hazard for the proposed disposal cell footprint and adjacent operating area, showing the distance the rocks will travel southward from the base of the Book Cliffs after breaking off from the top of the cliffs.

The rate of northward scarp retreat of the Book Cliffs, a compound scarp (Schumm and Chorley 1966) composed of a resistant caprock (sandstone of the Mesaverde Group) underlain by weaker rock (Mancos Shale), may be estimated from published scarp retreat rates for rock types in arid climates. Also, general scarp retreat rates have been estimated for geographic areas, such as the Paradox Basin region of the Colorado Plateau where Woodward-Clyde Consultants (1983) published a rate of 0.8 to 1.8 ft per 1,000 years. Schumm and Chorley (1983) published scarp retreat rates in semiarid to arid climates for sandstone as 0.65 to 3.3 ft per 1,000 years and for shale as 6.5 to 43 ft per 1,000 years. Because the compound scarp of the Book Cliffs is formed by the two rock types, a scarp retreat rate for the Book Cliffs

could be estimated at 5 ft per 1,000 years, which is roughly the average of the high range for sandstone and the low range for shale.

Eolian Processes

Windblown deposits are scarce at the site area. Earlier small-scale geologic mapping by Williams (1964) and Hintze et al. (2000) show the Crescent Flat area covered by eolian and alluvial deposits. More recent large-scale mapping of the area by Doelling (2001) shows instead that the Crescent Flat area is covered by alluvial mud. Only a few small areas of eolian deposits are mapped by Doelling (2001) near the site area, about 1 mi north of the site on the north (leeward) side of the Book Cliffs. Eolian processes are apparently of low significance to the site area at present; however, layers of windblown deposits may be present in the Quaternary alluvial mud. Windblown deposits would indicate drier climatic episodes in the Pleistocene and Holocene Epochs when eolian processes were more widespread.

Conclusion and Recommendations:

Based on evaluation of the results of the literature research, the geomorphological characteristics of the Crescent Junction Site indicate that it is apparently suitable for disposal of the Moab uranium mill tailings and contaminated material. Several concerns in areas around the periphery of Crescent Flat involving geomorphic processes are evaluated, and the results are reported in the following calculation sets: "Photogeologic Interpretation" (RAP Attachment 2, Appendix G) has results of evaluation of the rate of northward incision advance in the West Branch of Kendall Wash; "Site and Regional Geomorphology – Results of Site Investigations" (RAP Attachment 2, Appendix D) has results of evaluations for eastward migration of Crescent Wash, stream capture and formation of mantled pediment surfaces, landslides on the south slope of the Book Cliffs, and the extent of rock falls from the south side of the Book Cliffs.

Computer Source:

Not applicable.

References:

Carter, T.E., 1977. *Pediment Development Along the Book Cliffs, Utah and Colorado*, Geological Society of America Abstracts with Programs, 9(6) p. 714.

Dethier, D.P., 2001. "Pleistocene Incision Rates in the Western United States Calibrated Using Lava Creek B Tephra," Geological Society of America, *Geology*, 29(9), pp. 783–786.

Doelling, H.H., 2001. *Geologic Map of the Moab and Eastern Part of the San Rafael Desert 30' × 60' Quadrangles, Grand and Emery Counties, Utah, and Mesa County, Colorado*, Utah Geological Survey Map 180, scale 1:100,000.

Hansen, D.T., 1989. *Soil Survey of Grand County, Utah, Central Part*, U.S. Department of Agriculture, Soil Conservation Service, 60 sheets, scale 1:24,000.

Harty, K.M., 1993. *Landslide Map of the Moab 30' × 60' Quadrangle, Utah*, Utah Geological Survey Open-File Report 276, scale 1:100,000.

Hintze, L.F., G.C. Willis, D.Y.M. Laes, D.A. Sprinkel, and K.D. Brown, 2000. *Digital Geologic Map of Utah*, Utah Geological Survey Map 179DM, CD-ROM, scale 1:500,000.

Koons, E.D., 1955. "Cliff Retreat in the Southwestern United States," *American Journal of Science*, Vol. 253, pp. 44–52.

Rich, J.L., 1935. "Origin and Evolution of Rock Fans and Pediments," *Geological Society of America Bulletin*, Vol. 46, pp. 999–1024.

Schumm, S.A., and R.J. Chorley, 1966. "Talus Weathering and Scarp Recession in the Colorado Plateaus," *Zeitschrift für Geomorphologie*, Vol. 10, pp. 11–36.

Schumm, S.A., 1980. "Geomorphic Thresholds: the Concept and its Applications," *Institute of British Geographers Transactions*, Vol. 4, pp. 485–515.

Schumm, S.A., 1986. *Diffuse-Source Salinity: Mancos Shale Terrain,* U.S. Bureau of Land Management Technical Note 373.

Schumm, S.A., and R.J. Chorley, 1983. *Geomorphic Controls on the Management of Nuclear Waste*, prepared for U.S. Nuclear Regulatory Commission, Washington, D.C., NUREG/CR-3276.

Williams, P.L., compiler, 1964. *Geology, Structure, and Uranium Deposits of the Moab Quadrangle, Colorado and Utah*, U.S. Geological Survey Miscellaneous Geologic Investigations Map I-360, scale 1:250,000.

Woodward-Clyde Consultants, 1982. *Geologic Characterization Report for the Paradox Basin Study Region, Utah Study Areas, Volume I, Regional Overview*, unpublished technical report ONWI-290, prepared for the Office of Nuclear Waste Isolation, Battelle Memorial Institute, Columbus, Ohio, January.

Woodward-Clyde Consultants, 1983. *Overview of the Regional Geology of the Paradox Basin Study Region,* unpublished technical report ONWI-92, prepared for the Office of Nuclear Waste Isolation, Battelle Memorial Institute, Columbus, Ohio, March.

Woodward-Clyde Consultants, 1984. *Geologic Characterization Report for the Paradox Basin Study Region, Utah Study Areas, Volume VI, Salt Valley*, unpublished technical report ONWI-290, prepared for the Office of Nuclear Waste Isolation, Battelle Memorial Institute, Columbus, Ohio, December.

U.S. Department of Energy—Grand Junction, Colorado

Calculation Cover Sheet

Calc. No.: MOA-02-04-2007-1-07-01 **Doc. No.:** X0113500	**Discipline:** Geologic and Geophysical Properties	**No. of Sheets:** 16

Location: Attachment 2, Appendix D

Project: Moab Project

Site: Crescent Junction Disposal Site

Feature: Site and Regional Geomorphology – Results of Site Investigations

Sources of Data:

Reconnaissance geologic investigations in 2005 and 2006 in and immediately surrounding the site withdrawal area.

Purpose of Revision:

Revision is being issued to include results of site characterization activities in 2005 that identified additional geomorphic features, which were investigated in 2006. Also, the U.S. Nuclear Regulatory Commission questions on several features were addressed, and a change in the size and orientation of the disposal cell footprint necessitated revision of figures and a plate.

Sources of Formulae and References:

See References section.

Preliminary Calc. ☐ **Final Calc.** ☒ **Supersedes Calc. No. MOA-02-08-2005-1-08-00**

Author: Craig Goodknight (Name) 31 May 07 (Date) **Checked by:** [signature] (Name) 31 May 07 (Date)

[signature] (Name) 5-31-07 (Date)

Approved by: [signature] (Name) 5/31/07 (Date)

[signature] (Name) 31 May 07 (Date)

[signature] (Name) May 31, 07 (Date)

No text for this page

Problem Statement:

Preliminary site selection performed jointly by the U.S. Department of Energy (DOE) and the Contractor has identified a 2,300-acre withdrawal area in the Crescent Flat area just northeast of Crescent Junction, Utah, as a possible site for a final disposal cell for the Moab uranium mill tailings. The proposed disposal cell would cover approximately 250 acres. Based on the preliminary site-selection process, the suitability of the Crescent Junction Disposal Site is being evaluated from several technical aspects, including geomorphic, geologic, hydrologic, seismic, geochemical, and geotechnical. The objective of this calculation set is to identify and evaluate geomorphic features and processes that may affect the disposal site.

This calculation was initially prepared in August 2005 and included results from several field reconnaissance site visits, examination of low-sun-angle (LSA) and high-altitude vertical (HAV) aerial photographs of the site area taken in July 2005, and results of excavation of two test pits in the withdrawal area. Revision of this calculation set became necessary because 1) the size and orientation of the disposal cell footprint changed; 2) site characterization activities of geologic mapping, drilling of boreholes and coreholes, and excavation of more test pits identified additional geomorphic features in 2005 that were further investigated in 2006; and 3) additional information was included for some features as a result of responses to U.S Nuclear Regulatory Commission (NRC) review questions.

Information from this calculation is incorporated into Attachment 2 (Geology) of the Remedial Action Plan and Site Design for Stabilization of Moab Title I Uranium Mill Tailings at the Crescent Junction, Utah, Disposal Site (RAP), and summarized in the appropriate sections of the Remedial Action Selection (RAS) Report for the Moab Site.

Method of Solution:

Geomorphic features investigated are described according to the principal geomorphic processes (fluvial, mass movement, and eolian) represented at the site. Plate 1 shows the geomorphic features of the site withdrawal area and nearby surrounding area. LSA and HAV aerial photographs were inspected in conjunction with field checks of geomorphic features, and for some features, detailed investigation results are presented in the "Photogeologic Interpretation" calculation set (RAP Attachment 2, Appendix G). Locations of boreholes, coreholes, test pits, and mapped surficial and bedrock geology for the disposal cell footprint and nearby area are shown in Plate 1 of the "Surficial and Bedrock Geology of the Crescent Junction Disposal Site" calculation set (RAP Attachment 2, Appendix B).

Assumptions:

Not applicable.

Calculation:

None required.

Discussion:

Degradational (erosional) and aggradational (depositional) processes are represented by the geomorphic features in and near the site withdrawal area. Investigations of these areas related to the fluvial, mass movement, and eolian geomorphic processes and how they affect the disposal site are described in the following subsections.

Fluvial Processes

Kendall Wash Tributaries

The advance of headward incision of several tributaries of the West Branch of Kendall Wash was investigated along with an abandoned ancestral channel of the East Branch of Kendall Wash (Plate 1). Incision advance of the West Branch and the abandoned channel of the East Branch are best shown in

aerial photographs, and details of these investigations are in the "Photogeologic Interpretation" calculation set (RAP Attachment 2, Appendix G).

Incision advance northward of the tributaries of the West Branch is caused by sheet wash flows across the west side of Crescent Flat from infrequent heavy rains. Historic aerial photos show that the incision rate advance northward is approximately 1.3 to 2.3 feet (ft) per year, and that after about 1,600 years, incision northwestward of the West Branch could reach and possibly capture Crescent Wash. This possible capture would place a larger, high-energy drainage to within about 1,000 ft of the southwest corner of the disposal cell footprint (Plate 1).

Northward incision would reach the site access road much sooner, at about 250 years, and after about another 250 years, incision of the easternmost tributary could reach to just west of the southwest corner of the disposal cell. This north-trending tributary drainage (Figure 1) has been recently capturing more of the sheet wash flow because a culvert constructed under the site access road is channeling water southward (Figure 2) to an east branch of this drainage. After disposal cell construction, drainage westward around this cell and then southward will further increase and concentrate flows into this north-trending drainage, likely resulting in an increased rate of headward incision. Rock armoring of this drainage channel in the disposal cell design will be necessary to prevent northward advance of headward erosion from nearing the southwest corner of the disposal cell.

North of the Union Pacific Railroad, incision of the West Branch has not exposed Mancos Shale bedrock. Downstream from the railroad to old U.S. Highway 50, incision of the wash is as much as 8 ft deep and, in places, the wash cuts as much as 2 ft into weathered Mancos Shale. The confluence of the East and West Branches of Kendall Wash is just north of the large (approximately 15-ft diameter) concrete culvert pipe under Interstate Highway 70 (I-70). Kendall Wash passes through this large culvert pipe, which effectively sets the base level for the wash. Erosion by headward incision in both branches of the wash will continue for an unknown period in response to this base level. South of I-70 for about 0.5 mile (mi), Kendall Wash is incised as much as 10 ft deep, and the wash has cut as much as 4 ft into weathered Mancos Shale in numerous places. No ground water seepage was noted in the weathered Mancos Shale contacted in the wash bottom.

The East Branch of Kendall Wash drains in a southwesterly direction and has a much larger drainage area than the West Branch. Consequently, the East Branch is more deeply incised (as much as 15 ft) into the surface of Crescent Flat. Incision of the East Branch begins north of old U.S. Highway 50 and continues for about 2 mi upstream. In places, the incised bottom of the East Branch does not cut into Mancos Shale bedrock (Figure 3), but along most of its incised length the base of the wash is near the bedrock contact or has cut as much as 6 to 8 ft into weathered bedrock. No ground water seepage was noted in weathered Mancos Shale along the course of the East Branch.

Deep incision in the East Branch of Kendall Wash has advanced upstream, northeastward, capturing the ancestral East Branch that drained southward (Plate 1). A description of the ancestral course of the East Branch and possible timing of its capture and abandonment are in the "Photogeologic Interpretation" calculation set (RAP Attachment 2, Appendix G). Several tributaries draining from the north into the East Branch are deeply incised (as much as 10 ft) and headcuts are apparently advancing northward. These tributaries are 0.5 to 1.0 mi east of the disposal cell in the SE¼ of Section 23, SW¼ of Section 24, and NE¼ of Section 26. Their northward incision advance should not pose any erosion concerns to the disposal cell area.

Crescent Wash

The prominent incised meander of Crescent Wash near the northwest corner of Section 27 (Figure 4) was investigated to evaluate the possibility of further eastward migration toward the planned disposal cell. At the meander, Crescent Wash is incised to a depth of about 12 ft into sandy alluvium deposited by the ancestral Crescent Wash system. Gravel and boulders as much as 3 ft in diameter are exposed in the walls of the sandy alluvium incised by the wash. Recently transported sandstone boulders as large as 4 ft in diameter are in the wash bottom at the meander, and boulders as large as 8 ft are within 0.5 mi downstream in the wash. From the meander bend downstream for about 0.5 mi, incision of Crescent Wash has not cut into weathered Mancos Shale bedrock.

High flows, responsible for the coarse material in the wash bottom, down the normally dry Crescent Wash were seen in late summer and early fall 2005. Bank failure was noted on the east side of the meander bend (Figure 5), indicating active erosion is progressing eastward during moderately high rainfall events. After the most intense rainfall event of the season, on September 9 and 10, 2005, the depth of flow in the wash at the meander reached about 9 ft. At this high stand, water had flowed across the inside of the meander about 200 ft west of the main meander bend channel. This flow across an incipient cutoff channel indicates that, during another extremely high flow, the cutoff channel will be reoccupied and deepened, with the long-term tendency to occupy the cutoff and abandon the present meander bend channel. Occupation of the cutoff channel would tend to straighten the course of Crescent Wash, whose channel does not have a significant meander bend in its approximately 1.5-mi course south to I-70. Because of this tendency of Crescent Wash to change course to the cutoff channel and abandon the outside meander bend channel, erosion for more than a few tens of feet eastward from the present outside meander bend is unlikely.

Mantled Pediment Surfaces

A pediment surface on Mancos Shale that is mantled by coarse alluvium (composed mostly of sandstone) from ancestral Crescent Wash drainage courses stands about 100 ft above the present wash. This surface forms a long, low mesa west of Crescent Wash, nearly a mile west of the disposal cell footprint. This eroding pediment surface originally was slightly more extensive, and other pediment surfaces representing former Crescent Wash drainage courses were east of Crescent Wash to as far as the West Branch of Kendall Wash. East of Crescent Wash, erosion has removed most of the pediment, with only a few low hills of Mancos Shale remaining south of the site access road and the resistant pediment mantling material remaining as lag in some places.

The process of formation of the pediment surfaces mantled by alluvium involves stream capture of a steep-gradient drainage from the Book Cliffs by a low-gradient drainage formed on Mancos Shale (Schumm 1980). As described earlier in the section on Kendall Wash tributaries, the only area near the disposal site where this process could occur is by long-term headward incision advance by the West Branch of Kendall Wash to eventually (after an estimated 1,600 years) possibly capture Crescent Wash. This capture could result in the isolation of coarse Crescent Wash sediments downstream of the capture that could eventually mantle a new pediment surface. This process could occur, but it would be many thousands of years in the future and would not affect the disposal site area more than 0.5 mi to the east.

Mass Movement Processes

Landslides

The landslides mapped by Harty (1993) and Doelling (2001) in the Book Cliffs just north of the withdrawal area mainly have northerly aspects (Plate 1). One of these landslides, the large one in the south side of the Horse Heaven area, extends around the west end of the top of the Book Cliffs in the north-central part of Section 22 and has displaced some of the south face of the cliffs (Plate 1). This displacement is shown by a sandstone pillar of Blackhawk Formation that has slid down by more than 50 ft and a line of vegetation that extends eastward from that, marking the base of the slide (Figure 6).

Several small areas mapped as talus and colluvium by Doelling (2001) along the south-facing badlands slope of the Book Cliffs were investigated to determine if they represent small landslides. These areas form a tan to light-brown, discontinuous bench across the lower third of the gray slope of the Book Cliffs at an elevation of approximately 5,250 ft (Figure 4). Inspection of these benches that contain large sandstone blocks and, in places, intact beds that dip northward back into the slope, concluded that they represent remnants of ancestral landslides (Figure 7). The band of discontinuous benches is in the east part of Section 22 and the west part of Section 23 (Plate 1). The largest of these benches is at the west end of the band. These landslide remnants are very old, are no longer active, and apparently originated in much wetter climatic conditions during the Pleistocene, when wet conditions allowed landslide conditions to develop even on south-facing slopes.

Rock Falls

Rock-fall debris covers some of the badlands slope as talus along the south side of the 800-ft-high Book Cliffs (Figure 8). The dislodged rock is sandstone from the Blackhawk Formation and Castlegate Sandstone, both of the Mesaverde Group, which cap the Book Cliffs. This rock may roll and slide some distance beyond the base of the badland slopes; an example of this rock runout is "Big Rock", which is just north of the east-west access road north of the disposal cell footprint (Plate 1 and Figure 9). An investigation was conducted in October 2006 to evaluate how far this rock-fall material could run out along the base of the Book Cliffs and if it could affect the disposal cell. Results of this investigation are in the following paragraphs.

Because the axis of the disposal cell footprint trends east-northeast, the northeast part of the disposal cell will be the closest to the Book Cliffs. Therefore, the investigation along the slopes of the Book Cliffs was focused in the east part of Section 22 and the west part of Section 23. The angle of the badland slope up to the base of the Blackhawk Formation is 34 to 35 degrees. Where the slope is covered by talus, the angle is 33 to 35 degrees. The angle of repose on a bare rock surface of Mancos Shale is about 35 degrees (Koons 1955). Because the talus-covered slope angle (always less than the angle of repose) is very close to the angle of repose, this indicates cliff retreat rather than talus accumulation is presently the dominant process (Koons 1955).

An evaluation of rock-fall runout was made in the west part of Section 23 in the area of "Big Rock" to determine if runout could extend farther south of "Big Rock" and possibly affect the disposal cell. The evaluation was based on the method used by Evans and Hungr (1993) who suggested, based on empirical data, that a minimum shadow angle of about 27.5 degrees may be useful for establishing an estimate of maximum rock-fall runout distance. This method was also used in evaluation of rock-fall hazard in the Moab-Spanish Valley (Hylland and Mulvey 2003).

A schematic diagram showing the terms used in the rock-fall analysis and the location of the rock-fall area in relation to the disposal cell is in Figure 10. The source of rock fall is in the cliff starting near the base of the Blackhawk Formation. In the site area, the base of this cliff is at an elevation of approximately 5,700 ft. From this cliff base, the minimum shadow angle of 27.5 degrees determines the empirical rock-fall runout limit (Figure 10). The rock-fall shadow is the distance of rock-fall runout from the base of the talus slope out to the empirical runout limit. Within the rock-fall shadow is the rock-fall fahrböshung, which is the angle between the rock-fall source and the stopping point of the longest runout boulder (Evans and Hungr 1993).

Two profiles were selected for the calculation of rock-fall runout; the line of these profiles and their relation to the disposal cell footprint are shown in Figure 11. Shown in each of the profiles in Figure 12 are the elevations of the base of the cliff (rock-fall source) and the runout limit. Rock-fall limits for each profile are plotted on the map in Figure 11 and are shown in Figure 13 in a perspective from the top of the Book Cliffs along with "Big Rock" and the proposed disposal cell footprint.

Distances from the empirical rock-fall runout limits to the edge of the disposal cell footprint are approximately 900 ft for profile 1 and 950 ft for profile 2. This is far enough north away from the disposal cell and any infrastructure or access roads to not pose a rock-fall hazard. Slow scarp retreat northward of the Book Cliffs over time will continue to reduce this hazard to the disposal cell.

"Big Rock" (Figure 9 and Figure 13) sits about 150 ft south of the rock-fall runout limit calculated from nearby profile 1. This feature is evidence of an earlier fahrböshung when the rock-fall limit was farther south. A rough estimate of the rate of scarp retreat for the Book Cliffs in this area is 5 ft per 1,000 years. Maximum age of petroglyphs on "Big Rock" indicate that it could have fallen as long as 2,200 years or more ago. Because "Big Rock" is so far beyond (150 ft) the present rock-fall runout limit, it is likely that it could have fallen as much as 30,000 years ago.

Eolian Processes

No windblown deposits are on the surface of the withdrawal area or the immediately adjacent area. However, eolian-deposited sandy silt is preserved in places in the shallow subsurface as one or more thin, reddish-brown layers (less than 2 ft thick) in the gray alluvial mud overlying weathered Mancos Shale bedrock. Eolian material was seen in several test pits at depths of 5 to 10 ft, particularly in test pit 0151 at

a depth of 7 ft. Reddish-brown eolian layers were also exposed in places along the incised drainages of the West Branch (Figure 14) and the East Branch (Figure 3) of Kendall Wash. The eolian material is not present everywhere beneath the site because it was likely deposited in sheltered, lee sides of ridges or it was removed later by alluvial erosional channels, or a combination of both processes. This windblown layer was likely deposited during what is referred to as the altithermal period in the early Holocene, a post-glacial time of high temperatures and dry climate. A warm, dry climate regime such as this could develop relatively quickly (over a period of decades) and favor the accumulation of eolian deposits at the site.

Conclusion and Recommendations:

Fluvial geomorphic processes will have the most significant effect on the site area that includes the proposed disposal cell. The other geomorphic processes investigated—mass movement and eolian—will likely have negligible effects on the disposal cell and nearby area. Mass movement processes of landslides, rock fall, and scarp retreat are confined to the Book Cliffs, which are far enough away (approximately 1,000 ft at the closest point) to not affect the disposal cell. Eolian processes, active in drier times earlier in the Holocene, are not expressed at the site and apparently will not affect the site unless the climate becomes drier.

Long-term incision advance of the tributaries of the West Branch of Kendall Wash has the greatest potential of fluvial erosion processes to affect the disposal cell. Headward incision northward at a rate measured from historical aerial photographs of an eastern tributary to the West Branch could reach the southwest corner of the disposal cell in about 500 years. Increased flows in the drainage created by channeling of several drainages around the west side of the disposal cell will accelerate headcutting and shorten the time for erosion to reach the disposal cell corner. It is recommended that rock armoring of this drainage path be included in the engineering design of the disposal cell to prevent this headward erosion.

The tendency of Crescent Wash to migrate eastward toward the disposal cell is low because the wash channel will likely soon follow an incipient cutoff channel, resulting in a straightening of the wash course. Long-term incision advance of a tributary of the West Branch of Kendall Wash could capture the Crescent Wash drainage after approximately 1,600 years. At that time, the high-energy Crescent Wash channel could then be about 1,000 ft west of the disposal cell—probably far enough away not to pose an erosion threat to the cell.

Erosional incision advance of the present East Branch of Kendall Wash resulted in capture of an earlier drainage thousands of years ago. Incision advance of this wash and its tributaries will continue, but this erosion is 0.5 to 1.0 mi or more east of the disposal cell and will not affect the site.

Computer Source:

Not applicable.

References:

Doelling, H.H., 2001. *Geologic Map of the Moab and Eastern Part of the San Rafael Desert 30' × 60' Quadrangles, Grand and Emery Counties, Utah, and Mesa County, Colorado*, Utah Geological Survey Map 180, scale 1:100,000.

Evans, S.G., and O. Hungr, 1993. "The Assessment of Rockfall Hazard at the Base of Talus Slopes," *Canadian Geotechnical Journal*, Vol. 30, pp. 620–636.

Harty, K.M., 1993. *Landslide Map of the Moab 30' × 60' Quadrangle, Utah,* Utah Geological Survey Open File Report 276, scale 1:100,000.

Hylland, M.D., and W.E. Mulvey, 2003. *Geologic Hazards of Moab-Spanish Valley, Grand County, Utah*, Utah Geological Survey Special Study 107.

Koons, E.D., 1955. "Cliff Retreat in the Southwestern United States," *American Journal of Science,* Vol. 253, pp. 44–52.

Schumm, S.A., and R.J. Chorley, 1966. "Talus Weathering and Scarp Recession in the Colorado Plateaus," *Zeitschrift für Geomorphologie*, Vol. 10, pp. 11–36.

Figure 1. View north of incised north-trending tributary drainage to the West Branch of Kendall Wash.

Figure 2. View north-northwest of culvert under the site access road and water channeled southward to an east fork of the north-trending tributary to the West Branch of Kendall Wash.

Figure 3. View northeast of East Branch of Kendall Wash incised about 12 ft deep in SE¼ NE¼ Section 26; here, a red-brown eolian layer about 1 ft thick is exposed and the wash has not incised into Mancos Shale bedrock.

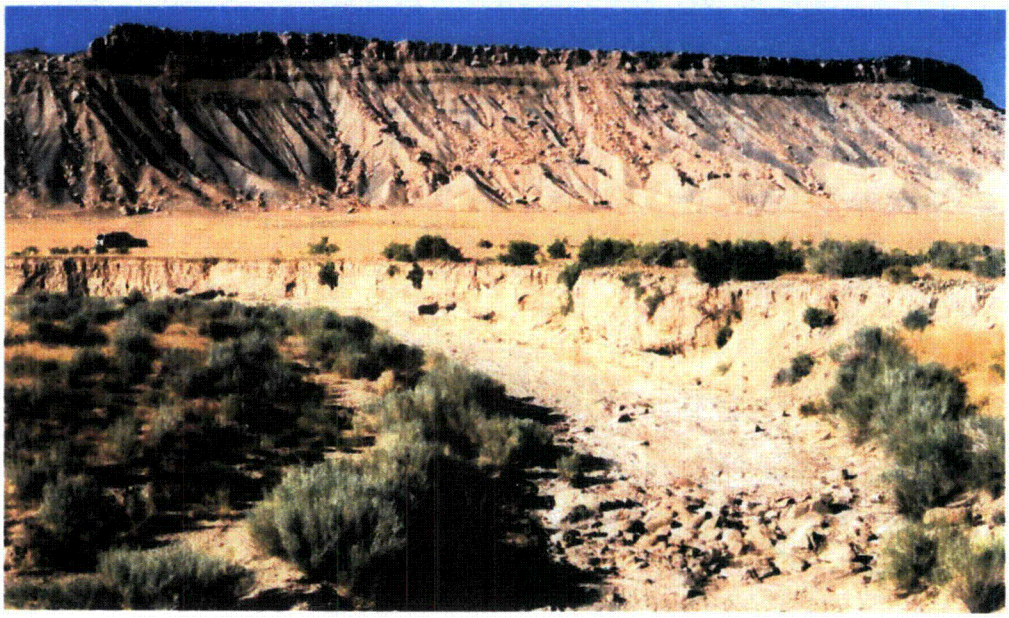

Figure 4. View northeast (upstream) of incised meander bend in Crescent Wash, just southwest of corner of Sections 21, 22, 27, and 28. Discontinuous tan bench in lower slope of the Book Cliffs marks remnants of ancestral landslides.

Figure 5. View south (downstream) of incised meander bend in Crescent Wash showing bank failure at left being removed by 2-ft deep storm flow, September 21, 2005.

Figure 6. View north of landslide at west end of the Book Cliffs in the north-central part of Section 22 where Blackhawk Formation sandstone has slid down more than 50 ft; vegetation (willows) marks a moist area at the base of the landslide.

Figure 7. View southwest along the badlands south face of the Book Cliffs and small bench at left that represents the remnant of an ancestral landslide.

Figure 8. View north of the sandstone blocks of the Blackhawk Formation and overlying, slabby Castlegate Sandstone that cover some of the badlands Mancos Shale slopes as talus.

Figure 9. View southwest of "Big Rock", just north of the east-west access road (note vehicle for scale); low mounds of dolomitic siltstone concretions are in middle distance near the northeast corner of the disposal cell footprint.

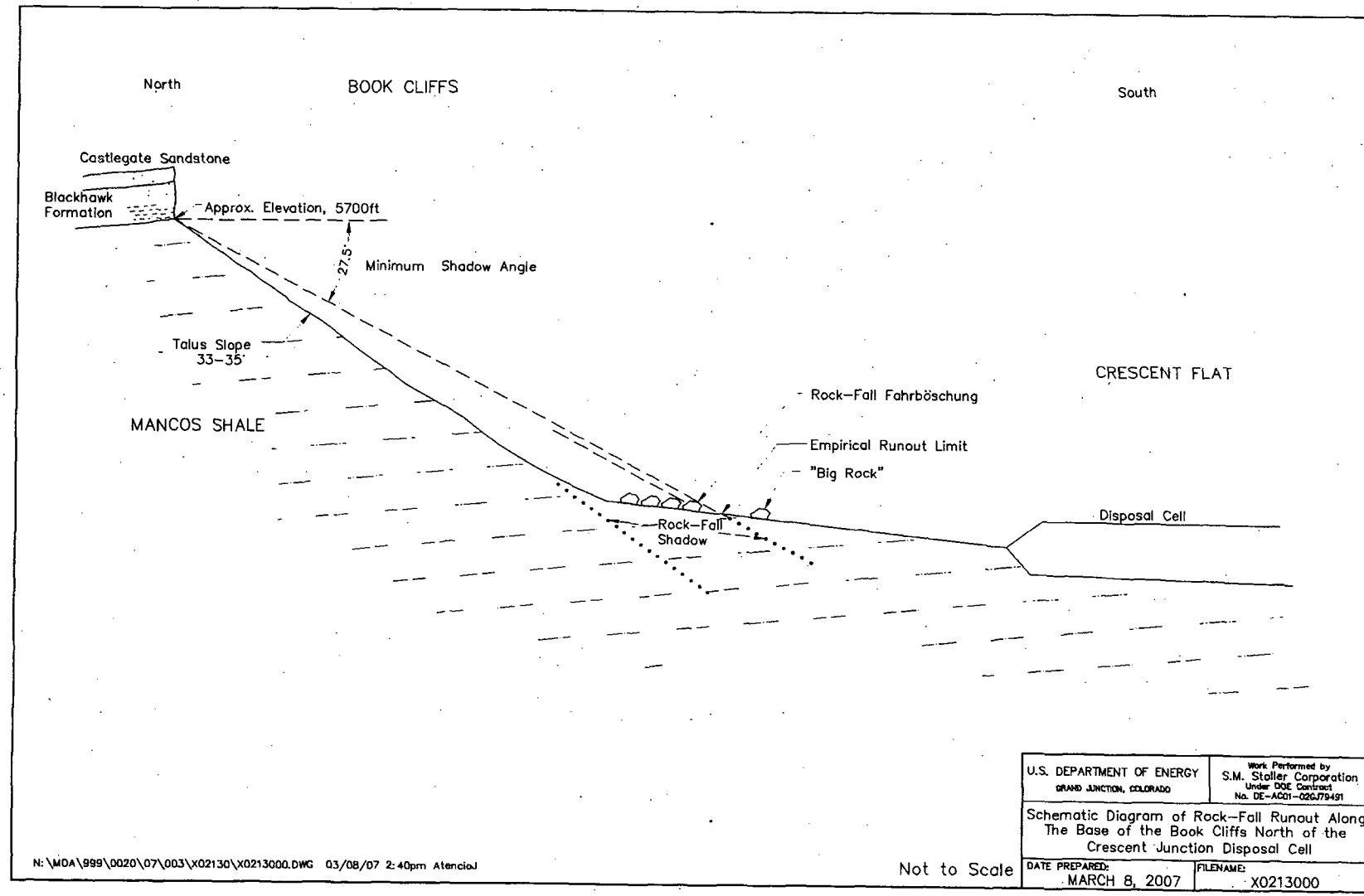

Figure 10. Schematic diagram of rock-fall runout along the base of the Book Cliffs north of the Crescent Junction Disposal Cell

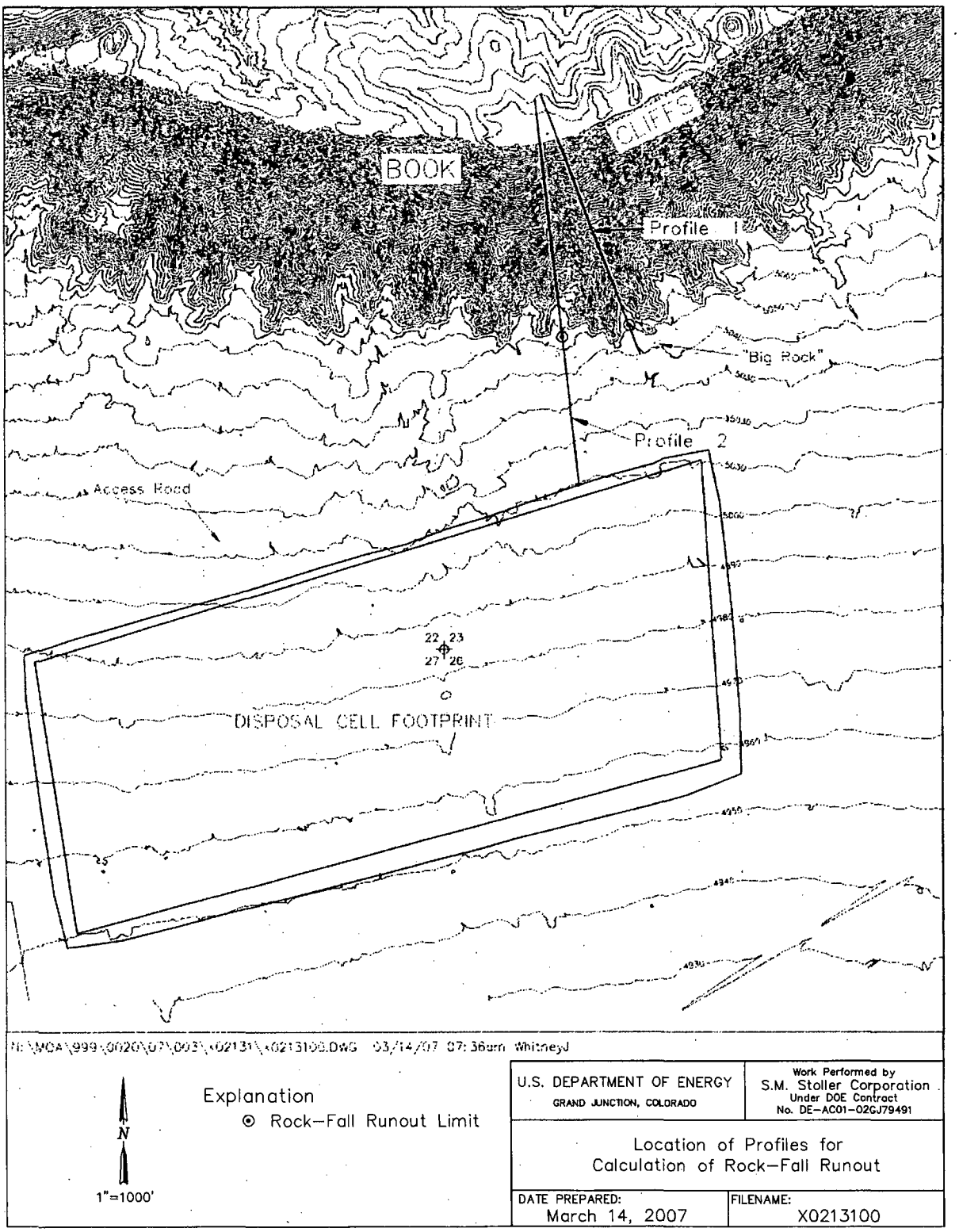

Figure 11. Location of profiles for calculation of rock-fall runout.

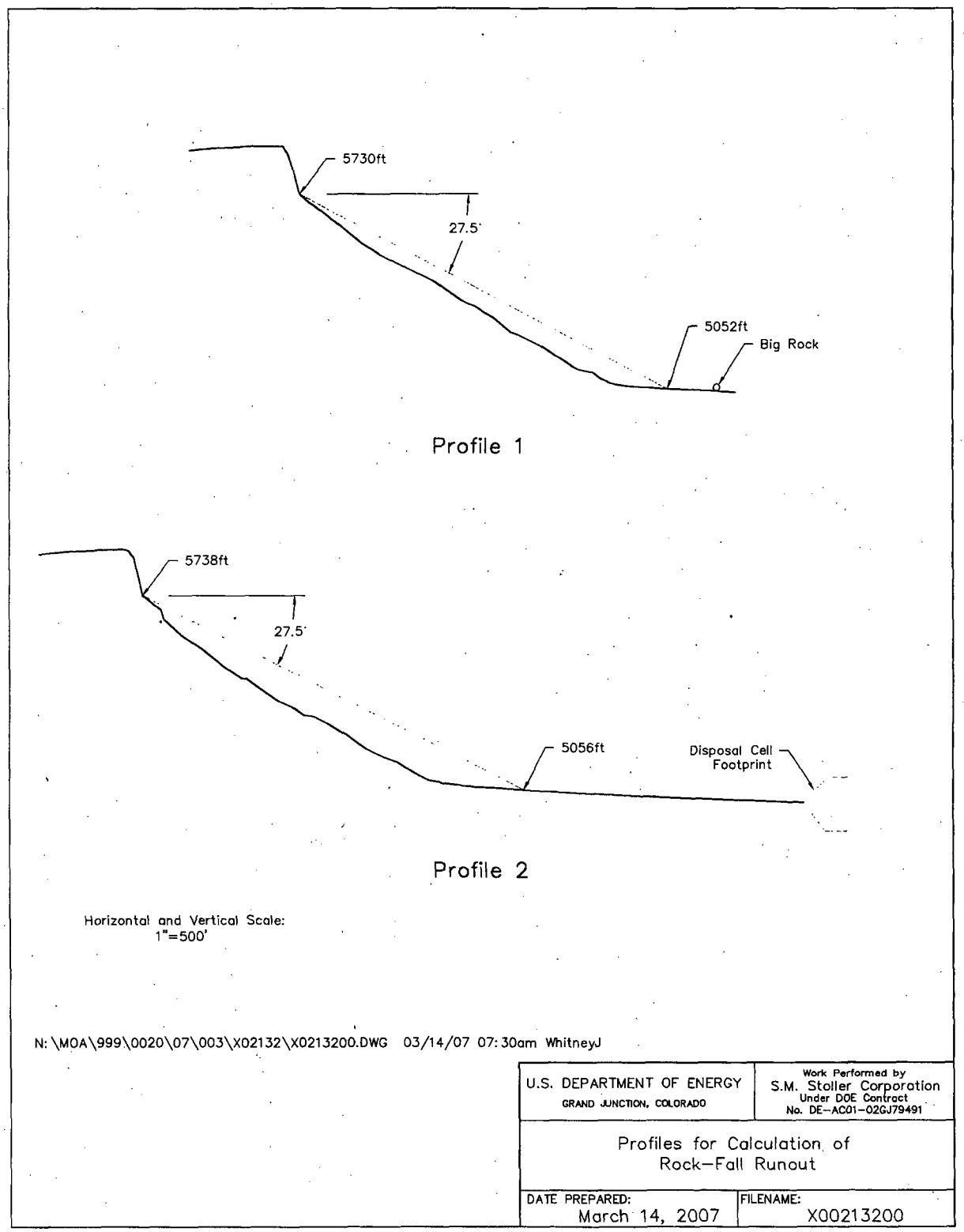

Figure 12. Profiles for calculation of rock-fall runout.

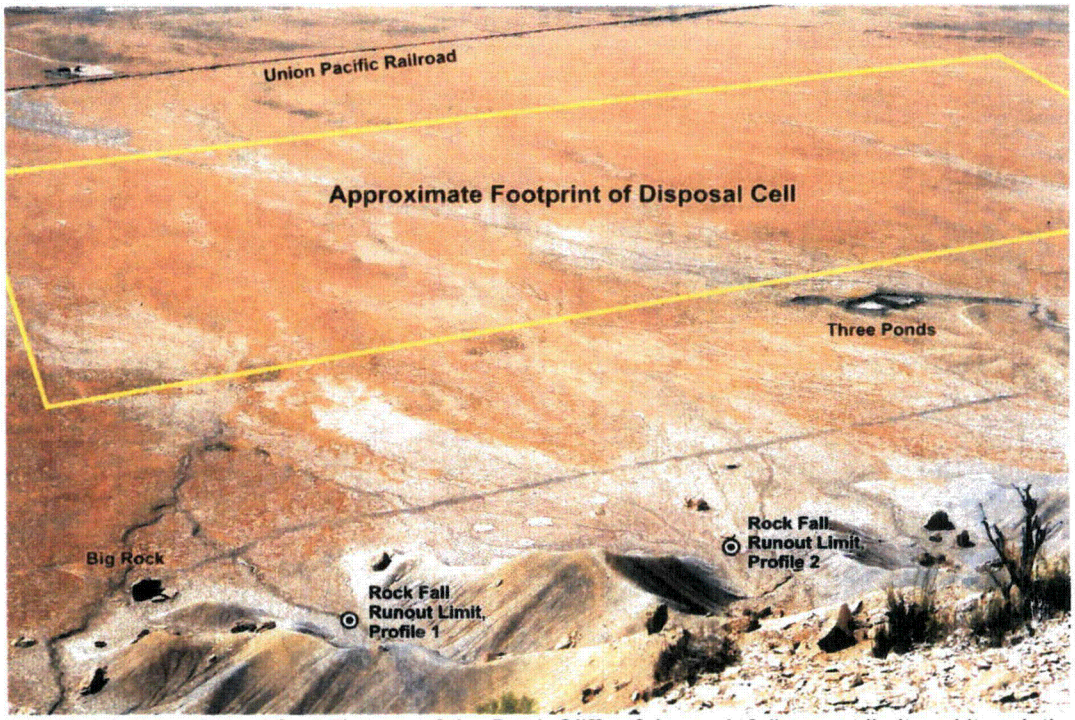

Figure 13. View southwest from the top of the Book Cliffs of the rock-fall runout limit and its relation to "Big Rock" and the proposed disposal cell footprint; "Big Rock" is approximately 800 ft from the disposal cell footprint.

Figure 14. View northwest along the incised West Branch of Kendall Wash of a thin, reddish-brown layer of eolian-deposited sandy silt in the thicker gray alluvial mud deposits.

THIS PAGE IS AN OVERSIZED DRAWING OR FIGURE,

THAT CAN BE VIEWED AT THE RECORD TITLED:

DRAWING NO.: X0213300, "PLATE 1 - GEOMORPHIC FEATURES OF THE CRESCENT JUNCTION DISPOSAL SITE WITHDRAWAL AREA AND IMMEDIATELY SURROUNDING AREA"

WITHIN THIS PACKAGE... OR, BY SEARCHING USING THE DOCUMENT/REPORT DRAWING NO. X0213300

D-04

U.S. Department of Energy—Grand Junction, Colorado

Calculation Cover Sheet

Calc. No.: MOA-02-04-2007-1-08-01 Doc. No.: X0113900	Discipline: Geologic and Geophysical Properties	No. of Sheets: 22

Location: Attachment 2, Appendix E

Project: Moab Project

Site: Crescent Junction Disposal Site

Feature: Site and Regional Seismicity – Results of Literature Research

Sources of Data:

Published reports and maps – see list of references at end of calculation set.

Purpose of Revision:

Added Chitwood (1994) and Doelling (2001) references for Little Grand Wash Fault.

Sources of Formulae and References:

See list of references at end of calculation set.

Preliminary Calc. ☐ **Final Calc.** ☒ **Supersedes Calc. No. MOA-02-11-2005-7-01-00**

Author: [signature] Name 5/25/07 Date

Checked by: [signature] Name 31 May 07 Date

[signature] Name 31 May 07 Date

[signature] Name 31/May 07 Date

[signature] Name MAY 31, 07 Date

Approved by: [signature] Name 5/31/07 Date

No text for this page

Problem Statement:

Determination of the suitability of the Crescent Junction Disposal Site as the repository for the Moab Uranium Mill tailings material, and development of the site and regional seismotectonic sections of the Remedial Action Plan and Site Design for Stabilization of Moab Title I Uranium Mill Tailings at the Crescent Junction, Utah, Disposal Site (RAP), requires a thorough review of available literature that applies to the Crescent Junction Site. The compiled list of references is presented at the end of this calculation set, and relevant information is summarized below.

This calculation will be incorporated into Attachment 2 (Geology) of the RAP and summarized in the appropriate sections of the Remedial Action Selection (RAS) report for the Moab Site.

Method of Solution:

This literature review is part of the seismotectonic calculation set to develop seismic design parameters for the disposal site. Specifically, the calculation set includes a review of the pertinent literature, development of an estimate of the Maximum Credible Earthquake (MCE) and determination of the resulting design vibratory ground motion at the site (peak horizontal ground acceleration). The objective of this literature review is to identify the appropriate previous studies and published data pertaining to seismicity in the area. This review will be used to support the calculation of the MCE and peak horizontal ground accelerations to be calculated specifically for the Crescent Junction Site.

Two studies for other Uranium Mill Tailings Remedial Action (UMTRA) sites in particular were referred to for this seismotectonic calculation set because of their similar project type and close proximity to the Crescent Junction Site. Specifically, the seismotectonic studies from the RAP for the Green River, Utah, UMTRA Site (DOE 1991a) and the Grand Junction UMTRA Site (DOE 1991b) were principal resources for this review. The Green River, Utah, Site is a 380,000-cubic-yard (yd^3) uranium disposal site located approximately 20 miles west of the Crescent Junction Site, while the Grand Junction, Colorado, Site is a 5.3-million-yd^3 uranium disposal site located approximately 95 miles east of the Crescent Junction Site. Although the Green River Site is closer to the Crescent Junction Site than the Grand Junction Site, the seismotectonic investigation for Green River Site was not as extensive as the investigation for Grand Junction. Therefore, the use of the Green River RAP as a reference is limited.

Assumptions:

It is assumed that the literature sources are reliable and representative of the current understanding of the seismotectonics of the region.

Calculation:

None required.

Criteria and Definitions:

The following are the standards and definitions that are applied to the evaluation of the seismicity of the Crescent Junction Site as specified in the Technical Approach Document (TAD) (DOE 1989).

Design life. As specified by the U.S. Environmental Protection Agency (EPA) *Code of Federal Regulations* Promulgated Standards for Remedial Actions at Inactive Uranium Processing Sites (40 CFR 192, Subpart A), the controls implemented at UMTRA Project Sites are to be effective for up to 1,000 years, to the extent reasonably achievable and, in any case, for at least 200 years. For the purpose of the seismic hazard evaluation, a 1,000-year design life is adopted.

Design earthquake. For UMTRA Project Sites, the magnitude(s) of the earthquake(s) that produces the largest on-site peak horizontal acceleration (PHA) and that produces the most severe effects upon the site is the design earthquake. This earthquake could be either a floating earthquake or an earthquake

whose magnitude is derived from a relationship between fault length and maximum magnitude. The latter case is applied for a verified or assumed capable fault of known rupture length.

Floating earthquake (FE). An FE is an earthquake within a specific seismotectonic province that is not associated with a known tectonic structure. Before assigning the FE magnitude, the earthquake history and tectonic character of the province are analyzed.

Capable fault. A capable fault is a fault that has exhibited one or more of the following characteristics:

- Movement at or near the ground surface at least once within the past 35,000 years or movement of a recurring nature within the past 500,000 years.
- Macroseismicity (magnitude 3.5 or greater) determined with instruments of sufficient precision to demonstrate a direct relationship with the fault.
- A structural relationship to a capable fault such that movement on one fault could be reasonably expected to cause movement on the other.

Acceleration. Acceleration is the mean of the peaks of the two orthogonal horizontal components of an accelerogram record, or PHA. The accelerations are determined from the corrected peak horizontal ground acceleration attenuation relationship based on distance and magnitude as developed by Campbell and Bozorgnia (2003). This relationship is an update to the Campbell (1981) relationship referenced in the TAD (DOE 1989). The mean-plus-one standard deviation (84th percentile) value is adopted. This value is considered a non-amplified PHA.

Surface acceleration. Surface acceleration is the site acceleration adjusted for the site soil attenuation or amplification effects.

Duration of strong earthquake ground motion. Duration is defined, after Krinitzsky and Chang (1977), as the bracketed time interval in which the acceleration is greater than 0.05g. The methodology of Krinitzsky and Chang (1977) is applied in estimating the duration of strong ground motion at a particular site.

Magnitude and intensity. Magnitude is the base-10 logarithm of amplitude of the largest deflection observed on a torsion seismograph 100 kilometers (km) from the epicenter (Richter 1958). This local magnitude value may not be the same as the body-wave and surface-wave magnitudes derived from measurements at teleseismic distances. Unless specified otherwise, Richter magnitude values for values less than 6.5 are used in UMTRA Project seismic hazard evaluations.

Intensity is the index of the effects of any earthquake on the human population and structures. The most commonly applied scale is the 1931 Modified Mercalli (MM) Intensity Scale, which will be used in this study.

Because pre-instrumental earthquake records are reported in intensity and more recent instrumental records are in magnitude, there may be a need to relate these values. The relationship developed by Gutenburg and Richter (1956) is used:

$$M = 1 + 2/3\ Io$$

Where M = magnitude in the Richter scale and Io = Modified Mercalli intensity in the epicentral area.

Maximum earthquake. The term Maximum Earthquake (ME) was defined by Krinitzsy and Chang (1977) as the largest earthquake that is reasonably expected on a given structure or within a given area. No recurrence interval is specified for such an event.

Local regional study area. The regional study area is selected by calculating the distance at which the largest magnitude earthquake possible for a region, as determined by Algermissen et al. (1982), produces the minimum accepted on-site design acceleration (0.10 g). All further characterization work is then limited to this region. Using this definition, the maximum earthquake for the region as determined by

Algermissen et al. (1982) is magnitude 6.1. Using Campbell (1981) attenuation relations for constrained, 84th-percentile values, distances within 29 km of the site are considered within the local regional study area.

Expanded regional study area. Although UMTRA defines the study area as discussed above, the U.S. Nuclear Regulatory Commission (NRC) for 10 CFR 100, Appendix A, requires an investigation within 200 miles of the site. For purposes of this seismotectonic evaluation, capable faults, historical earthquakes, and floating earthquakes associated with neighboring tectonic provinces that lie within 200 miles of the site and are capable of producing a minimum on-site acceleration of 0.10g or greater will be evaluated in the expanded regional study area.

Discussion:

Seismotectonic Setting

The Crescent Junction Site is located in the northern portion of the Colorado Plateau tectonic province (Figure 1). The Colorado Plateau is a broad, roughly circular region of relative structural stability within a more structurally active region of disturbed mountain systems. Broad basins and uplifts, monoclines, and belts of anticlines and synclines are characteristic of the plateau (Kelley 1979). These basins and uplifts are generally considered to be inactive under the present seismotectonic regime (DOE 1991b). All three of the referenced UMTRA Sites are located within the northern portion of the Colorado Plateau physiographic and tectonic province.

The Colorado Plateau is surrounded by the provinces of the Wyoming Basin and Middle Rocky Mountains to the north, the Basin and Range province to the west and south, the Intermountain Seismic Belt (ISB) to the west, and the Rio Grande Rift and the Southern Rocky Mountains to the east (Keller et al. 1979; Kelley and Clinton 1960; Kelley 1979; Allenby 1979; Kirkham and Rogers 1981). The boundaries of the provinces vary between authors; the Southern Rocky Mountains are divided into the Eastern and Western Mountain Province by Kirkham and Rogers (1981).

Within the Colorado Plateau, the Crescent Junction Site lies in the northwestern part of the Paradox Basin (in the Paradox Fold and Fault Belt), approximately 8 miles south of the Uinta Basin sub-province. The Book Cliffs, less than 1 mile north of the Crescent Junction Site, are the erosional escarpment on the south flank of the Uinta Basin. As shown in Figure 2, additional sub-provinces in the area include the San Rafael Swell to the west; Henry Basin, White Canyon Slope, Monument Upwarp, Blanding Basin, and Four Corners Platform to the south; the San Juan Dome to the east; and the Uncompahgre Uplift to the northeast (Kelley 1955).

The Paradox Basin is characterized by complex systems of northwest-trending normal faults and landslide and slump features. Typical salt anticlinal collapse features extend to within about 2 miles of the site. These features have been active during Quaternary time and may be active today. However, since they result from very gradual processes of salt dissolution and flow, they are not likely capable of generating large earthquakes. Kirkham and Rogers (1981) estimate the maximum earthquakes possible on these features to be about magnitude 5 (DOE 1991b, Kelley and Clinton 1960).

- **Intermountain Seismic Belt (ISB)**

  The ISB (Smith and Sbar 1974; DOE 1991a) is a zone of pronounced earthquake activity extending north from Arizona and terminating in northwestern Montana. It is described by Ryall et al. (1966) as being surpassed in seismic activity in the United States only by the California and Nevada seismic zones. The ISB is coincident with the boundary between the Basin and Range province and the Colorado Plateau/Middle Rocky Mountains. The largest historical event in the ISB was the 1959 Hebgen Lake earthquake of Richter magnitude 7.7 plus or minus 0.2. More than 15 events with magnitudes greater than 6 have been reported since the mid 1800s. The site lies approximately 50 miles east of the highly active ISB.

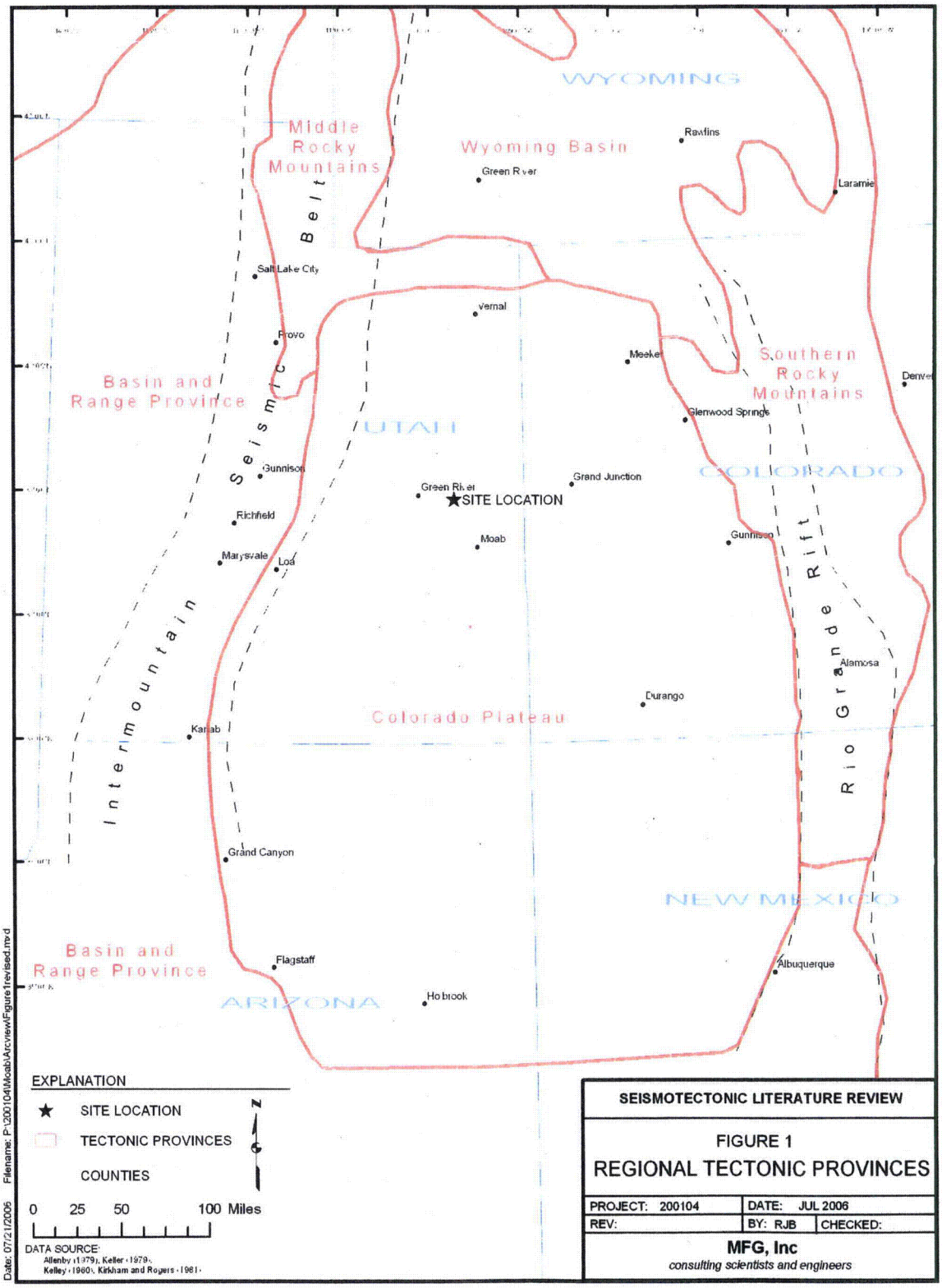

Figure 1. Regional Tectonic Provinces

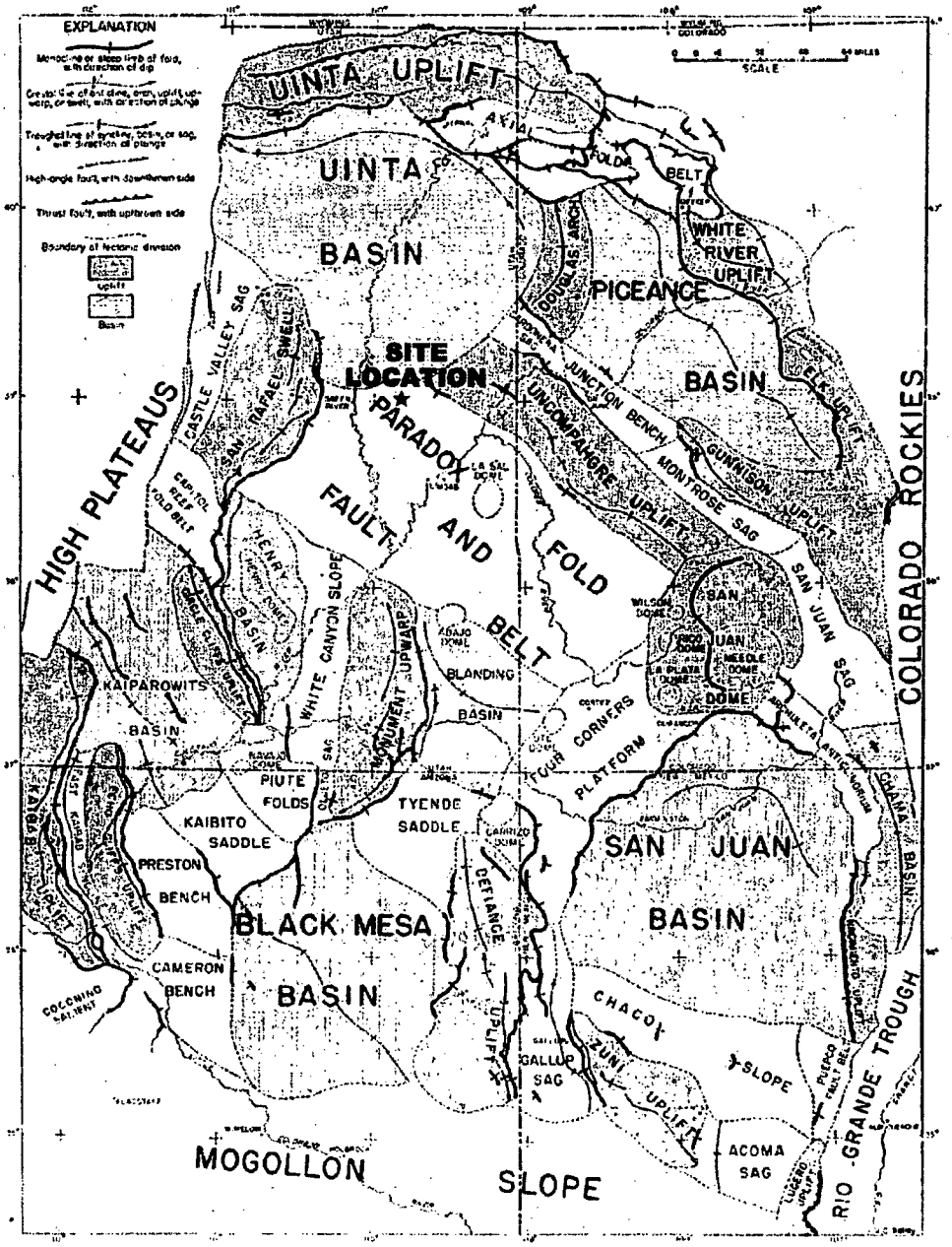

SOURCE: VINCENT C. KELLEY, 1955.

SEISMOTECTONIC LITERATURE REVIEW		
FIGURE 2		
TECTONIC SUB–PROVINCES OF THE COLORADO PLATEAU		
PROJECT: 200104	DATE: JULY 2006	
REV:	BY: TGB	CHECKED:
MFG, Inc. *consulting scientists and engineers*		

E:\200104\tectonic.dwg

Figure 2. Tectonic Sub-Provinces of the Colorado Plateau

- **Rio Grande Rift**

  The Rio Grande Rift (Kirkham and Rogers 1981, DOE 1991a) is a north-south-trending extensional graben feature that extends from Chihuahua, Mexico, to northern Colorado. The rift was initiated in Neogene time and has experienced continued activity through the Quaternary. The rift is characterized by Neogene basin-fill sedimentary rocks; a bimodal suite of mafic and silicic igneous rocks; and abundant features suggesting recently active faults, such as fault scarps in young alluvium, abrupt mountain fronts that exhibit faceted spurs, and deep, narrow linear valleys. A high percentage of all the potentially capable faults in Colorado and New Mexico lie within this province. Well-defined evidence of repeated Late Quaternary movement is abundant on several faults in the southern portion of the province, whereas such evidence is obscure in the northern portion. The closest approach of the Rio Grande Rift to the site area is about 270 km (170 miles).

- **Wyoming Basin**

  The Wyoming Basin (DOE 1991a) consists of a series of broad structural and topographic basins that merge with and resemble the adjoining part of the Colorado Plateau (Hunt 1967). These basins are partly filled with Tertiary deposits and are separated by low anticlinal uplifts of older rocks. The earthquake history of the Wyoming Basin is apparently similar to the widely distributed, low- to moderate-magnitude pattern of the stable interior portion of the Colorado Plateau. Witkind (1975) identified numerous suspected active faults in the Wyoming Basin along the Colorado-Wyoming border between 107 and 108 degrees west longitude, which may represent a continuation of structures associated with the Rio Grande Rift in Colorado. However, these faults are not known to have been associated with seismic activity.

- **Southern Rocky Mountains/Mountain Provinces**

  The Mountain Provinces are divided into the Eastern and Western Mountain Provinces by Kirkham and Rogers (1981). The Eastern Mountain Province includes the Front and Medicine Bow Ranges, Middle and South Parks, and the east flanks of the Mosquito and Sangre de Cristo Ranges. Most of the faults in this province have Laramide, late Paleozoic, or even Precambrian ancestry. Several of the faults show considerable Neogene movement. A few of these faults have moved during the Quaternary. The distribution, orientation, and character of Neogene movement on these faults suggest rejuvenation is related to the extensional stresses responsible for rifting. The Western Mountain Province includes the San Juan Mountains, Elk and West Elk Mountains, west flank of the Sawatch Range, White River uplift, and Gunnison uplift. Neogene faults are relatively scarce in this province. Many of the faults that are present are not truly tectonic features, but rather are the results of evaporate flowage or caldera collapse. Despite an apparent absence of major Neogene tectonic faults, numerous earthquakes have been felt and/or instrumentally located in the province. The site is located approximately 200 km (130 miles) from the nearest portion of the Southern Rocky Mountain province.

Quaternary Faults

Quaternary faults and folds were evaluated using the USGS Quaternary Fault and Fold database (USGS 2002) and the Quaternary Fault and Fold database from the Utah Geological Survey (Black et al. 2003). An initial search for critical Quaternary faults was conducted using the minimum fault lengths given in NRC document 10 CFR 100, Appendix A, as shown in Table 1. In addition to faults included in the Quaternary Fault and Fold database, faults of undetermined age that are shown on geologic maps in the area (Williams 1964, Gualtieri 1988, Witkind 1995, Williams and Hackman 1971), were considered if the PHA associated with these structures (if considered Quaternary) is greater than 0.1 g. Quaternary faults that are within the expanded regional study area are presented in Figure 3 and in Appendix A. Faults that are within 40 miles of the site are shown on Figure 3 and are described below. Faults that are included in the Quaternary Fault and Fold database retain the original four-digit numbering system of the database. Faults from other sources are labeled with a single-digit number.

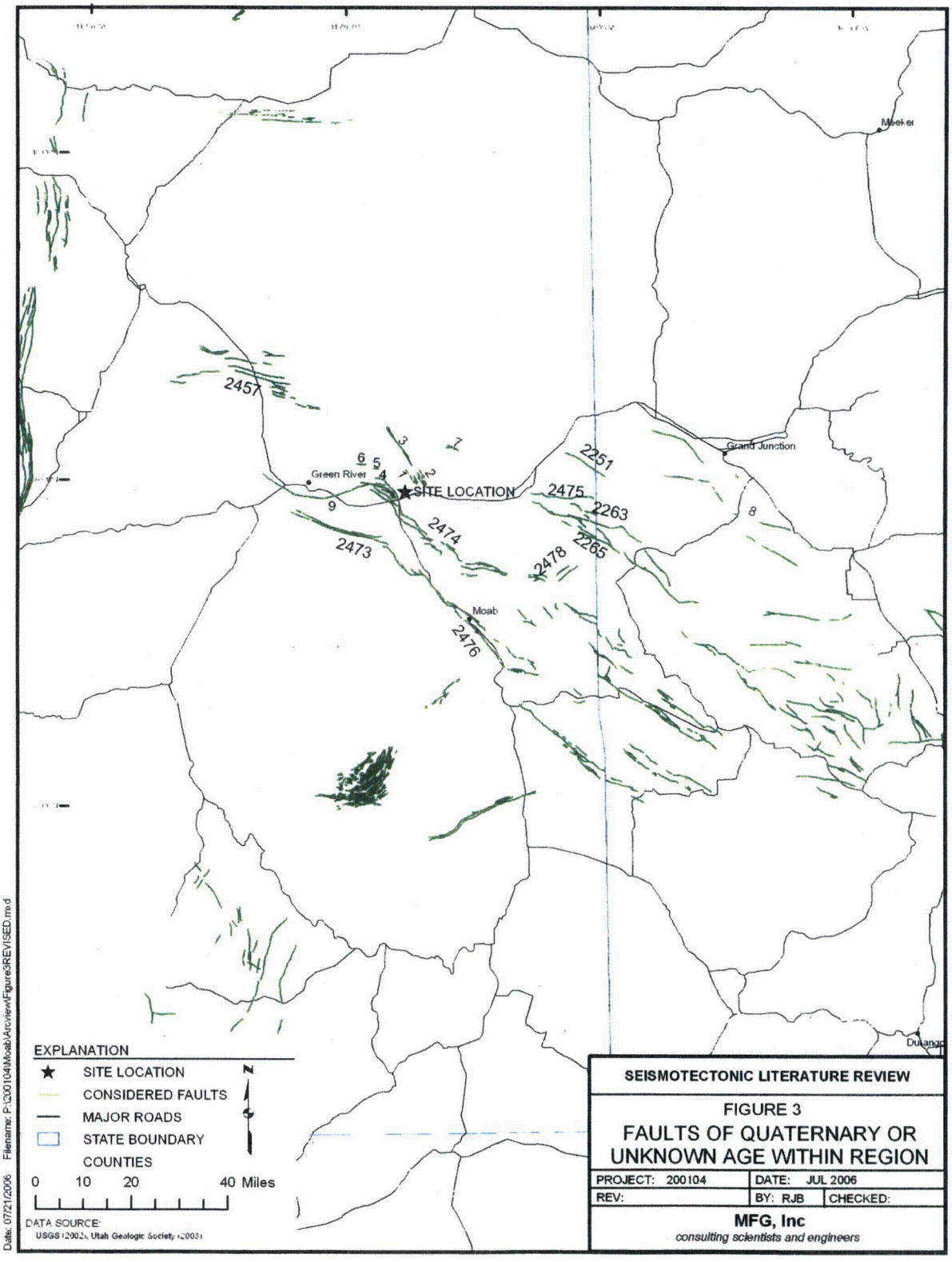

Figure 3. Faults of Quaternary or Unknown Age Within Region

Table 1. Minimum Length of Fault to be Considered in Establishing MCE

Distance from Site		Minimum Length	
Miles	**Kilometers**	**Miles**	**Kilometers**
0 to 20	0 to 32	1	1.6
Greater than 20 to 50	Greater than 32 to 80	5	8
Greater than 50 to 100	Greater than 80 to 161	10	16
Greater than 100 to 150	Greater than 160 to 240	20	32
Greater than 150 to 200	Greater than 240 to 320	40	64

- **Salt Valley and Cache Valley Faults (2474)**

As described in Black et al. (2003), the faults are within a northwest-trending zone of folding, faulting, and warping related to dissolution and collapse of the Salt Valley Anticline in eastern Utah, north of Moab. Collapse of the Salt Valley Anticline appears to largely post-date late Pliocene deposition of exotic fluvial gravels (likely derived from a since-eroded source in the Book Cliffs) on the rim and floor of Salt Valley and formation of an erosion surface on the flank of the anticline. Small depositional basins within Salt Valley containing Bishop ash (~740 thousand years ago [ka]) and Lava Creek B ash (670 ka) were localized by salt dissolution and collapse and/or salt flow during early and middle Quaternary time and record syn and post-depositional folding and faulting. Faults are parallel and appear related to the major older structures of the anticline.

At the lower end of the valley, slightly tilted and relatively undeformed middle- to late-Quaternary basin fill deposits unconformably overlie older, more deformed units. Structural relations exposed at other localities in the valley suggest that Quaternary sediments have been deformed and localized by movement within salt diapirs of the Paradox Formation. Playas and mudflats in upper Salt Valley indicate active deformation (due to salt flow or dissolution) and damming of surface runoff. A stream that crosses the south end of the Salt Valley Anticline at a high angle is entrenched and bordered by probable late-Holocene terraces north of the anticline. The stream is braided and unentrenched in the short reach within Salt Valley, suggesting that the core of the anticline is presently subsiding and causing stream aggradation. In Cache Valley, a Quaternary erosion surface that apparently postdates collapse-related deformation is displaced by a major bedrock fault and may have been tilted. East of Cache Valley, Colorado River terraces are tilted upstream on the upstream side of the Cache Valley Anticline, indicating that salt flowed into the collapsed structure during Quaternary time. The timing of the most recent paleoevent is Quaternary (<1.6 million years ago [Ma]). The slip rate is unknown, but is likely to be less than 0.2 millimeters per year (mm/yr). The length of the fault is 58 km (Black et al. 2003).

Reports by Woodward-Clyde (1984, 1996), based on map and seismic reflection data, found no evidence of Quaternary tectonic deformation of these structures. Surface faults occurred as a result of dissolution and collapse of the salt anticline during the Cenozoic era. Surface faults are not interpreted to extend below the top of salt, limiting the rupture depth to approximately 2 km, and are not structurally related to underlying pre-salt faults. Due to the shallow nature of the faults, large shear stresses are not sustained and potential rupture areas will be limited in extent such that significant earthquakes cannot be generated.

In 1979, a seismic monitoring program was initiated to assess the seismicity of the Paradox Basin at the microearthquake level. The report by Woodward-Clyde (1984) indicated that from 1979 through 1984, only two events were detected in the Salt Valley area (local magnitude (M_L) of 1.2, and 2.1). They concluded that the seismicity associated with the study area is generally diffusely distributed and of low level and small magnitude, consistent with the longer historical record of the interior of the Colorado Plateau. From these data, it is assumed that there is no seismicity associated with the Salt and Cache Valley faults, and the faults are not considered capable.

- **Tenmile Graben (2473)**

  The Tenmile Graben, which is approximately 35 km in length, is a narrow zone of faulting displacing Cretaceous and Jurassic bedrock along Salt Wash southeast of Green River. The graben is on the northwestern edge of an area typified by northwest-trending, elongated oval valleys that are collapsed or depressed anticlines. The graben is probably related to salt dissolution, but was included in the Quaternary Fault and Fold database as a Class B fault to indicate the possibility of a tectonic component (Black et al. 2003). Inclusion in the Quaternary database was based on a possible structural association with the Moab Fault (Hecker 1993). The youngest rocks offset by this fault are the upper members of the Cretaceous Mancos Shale (Doelling 2001). No Tertiary rocks are preserved along the Tenmile Graben. Quaternary alluvium and eolian sediments do not appear offset by any of the faults (Doelling 2001).

  Woodward-Clyde Consultants (1996) evaluated the potential seismic hazards for the uranium mill tailings site in Moab, Utah. Microearthquake studies in the region from 1979 to 1987 show no evidence for earthquakes associated with the Tenmile Graben. Structural incongruities between the Moab faults and the Tenmile Graben suggest that if fault ruptures did occur, they would most likely be arrested at the incongruity. A kinematic incongruity between Tenmile Graben and the Moab faults is indicated by a change in strike of 35 degrees, an opposite sense of total net displacement, and differences in structural style between these faults.

  They concluded that the Tenmile Graben may be structurally related to the Moab Fault in that both may have formed during Tertiary extension, but the fault is not expected to rupture with the Moab Fault, nor is there any definitive evidence that the Tenmile Graben is a capable structure. They found no evidence for Quaternary deformation of the Tenmile Graben and did not consider the graben as a capable fault for seismic-hazard assessment purposes. From these data, it is assumed that there is no seismicity associated with the Tenmile Graben, and the structure is not considered capable.

- **Moab Fault and Spanish Valley Faults (2476)**

  The Moab Fault and Spanish Valley faults are approximately 68 km in length and consist of a northwest-trending zone of faulting and warping from collapse of the Moab Valley Anticline from salt dissolution. The faults are related to salt dissolution, but were included in the Quaternary Fault and Fold database as Class B faults to indicate the possibility of a tectonic component (Black et al., 2003). Inclusion of the Moab and Spanish Valley faults in the Quaternary database was based on indirect geomorphic and stratigraphic evidence, primarily for Quaternary salt-dissolution collapse that may or may not be associated with faulting (Woodward Clyde 1996).

  Collapse of the Moab Valley Anticline appears to largely post-date deposition of early and middle Pleistocene alluvium on and near the rim of the valley (Harden et al. 1985). A well-preserved relic canyon on the rim of Moab Canyon, whose headwaters were apparently removed by collapse of the anticline, probably formed during late Tertiary to early Quaternary time (Oviatt 1988). Distribution of middle Pleistocene through Holocene alluvial deposits suggests differential subsidence in Spanish Valley (due to tectonism or salt dissolution/migration). Marshes at the lower end of Spanish Valley may be evidence of Holocene subsidence. Woodward-Clyde Consultants (1996) indicates the youngest rocks or structures demonstrably displaced by the Moab Fault are Cretaceous or Tertiary in age, and did not consider the faults as capable faults for seismic-hazard assessment purposes. Timing of most recent paleoevent is Quaternary (<1.6 Ma). The slip rate is unknown, but is likely less than 0.2 mm/yr. (Black et al. 2003).

  Based on detailed mapping, structural evidence, and geophysical data, Olig et al. (1996) determined that the faults within the Moab and Spanish Valley are most likely related to salt-dissolution. They concluded that the primary movement on the Moab Fault is tectonic and occurred during a period of Tertiary extension. Everywhere that Quaternary sediments have been mapped in relation to the Moab Fault, they bury the fault and do not appear to be offset by it. In addition, most, if not all, of the slip on the Moab Fault is pre-Quaternary, and that the Moab Fault is a shallow structure that probably soles into the Moab salt-cored anticline within 2-km depth along much of its length. Therefore, it would most likely not be capable of producing significant earthquakes.

A seismographic network operating in the Paradox Basin from 1979 to 1987 revealed no microearthquakes that could definitely be associated with the Moab Fault. A few earthquakes occurred in the vicinity of the fault, but they appear to be part of the broad pattern of scattered seismicity characteristic of the Colorado Plateau interior. Additionally, no earthquakes from 1987 through 1994 have been recorded by the University of Utah Seismographic Stations, which locate events in the vicinity of the Moab Fault (Woodward Clyde 1996). From these data, it is assumed that there is no seismicity associated with the Moab Fault, and the structure is not considered capable.

- **Price River Area Faults (2457)**

  The Price River Area faults are generally east-west striking faults along the Price River west of the Book Cliffs. The faults are in a long, sinuous area along the base of the Book Cliffs termed the Mancos Shale Lowlands and characterized by sloping pediments, rugged badlands, and narrow flat-bottomed alluvial valleys in Cretaceous rock. Some faults within the zone displace pre Wisconsin-age pediments less than 2 meters. Structural relations indicate that the fault zone forms the crest of a broad, collapsed anticline. The fault zone is similar in trend, pattern, and length to faults along the crest of the Moab Valley Anticline (2476), although it is not as strongly developed. The faults are inferred to be related to a salt anticline at the northern margin of the Paradox Basin but were included in the Quaternary Fault and Fold database as Class B faults to indicate the possibility of a tectonic component (Black et al. 2003). Early- to middle-Pleistocene pediments north of the fault zone steepen sharply at the base of the Book Cliffs, and may be warped due to elastic rebound of the Mancos Shale during erosional unloading and/or monoclinal folding. The ancestral course of Whitmore Canyon (near Sunnyside) also appears to be warped. Timing of most recent paleoevent is Quaternary (<1.6 Ma). The slip rate is unknown, but is likely <0.2 mm/yr. The fault length is 51 km. (Black et al. 2003). For the purposes of this report, the Price River Area faults are considered capable faults.

- **Little Dolores River Fault (2251)**

  The Little Dolores River Fault extends from Utah into Colorado on the northeast flank of the Uncompahgre uplift. Evidence for Quaternary movement on this fault was cited in Witkind (1976) based on personal communication with Fred Cater. Based on the timing of abandonment of Unaweep Canyon, Cater (1966) indicated uplift of the Uncompahgre Plateau began in the mid-Pliocene and continued into the Pleistocene, resulting in as much as 640 meters of differential uplift. Despite the lack of evidence of faulted Quaternary deposits along the Little Dolores River Fault, it has been classified as a Quaternary fault (Howard et al. 1978; Kirkham and Rogers 1981; Colman 1985), and no references have been published that refute this age assignment. The timing of the most recent paleoevent is Quaternary (<1.6 Ma). Despite a lack of evidence for offset in Quaternary deposits, faults associated with the Uncompahgre uplift are often considered to have experienced Quaternary movement. The slip-rate category is unknown, but likely less than 0.2 mm/yr. The length of fault is 16 km (Black et al. 2003). For purposes of this report, the Little Dolores River Fault is considered a capable fault.

- **Sand Flat Graben Faults (2475)**

  The Sand Flat Graben faults include the northern graben-bounding fault (Dry Gulch Fault) and subsidiary within the Sand Flat Graben. The southern graben-bounding fault is included in the discussion of the Ryan Creek Fault zone (2263). The faults are west to northwest trending within the Sand Flat Graben along the southwestern margin of the Uncompahgre uplift northeast of the Paradox Basin. The Uncompahgre uplift is a northwest-trending, east-tilted fault block. The Uinta Basin borders the northwest end of the uplift. Faults are part of a regional zone of northwest- to west-trending normal faults along the Utah–Colorado border, within a monoclinal flexure that forms the southwest margin of the Uncompahgre uplift. Different movement histories and cumulative Quaternary displacements have been inferred for the fault zone based on studies of Unaweep Canyon and related drainage changes, but most studies suggest that differential uplift has continued into the early or late Pleistocene. Diversion of drainage (ancestral Colorado River from Unaweep Canyon), which followed impoundment and formation of a lake, occurred about 775 ka (Perry and

Annis 1990). The timing of the most recent paleoevent is Quaternary (<1.6 Ma). The slip rate is unknown, but is likely less than 0.2 mm/yr. The fault length is 23 km. For purposes of this report, the Sand Flat Graben faults are considered capable faults.

- **Ryan Creek Fault Zone (2263)**

  The Ryan Creek Fault zone trends east-west along the southwestern margin of the Uncompahgre uplift. Approximately half of the fault length is in Utah. The fault extends east into Colorado from the flank of Haystack Peaks parallel to Ryan Gulch, and then bends southeast toward Unaweep Canyon. Individual faults in the fault zone form the southern margin of the Sand Flat Graben in Utah and the northeast margin of the Ute Creek Graben in Colorado. The Ryan Creek Fault zone lies on the southwestern margin of the Uncompahgre uplift along the Utah-Colorado border. Evidence for Quaternary movement on this fault zone is cited in Witkind (1976) based on personal communication with Fred Cater. Cater (1966) indicated uplift of the Uncompahgre Plateau began in the mid-Pliocene and continued into the Pleistocene, resulting in as much as 640 meters of differential uplift. Despite the lack of evidence of faulted Quaternary deposits along the Ryan Creek Fault zone, it has been classified as a Quaternary fault (Howard et al. 1978; Kirkham and Rogers 1981; Colman 1985), and no references have been published that refute this age assignment. Timing of the most recent paleoevent is Quaternary (<1.6 Ma). A small earthquake (M_L 2.9) and several aftershocks in 1985 may have occurred on the Ryan Creek Fault zone (Ely et al. 1986). The slip-rate is unknown, but is likely less than 0.2 mm/yr. The fault length is 39 km. (Black et al. 2003). For purposes of this report, the Ryan Creek Fault is considered a capable fault.

- **Granite Creek Fault Zone (2265)**

  The Granite Creek Fault zone is a northwest-trending fault zone, which extends from Utah into Colorado north of Steamboat Mesa on the southwest flank of the Uncompahgre uplift. Williams (1964) mapped Quaternary deposits as both concealing and abutting the fault. Cater (1966) indicated uplift of the Uncompahgre Plateau began in the mid-Pliocene and continued into the Pleistocene, resulting in as much as 640 meters of differential uplift. Despite the lack of evidence of faulted Quaternary deposits along the Granite Creek Fault zone, it has been classified as a Quaternary fault (Kirkham and Rogers 1981; Colman 1985), and no references have been published that refute this age assignment. The Granite Creek Fault zone consists of high-angle normal faults that are mostly down-to-the-northeast. The fault lies in a tectonically weakened area above the ancestral Uncompahgre Fault zone (Stone 1977).

  The possibility of Granite Creek and Ryan Creek fault systems being connected was investigated. However, the two fault systems appear to be separate based on mapping by Doelling (2001) and their depiction in a cross section by Ely et al. (1986). In addition, MCE calculations are based on total length of fault trace from farthest reaches of the fault. Because the Granite Creek and Ryan Creek faults are roughly parallel and overlapping, the total fault trace would not increase if they are considered collectively. Several faults of similar strike parallel the Granite Creek Fault to the northeast. The Granite Creek faults are mostly down to the northeast. Granite Creek faults were named by Heyman (1983), but Doelling (2001) does not show that name for the faults on his map. Both Granite Creek and Ryan Creek faults may merge at depth with the major uplift-bounding (Uncompahgre) reverse fault.

  Offset of Quaternary deposits is inconclusive since Williams (1964) showed Quaternary deposits as abutting against the fault and concealing the fault. However, faults associated with the Uncompahgre uplift are often considered to have experienced Quaternary movement. Based on the timing of abandonment of Unaweep Canyon, Cater (1966) indicated uplift of the Uncompahgre Plateau began in the mid-Pliocene and continued into the Pleistocene, resulting in as much as 640 meters of differential uplift. The slip-rate category is unknown, but is likely less than 0.2 mm/yr. The fault length is 23 km. For purposes of this report, the Granite Creek Fault zone is considered a capable fault.

- **Fisher Valley Faults (2478)**

  The Fisher Valley faults are a result of late Quaternary folding and warping in Fisher Valley from salt dissolution and collapse. Fisher Valley is on the crest of a long anticlinal structure that includes Salt and Cache Valleys in Utah and Sinbad and Roc Creek Valleys in Colorado. The valley formed from collapse of the anticline (Onion Creek diapir) due to salt dissolution. The faults border and define Fisher Valley. Formation of the valley by collapse of the anticline beheaded streams whose broad, shallow channels are preserved on the valley rim. Upper Cenozoic deposits, by far the thickest sequence in the Paradox Basin (>125 meters thick), have ages between greater than 2.5 Ma (based on paleomagnetic analysis) and about 250 ka (based on secondary carbonate accumulation rates) and record episodic deformation from movements of the Onion Creek salt diapir and basin subsidence (resulting from salt flowage into the diapir and/or salt dissolution and collapse). The timing of the most recent paleoevent is Quaternary (<1.6 Ma), based on tephrochronology, soil development, and stream dissection rate. Young basin fill deposits demonstrating recent movement are absent, but evidence for rapid incision (3 mm/y based on 14C dates), and steep, unstable slopes where Onion Creek cuts through the cap rock, suggest that the diapir may be presently active. The slip rate is unknown, but is likely less than 0.2 mm/yr. The fault length is 16 km. (Black et al. 2003). For purposes of this report, the Fisher Valley faults are considered capable faults.

- **Unnamed Faults in the Westwater and Hatch Mesa Quadrangles (1 through 7)**

  The unnamed faults in the Westwater 30-ft × 60-ft quadrangle map are of undocumented age. Faults 1, 2, and 3 are associated with the Thompson Anticline. Walton (1956) early suggested that the Thompson Anticline is on trend with the Onion Creek–Sinbad Valley salt structures and had a similar origin. The pattern of keystone collapse faulting in the Thompson Anticline is characteristic of salt structures. Mobil-American Petrofina Elba Flats unit 1-30 penetrated 178 ft of salt a short distance east of the Sego Canyon quadrangle, showing that salt does extend beneath the Thompson Anticline.

  Mapping by Willis (1986) of the Sego Canyon quadrangle describes the faults as subparallel, high-angle, normal faults that trend N 20° W. Offsets range to nearly 90 ft. Evidence suggests that fault movements in the Sego Canyon quadrangle occurred well after deposition of units and may coincide with uplift of the Colorado Plateau. The movement appears brittle, with jagged, broken sandstone blocks and small splintery branching faults extending from the major ones. Drainage patterns also support late movement on the faults. Late movement and the graben arrangement of the faults support the idea that salt dissolution may be responsible for their presence.

  The faults are described by Gualtieri (1988) as "high-angle normal faults and are the result of subsidence following the exsolution of salt." Thus, the faults may have initiated due to salt movement, similar to other salt-related features of the Paradox Fold and Fault Belt. There is currently a lack of evidence suggesting Quaternary displacement.

  A preliminary field investigation of several of the unnamed faults was conducted by Craig Goodknight of S.M. Stoller and Greg Smith, a consultant, on November 22, 2005. Unnamed faults 1 and 2 were investigated for evidence of Quaternary displacement. These faults, associated with the Thompson Anticline (Willis 1986; Doelling 2001), showed no evidence of Quaternary movement (no Quaternary deposits were displaced by the faults). Farther to the north, unnamed fault 3 was not investigated, but it is of similar strike and also occurs along the Thompson Anticline. It was concluded that no recent movement has occurred along these faults associated with the Thompson Anticline, and that they reflect slow, incipient subsidence related to dissolution of deep salt deposits along the northeast edge of the Paradox Basin. Based on these data, unnamed faults 1, 2, and 3 are not considered capable faults.

  Also as part of the field investigation, several faults in the northern part of the system of Salt and Cache Valley faults were checked for evidence of Quaternary movement. These west-northwest-striking faults are east and west of Floy Wash in the Hatch Mesa 7.5-minute quadrangle (Chitwood 1994; Doelling 2001). Associated with the Salt Valley Anticline, these faults showed no evidence of Quaternary movement (no displacement of Quaternary deposits by the faults). Just to the north of these faults in the Westwater 30-ft × 60-ft quadrangle, unnamed faults 4, 5, and 6 were not

investigated, but are of similar strike and appear to be related to the Salt Valley Anticline. It was similarly concluded that no Quaternary movement has occurred on these faults associated with the Salt Valley Anticline, and that they are also related to dissolution of deep salt deposits in the northern Paradox Basin. Based on these data, unnamed faults 4, 5, and 6 are not considered capable faults.

Unnamed Fault 7 is not related to either the Salt Valley or Thompson anticlines. In mapping of the Sego Canyon quadrangle, Willis (1986) calls this feature the Bull Canyon Fault. He describes it as an east-west-trending fault that crosses the Cisco Anticlinal axis. Wells drilled on the Cisco Anticline encountered Precambrian rocks without passing through Paradox Basin salt-bearing rocks. Overall outcrop patterns suggest that the folding may have occurred between the Late Cretaceous and early Eocene, similar to other structures in the region that have been attributed to Laramide disturbances. Walton (1956) suggests that the Cisco Anticline is directly related to faulting along the steep western flank of the Uncompahgre uplift and is a drape fold over that structure. Additional field investigations into the origin of the fault have not been conducted for this report. For the purposes of this report, unnamed Fault 7 will be considered a capable fault.

- **Cactus Park-Bridgeport Fault**

Seismotectonic stability investigations performed for the uranium mill tailings site at Grand Junction (DOE 1991b) concluded Fault 8 is the design fault for the Grand Junction Site. Although Fault 8 does not meet the minimum requirements as shown in Table 1 for the Crescent Junction site, it is included here for completeness. The fault is referred to as Fault 8 (Fault 71 of Kirkham and Rogers 1981) in the DOE (1991b) report and as "unnamed fault near Bridgeport" in the Quaternary Fault and Fold Database (USGS 2002). It is described as being the eastern extension of the East Creek monocline. Observation by photos, aerial reconnaissance, and in the field showed no evidence of Quaternary activity on this fault. However, based on regional seismicity trends and geologic and geomorphic evidence, the Uncompahgre Uplift may be experiencing regional tectonic movement at the present time. Due to the association of Fault 8 with an active regional structure, the fault was considered capable. The fault was estimated to have a length of 11.0 km, with the closest approach to the Grand Junction site of 9.0 km. The MCE associated with this fault was estimated to have a compressional body wave magnitude (m_b) of 6.8 (based on fault length/magnitude relationship of Bonilla et al 1984). The resulting nonamplified PHA at the Grand Junction Site was estimated to be 0.42 g, based on acceleration/attenuation relationships developed by Campbell (1981) (DOE 1991b).

Fault 8 appears to be the southern portion of the Cactus Park-Bridgeport Fault, as shown in recent mapping of Laramide structures along the northern Uncompahgre Plateau (Livaccari and Hodge 2005). This recent mapping shows the Cactus Park and Bridgeport Fault as connected, with a surface trace approximately 14 miles in length. This west-northwest-striking left lateral strike slip fault is as close as about 8 km to the Cheney Site. Evidence from mapping indicates the fault may have had reactivated Quaternary movement (Livaccari and Hodge 2005). For the purposes of this report, the Cactus Park-Bridgeport Fault is considered a capable fault.

- **Little Grand Wash Fault**

The Little Grand Wash Fault, more recently known as the Little Grand Fault, is an arcuate normal fault/graben system extending over a total length of approximately 47 km. It extends from the northwestern corner of the Salt Valley Graben to the east flank of the San Rafael Swell. Over most of its length it separates the Jurassic Morrison Formation from the Cretaceous Mancos Shale with stratigraphic offsets of several thousand feet. It has not been identified as a suspected Quaternary fault in the Quaternary Fault and Fold Database (Black et al. 2003).

Because of its length and proximity to the Green River Site, this fault was considered to be the most critical fault in the seismotectonic study performed for the Green River Site (DOE 1991a). The fault is clearly marked in the field by prominent bedrock scarps, lithologic changes, and extensive linear travertine deposits such as are presently forming at Crystal Geyser on the Green River approximately 3 km south of the Green River Site. However, detailed examination of the fault trace did not reveal any evidence of Late Quaternary movement. The fault trace, when viewed in detail, is highly dissected and is crossed by numerous washes. Alluvium in these washes shows no evidence of

tectonic disturbance. Talus and colluvial slopes that mantle the fault trace in many places are not deformed. Fault scarps are formed only where rocks of the hanging and foot walls are of contrasting degrees of resistance to erosion. Near Crystal Geyser the contrast of the relatively durable Morrison Formation with the nonresistant Mancos Shale has produced steep cliffs that mark the fault trace. Where shale of similar composition lies on both sides of the fault, scarps are indistinct or absent (DOE 1991a). Mapping done by Chitwood (1994) and Doelling (2001) did not observe any offset of Quaternary deposits.

The evidence from the Green River investigation indicates that the Little Grand Wash Fault is of Laramide age and is not capable under the present seismotectonic regime. The prominent bedrock scarps that mark the fault trace have been produced by erosion during Late Tertiary to Holocene time. Gradual creep, produced by salt solution at depth, may be presently occurring, but no conclusive evidence for it was seen (DOE 1991a). Based on these data, the Little Grand Wash Fault is not considered a capable fault.

Historical Earthquakes

Instrumentally and historically recorded earthquakes within a study area of 200 miles around the site were documented using the National Earthquake Information Center (NEIC) website (NEIC 2005). Databases searched included USGS/NEIC Preliminary Determinations of Epicenters monthly, weekly, and daily listings; Significant U.S. Earthquakes; and Eastern, Central, and Mountain States of the United States. The earthquakes are shown graphically in Figure 4 and also in table form in Appendix B.

Maximum Credible Earthquakes

A study by Kirkham and Rogers (1981) estimated the MCEs of tectonic provinces within the state of Colorado. In addition, the RAP for the Grand Junction/Cheney disposal site (DOE 1991b) estimated maximum earthquakes associated with regional tectonic provinces. Table 2 summarizes these estimates for the provinces within this study region.

Table 2. Estimate of Maximum Credible Earthquakes Associated with Tectonic Provinces

Tectonic Province	Maximum Credible Earthquake (MCE)	
	Kirkham and Rogers (1981)	DOE (1991b)
Rio Grande Rift	6 to 7.5	6.5 to 7.5
Eastern Mountain	6 to 6.75	
Western Mountain	6 to 6.5	
Colorado Plateau	5.5 to 6.5	6.5
Paradox Basin		4 to 5
Intermountain Seismic Belt		7.0-7.9
Wyoming Basin		5.7 to 6.5

Peak Ground Accelerations

A contour map for PHA in rock with 90 percent probability to not being exceeded in 50 years is presented for the contiguous United States by Algermissen et al. (1990), showing the site to have a PHA of 0.025 g. Contour maps developed for the National Seismic Hazard Mapping Project (Frankel et al. 2002a and 2002b) show the peak acceleration to be 0.045 g with a 10 percent probability of exceedance in 50 years, and 0.12 g with a 2 percent probability of exceedance in 50 years.

Halling et al. (2002) developed peak acceleration maps for the State of Utah. In this study, the MCEs for all known or suspected Quaternary faults in the state were calculated using relationships developed by Wells and Coppersmith (1994). Ground motion was attenuated across the state using three different attenuation relationships. Contours of peak horizontal bedrock accelerations were developed. The peak ground acceleration for the Crescent Junction Site was estimated to be approximately 0.5 g.

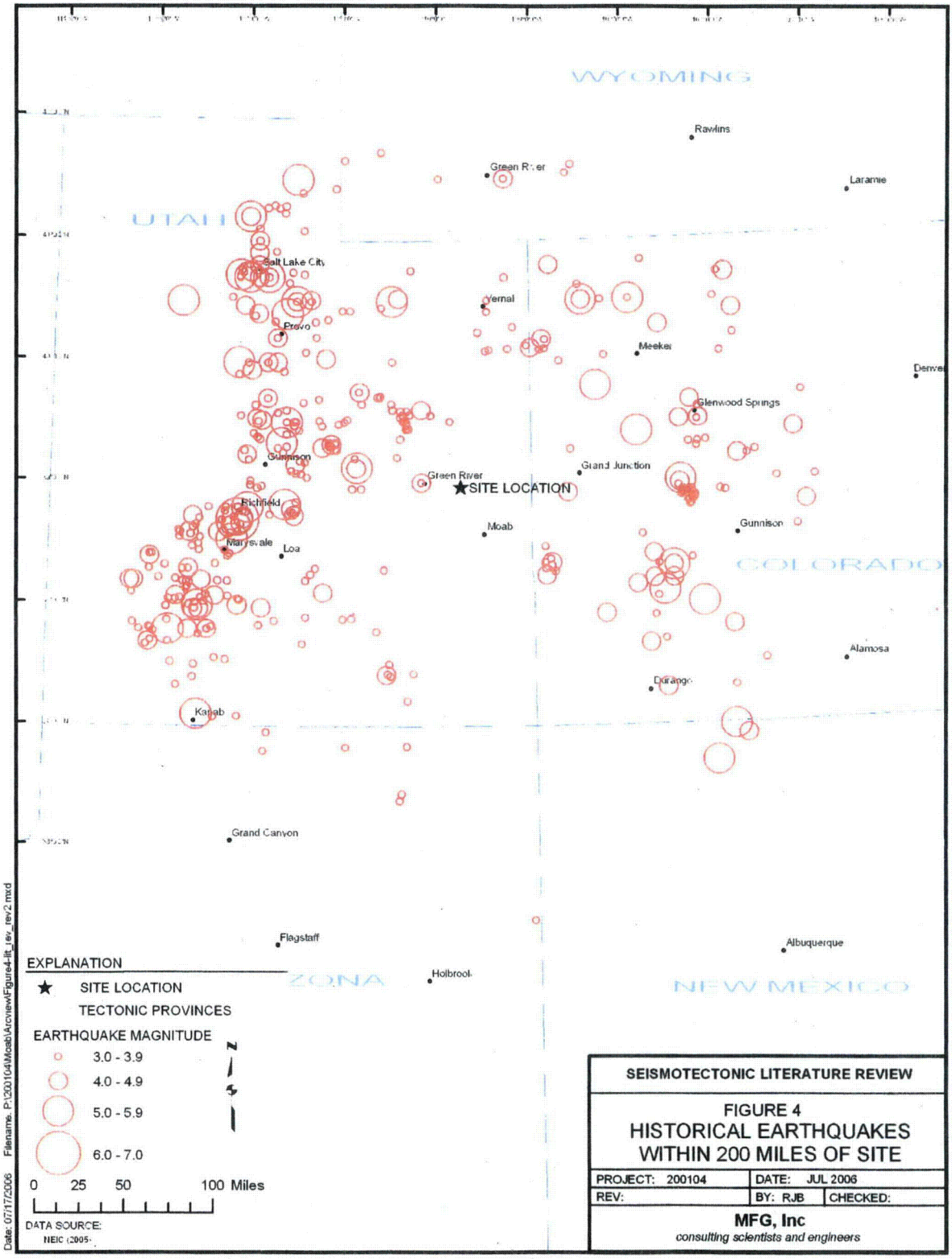

Figure 4. Historical Earthquakes Within 200 Miles of Site

These ground accelerations were predominately influenced by predicted ground motion from the Tenmile Graben Fault.

For comparison purposes only, the peak ground accelerations determined for the UMTRA sites at Green River and Grand Junction/Cheney Disposal Site were investigated. The seismotectonic stability study performed for the Green River Disposal Site recommended the design acceleration based on a floating earthquake of magnitude (ML) 6.2 occurring 15 km (9.5 miles) from the site, resulting in a peak ground acceleration of 0.21 g.

Seismotectonic stability studies done for the Grand Junction mill tailings/Cheney Disposal Site identified a fault (Fault 8) with a length of 11.0 km at a distance of 9.0 km from the site. Although no evidence of Quaternary displacement was proven, it was considered to be capable on the basis of its apparent association with a possibly active regional structure, the Uncompahgre Uplift. This fault was adopted as the design fault for the Cheney Disposal Site, resulting in a recommended design acceleration of 0.42 g.

Conclusion and Recommendations:

A thorough review of available literature that applies to the Crescent Junction Site is required to determine the suitability of the Crescent Junction Disposal Site as the repository for the Moab uranium mill tailings material and to develop the site and regional seismotectonic sections of the RAP The results of this review indicate that there are nine Quaternary fault systems within 40 miles of the site that have been numbered using the identification system in the USGS database. The closest fault systems to the Crescent Junction Site are the Salt Valley and Cache Valley faults (2474). However, these faults appear related to dissolution and collapse of the Salt Valley Anticline in eastern Utah, north of Moab. An additional nine faults have been identified that warrant consideration in the development of the seismicity of the Crescent Junction Site. Further analysis of the faults and historical earthquake events will be performed in additional calculation sets to determine the MCE and associated ground accelerations.

Computer Source:

Not applicable.

References:

10 CFR 100. U.S. Nuclear Regulatory Commission (NRC), "Seismic and Geologic Siting Criteria for Nuclear Power Plants," *Code of Federal Regulations,* Appendix A.

40 CFR 192. U.S. Environmental Protection Agency (EPA), "Promulgated Standards for Remedial Actions at Inactive Uranium Processing Sites," *Code of Federal Regulations,* Subpart A.

Algermissen, S.T., D.M. Perkins, P.C. Thenhause, S.L. Hanson, and B.L. Bender, 1982. *Probabilistic Estimates of Maximum Acceleration and Velocity in Rock in the Contiguous United States*, U.S. Geological Survey Open-File Report 82-1033.

Algermissen, S.T., D.M. Perkins, P.C. Thenhause, S.L. Hanson, and B.L. Bender, 1990. *Probabilistic Earthquake Acceleration and Velocity Maps for the United States and Puerto Rico*, U.S. Geological Survey Miscellaneous Field Studies Map MF-2120.

Allenby, R.J., 1979. Letter section: "Implications of Very Long Baseline Interferometry Measurements on North American Intra-Plate Crustal Deformation," *Tectonophysics*, Vol. 60, pp. T27–T35.

Black, B.D., S. Hecker, M.D. Hylland, G.E. Christenson, and G.N. McDonald, 2003. *Quaternary Fault and Fold Database and Map of Utah*, Utah Geological Survey Map 193DM, CD-ROM, scale 1:500,000.

Campbell, K. W., 1981. *Near-Source Attenuation of Peak Horizontal Acceleration*, Bulletin of the Seismological Society of America, 71(6), pp. 2039–2070, December.

Campbell, K.W., and Y. Bozorgnia, 2003. *Updated Near-Source Ground-Motion (Attenuation) Relations for the Horizontal and Vertical Components of Peak Ground Acceleration and Acceleration Response Spectra,* Bulletin of the Seismological Society of America, 93(1), pp. 314–331, February.

Cater, F.W., Jr., 1966. *Age of the Uncompahgre Uplift and Unaweep Canyon, West-Central Colorado,* U.S. Geological Survey Professional Paper 550-C, pp. C86–C92.

Chitwood, J.P., 1994. *Provisional Geologic Map of the Hatch Mesa Quadrangle, Grand County, Utah,* Utah Geological Survey Map 152, scale 1:24,000.

Colman, S.M., 1985. *Map Showing Tectonic Features of Late Cenozoic Origin in Colorado,* U.S. Geological Survey Miscellaneous Geologic Investigations Map I-1566, scale 1:1,000,000.

DOE (U.S. Department of Energy), 1989. *Technical Approach Document, Revision II,* AL 050425.0002, United States Department of Energy, Uranium Mill Tailings Remedial Action Project, December.

DOE (U.S. Department of Energy), 1991a. *Remedial Action Plan and Final Design for Stabilization of the Inactive Uranium Mill Tailings at Green River, Utah.*

DOE (U.S. Department of Energy), 1991b. *Remedial Action Plan and Site Design for Stabilization of the Inactive Uranium Mill Tailings Site at Grand Junction, Colorado.*

Doelling, H.H., 2001. *Geologic Map of the Moab and Eastern Part of the San Rafael Desert 30' × 60' Quadrangles, Grand and Emery Counties, Utah, and Mesa County, Colorado,* Utah Geological Survey Map 180, scale 1:100,000.

Ely, R.W., I.G. Wong, and P. Chang, 1986. "Neotectonics of the Uncompahgre Uplift, Eastern Utah and Western Colorado," in Rogers, W.P. and R.M. Kirkham, editors, *Contributions to Colorado Seismicity and Tectonics – a 1986 Update,* Colorado Geological Survey Special Publication, pp. 75–92.

Frankel, A., C. Mueller, T. Barnhard, D. Perkins, E. Leyendecker, N. Dickman, S. Hanson, and M. Hopper, 2002a. *Seismic-Hazard Maps for the Conterminous United States, Map A – Horizontal Peak Acceleration With 10% Probability of Exceedance in 50 years,* U.S. Geological Survey Open-File Report 97-131-A.

Frankel, A., C. Mueller, T. Barnhard, D. Perkins, E. Leyendecker, N. Dickman, S. Hanson, and M. Hopper, 2002b. *Seismic-Hazard Maps for the Conterminous United States, Map C – Horizontal Peak Acceleration With 2% Probability of Exceedance in 50 Years,* U.S. Geological Survey Open-File Report 97-131-C.

Gaultieri, J. L, 1988. *Geologic Map of the Westwater 30' × 60' Quadrangle, Grand and Uintah Counties, Utah, and Garfield and Mesa Counties, Colorado,* U.S. Geological Survey Miscellaneous Investigations Series Map I-1765, scale: 1:100,000.

Gutenburg, B., and C.F. Richter, 1956. *Earthquake Magnitude, Intensity, Energy, and Acceleration,* Bulletin of the Seismological Society of America, 46(1), pp. 105–145.

Halling, M.W., J.R. Keaton, L.R. Anderson, and W. Kohler, 2002. *Deterministic Maximum Peak Bedrock Acceleration Maps for Utah,* Utah Geological Survey Miscellaneous Publication 02-11, July.

Harden, D.R., N.E. Biggar, and M.L. Gillam, 1985. "Quaternary Deposits and Soils in and Around Spanish Valley, Utah," in Weide, D.L., editor, *Soils and Quaternary Geology of the Southwestern United States,* Geological Society of America Special Paper 203, pp. 43–64.

Hecker, S., 1993. *Quaternary Tectonics of Utah with Emphasis on Earthquake-Hazard Characterization,* Utah Geological Survey Bulletin 127.

Heyman, O.G., 1983. "Distribution and Structural Geometry of Faults and Folds Along the Northwestern Uncompahgre Uplift, Western Colorado and Eastern Utah," in Averett, W.R., editor, *Northern Paradox Basin – Uncompahgre Uplift*, Grand Junction Geological Society, pp. 45–57.

Howard, K., J. Aaron, E. Brabb, M. Brock, H. Gower, S. Hunt, D. Milton, W. Muehlberger, J. Nakata, G. Plafker, D. Prowell, R. Wallace, and I. Witkind, 1978. *Preliminary Map of Young Faults in the United States as a Guide to Possible Fault Activity*, U.S. Geological Survey Miscellaneous Field Studies Map MF-916, 2 sheets, scale 1:5,000,000.

Hunt, C.B., 1967. *Physiography of the United States*, W.H. Freeman and Company, San Francisco, California.

Jones, R.W., 1959. *Origin of Salt Anticlines of Paradox Basin*, American Association of Petroleum Geologists Bulletin, 43(8), pp. 1869–1895.

Keller, G., L. Braile, and P. Morgan, 1979. *Crustal Structure, Geophysical Models and Contemporary Tectonism of the Colorado Plateau*, Tectonophysics, Vol. 61, pp. 131–147.

Kelley, V.C., 1955. *Regional Tectonics of the Colorado Plateau and Relationship to the Origin and Distribution of Uranium*, University of New Mexico Publications in Geology No. 5.

Kelley, V.C., and N. Clinton, 1960. *Fracture Systems and Tectonic Elements of the Colorado Plateau*, University of New Mexico Publications in Geology No. 6.

Kelley, V.C., 1979. *Tectonics of the Colorado Plateau and New Interpretation of Its Eastern Boundary*, Tectonophysics, Vol. 61, pp. 97–102.

Kirkham, R.M. and W.P. Rogers, 1981. *Earthquake Potential in Colorado, a Preliminary Evaluation*, Colorado Geological Survey Bulletin 43.

Krinitzsky, E.L., and F.K. Chang (1977). *State-of-the-Art for Assessing Earthquake Hazards in the United States, Report 7: Specifying Peak Motions for Design Earthquakes*, U.S. Army Engineer Waterways Experiment Station, Miscellaneous Paper S-74-1, Vicksburg, Mississippi.

Livaccari, R., and J. Hodge, 2005. *Laramide and Quaternary-Age Faulting Along the Northern Uncompahgre Plateau, Western Colorado*, Geological Society of America Abstracts with Programs, Rocky Mountain Section, 37(6) p. 34.

National Earthquake Information Center (NEIC), 2005. *Circular Area Search of Historical Earthquakes*: http://neic.usgs.gov/neis/epic/

Olig, S.S., C.H. Fenton, J. McCleary, and I.G. Wong, 1996. "The Earthquake Potential of the Moab Fault and Its Relation to Salt Tectonics in the Paradox Basin, Utah," in Huffman, A.C., Jr., W.R. Lund, and L.H. Godwin, editors, *Geology and Resources of the Paradox Basin*, Utah Geological Association Guidebook 25, pp. 251–264.

Oviatt, C.G., 1988. "Evidence for Quaternary Deformation in the Salt Valley Anticline, Southeastern Utah," in Doelling H.H., C.G.Oviatt, and P.W. Huntoon, editors, *Salt Deformation in the Paradox Region*, Utah Geological and Mineral Survey Bulletin 122, pp. 63–76.

Perry, T., and D. Annis, 1990. *Pleistocene History of the Gunnison River in Unaweep Canyon, Colorado, and Implications for Colorado Plateau Uplift*, Geological Society of America Abstracts with Programs, 22(3), p. 75.

Richter, C.F., 1958. *Elementary Seismology*, W. H. Freeman and Company, San Francisco, California.

Ryall, A., D. Slemmons, and L. Gedney, 1966. *Seismicity, Tectonism, and Surface Faulting in the Western United States During Historic Time*, Seismological Society of America Bulletin, Vol. 56, pp. 1105–1135.

Shoemaker, E.M., J.E. Case, and D.P. Elston, 1958. "Salt Anticlines of the Paradox Basin," in Sanborn, A.R., editor, *Guidebook to the Geology of the Paradox Basin,* Intermountain Association of Petroleum Geologists, Ninth Annual Field Conference, pp. 39–59.

Smith, R., and M. Sbar, 1974. *Contemporary Tectonics and Seismicity of the Western United States with Emphasis on the Intermountain Seismic Belt*, Geological Society of America Bulletin, Vol. 85, pp. 1205–1218.

Stone, D.S., 1977. "Tectonic History of the Uncompahgre Uplift," in Veal, H.K., editor, *Exploration Frontiers of the Central and Southern Rockies*, Rocky Mountain Association of Geologists, 1977 Field Conference Guidebook, pp. 23–30.

USGS (U.S. Geological Survey), 2002. *Quaternary Fault and Fold Database*, http://Qfaults.cr.usgs.gov/

Walton, P.T., 1956. "Structure of the North Salt Valley-Cisco Area, Grand County, Utah," in Peterson, J.A., ed., *Geology and Economic Deposits of East-Central Utah,* Intermountain Association of Petroleum Geologists, Seventh Annual Field Conference Guidebook, pp. 186–189.

Wells, D.L., and K.J. Coppersmith, (1994). *New Empirical Relationships Among Magnitude, Rupture Length, Rupture Area, and Surface Displacement*, Bulletin of the Seismological Society of America, Vol. 84, pp. 974–1002.

Williams, P. L., compiler, 1964. *Geology, Structure, and Uranium Deposits of the Moab Quadrangle, Colorado and Utah*, U.S. Geological Survey Miscellaneous Geologic Investigations Map I-360, scale 1:250,000.

Williams, P.L., and R.J. Hackman, 1971. *Geology of the Salina Quadrangle, Utah*, U.S. Geological Survey Miscellaneous Geologic Investigations Map I-591, scale 1:250,000.

Willis, G.C., 1986. *Provisional Geologic Map of the Sego Canyon Quadrangle, Grand County, Utah*, Utah Geological and Mineral Survey Map 89, scale 1:24,000.

Witkind, I., 1975. *Preliminary Map Showing Known and Suspected Active Faults in Wyoming*, U.S. Geological Survey Open-File Report 75-249.

Witkind, I., 1976. *Preliminary Map Showing Known and Suspected Active Faults in Colorado*, U.S. Geological Survey Open-File Report 76-154, 42 sheets, scale 1:500,000.

Woodward-Clyde Consultants, 1984. *Geologic Characterization Report for the Paradox Basin Study Region, Utah Study Areas, Volume VI, Salt Valley*, Walnut Creek, California, unpublished consultant's report for Battelle Memorial Institute, Office of Nuclear Waste Isolation, ONWI-290, scale 1:62,500.

Woodward-Clyde Consultants, 1996. *Evaluation and Potential Seismic and Salt Dissolution Hazards at the Atlas Uranium Mill Tailings Site, Moab, Utah,* Oakland, California, unpublished consultant's report for Smith Environmental Technologies and Atlas Corporation, SK9407.

End of current text

Appendix A

Quaternary and Undated Faults Within Expanded Study Region

SITE AND REGIONAL SEISMICITY - RESULTS OF LITERATURE REVIEW
APPENDIX A:
QUATERNARY AND UNDATED FAULTS WITHIN EXPANDED SITE REGION

Name	Number	Age of Most Recent Prehistoric Deformation (ya)	Slip-rate (mm/yr)	Fault Length (km)	Fault Type	Distance from site (miles)[1]
Salt and Cache Valleys faults (Class B)	2474	Class B	<0.2	57.9	N	1.8
unnamed fault in Westwater Quad, R19E, T21S (no. 1)	1			8.0		2.4
unnamed fault in Westwater Quad, R20E, T21S (no. 2)	2			6.4		3.1
unnamed fault in Westwater Quad, R18E, T21S (no. 4)	4			2.9		4.9
unnamed fault in Westwater Quad, R19E, T19S (no. 3)	3			15.7		5.3
Little Grand fault	9			47.0	N	6.5
unnamed fault in Westwater Quad, R18E, T20S (no. 5)	5			1.9		7.0
unnamed fault in Westwater Quad, R17E, T20S (no. 6)	6			3.3		9.6
Ten Mile graben faults (Class B)	2473	Class B	<0.2	34.6	N	10.5
unnamed fault in Westwater Quad, R21E, T0S (no. 7)	7			4.4		12.4
Moab fault and Spanish Valley faults (Class B)	2476	Class B	<0.2	72.4	N	12.5
Price River area faults (Class B)	2457	<1,600,000	<0.2	50.9	N	24.8
Sand Flat graben faults	2475	<1,600,000	<0.2	23.1	N	26.4
Ryan Creek fault zone	2263	<1,600,000	<0.2	39.5	N	26.6
Fisher Valley faults (Class B)	2478	Class B	<0.2	15.9		31.0
Granite Creek fault zone	2265	<1,600,000	<0.2	22.7	N	33.4
Castle Valley faults (Class B)	2477	Class B	<0.2	12.4		34.2
Little Doloras River fault	2251	<1,600,000	<0.2	15.7	R	34.5
unnamed fault in Salina Quad, R13E, T24S				19.6		36.0
Sinbad Valley graben (Class B)	2285	<1,600,000	<0.2	31.8		39.3
Lockhart fault (Class B)	2510	Class B	<0.2	15.7		40.8
Unnamed fault of Lost Horse Basin	2264	<1,600,000	<0.2	8.1		40.8
unnamed fault in Salina Quad, R11E, T22S				22.7		41.6
unnamed fault in Salina Quad, R11E, T21S				14.0		42.1
unnamed fault in Price Quad, R12E, T19S				13.7		42.4
unnamed fault in Salina Quad, R12E, T24S				10.1		42.6
unnamed fault in Salina Quad, R12E, T23S				9.0		43.5
unnamed fault in Salina Quad, R16E, T28S				9.0		43.9
unnamed fault in Salina Quad, R11E, T23S				25.8		44.7
unnamed fault in Salina Quad, R11E, T24S				9.8		47.0
Unnamed fault near Pine Mountain	2267	<1,600,000	<0.2	30.7		47.2
unnamed fault in Price Quad, R16E, T13S				9.5		48.6
Paradox Valley graben (Class B)	2286	<1,600,000	<0.2	56.4	N	49.6
Lisbon Valley fault zone (Class B)	2511	<1,600,000	<0.2	37.5		50.9
Redlands fault complex	2252	<1,600,000	<0.2	21.1	N,R	53.1
Needles fault zone (Class B)	2507	Class B	<0.2	28.5		53.9
Shay graben faults (Class B)	2513	Class B	<0.2	39.5		68.1
Cactus Park-Bridgeport fault	8			22.5		70.0
Big Gypsum Valley graben (Class B)	2288	Class B	<0.2	33.1		70.9
Southern Joes Valley fault zone	2456	<750,000	<0.2	47.2		77.2
Unnamed faults of Pinto Mesa	2277	<1,600,000	<0.2	19.7		78.4
Unnamed faults south of Love Mesa	2271	<1,600,000	<0.2	17.6		78.8
Joes Valley fault zone, east fault	2455	<15,000	0.2-1	56.6		79.0
Duchesne-Pleasant Valley fault system (Class B)	2414	<1,600,000	<0.2	45.3	N	79.1
Monitor Creek fault	2268	<1,600,000	<0.2	30.1		79.1
Joes Valley fault zone, west fault	2453	<15,000	0.2-1	57.2		81.1
Joes Valley fault zone, intragraben faults	2454	<15,000	<0.2	34.0		82.9

Name	Number	Age of Most Recent Prehistoric Deformation (ya)	Slip-rate (mm/yr)	Fault Length (km)	Fault Type	Distance from site (miles)[1]
Pleasant Valley fault zone, unnamed faults	2425	<1,600,000	<0.2	31.0	N	86.1
Pleasant Valley fault zone, graben	2426	<750,000	<0.2	17.6		88.3
Roubideau Creek fault	2270	<15,000	<0.2	20.5		88.7
Bright Angel fault system (Class B)	2514	<1,600,000	<0.2	102.3		89.6
Snow Lake graben	2452	<15,000	<0.2	25.4		89.7
Wasatch monocline (Class B)	2450	<1,600,000	<0.2	103.5	?	90.3
White Mountain area faults	2451	<1,600,000	<0.2	16.4		90.5
Unnamed fault at Red Canyon	2279	<1,600,000	<0.2	24.2		90.9
Gooseberry graben faults	2424	<750,000	<0.2	22.6		93.1
Unnamed faults near San Miguel Canyon (Class B)	2284	Class B	<0.2	32.1		94.5
Thousand Lake fault	2506	<750,000	<0.2	48.3		97.2
Unnamed fault at Hanks Creek	2281	<1,600,000	<0.2	17.5		99.0
Gunnison fault	2445	<15,000	<0.2	42.0	N	104.3
Aquarius and Awapa Plateaus faults	2505	<1,600,000	<0.2	35.7		108.6
Red Rocks fault	2291	<1,600,000	<0.2	38.3		111.8
Valley Mountains monocline (Class B)	2449	<1,600,000	<0.2	38.6		112.9
Paunsaugunt fault	2504	<1,600,000	<0.2	44.1		118.0
Wasatch fault zone, Nephi section	2351h	<15,000	1-5	43.1		119.9
Wasatch fault zone, Provo section	2351g	<15,000	1-5	58.8		122.2
Sevier fault	2355	<1,600,000	<0.2	41.3	N	126.4
East Tintic Mountains (west side) faults	2420	<750,000	<0.2	33.1		129.6
Sevier Valley-Marysvale-Circleville area faults	2500	<750,000	<0.2	34.9		133.7
Bear River fault zone	730	<15,000	0.2-1	33.2		140.4
Hogsback fault, southern section	732b	<130,000	1-5	38.3		144.3
Cannibal fault	2337	<130,000	<0.2	49.3		148.9
Sevier/Toroweap fault zone, Sevier section	997a	<130,000	0.2-1	88.7		155.4
West Kaibab fault system	994	<1,600,000	<0.2	82.9	N	187.7
Frontal fault	2302	<130,000	0.2-1	75.0	N,R	190.1
Central Kaibab fault system	993	<1,600,000	<0.2	71.5	N	192.3
Sevier/Toroweap fault zone, northern Toroweap section	997b	<130,000	<0.2	80.9		198.5
Almy fault zone	742	<1,600,000	<0.2	10.7		
Andrus Canyon fault	1013	<1,600,000	<0.2	5.6		
Annabella graben faults	2472	<15,000	<0.2	12.5		
Antelope Range fault	2517	<750,000	<0.2	24.5		
Arrowhead fault zone	953	<130,000	<0.2	5.2		
Aubrey fault zone	995	<130,000	<0.2	53.1		
Babbitt Lake fault zone	954	<750,000	<0.2	7.6		
Bald Mountain fault	2390	<1,600,000	<0.2	2.3		
Bangs Canyon fault	2256	<1,600,000	<0.2	6.3		
Basalt Mountain fault (Class B)	2299	Class B	<0.2	7.0		
Bear Lake (west side) fault (Class B)	2531	<1,600,000	<0.2	5.5		
Bear River Range faults	2410	<1,600,000	<0.2	62.9	N, D	
Beaver Basin faults, eastern margin faults	2492a	<15,000	<0.2	34.2		
Beaver Basin faults, intrabasin faults	2492b	<15,000	<0.2	38.9		
Beaver Ridge faults	2464	<130,000	<0.2	14.2		
Big Pass faults	2366	<1,600,000	<0.2	17.3		
Black Mesa fault zone	2006	<1,600,000	<0.2	18.5		
Black Mountains faults	2487	<750,000	<0.2	25.9		
Black Point/Doney Mountain fault zone	957	<750,000	<0.2	23.8	N	
Black Rock area faults	2461	<130,000	<0.2	8.2		
Blue Springs Hills faults	2363	<750,000	<0.2	2.5		
Bright Angel fault zone	991	<1,600,000	<0.2	66.0	N	

Name	Number	Age of Most Recent Prehistoric Deformation (ya)	Slip-rate (mm/yr)	Fault Length (km)	Fault Type	Distance from site (miles)[1]
Broadmouth Canyon faults	2377	<130,000	<0.2	3.4		
Buckskin Valley faults (Class B)	2499	Class B	<0.2	3.5		
Busted Boiler fault	2274	<130,000	<0.2	18.0		
Cactus Park fault	2258	<1,600,000	<0.2	1.9		
Calabacillas fault	2035	<750,000	<0.2	31.3		
Cameron graben and faults	988	<750,000	<0.2	10.8		
Campbell Francis fault zone	959	<750,000	<0.2	10.1		
Canones fault (Class B)	2003	<1,600,000	<0.2	29.4		
Cataract Creek fault zone	990	<1,600,000	<0.2	51.1	N	
Cattle Creek anticline (Class B)	2293	Class B	<0.2	8.6		
Cedar City-Parowan monocline (and faults)	2530	<15,000	<0.2	24.8		
Cedar Ranch fault zone	961	<750,000	<0.2	10.2		
Cedar Valley (north end) faults	2529	<130,000	<0.2	15.5		
Cedar Valley (south side) fault	2408	<750,000	<0.2	2.8		
Cedar Valley (west side) faults	2527	<750,000	<0.2	12.8		
Cedar Wash fault zone	962	<750,000	<0.2	11.6		
Chicken Springs faults	780	<15,000	<0.2	13.7		
Cimmarron fault, Blue Mesa section	2290c	<1,600,000	<0.2	22.5		
Cimmarron fault, Bostwick Park section (Class B)	2290a	Class B	<0.2	11.2		
Cimmarron fault, Poverty Mesa section (Class B)	2290b	Class B	<0.2	24.1		
Citadel Ruins fault zone	963	<1,600,000	<0.2	4.5		
Clear Lake fault zone (Class B)	2436	<15,000	<0.2	35.5		
Clover fault zone	2396	<130,000	<0.2	4.0		
County Dump fault	2038	<1,600,000	<0.2	35.3		
Cove Fort fault zone (Class B)	2491	Class B	<0.2	22.2		
Crater Bench faults	2433	<15,000	<0.2	15.9		
Crawford Mountains (west side) fault	2346	<130,000	<0.2	25.3		
Cricket Mountains (north end) faults	2434	<750,000	<0.2	2.8		
Cricket Mountains (west side) fault	2460	<15,000	<0.2	41.0		
Cross Hollow Hills faults	2524	<1,600,000	<0.2	5.3		
Curlew Valley faults	3504	<15,000	<0.2	20.0		
Dayton fault (Class B)	2370	Class B	<0.2	16.3		
Deadman Wash faults	964	<1,600,000	<0.2	1.8		
Deep Creek Range (east side) faults	2416	<750,000	<0.2	20.7		
Deep Creek Range (northwest side) fault zone	2403	<130,000	<0.2	10.7		
Deseret faults	2435	<750,000	<0.2	7.1		
Diamond Gulch faults	2393	<1,600,000	<0.2	20.2		
Doloras fault zone (Class B)	2289	Class B	<0.2	15.2		
Dolphin Island fracture zone	2367	<750,000	<0.2	19.2		
Double Knobs fault	966	<1,600,000	<0.2	6.0		
Double Top fault zone	965	<1,600,000	<0.2	6.1		
Drum Mountains fault zone	2432	<15,000	<0.2	51.5	N	
Dry Wash fault and syncline	2496	<130,000	<0.2	18.6		
Duncomb Hollow fault	743	<1,600,000	<0.2	2.4		
Dutchman Draw fault	1003	<130,000	<0.2	16.3	N	
East Cache fault zone, central section	2352b	<15,000	0.2-1	16.5		
East Cache fault zone, northern section	2352a	<750,000	<0.2	25.7		
East Cache fault zone, southern section	2352c	<130,000	<0.2	22.1		
East Canyon (east side) fault (Class B)	2350	<1,600,000	<0.2	28.9		
East Canyon fault, Northern East Canyon section (Class B)	2354a	Class B	<0.2	22.5		
East Canyon fault, Southern East Canyon section	2354b	<750,000	<0.2	8.4		
East Dayton-oxford fault	3509	<130,000	<0.2	23.2	N	

Name	Number	Age of Most Recent Prehistoric Deformation (ya)	Slip-rate (mm/yr)	Fault Length (km)	Fault Type	Distance from site (miles)[1]
East Great Salt Lake fault zone, Antelope Island section	2369c	<15,000	0.2-1	35.1		
East Great Salt Lake fault zone, Fremont Island section	2369b	<15,000	0.2-1	30.1		
East Great Salt Lake fault zone, Promontory section	2369a	<15,000	0.2-1	49.2	N	
East Kamas fault	2391	<1,600,000	<0.2	14.6		
East Lakeside Mountains fault zone	2368	<1,600,000	<0.2	36.0		
East Pocatello valley faults	3507	<15,000	<0.2	6.8		
Eastern Bear Lake fault, central section	2364b	<15,000	<0.2	23.8		
Eastern Bear Lake fault, southern section	2364c	<15,000	0.2-1	34.8		
Eastern Bear Valley fault (Class B)	734	Class B	<0.2	47.2		
Eastern Pilot Range fault	2371	<1,600,000	<0.2	10.6		
East-Side Chase Gulch fault	2317	<130,000	<0.2	30.7		
Ebert Tank fault zone	967	<750,000	<0.2	3.1		
Eleven Mile fault	2318	<130,000	<0.2	4.7		
Elk Mountain fault	736	<1,600,000	<0.2	7.8		
Ellison Gulch scarp (Class B)	2304	Class B	<0.2	1.2		
Elsinore fault (fold)	2470	<1,600,000	<0.2	28.1		
Embudo fault, Hernandez section	2007b	<1,600,000	<0.2	31.6		
Embudo fault, Pilar section	2007a	<130,000	<0.2	38.7		
Eminence fault zone	992	<1,600,000	<0.2	36.0		
Enoch graben faults	2528	<15,000	<0.2	17.2		
Enterprise faults	2516	<750,000	<0.2	8.4		
Escalante Desert (east side) faults	2526	<15,000	<0.2	6.4		
Escalante Desert faults (Class B)	2488	Class B	<0.2	6.6		
Escalante Desert faults near Zane	2518	<130,000	<0.2	3.9		
Faults in Raft River Valley	3503	<750,000	<0.2	35.2		
Faults near Garcia	2323	<130,000	<0.2	3.4		
Faults near Monte Vista	2315	<1,600,000	<0.2	16.2		
Faults near of Cochiti Pueblo	2142	<1,600,000	<0.2	32.2		
Faults north of Placitas	2043	<750,000	<0.2	10.5		
Faults of Cove Creek Dome	2462	<1,600,000	<0.2	18.8		
Faults of the northern Basaltic Hills	2322	<1,600,000	<0.2	12.6		
Faults on north flank of Phil Pico Mountains	744	<130,000	<0.2	4.4		
Fish Springs fault	2417	<15,000	<0.2	29.7		
Foote Range fault	2429	<750,000	<0.2	3.1		
Fremont Wash faults	2495	<750,000	<0.2	7.2		
Frog Valley fault	2389	<1,600,000	<0.2	4.6		
Gallina fault	2001	<1,600,000	<0.2	39.3		
Glade Park fault	2254	<1,600,000	<0.2	9.4	R	
Goose Creek Mountains faults (Class B)	2356	Class B	<0.2	4.0		
Grand Hogback monocline (Class B)	2331	Class B	<0.2	22.0		
Grand Wash fault zone	1005	<130,000	<0.2	34.9	N	
Gray Mountain faults	1018	<1,600,000	<0.2	23.6		
Greenhorn Mountain fault (Class B)	2297	Class B	<0.2	21.5		
Grouse Creek and Dove Creek Mountains faults	2357	<750,000	<0.2	47.7		
Guaje Mountain fault	2027	<15,000	<0.2	10.7		
Gunlock fault (Class B)	2515	Class B	<0.2	7.5		
Gyp Pocket graben and faults	1001	<130,000	<0.2	11.8	N	
Hansel Mountains (east side) faults	2359	<750,000	<0.2	14.7		
Hansel Valley (valley floor) faults	2360	<750,000	<0.2	19.5		
Hansel Valley fault	2358	<150	<0.2	13.0		
Hidden Tank fault zone	970	<750,000	<0.2	10.2		
Hogsback fault, northern section	732a	<750,000	0.2-1	22.4		

Name	Number	Age of Most Recent Prehistoric Deformation (ya)	Slip-rate (mm/yr)	Fault Length (km)	Fault Type	Distance from site (miles)[1]
House Range (west side) fault	2430	<15,000	<0.2	45.5	N	
Hurricane fault zone, Anderson Junction section	998c	<15,000	0.2-1	42.2		
Hurricane fault zone, Ash Creek section	998b	<15,000	<0.2	32.0		
Hurricane fault zone, Cedar City section	998a	<15,000	<0.2	13.2		
Hurricane fault zone, Shivwitz section	998d	<130,000	<0.2	56.5	N	
Hurricane fault zone, southern section	998f	<1,600,000	<0.2	66.6	N	
Hurricane fault zone, Whitmore Canyon section	998e	<15,000	<0.2	28.5		
Hyrum fault	2374	<1,600,000	<0.2	3.1		
James Peak fault	2378	<130,000	<0.2	6.3		
Japanese and Cal Valleys faults	2447	<750,000	<0.2	30.1		
Jemez-San Ysidro fault, Jemez section	2029a	<1,600,000	<0.2	24.1		
Jemez-San Ysidro fault, San Ysidro section	2029b	<1,600,000	<0.2	30.1		
Johns Valley fault (Class B)	2539	Class B	<0.2	2.1		
Joseph Flats area faults and syncline (Class B)	2468	Class B	<0.2	3.2		
Juab Valley (west side) faults (Class B)	2423	<750,000	<0.2	13.2		
Judd Mountain fault	1597	<1,600,000	<0.2	20.4		
Killarney faults	2336	<1,600,000	<0.2	5.6		
Kolob Terrace faults	2525	<750,000	<0.2	12.1		
Koosharem fault	2503	<1,600,000	<0.2	2.2		
La Bajada fault	2032	<1,600,000	<0.2	40.3		
La Canada del Amagre fault zone	2005	<1,600,000	<0.2	17.2		
Ladder Creek fault	2255	<1,600,000	<0.2	6.2		
Lakeside Mountains (west side) fault (Class B)	2384	Class B	<0.2	4.7		
Large Whiskers fault zone	972	<1,600,000	<0.2	11.6		
Las Tablas fault	2020	<1,600,000	<0.2	14.8		
Lee Dam faults	973	<1,600,000	<0.2	7.6		
Leupp faults	1017	<750,000	<0.2	32.2		
Lime Mountain fault	2415	<1,600,000	<0.2	10.6		
Little Diamond Creek fault	2411	<750,000	<0.2	20.0		
Little Rough Range faults	2458	<750,000	<0.2	3.2		
Little Valley faults	2439	<15,000	<0.2	19.2		
Littlefield Mesa faults	1008	<750,000	<0.2	21.2		
Lobato Mesa fault zone	2004	<1,600,000	<0.2	21.3		
Lockwood Canyon fault zone	974	<1,600,000	<0.2	20.8		
Log Hill Mesa graben	2275	<130,000	<0.2	9.5		
Long Ridge (northwest side) fault	2422	<1,600,000	<0.2	20.8		
Long Ridge (west side) faults	2421	<750,000	<0.2	15.2		
Lookout Pass fault	2404	<1,600,000	<0.2	3.9		
Los Cordovas faults	2022	<1,600,000	<0.2	12.2		
Lucky Boy fault	2314	<1,600,000	<0.2	11.1		
Main Street fault zone	1002	<130,000	<0.2	87.3	N	
Malpais Tank faults	975	<750,000	<0.2	4.6		
Mantua area faults	2373	<750,000	<0.2	21.1		
Maple Grove faults	2443	<15,000	<0.2	12.8		
Markagunt Plateau faults (Class B)	2535	<750,000	<0.2	56.4		
Martin Ranch fault	731	<15,000	0.2-1	3.7		
Maverick Butte faults	976	<750,000	<0.2	3.7		
Meadow-Hatton area faults	2466	<15,000	<0.2	4.0		
Mesa Butte North fault zone	987	<1,600,000	<0.2	22.6		
Mesita fault	2015	<130,000	<0.2	27.9		
Mesquite fault	1007	<130,000	<0.2	36.2		
Michelbach Tank faults	978	<750,000	<0.2	13.4		

Name	Number	Age of Most Recent Prehistoric Deformation (ya)	Slip-rate (mm/yr)	Fault Length (km)	Fault Type	Distance from site (miles)[1]
Mineral Hot Springs fault	2320	<130,000	<0.2	7.8		
Mineral Mountains (northeast side) fault (Class B)	2490	Class B	<0.2	14.2		
Mineral Mountains (west side) faults	2489	<15,000	<0.2	36.6		
Morgan fault, central section	2353b	<15,000	<0.2	4.9		
Morgan fault, northern section	2353a	<750,000	<0.2	7.9		
Morgan fault, southern section	2353c	<750,000	<0.2	2.3		
Mosquito fault	2303	<130,000	<0.2	51.5		
Mountain Home Range (west side) faults	2480	<1,600,000	<0.2	26.4		
Nacimiento fault, northern section	2002a	<1,600,000	<0.2	35.9		
Nacimiento fault, southern section	2002b	<1,600,000	<0.2	45.2		
Nambe fault	2024	<1,600,000	<0.2	47.8		
North Bridger Creek fault	737	<1,600,000	<0.2	4.2		
North Hills faults	2522	<750,000	<0.2	5.0		
North of Wah Wah Mountains faults	2459	<750,000	<0.2	12.5		
North Promontory fault	2361	<15,000	<0.2	25.8		
North Promontory Mountains fault	2362	<1,600,000	<0.2	6.3		
Northern Boundary fault system	2309	<750,000	<0.2	49.0		
Northern Sangre de Cristo fault, Blanca section	2321c	<15,000	<0.2	6.7		
Northern Sangre de Cristo fault, Crestone section	2321a	<15,000	<0.2	79.1	N	
Northern Sangre de Cristo fault, San Luis section	2321d	<15,000	<0.2	59.1	N	
Northern Sangre de Cristo fault, Zapata section	2321b	<15,000	<0.2	25.8		
Ogden Valley North Fork fault	2376	<750,000	<0.2	26.1		
Ogden Valley northeastern margin fault	2379	<1,600,000	<0.2	12.8		
Ogden Valley southwestern margin faults	2375	<750,000	<0.2	17.8		
Oquirrh fault zone	2398	<15,000	<0.2	21.1		
Overton Arm faults	1119	<130,000	<0.2	50.9		
Pajarito fault	2008	<130,000	<0.2	49.4		
Paragonah fault	2534	<130,000	0.2-1	27.2		
Parleys Park faults (Class B)	2388	Class B	<0.2	3.4		
Parowan Valley faults	2533	<15,000	<0.2	16.3		
Pavant faults	2438	<15,000	<0.2	30.1		
Pavant Range fault	2442	<15,000	<0.2	14.2		
Pearl Harbor fault zone	981	<1,600,000	<0.2	15.3		
Picuris-Pecos fault	2023	<1,600,000	<0.2	98.2	N	
Pilot Range faults	1599	<1,600,000	<0.2	40.2		
Pine Ridge faults (Class B)	2512	Class B	<0.2	5.5		
Pine Valley (south end) faults	2482	<1,600,000	<0.2	10.7		
Pine Valley faults	2481	<750,000	<0.2	3.7		
Pleasant Valley fault zone, Dry Valley graben	2427	<750,000	<0.2	12.4		
Pojoaque fault zone	2010	<1,600,000	<0.2	46.5		
Porcupine Mountain faults	2380	<130,000	<0.2	34.6	N	
Pot Creek faults	2394	<1,600,000	<0.2	13.4		
Puddle Valley fault zone	2383	<15,000	<0.2	6.5		
Puye fault	2009	<130,000	<0.2	16.7		
Raft River Mountains fault	2448	<750,000	<0.2	1.5		
Red Canyon fault scarps	2471	<15,000	<0.2	9.4		
Red Hills fault	2532	<130,000	<0.2	13.8		
Red House faults	983	<750,000	<0.2	3.4		
Red River fault zone	2019	<1,600,000	<0.2	10.0		
Rendija Canyon fault	2026	<130,000	<0.2	11.1		
Ridgway fault	2276	<1,600,000	<0.2	23.8		
Rimmy Jim fault zone	984	<1,600,000	<0.2	8.2		

Name	Number	Age of Most Recent Prehistoric Deformation (ya)	Slip-rate (mm/yr)	Fault Length (km)	Fault Type	Distance from site (miles)[1]
Rock Creek fault	729	<15,000	0.2-1	40.5	N	
Round Valley faults	2400	<750,000	<0.2	12.8	N	
Ryckman Creek fault	740	<1,600,000	<0.2	5.3		
Sage Valley fault	2444	<1,600,000	<0.2	10.5		
Saint John Station fault zone	2397	<130,000	<0.2	5.2		
Saleratus Creek fault	2365	<750,000	<0.2	37.6		
San Felipe fault, Algodones section	2030b	<1,600,000	<0.2	15.9		
San Felipe fault, Santa Ana section	2030a	<1,600,000	<0.2	43.8		
San Francisco fault	2031	<1,600,000	<0.2	25.7		
San Francisco Mountains (west side) fault	2486	<750,000	<0.2	41.4		
Sand Hill fault zone	2039	<1,600,000	<0.2	35.6		
Sawatch fault, northern section	2308a	<130,000	<0.2	34.0		
Sawatch fault, southern section	2308b	<15,000	<0.2	41.1		
Sawyer Canyon fault	2028	<130,000	<0.2	8.4		
Scipio fault zone	2441	<15,000	<0.2	12.5		
Scipio Valley faults	2440	<15,000	<0.2	7.3		
Sevier Valley fault	2502	<1,600,000	<0.2	7.4		
Sevier Valley faults and folds (Class B)	2537	<130,000	<0.2	23.6		
Sevier Valley faults north of Panguitch	2536	<130,000	<0.2	6.2		
Sevier/Toroweap fault zone, central Toroweap section	997c	<15,000	<0.2	60.4	N	
Sevier/Toroweap fault zone, southern Toroweap section	997d	<750,000	<0.2	18.8		
Shadow Mountain grabens	989	<750,000	<0.2	10.4		
Sheeprock fault zone	2405	<130,000	<0.2	11.7		
Sheeprock Mountains fault	2419	<1,600,000	<0.2	6.7		
Silver Island Mountains (southeast side) fault	2382	<15,000	<0.2	1.8		
Silver Island Mountains (west side) fault	2381	<1,600,000	<0.2	6.4		
Simpson Mountains faults	2418	<750,000	<0.2	10.8		
Sinagua faults	986	<130,000	<0.2	4.9		
Sinbad Valley graben (Class B)	2385	<1,600,000	<0.2	9.9		
Skull Valley (mid-valley) faults	2387	<15,000	<0.2	54.8	N	
Snake Valley fault	1246	<15,000	<0.2	41.1		
Snake Valley faults	2428	<15,000	<0.2	45.3	N	
South Granite Mountains fault system, Seminoe Mountains section (Class B)	779e	Class B	<0.2	35.0		
Southern Oquirrh Mountains fault zone	2399	<130,000	<0.2	24.1		
Southern Sangre de Cristo fault zone, San Pedro section	2017a	<130,000	<0.2	24.4		
Southern Sangre de Cristo fault, Cañon section	2017e	<15,000	<0.2	15.2		
Southern Sangre de Cristo fault, Hondo section	2017d	<15,000	<0.2	22.2		
Southern Sangre de Cristo fault, Questa section	2017c	<15,000	<0.2	17.8		
Southern Sangre de Cristo fault, Urraca section	2017b	<15,000	<0.2	21.9		
Southern Snake Range fault zone	1433	<130,000	<0.2	27.5	N	
SP fault zone	958	<130,000	<0.2	12.5		
Spring Creek fault	738	<1,600,000	<0.2	2.3		
Spry area faults	2498	<750,000	<0.2	5.1		
Stansbury fault zone	2395	<15,000	<0.2	49.8	N	
Stinking Springs fault	2413	<130,000	0.2-1	10.0		
Strawberry fault	2412	<15,000	<0.2	31.9		
Strong fault	2021	<1,600,000	<0.2	8.1		
Sublette Flat fault	733	<750,000	<0.2	36.0		
Sugarville area faults	2437	<15,000	<0.2	4.3		
Sunshine faults	1000	<130,000	<0.2	29.2	N	
Sunshine Trail graben and faults	999	<130,000	<0.2	17.0	N	

Name	Number	Age of Most Recent Prehistoric Deformation (ya)	Slip-rate (mm/yr)	Fault Length (km)	Fault Type	Distance from site (miles)[1]
Sunshine Valley faults	2016	<130,000	<0.2	14.1		
Swasey Mountain (east side) faults	2431	<750,000	<0.2	3.8		
Tabernacle faults	2465	<15,000	<0.2	7.9		
The Pinnacle fault	739	<1,600,000	<0.2	2.3		
Tijeras-Cañoncito fault system, Galisteo section	2033a	<1,600,000	<0.2	37.1		
Topliff Hill fault zone	2407	<130,000	<0.2	19.9		
Towanta Flat graben (Class B)	2401	<750,000	<0.2	5.2		
Tushar Mountains (east side) fault	2501	<1,600,000	<0.2	18.5		
Uinkaret Volcanic field faults	1012	<1,600,000	<0.2	18.5		
Unnamed fault along Grand Hogback monocline (Class B)	2292	Class B	<0.2	2.4		
Unnamed fault at Big Dominquez Creek	2260	<1,600,000	<0.2	3.9		
Unnamed fault at Little Dominquez Creek	2261	<1,600,000	<0.2	14.2		
Unnamed fault at northwest end of Paradox Valley (Class B)	2287	Class B	<0.2	5.1		
Unnamed fault east of Whitewater	2257	<1,600,000	<0.2	1.9		
Unnamed fault near Bridgeport	2259	<1,600,000	<0.2	11.0		
Unnamed fault near Escalante	2262	<1,600,000	<0.2	1.6		
Unnamed fault near Johnson Spring	2282	<1,600,000	<0.2	7.1		
Unnamed fault near Wolf Hill	2266	<1,600,000	<0.2	15.2		
Unnamed fault north of Horsefly Creek	2280	<1,600,000	<0.2	8.1		
Unnamed fault of Missouri Peak	2312	<130,000	<0.2	5.9		
Unnamed fault south of Shavano Peak	2311	<1,600,000	<0.2	5.8		
Unnamed fault southeast of China Mountain	1598	<1,600,000	<0.2	2.9		
Unnamed fault west of Buena Vista	2310	<1,600,000	<0.2	2.7		
Unnamed fault west of White Rock Mountains	1437	<1,600,000	<0.2	27.7		
Unnamed fault zone in Ferber Hills	1721	<1,600,000	<0.2	37.3		
Unnamed faults along the Grand Hogback monocline near Fourmile Creek (Class B)	2294	Class B	<0.2	2.5		
Unnamed faults along the Grand Hogback monocline near Freeman Creek (Class B)	2295	Class B	<0.2	5.7		
Unnamed faults at Clay Creek	2283	<1,600,000	<0.2	9.2		
Unnamed faults east of Atkinson Masa	2269	<1,600,000	<0.2	41.1	N	
Unnamed faults east of Roubideau Creek (Class B)	2272	Class B	<0.2	11.7		
Unnamed faults in Williams Fork Valley	2300	<750,000	<0.2	18.4		
Unnamed faults near Burns (Class B)	2296	Class B	<0.2	13.3		
Unnamed faults near Cottonwood Creek	2278	<1,600,000	<0.2	10.8		
Unnamed faults near Loma Barbon	2045	<1,600,000	<0.2	1.2		
Unnamed faults near Picuda Peak	2041	<1,600,000	<0.2	10.6		
Unnamed faults near Twin Lakes Reservoir	2307	<1,600,000	<0.2	14.0		
Unnamed faults northwest of Leadville	2306	<1,600,000	<0.2	18.8		
Unnamed faults of Jemez Mountains, caldera margin section (Class B)	2143c	<750,000	<0.2	20.3		
Unnamed faults of Jemez Mountains, intracaldera section (Class B)	2143d	<1,600,000	<0.2	11.3	N	
Unnamed faults of Jemez Mountains, Toledo caldera section (Class B)	2143b	<1,600,000	<0.2	10.9		
Unnamed faults of Jemez Mountains, Valles caldera section (Class B)	2143a	<1,600,000	<0.2	16.7		
Unnamed faults of Red Hill (Class B)	2298	Class B	<0.2	6.1		
Unnamed faults on southeast side of Kern Mountains	1256	<1,600,000	<0.2	11.4	N	
Unnamed faults south of Leadville	2305	<1,600,000	<0.2	12.8		
Unnamed faults southeast of Montrose (Class B)	2273	Class B	<0.2	9.2		
Unnamed syncline northeast of Carbondale (Class B)	2333	Class B	<0.2	1.5		

Name	Number	Age of Most Recent Prehistoric Deformation (ya)	Slip-rate (mm/yr)	Fault Length (km)	Fault Type	Distance from site (miles)[1]
Unnamed syncline northwest of Carbondale (Class B)	2334	Class B	<0.2	1.9		
Unnamed syncline southwest of Carbondale (Class B)	2332	Class B	<0.2	3.0		
Unnamed syncline west of Carbondale (Class B)	2335	Class B	<0.2	0.6		
Utah Lake faults	2409	<15,000	<0.2	30.8		
Vernon Hills fault zone	2406	<130,000	<0.2	3.7		
Villa Grove fault zone	2319	<15,000	<0.2	19.0		
Volcano Mountain faults	2520	<750,000	<0.2	2.9		
Wah Wah Mountains (south end near Lund) fault	2485	<130,000	<0.2	40.2		
Wah Wah Mountains faults	2483	<1,600,000	<0.2	53.6		
Wah Wah Valley (west side) faults (Class B)	2484	Class B	<0.2	2.1		
Wasatch fault zone, Brigham City section	2351d	<15,000	0.2-1	37.3		
Wasatch fault zone, City section	2351a	<130,000	<0.2	39.6		
Wasatch fault zone, Clarkston Mountain section	2351b	<130,000	<0.2	10.4		
Wasatch fault zone, Collinston section	2351c	<15,000	<0.2	29.7		
Wasatch fault zone, Fayette section	2351j	<15,000	<0.2	15.6		
Wasatch fault zone, Levan section	2351i	<15,000	<0.2	30.1		
Wasatch fault zone, Salt Lake City section	2351f	<15,000	1-5	42.5		
Wasatch fault zone, Weber section	2351e	<15,000	1-5	56.2		
Washington fault zone, Mokaac section	1004b	<130,000	<0.2	11.2	N	
Washington fault zone, northern section	1004a	<15,000	<0.2	36.2	N	
Washington fault zone, Sullivan Draw section	1004c	<130,000	<0.2	34.5	N	
West Cache fault zone, Clarkston fault	2521a	<15,000	0.2-1	13.0		
West Cache fault zone, Junction Hills fault	2521b	<15,000	<0.2	24.3		
West Cache fault zone, Wellsville fault	2521c	<15,000	<0.2	19.9		
West Pocatello Valley faults	3506	<1,600,000	<0.2	7.7		
West Valley fault zone, Granger fault	2386b	<15,000	0.2-1	16.0	N	
West Valley fault zone, Taylorsville fault	2386a	<15,000	<0.2	15.1	N	
Western Bear Lake fault	622	<15,000	<0.2	58.2		
Western Bear Valley faults	735	<1,600,000	<0.2	12.4		
Western Boundary fault	2313	<1,600,000	<0.2	20.1		
West-Side Chase Gulch fault	2316	<130,000	<0.2	2.7		
Wheeler fault zone and graben	1006	<750,000	<0.2	45.3		
White Sage Flat faults	2467	<130,000	<0.2	11.8		
Whitney Canyon fault	741	<15,000	<0.2	5.5		
Williams Fork Mountains fault	2301	<15,000	0.2-1	37.7		
Woodruff fault	3508	<1,600,000	<0.2	12.5		
Yampai graben	996	<1,600,000	<0.2	6.9		
Zia fault	2046	<750,000	<0.2	32.4		

Class B=Geologic evidence demonstrates the existence of Quaternary deformation, but either (1) the fault might not extend deeply enough to be a potential source of significant earthquakes, or (2) the currently available geologic evidence is too strong to confidently assign the feature to Class C but not strong enough to assign it to Class A.
Fault Type: N=normal, R=reverse, D=Dextral

[1]Distance from site only measured for those faults meeting the minimum length requirements as given in NRC 10 CFR part 100, Appendix A. Other faults have minimal impact on site.

Appendix B

NEIC: Earthquake Search Results

SITE AND REGIONAL SEISMICITY - RESULTS OF LITERATURE REVIEW
APPENDIX B:
NEIC: Earthquake Search Results

UNITED STATES GEOLOGICAL SURVEY

EARTHQUAKE DATA BASE

FILE CREATED: Tue Jul 26 09:46:31 2005
Circle Search Earthquakes= 598
Circle Center Point Latitude: 38.970N Longitude: 109.790W
Radius: 320.000 km
Catalog Used: PDE
Data Selection: Historical & Preliminary Data
Catalog Used: PDE
Data Selection: Preliminary Data Only
Catalog Used: SRA
Data Selection: Eastern, Central and Mountain States of U.S. (SRA)
Catalog Used: USHIS
Data Selection: Significant U.S. Earthquakes (USHIS)

This file includes all earthquakes in PDE, SRA, and USHIS databases within 200 miles (320 km) of site with magnitudes greater than or equal to 3.0 and intensities greater than or equal to 4.0.
Data has been declustered to remove aftershocks and foreshocks

CATALOG SOURCE	DATE YEAR	MO	DA	ORIGIN TIME	COORDINATES LAT	LONG	DEPTH km	MAGNITUDES mb	Ms	Other Value	Other Scale	INFORMATION (see below for explanation of symbols) INT	EF	MAP	FPS	MO	DEP	IDE	PFD	FLG	D	T	S	V	N	W	G	RADIAL DIST (km)	Converted Magnitude
	Largest magnitude earthquake possible for region 016 as determined by Algermissen et al. (1982)																											29	6.1
	at furthest distance from site such that PHA from event is 0.1 g or greater																												
SRA	1850	2	22	22	40.7	-111.8						4																257	3.7
SRA	1853	12	1	1845	40	-111.8						5																207	4.3
SRA	1859	8	28		37.7	-112.8						4																298	3.7
SRA	1871	10			40.5	-108.5						6																202	5.0
SRA	1873	7	31	315	38.3	-112.6						5																255	4.3
SRA	1873	12	27	3	41	-111.9						4																288	3.7
SRA	1874	6	18	6	40.7	-111.8						4																257	3.7
SRA	1876	3	22		39.5	-111.6						6																166	5.0
SRA	1877	1	1		38.8	-112.1						4																201	3.7
SRA	1878	8	14		38.6	-112.6						5																247	4.3
SRA	1880	9	17	627	40.7	-111.8						5																257	4.3
SRA	1882	2	11	830	37.3	-107						4																306	3.7
SRA	1883	9	28	11	39.9	-112.1						4																223	3.7
SRA	1885	10	26	610	38.3	-113						4																289	3.7
SRA	1885	12	17	1	38.2	-112.3						4																234	3.7
SRA	1887	12	5	1530	37.1	-112.5						6																315	5.0
SRA	1889	1	15	22	39.5	-107.3						5																222	4.3
SRA	1889	12	7	11	39.3	-111.6						4																160	3.7
SRA	1891	12		21	40.5	-108						6																228	5.0
SRA	1894	1	1	10	37.9	-107.8						4																210	3.7
SRA	1894	2	5	330	38.8	-112.4						4																227	3.7
SRA	1894	7	18	2250	41.2	-112						6																311	5.0
SRA	1895	3	22	20	40.5	-107.1						4																286	3.7
SRA	1895	7	27	2225	39.5	-111.5						4																158	3.7
SRA	1896	9	12	130	39.7	-111.8						4																191	3.7
SRA	1897	8	3	7	38.2	-107.8						5																193	4.3
SRA	1899	11	10	9	38.3	-112.6						4																255	3.7
SRA	1899	12	13	1350	40.7	-111.8						4																257	3.7
SRA	1899			230	40.5	-108						4																228	3.7
SRA	1900	5	0	0	36.9	-106.9						5																	4.3
SRA	1900	8	1	745	40	-112.1						7																229	5.7
SRA	1901	8	11	18	40.2	-111.7						4																213	3.7
SRA	1901	11	14	432	38.7	-112.1						9																202	7.0
SRA	1901	11	15	10	38.8	-106.2						5																311	4.3
SRA	1902	7	31	7	38.3	-112.6						4																255	3.7

CATALOG SOURCE	DATE			ORIGIN	COORDINATES		DEPTH	MAGNITUDES				INFORMATION (see below for explanation of symbols)																RADIAL DIST. (km)	Converted Magnitude
										Other		INT	EFF	MAP	FPS	MO	DEP	IDE	PFD	FLG	D	T	S	V	N	W	G		
	YEAR	MO	DA	TIME	LAT	LONG	km	mb	Ms	Value	Scale																		
SRA	1903	7	23	834	41.1	-111.9						4																297	3.7
SRA	1906	4			40.5	-108.3						4																212	3.7
SRA	1906	5	24	2110	41.2	-112						5																311	4.3
SRA	1908	4	15		38.4	-113						5																286	4.3
SRA	1910	1	10	13	38.7	-112.1						6																202	5.0
SRA	1910	5	22	1428	40.7	-111.8						7																257	5.7
SRA	1910	7	26	130	41.5	-109.3						5																283	4.3
SRA	1913	10	20	10	37.8	-112.4						4																262	3.7
SRA	1913	11	11	2155	38.1	-107.7						6																206	5.0
SRA	1914	4	8	1606	41	-111.9						5																288	4.3
SRA	1914	5	13	1715	41.2	-112						7																311	5.7
SRA	1915	7	15	22	40.4	-111.6						6																221	5.0
SRA	1915	8	11	1020	40.5	-112.7						6																301	5.0
SRA	1916	2	5	625	40	-111.8						5																207	4.3
SRA	1919	5	7	2330	39.5	-111.6						4																166	3.7
SRA	1920	12	29	250	39.5	-107.5						5																206	4.3
SRA	1921	2	4	826	38.6	-106.3						4																305	3.7
SRA	1921	9	29	1412	38.7	-112.1				5.2	UK	8																202	5.2
SRA	1923	5	14	1210	38.2	-113.2						5																309	4.3
SRA	1926	12	19	330	40	-112						4																221	3.7
SRA	1928	4	30	1550	37.8	-107						5																276	4.3
SRA	1930	7	28	935	41.5	-109.3						4																283	3.7
SRA	1932	11	11	10	40.5	-111.5						4																224	3.7
SRA	1933	1	20	1305	37.8	-112.8						6																293	5.0
SRA	1934	4	7	216	41.5	-111.5				5.5	ML	3																316	5.5
SRA	1935	7	9	1059	40.7	-111.8						4																257	3.7
SRA	1935	10	6	3	37.9	-111.4						4																183	3.7
SRA	1937	2	18	630	37.8	-112.6						5																277	4.3
SRA	1938	6	30	1337	40.7	-111.8						5																257	4.3
SRA	1940	11	23	13	39.3	-111.6						4																160	3.7
SRA	1941	8	29	1134	37.3	-107.7						5																260	4.3
SRA	1942	3	28	141030	38.5	-112.5						4																241	3.7
SRA	1942	6	4	2304	39.6	-111.6						4																171	3.7
SRA	1942	7	23	1940	40.5	-108.5						5																202	4.3
SRA	1943	1	16	115018	37.7	-113						5																313	4.3
SRA	1943	2	22	1420	40.7	-112						6																269	5.0
SRA	1943	3	12	1345	39.4	-111.6						4																163	3.7
SRA	1943	8	14	540	38.2	-111.4						4																164	3.7
SRA	1943	11	3	1030	38.6	-112.3						5																221	4.3
SRA	1944	9	9	41220	39	-107.5						6																198	5.0
SRA	1944	10	5	1405	39.2	-106.8						4																259	3.7
SRA	1945	3	28	1040	39.7	-111.8						4																191	3.7
SRA	1945	4	29	1708	37.7	-107.7						4																230	3.7
SRA	1945	11	18	10741	38.8	-112						6																192	5.0
SRA	1946	1	31	2245	39.6	-107.3						4																225	3.7
SRA	1946	10	25	1653	40.7	-112.1						4																275	3.7
SRA	1947	3	28	1102	40.7	-111.9						5																263	4.3
SRA	1948	11	4	1318	39.3	-111.6						4																160	3.7
SRA	1949	3	7	650	40.7	-111.8						6																257	5.0
SRA	1950	1	18	15551	40.5	-110.5				5.3	UK	5																180	5.3
SRA	1950	5	5	735	38.2	-112.2						4																226	3.7
SRA	1950	5	8	2235	40	-111.7						5																200	4.3
SRA	1951	1	23	1333	39.7	-111.8						4																191	3.7
SRA	1951	8	12	26	40.2	-111.7						5																213	4.3
SRA	1952	7	22	1	40	-111.8						4																207	3.7
SRA	1952	9	28	20	40.4	-111.9						5																240	4.3
SRA	1953	4	18	515	38.6	-112.1						4																204	3.7
SRA	1953	5	24	25429	40.5	-111.5						5																224	4.3
SRA	1953	7	30	545	39	-110.2						5																35	4.3
SRA	1953	8	16	16	40.8	-112						4																277	3.7
SRA	1953	10	22	3	37.8	-112.4						5																262	4.3
SRA	1954	2	21	202051	40	-108.75						4																145	3.7

CATALOG SOURCE	DATE			ORIGIN	COORDINATES		DEPTH	MAGNITUDES				INFORMATION (see below for explanation of symbols)																RADIAL DIST (km)	Converted Magnitude
										Other		INT	EFF	MAP	FPS	MO	DEP	IDE	PFD	FLG	D	T	S	V	N	W	G		
	YEAR	MO	DA	TIME	LAT	LONG	km	mb	Ms	Value	Scale																		
SRA	1954	3	31	14	39	-110.2						4																35	3.7
SRA	1955	2	2	1923	40.8	-111.9						5																271	4.3
SRA	1955	2	10	1730	40.4	-106.9						5																294	4.3
SRA	1955	3	27	1213	38.3	-111.3						4																150	3.7
SRA	1955	5	12	2257	40.9	-111.9						5																279	4.3
SRA	1955	8	3	63942	38	-107.3						6																242	5.0
SRA	1956	2	12	3	40.5	-109.5						4																171	3.7
SRA	1956	10	3	202140	41.5	-110						4																281	3.7
SRA	1957	7	18	152420	40	-110.5						4																129	3.7
SRA	1958	2	13	2252	40.5	-111.5						6																224	5.0
SRA	1958	11	28	133039	39.7	-111.8						5																191	4.3
SRA	1958	12	11	930	39.5	-111						4																119	3.7
SRA	1959	2	27	221952	38	-112.5						6																259	5.0
SRA	1959	9	17	620	38.4	-112.2						4																218	3.7
SRA	1960	10	11	80530.5	38.3	-107.6	49			5.5	mb	6																204	5.5
SRA	1960	10	17	16	39.2	-106.9						5																251	4.3
SRA	1961	4	16	50239.3	39.33	-111.65						6																165	5.0
SRA	1961	5	6	161220.7	39.6	-110.2	25					5																78	4.3
SRA	1961	11	27	5545.7	39	-106.1	33					4																319	3.7
SRA	1962	1	13	1333	38.4	-107.8				4.4	ML	4																184	4.4
SRA	1962	2	5	144551.1	38.2	-107.6	25			4.7	ML	5																208	4.7
SRA	1962	6	5	222945	38	-112.1	33			4.5	ML																	228	4.5
SRA	1962	8	19	173241.4	38.05	-112.09	7			3.2	ML																	224	3.2
SRA	1962	9	5	160427.8	40.72	-112.09	7	5.1		5.2	ML	6																276	5.2
SRA	1962	9	7	165023.8	39.2	-110.89	7			3.1	ML																	98	3.1
SRA	1962	12	11	102813.5	39.36	-110.42	7			3.4	ML																	69	3.4
SRA	1963	4	15	221824.6	39.59	-110.35	7	4.2		3.4	ML														N				3.4
SRA	1963	4	24	133303.3	39.44	-110.33	7	4.6		3.3	ML														N				3.3
SRA	1963	6	19	83844.9	38.02	-112.53	7	4.2		3.7	ML																	261	3.7
SRA	1963	7	7	192039.6	39.53	-111.91	7	4.9		4.4	ML	6																193	4.4
SRA	1963	7	9	202525.8	40.03	-111.19	7	4.1		4	ML		F															168	4.0
SRA	1963	9	30	91739.3	38.1	-111.22	7	4.5		4.3	ML																	157	4.3
SRA	1963	11	13	61730.1	38.3	-112.66	7	3.8		3.2	ML																	260	3.2
SRA	1963	12	24	145108.8	39.56	-110.32	7	4.1		3	ML														N				3
SRA	1964	1	17	1503.5	38.19	-112.62	7			3.3	ML																	261	3.3
SRA	1964	8	5	151756.2	38.95	-110.92	7			3	ML																	97	3.0
SRA	1964	8	24	15100.6	38.77	-112.23	7			3.1	ML																	212	3.1
SRA	1964	9	6	190333.8	39.18	-111.46	7			3.1	ML																	146	3.1
SRA	1965	1	14	123010.8	39.44	-110.35	7	4.5		3.3	ML														N				3.3
SRA	1965	5	30	173104.1	39.4	-106.3	33	4.3																				305	4.3
SRA	1965	6	27	192408.7	39.51	-110.38	7	4		3.1	ML	3																	
SRA	1965	6	29	74628.7	39.5	-110.39	7	4.3		3.2	ML																		
SRA	1965	7	13	180315.4	37.71	-112.98	7			3	ML																	311	3.0
SRA	1965	7	18	35551.4	39.5	-109.9	33	3.1																				59	3.1
SRA	1965	7	20	144924.9	38.03	-112.44	7			3	ML																	253	3.0
SRA	1965	9	10	214744.6	39.43	-111.47	7			3	ML																	153	3.0
USHIS	1966	1	23	15638	36.98	-107.02	3	5.1		4.99	Mw	7	F																5.0
SRA	1966	4	23	202053.3	39.1	-111.55	7	4.4		3.5	ML																	153	3.5
SRA	1966	5	20	134047.9	37.98	-111.85	7	4.3		4.1	ML																	210	4.1
SRA	1966	7	6	54708.4	40.09	-108.95	7	4.1		3.7	ML																		3.7
SRA	1966	7	30	32531	39.44	-110.36	7	4.1		3.1	ML																		
SRA	1966	9	4	95234.5	38.3	-107.6	33	4.2																				204	4.2
SRA	1966	10	21	71348.9	38.2	-113.16	7			4.2	ML																	305	4.2
SRA	1966	11	1	74028	40.2	-106.9	33	4		3.9	ML																	283	3.9
SRA	1966	11	11	164534.6	39.6	-110.5	15	3.2																	N				
SRA	1966	12	19	205233.3	39	-106.5	5	4.6		3.3	ML	3																284	3.3
SRA	1967	1	12	35206.2	38.98	-107.51	33	4.4																				197	4.4
SRA	1967	1	16	92245.9	37.67	-107.86	33	4.1																				221	4.1
SRA	1967	1	18	61200.6	40.05	-107.05	33	3.8																				264	3.8
SRA	1967	2	5	100716.6	39.55	-110.1	33	3																				69	3.0
SRA	1967	2	15	32803.5	40.11	-109.05	7	4.5		4	ML	5																141	4.0
SRA	1967	4	4	225339.5	38.32	-107.75	33	4.5		3	ML																	191	3.0

CATALOG SOURCE	DATE			ORIGIN	COORDINATES		DEPTH	MAGNITUDES				INFORMATION (see below for explanation of symbols)																	RADIAL DIST (km)	Converted Magnitude
										Other		INT	EFF	MAP	FPS	MO	DEP	IDE	PFD	FLG	D	T	S	V	N	W	G		
	YEAR	MO	DA	TIME	LAT	LONG	km	mb	Ms	Value	Scale																			
SRA	1967	7	22	215127.4	38.8	-112.22	7	4.2		3.6	ML																		211	3.6
SRA	1967	9	24	50028.6	40.71	-112.1	7	3.7		3	ML	5																	276	3.0
SRA	1967	10	4	102012.8	38.54	-112.16	7	5.2		5.2	ML	7																	211	5.2
SRA	1967	10	25	24134.6	39.47	-110.35	0	4		3.2	ML																		73	3.2
SRA	1967	10	25	55308.8	39.46	-110.34	2	4		3.1	ML																			
SRA	1967	12	7	133322.5	41.29	-111.74	7	4.3		3.7	ML	3																	306	3.7
SRA	1967	12	10	193000.1	36.68	-107.21	0	5.1																	N					5.1
SRA	1968	1	16	94252.1	39.27	-112.04	7	4		3.9	ML																		197	3.9
SRA	1968	2	20	63426.4	41.72	-110.61	7	3.7		3.2	ML																		313	3.2
SRA	1968	6	2	185923.2	39.21	-110.45	7	3.8		3.3	ML																		62	3.3
SRA	1968	6	23	201613	39.31	-107.41	33	3.8																					209	3.8
SRA	1968	9	24	21049.6	38.04	-112.08	7	4		3.6	ML																		224	3.6
SRA	1968	11	17	143338.2	39.52	-110.97	7	4.6		3.5	ML																		118	3.5
SRA	1969	4	10	83705.5	38.66	-112.07	7			3.6	ML																		200	3.6
SRA	1969	5	23	52451.6	39.02	-111.97	7	4		3.3	ML																		188	3.3
SRA	1969	9	10	210000.1	39.41	-107.95	0	5.3				5													N					5.3
SRA	1970	2	3	55935.6	37.92	-108.31	33	4																					173	4.0
SRA	1970	2	21	61348	39.49	-110.35	7	4.1		3.1	ML																		75	3.1
SRA	1970	4	14	104054.1	39.65	-110.82	7	4.2		3	ML																		116	3.0
SRA	1970	4	18	104211	37.87	-111.72	7	4.4		3.7	ML																			3.7
SRA	1970	4	21	85352.4	40.1	-108.9	4	4.3		3.9	ML	5																	146	3.9
SRA	1970	5	23	225523.2	38.06	-112.47	7	4.6		3.9	ML																		254	3.9
SRA	1970	10	25	74821.9	39.17	-111.41	7			3.1	ML																		141	3.1
SRA	1971	1	7	203952.1	39.49	-107.31	33	4.3		3.8	ML	5																	221	3.8
SRA	1971	3	18	90859.9	40.7	-106.97	10	4.4				5																	308	4.4
SRA	1971	4	22	230102.8	39.41	-111.94	7			3.1	ML	3																	191	3.1
SRA	1971	6	23	60835.9	38.61	-112.71	7	4.6		3.1	ML																		256	3.1
SRA	1971	7	10	172236.8	40.24	-109.6	7	3.8		3.7	ML																		141	3.7
SRA	1971	11	10	141023	37.8	-113.1	7	4.5		3.7	ML		F																316	3.7
SRA	1971	11	12	93044.6	38.91	-108.68	5			4	ML	3																	96	4.0
SRA	1971	12	15	125814.5	36.791	-111.824	5			3	ML																		300	3.0
SRA	1972	1	3	102038.9	38.65	-112.17	7	4.6		4.4	ML	6																	209	4.4
SRA	1972	6	2	31548.2	38.67	-112.07	7	4.6		4	ML	5																	200	4.0
SRA	1972	10	1	194229.5	40.51	-111.35	7	4.7		4.3	ML	6																	216	4.3
SRA	1972	10	16	214931.2	40.42	-111.02	7	4.1		3.4	ML	4																		3.4
SRA	1972	11	16	21745.2	37.53	-112.77	7			3.6	ML	3																	305	3.6
PDE	1973	2	9	173837	36.43	-110.425	5			3.2	ML						4		P										287	3.2
SRA	1973	2	18	93139.6	38.1	-113.18	7			3.3	ML																		310	3.3
SRA	1973	5	17	16	39.793	-108.366	0	5.4	4.1	5.7	UK						3		P						E					5.7
PDE	1973	7	16	63642.8	39.149	-111.508	10	4.2									1		P										149	4.2
PDE	1974	3	31	115847.1	40.703	-107.053	5			3.5	ML	2	F				4		P										303	3.5
PDE	1974	4	29	73551.8	37.814	-112.983	5	4.4		3.2	ML	3	F				4		P										306	3.2
PDE	1974	11	4	90228	38.341	-112.325	17	4.3		3.9	ML	3	F				4		P										231	3.9
PDE	1975	1	30	144840.3	39.27	-108.646	5	4.4		3.7	ML		F				4		P										104	3.7
PDE	1975	9	10	63942.5	38.483	-112.563	5			3.3	ML		F				4		P										247	3.3
PDE	1975	10	6	155046.9	39.072	-111.447	5	4.2		3.2	ML	2	F				4		P										143	3.2
SRA	1976	4	19	233545.5	35.39	-109.1	5			3.5	ML	5													?					3.5
SRA	1976	7	30	221900.2	40.75	-110.3	7			3.1	MD																		202	3.1
SRA	1976	8	13	103021.1	38.42	-112.18	7			3.1	MD																		216	3.1
PDE	1976	8	19	132953.3	39.272	-111.08	2			3.3	ML						4		P										116	3.3
PDE	1976	10	6	111504.1	39.081	-111.505	2			3	ML						4		P										148	3.0
SRA	1976	11	26	222629.4	39.51	-111.26	7			3.1	ML																		140	3.1
PDE	1977	2	9	4216.4	39.306	-111.154	7			3.4	ML		F				4		P										123	3.4
SRA	1977	6	3	13722	39.65	-110.51	7			3.2	MD																		97	3.2
PDE	1977	9	24	111648.4	39.309	-107.311	5	4		3	ML						4		P										217	3.0
SRA	1977	9	30	101920	40.47	-110.47	6	5		4.5	ML	6																		4.5
SRA	1977	11	29	213123.4	36.82	-110.99	7			3	MD																		260	3.0
SRA	1978	2	24	194948.8	38.33	-112.84	2			3.5	ML																		274	3.5
PDE	1978	3	9	63051.8	40.761	-112.081	9			3.3	ML	6	D				4		P										279	3.3
PDE	1978	5	29	164518	39.275	-107.322	5			3	ML						4		P										216	3.0
PDE	1978	9	23	82006.6	39.319	-111.093	2			3	ML						4		P										119	3.0
PDE	1978	12	9	145948.3	38.658	-112.527	4			3.3	ML						4		P										240	3.3

CATALOG SOURCE	DATE			ORIGIN	COORDINATES		DEPTH	MAGNITUDES				INFORMATION (see below for explanation of symbols)																	RADIAL DIST (km)	Converted Magnitude
										Other		INT	EFF	MAP	PS	MO	DEP	IDE	PFD	FLG	D	T	S	V	N	W	G		
	YEAR	MO	DA	TIME	LAT	LONG	km	mb	Ms	Value	Scale																			
PDE	1979	1	20	65908.4	40.818	-107.861	5			3.3	ML						4		P										263	3.3
PDE	1979	2	24	124338.2	41.653	-110.998	5			3.5	ML						4		P										314	3.5
PDE	1979	3	19	145929.7	40.177	-108.895	2			3.3	ML	4	F				4		P										154	3.3
PDE	1979	4	30	20710.3	37.883	-111.016	7			3.8	ML	4	F				4		P										161	3.8
PDE	1979	10	6	101235.2	39.286	-111.687	7			3.2	ML		F				4		P										167	3.2
SRA	1979	10	23	41719.9	37.89	-110.93	7			3.5	ML		F																155	3.5
PDE	1980	5	24	100336.3	39.937	-111.966	5	5		4.2	ML	5	F				4		P										215	4.2
PDE	1981	2	20	91301.4	40.334	-111.723	7	4.7		3.9	ML	5	F				4		P										224	3.9
PDE	1981	5	14	51104.1	39.481	-111.06	1	4.5		3.5	ML	5	F				4		P										123	3.5
SRA	1981	5	29	30902.2	36.83	-110.37	1			3	MD																		242	3.0
SRA	1981	8	8	62016.9	38.05	-112.8	1			3.3	MD																		281	3.3
PDE	1981	9	10	75509.32	37.511	-110.542	7			3.1	ML						4		P										174	3.1
PDE	1981	9	21	80133.93	39.578	-110.44	7			3.2	ML	3	F				3		P										87	3.2
SRA	1981	9	22	50359.4	39.59	-110.39	8			3	ML		F																	
PDE	1982	2	12	104413.7	37.405	-112.545	7			3.6	ML						4		P										297	3.6
PDE	1982	5	24	121327	38.706	-112.041	8	4.7		4	ML	6	D				4		P										197	4.0
SRA	1983	1	27	233711.8	37.778	-110.674	7			3.3	MD																		153	3.3
SRA	1983	3	22	111235.1	39.546	-110.422	2			3.1	MD		F																	
PDE	1983	5	3	124338.1	38.288	-110.592	7			3	ML						3		P										102	3.0
PDE	1983	8	14	190830.7	38.359	-107.402	5			3.4	ML	2	F				4		P										218	3.4
SRA	1983	8	29	125311.5	41.083	-111.427	10			3	ML		F																272	3.0
PDE	1983	9	24	165745.8	40.789	-108.837	5			4.1	ML	3	F				4		P										217	4.1
PDE	1983	10	8	115754.2	40.746	-111.993	4	4.5		4.3	ML	6	D				3		P										272	4.3
PDE	1983	12	9	85841.34	38.583	-112.582	7	4.3		3.6	ML	3	F				4		P										246	3.6
SRA	1984	3	1	181300.9	41.539	-108.638	2			3.2	MD																		301	3.2
PDE	1984	3	21	111930.3	39.331	-111.096	1			3.5	ML		F				4		P										119	3.5
PDE	1984	5	14	101417.3	39.322	-107.228	5			3.2	ML	4	F				4		P										224	3.2
PDE	1984	8	16	141921.8	39.383	-111.904	9			3.7	ML	4	F				4		P										188	3.7
SRA	1984	9	14	190426.3	41.61	-108.582	2			3.2	MD																		310	3.2
SRA	1985	6	27	103629.5	39.558	-110.396	1			3	MD																		83	3.0
SRA	1985	10	7	203340.1	40.407	-109.498	21			3	MD																		161	3.0
PDE	1986	3	24	224023.5	39.236	-112.009	0	4.7		4.4	ML	5	F				4		P										194	4.4
PDE	1986	5	14	150257.4	37.429	-110.561	5			3.2	ML						4		P										183	3.2
PDE	1986	6	5	80541.8	41.267	-111.686	7			3.6	ML		F				4		P										301	3.6
PDE	1986	8	22	132633.4	37.42	-110.574	5			4	ML	5	F				4		P										185	4.0
PDE	1986	8	26	20602.61	38.9	-107.041	5			3.1	ML	3	F				4		P										238	3.1
PDE	1986	9	3	62050.98	38.912	-107.09	5			3.5	ML	5	F				4		P										234	3.5
PDE	1986	10	5	154733.5	38.64	-112.559	1			3.3	ML	3	F				4		P										243	3.3
SRA	1986	11	7	13153.7	37.43	-110.297	1			3	MD																		176	3.0
PDE	1987	3	5	30250.49	40.442	-110.616	1	4		3.7	ML	4	F				4		P										178	3.7
PDE	1987	3	11	153103	39.25	-111.636	1			3	ML		F				4		P										162	3.0
PDE	1987	4	4	62434.82	37.675	-113.027	5			3	ML	5	F				4		P										317	3.0
PDE	1987	6	26	123627.5	38.738	-111.77	5			3.5	ML						4		P										173	3.5
PDE	1987	9	2	50020.55	38.559	-112.695	1			3.4	ML						4		P										256	3.4
PDE	1987	10	19	71709.71	39.664	-111.427	0			3.8	ML	4	F				3		P										160	3.8
PDE	1987	12	16	174307.6	39.291	-111.229	5			4	ML						4		P										129	4.0
PDE	1988	1	15	73329.2	37.515	-106.684	5			3.1	ML		F				4		P										316	3.1
PDE	1988	2	14	183240.5	40.626	-108.532	5			3.3	ML	4	F				4		P										213	3.3
PDE	1988	7	10	204559.4	41.225	-111.629	7			3.6	ML						4		P										295	3.6
PDE	1988	7	11	114656	39.192	-111.988	1			3.1	ML	4	F				4		P										191	3.1
PDE	1988	7	15	3809.59	36.374	-110.448	5			3.3	ML						4		P										293	3.3
PDE	1988	8	14	200303.9	39.128	-110.869	9	5.5		5.3	ML	6	D	U			4		P									S	95	5.3
PDE	1988	9	21	175825.9	39.308	-111.165	9			3.1	MD						4		P										124	3.1
PDE	1988	11	6	153058.8	40.722	-111.418	11			3.3	ML	5	F				4		P										239	3.3
PDE	1989	1	30	40622.78	38.824	-111.614	24	5	4.8	5.4	ML	6	D	U		M	4		P										158	5.4
PDE	1989	4	9	112419.4	40.419	-110.942	9			3.2	ML	2	F				4		P										188	3.2
PDE	1989	5	13	210148.8	38.473	-108.924	7			3.1	MD						4		P										93	3.1
PDE	1989	8	9	152833.4	38.188	-112.589	2			3.3	MD		F				4		P										258	3.3
PDE	1989	11	19	32113.61	38.055	-107.767	5			3	ML		F				4		P										203	3.0
PDE	1990	2	5	102325.2	39.504	-111.517	10			3.1	ML	3	F				4		P										160	3.1
PDE	1990	4	7	153754.9	40.082	-109.519	3			3.5	ML						4		P										125	3.5
PDE	1990	6	25	171533.5	38.952	-110.828	11			3	MD						4		P										89	3.0

CATALOG SOURCE	DATE			ORIGIN	COORDINATES		DEPTH	MAGNITUDES				INFORMATION (see below for explanation of symbols)																		RADIAL DIST (km)	Converted Magnitude
										Other		INT	EFF	MAP	FPS	MO	DEP	IDE	PFD	FLG	D	T	S	V	N	W	G		
	YEAR	MO	DA	TIME	LAT	LONG	km	mb	Ms	Value	Scale																				
PDE	1990	9	1	181229.4	39.299	-111.135	7			3.3	MD						4		P										121	3.3
PDE	1990	9	12	213857.6	39.701	-106.206	5			3	ML	5	F				4		P										319	3.0
PDE	1990	10	23	84912.5	38.733	-111.525	1			3.2	MD						4		P										152	3.2
PDE	1991	1	26	214938	37.681	-111.429	9			3.3	ML	3	F				3		P										202	3.3
PDE	1991	2	21	112345.6	38.96	-111.901	1	3.4		3.4	ML	4	F				4		P										182	3.4
PDE	1991	3	2	84137.49	40.091	-109.483	1	3		3.3	ML						4		P										127	3.3
PDE	1991	3	22	145959.2	37.817	-112.997	3	3.2		3.1	ML		F				4		P										307	3.1
PDE	1991	4	20	125651.1	38.049	-112.728	2	4		3.8	ML	4	F				4		P										275	3.8
PDE	1991	5	23	73840.57	39.298	-111.149	12	3.5		3.6	ML	3	F				3		P										122	3.6
PDE	1991	6	25	210213.6	37.209	-110.358	1			3	MD						4		P										201	3.0
PDE	1991	8	21	134706.3	39.364	-111.878	3			3	ML						4		P										185	3.0
PDE	1991	11	8	131505.3	40.1	-109.286	2	3.4		3.8	ML	3	F				4		P										132	3.8
PDE	1991	12	21	202635.7	37.567	-112.322	7	3.6		3.8	ML	3	F				4		P										270	3.8
PDE	1992	3	16	144249.5	40.465	-112.043	12	4.4		4.2	ML	5	F				4		P										254	4.2
PDE	1992	5	15	213624	38.563	-107.914	5					4	F				4		P											3.7
PDE	1992	6	24	73120.21	38.783	-111.554	0	4.4		4.4	ML		F				4		P										154	4.4
PDE	1992	7	5	181729	35.982	-112.219	5	4					F				4		P											4.0
PDE	1992	9	10	62012.6	39.702	-110.632	0			3.4	MD						4		P										108	3.4
PDE	1992	9	24	143541	37.974	-112.533	3			3.1	MD						4		P										263	3.1
PDE	1993	1	21	90120.4	39.712	-110.622	1	3.4																	C					3.4
PDE	1993	2	25	112714.4	39.69	-111.263	8			3.1	MD						4		P										150	3.1
PDE	1993	3	15	104849.9	39.552	-112.075	5			3.3	ML						4		P										207	3.3
PDE	1993	5	13	161326.1	40.126	-109.087	5			3	ML						4		P										141	3.0
PDE	1993	5	27	62153.98	37.084	-112.089	10	3.3		3.5	ML	3	F				3		P										290	3.5
PDE	1993	6	16	72224.2	38.06	-112.688	5			3.5	MD						4		P										272	3.5
PDE	1993	7	8	40352.25	39.227	-106.715	5			3.1	ML		F				4		P										267	3.1
PDE	1993	7	20	35703.06	38.767	-112.056	2			3.6	MD	5	F				4		P										197	3.6
PDE	1993	9	27	112100.9	39.333	-111.159	1			3.3	MD						4		P										124	3.3
PDE	1993	10	5	22409.85	38.135	-112.622	5			3.1	ML						3		P										263	3.1
PDE	1993	10	21	220716.3	38.979	-111.861	5			3.5	MD	4	F				4		P										179	3.5
PDE	1993	11	6	73003.44	37.876	-112.812	5			3	ML						4		P										290	3.0
PDE	1994	5	6	224246	40.078	-111.402	1			3.2	MD						3		P										185	3.2
PDE	1994	6	3	42529.08	38.449	-112.229	5			3.3	ML						4		P										219	3.3
PDE	1994	9	6	34837.63	38.078	-112.327	5	3.9		4.3	ML	4	F				4		P										242	4.3
PDE	1994	9	10	63341.76	39.468	-111.52	5			3.7	ML	4	F				4		P										159	3.7
PDE	1994	9	13	60123.01	38.151	-107.976	10	4.4		4.6	ML	6	D				4		P										182	4.6
PDE	1994	11	3	114010.1	40.04	-108.269	5			3.4	ML						4		P										176	3.4
PDE	1994	11	17	111101.2	38.216	-112.728	5			3.6	MD		F				4		P										269	3.6
PDE	1994	11	19	180144.6	37.786	-112.954	5			3.1	ML	4	F				4		P										305	3.1
PDE	1994	11	23	163049	39.5	-111.52	5			3.3	ML	3	F				4		P										160	3.3
PDE	1995	3	20	124616.4	40.179	-108.925	5	4.2		4.1	ML	5	F				4		P										153	4.1
PDE	1995	4	27	195558.1	38.088	-112.419	5			3.7	MD						4		P										249	3.7
PDE	1995	7	6	2223.31	39.926	-111.629	10			3.3	ML						4		P										190	3.3
PDE	1995	7	21	172146.9	38.226	-112.904	5			3.6	ML						4		P										283	3.6
PDE	1995	10	8	62502.61	40.909	-111.716	5			3.2	ML		F				4		P										270	3.2
PDE	1995	11	3	70941.84	37.993	-112.826	1			3.1	MD						4		P										286	3.1
PDE	1995	12	3	230542.6	38.195	-112.657	0			3.1	MD						4		P										264	3.1
PDE	1995	12	6	42528.23	40.737	-111.54	10	3.4		3.5	ML	5	F				4		P										246	3.5
PDE	1995	12	31	121107.9	38.988	-111.974	1			3.1	MD						4		P										189	3.1
PDE	1996	1	6	125558.6	39.12	-110.878	0	4.3		4.2	MD	5	F				4		P										95	4.2
PDE	1996	2	2	21114.62	39.467	-111.23	1			3.2	ML						4		P										135	3.2
PDE	1996	12	6	135314.4	39.706	-110.658	3			3.4	ML						3		P										110	3.4
PDE	1996	12	28	113502.8	37.855	-113.166	5			3.2	ML						3		P										319	3.2
PDE	1997	4	14	93048.42	39.048	-111.389	5			3.1	MD						3		P										138	3.1
PDE	1997	8	13	142401.4	38.006	-112.592	5			3.7	ML						3		P										266	3.7
PDE	1997	9	17	3900.1	40.535	-112.179	1			3	ML						3		P										268	3.0
PDE	1997	10	20	70220.73	37.834	-111.879	10			3.1	ML						3		P										221	3.1
PDE	1998	1	2	72829.08	38.206	-112.467	5			4.5	ML		F				3		P										248	4.5
PDE	1998	1	5	22046.04	40.202	-111.291	5			3	ML						3		P										187	3.0
PDE	1998	1	30	215315.2	37.968	-112.547	5	4		4	ML		F				3		P										264	4.0
PDE	1998	2	5	51956.62	39.751	-110.846	1	3.6		3.7	ML		F				3		P										125	3.7
PDE	1998	3	29	121242	38.25	-111.35	3	3		3.2	ML		F				3		P										157	3.2

CATALOG SOURCE	DATE			ORIGIN	COORDINATES		DEPTH	MAGNITUDES				INFORMATION (see below for explanation of symbols)																	RADIAL DIST (km)	Converted Magnitude
										Other		INT	EFF	MAP	FPS	MO	DEP	IDE	PFD	FLG	D	T	S	V	N	W	G		
	YEAR	MO	DA	TIME	LAT	LONG	km	mb	Ms	Value	Scale																			
PDE	1998	4	10	200716	38.419	-113	5			3.9	ML		F				3		P										285	3.9
PDE	1998	6	18	110040	37.97	-112.49	2	4		4.2	ML		F				3		P										260	4.2
PDE	1999	1	8	152415.2	38.762	-111.554	0	3.5		3.8	ML						3		P										154	3.8
PDE	1999	1	14	103651	38.42	-112.98	5			3.2	ML		F				3		P										284	3.2
PDE	1999	1	26	214928	38.71	-112.49	1			3.2	ML						3		P										236	3.2
PDE	1999	1	30	90547	37.55	-112.21	1	3.2		3	ML						3		P										263	3.0
PDE	1999	2	23	32041	37.08	-112.33	10			3.1	ML						3		P										305	3.1
PDE	1999	3	9	123909	37.82	-112.36	0	3.4		3.5	ML						3		P										258	3.5
PDE	1999	4	19	144232	38.72	-112.14	0			3.5	ML		F				3		P										205	3.5
PDE	1999	4	25	52207	37.76	-112.49	2			3.1	ML						3		P										271	3.1
PDE	1999	6	3	153534.3	38.293	-108.921	4			3.6	ML		F				3		P										106	3.6
PDE	1999	6	30	152732.6	40.65	-111.576	11	3.5		3.7	ML		F				3		P										241	3.7
PDE	1999	7	6	220545.2	38.319	-108.859	5			3.5	ML		F				3		P										108	3.5
PDE	1999	7	19	102638	40.33	-111.3	1			3.2	ML						3		P										198	3.2
PDE	1999	8	4	183312	38.59	-112.18	0			3.3	ML		F				3		P										211	3.3
PDE	1999	10	11	224315	38.76	-112.02	2			3.9	ML		F				3		P										194	3.9
PDE	1999	10	22	175115.6	38.077	-112.727	5			4.2	ML		F				3		P										274	4.2
PDE	1999	12	22	80331	38.75	-111.53	2	4.1		3.9	ML						3		P										152	3.9
PDE	2000	3	7	21604	39.75	-110.84	1	4.3		4.2	ML		F				3		P									S	125	4.2
PDE	2000	3	15	121427.5	38.367	-108.867	5			3.3	ML						3		P										104	3.3
PDE	2000	5	26	32404.59	38.074	-112.192	0	3		3.6	ML						3		P										231	3.6
PDE	2000	5	27	215818.8	38.341	-108.859	5			4.3	ML		F				3		P										106	4.3
PDE	2000	6	20	175546	40.69	-109.31	1			3	ML						3		P										195	3.0
PDE	2000	8	3	133412	39.58	-111.69	5			3.2	ML						3		P										177	3.2
PDE	2000	11	11	211753	40.28	-109.23	5			3.7	ML						3		P										153	3.7
PDE	2000	12	10	193901	40.5	-111.35	13			3	ML						3		P										216	3.0
PDE	2001	2	23	214350	38.73	-112.56	0			4.1	ML		F				3		P										241	4.1
PDE	2001	5	24	24040	40.382	-111.938	0	2.9		3.3	ML		F				3		P										241	3.3
PDE	2001	7	8	135551	40.741	-112.069	13			3.4	ML	3	F				3		P										276	3.4
PDE	2001	7	19	201534	38.731	-111.521	3	4.5		4.3	ML		F				3		P										152	4.3
PDE	2001	8	9	223854.5	39.66	-107.378	5			4	ML	4	F				3		P										221	4.0
PDE	2001	11	5	83423.02	38.851	-107.384	1			3.4	ML		F				3		P										209	3.4
PDE	2001	11	19	213625.1	38.557	-112.483	1			3.6	ML						3		P										238	3.6
PDE	2002	1	8	172606	37.34	-112.71	8			3.2	ML						3		P										313	3.2
PDE	2002	1	31	181745.5	40.287	-107.693	5			4.3	ML	3	F				3		P										231	4.3
PDE	2002	3	30	213843.9	38.853	-107.386	1			3.1	ML														C					3.1
PDE	2002	6	3	32523.98	38.907	-107.418	1			3.3	ML														C					3.3
PDE	2002	6	6	122910	38.34	-108.93	1			3.2	ML						3		P										102	3.2
PDE	2002	6	14	74546	41.39	-111.44	7			3.1	ML						3		P										303	3.1
PDE	2002	6	20	221704.8	38.908	-107.416	1			3.6	ML														C					3.6
PDE	2002	8	12	13140	38.15	-112.61	0			3.4	ML						3		P										261	3.4
PDE	2002	8	24	153719.7	38.92	-107.481	1			3.2	ML														C					3.2
PDE	2002	9	10	161811.4	38.789	-107.412	1			3.3	ML														C					3.3
PDE	2002	9	26	103210	37.41	-110.53	3			3	ML						3		P										184	3.0
PDE	2002	11	8	125522	38.84	-111.5	5			3.2	ML						3		P										148	3.2
PDE	2002	11	26	54616.37	38.904	-107.448	1			3.1	ML														C					3.1
PDE	2003	1	3	50212	41.271	-111.815	12	3.4		3.7	ML	4	F				3		P										308	3.7
PDE	2003	2	11	90042	38.697	-112.259	0			3.3	ML	3	F				3		P										216	3.3
PDE	2003	4	17	10419	39.516	-111.857	0	4.7		4.4	ML	5	F				1		P										188	4.4
PDE	2003	7	8	22033	36.95	-111.79	6			3.3	ML						3		P										284	3.3
PDE	2003	7	12	15440	41.283	-111.622	9			3.7	ML	3	F				3		P										300	3.7
PDE	2003	8	8	61105.19	38.907	-107.458	1			3.4	ML														C					3.4
PDE	2003	11	17	231852	40.35	-111.17	12			3	ML						3		P											3.0
PDE	2003	11	29	223308	38.45	-112.49	1			3.1	ML						3		P										241	3.1
PDE	2003	12	27	3924	39.644	-111.929	1			3.8	ML	3	F				3		P										199	3.8
PDE	2004	4	15	45359.34	38.87	-107.35	1			3.1	ML														C					3.1
PDE-W	2004	9	19	60943.8	38.853	-107.358	1			3.5	ML						3		P										211	3.5
PDE	2004	10	11	5841.02	38.825	-107.425	1			3.3	ML														C					3.3
PDE-W	2004	11	7	65459	38.236	-108.915	0			4.1	ML	4	F				3		P										111	4.1
PDE	2004	11	13	182830.4	38.875	-107.497	1			3.2	ML														C					3.2
PDE-W	2005	3	14	53327	39.509	-111.895	1			3	ML						3		P										191	3.0
PDE	2005	4	30	45704.76	38.918	-107.393	1			3.1	ML														C					3.1

CATALOG SOURCE	DATE			ORIGIN	COORDINATES		DEPTH	MAGNITUDES				INFORMATION (see below for explanation of symbols)																RADIAL DIST (km)	Converted Magnitude
										Other		INT	EFF	MAP	FPS	MO	DEP	IDE	PFD	FLG	D	T	S	V	N	W	G		
	YEAR	MO	DA	TIME	LAT	LONG	km	mb	Ms	Value	Scale																		
PDE-W	2005	5	2	172955.8	38.795	-107.393	1			3.2	ML	.													C				3.2
PDE-W	2005	5	13	142604.3	38.835	-107.372	1			3.3	ML	.													C				3.3
PDE-W	2005	5	18	192146	41.425	-111.09	1			3.3	ML	.	.	.	.	.	3	.	P	.	.	.	.	.	.	.	.	294	3.3
PDE-W	2005	5	30	14921.14	38.889	-107.474	1			3.3	ML	.													C				3.3
PDE-W	2005	6	8	84600.4	38.953	-107.527	1			3.5	ML	.													C				3.5
PDE-Q	2005	6	24	130133	37.511	-112.534	6			3.6	ML	3	F	.	.	.	3	.	P	.	.	.	.	.	.	.	.	289	3.6
PDE-Q	2005	7	20	70615	38.601	-112.691	1			3.5	ML	.	.	.	.	.	3	.	P	.	.	.	.	.	.	.	.	255	3.5
PDE-W	2005	7	25	115128.3	38.831	-107.415	1			3.1	ML	.													C				3.1

INFORMATION

INFORMATION (IEFM DTSVNWG on Screen Search): Dots are used in place of blanks to aid in the distinction between the columns. Read the sub-headers vertically.

Intensity (sub-header INT):
Maximum intensity on the Modified Mercalli Intensity Scale of 1931 (Wood and Neumann, 1931) or any similar 12-point intensity scale. It may also be an MMI value approximated from other intensity scales such as Ross-Forel or Japan Meteorological Agency. Possible intensity values are 1 - 9; X = 10; E = 11; T = 12.

Cultural Effects (sub-header EFF):
The most severe effect is listed (C = Casualities; D = Damage; F = Felt; H = Heard). Note that casualties includes human deaths or injuries. Domestic animal casualties are considered to be damage.

Isoseismal Map (sub-header MAP): (Expanded Format only)
Indicates the publication where an isoseismal map for this event has been published.
- U = United States Earthquakes.
- E = Earthquake Notes. (Now Seismological Research Letters)
- P = Preliminary Determination of Epicenters.
- W = Wellington (New Zealand Seismology Reports, Wellington, N.Z.).
- N = Nature Magazine.
- S = Bulletin of the Seismological Society of America.

Fault Plane Solution (sub-header FPS):
Coded as an "F" to indicate the availability of a fault plane solution in the publication, "Preliminary Determination of Epicenters, Monthly Listing".

Moment Tensor Solution (sub-header MO):
Coded as an "G" to indicate the availability of a moment tensor solution in the publication "Preliminary Determination of Epicenters, Monthly Listing" (Sipkin, 1982; Dziewonski, 1980; and Hanks and others, 1979).

ISC Alternate Depth Indicator (sub-header DEP):
A "D" in this column indicates that a pP depth is given, but the pP depth is not the adopted depth in the hypocenter solution.

International Data Exchange (sub-header IDE):
An "X" in this column identifies the event as a "IDE" earthquake.

Preferred Solution (sub-header PFD):
A "P" in this column designates a preferred solution. Earthquake hypocenters which are located within a seismic network, such as Pasadena or Berkeley, or seismic catalogs which have undergone critical review during their compilation will be designated as a preferred solution.

Flag (sub-header FLG): Currently not used.

PHENOMENA

Diastrophism: (sub-header D)
- F = Faulting.
- U = Uplift.
- S = Subsidence.
- 3 = Uplift and Subsidence.
- 4 = Uplift and Faulting.
- 5 = Faulting and Subsidence.
- 6 = Faulting with Uplift and Subsidence.
- 7 = Uplift or Subsidence.
- 8 = Faulting and Uplift or Subsidence.

Tsunami: (sub-header T)
- T = Tsunami generated.
- Q = Questionable Tsunami.

Seiche: (sub-header S)
- S = Seiche.
- Q = Questionable Seiche.

Volcanism: (sub-header V)
- V = Earthquake associated with volcanism.

Non-Tectonic: (sub-header N)
- E = Explosion.
- I = Collapse.
- C = Coal bump or Rockburst in a coal mine.
- R = Rockburst.
- M = Meteoritic.
- N = Either known to be or likely to be of non-tectonic origin.
- ? = Classified as an earthquake, but a non-tectonic origin cannot be ruled out.
- V = Reservoir induced earthquake.

Guided Waves in Atmospheric And/Or Ocean: (sub-header W)
- T = T-wave.
- A = Acoustic wave.
- G = Gravity wave.
- B = Both A and G.
- M = T-wave plus and A or G.

Miscellaneous Phenomena: (sub-header G)
- L = Liquefaction.
- G = Geyser.
- S = Landslides and/or Avalanches.
- B = Sandblows.
- C = Ground cracks not known to be an expression of faulting.
- V = Lights or other visual phenomena seen.
- O = Olfactory (Unusual odors noted).
- M = More than one of these phenomena observed.

U.S. Department of Energy—Grand Junction, Colorado

Calculation Cover Sheet

Calc. No.: MOA-02-04-2007-1-09-02 **Discipline:** Geologic and Geophysical Properties **No. of Sheets:** 22
Doc. No.: X0115500

Location: Attachment 2, Appendix F

Project: Moab Project

Site: Crescent Junction Disposal Site

Feature: Site and Regional Seismicity – Results of Maximum Credible Earthquake Estimation and Peak Horizontal Acceleration

Sources of Data:

See list of references at end of calculation set.

Purpose of Revision:

Revisions to this calculation set have been made in response to Nuclear Regulatory Commission comments G9 and G10.

Sources of Formulae and References:

See list of references at end of calculation set.

Preliminary Calc. ☐ **Final Calc.** ☒ **Supersedes Calc. No.** MOA-02-08-2006-1-09-01

	Name	Date
Author:	Roslyn Stein	5/25/07
Checked by:	Craig Goodknight	31 May 07
	John E Ellis	5/31/07
	Mark Kautsky	5-31-07
	Duncan Foley	May 31, 07
Approved by:	Kent Kruger	5/31/07

No text for this page

Problem Statement:

Determination of the suitability of the Crescent Junction Disposal Site as the repository for the Moab uranium mill tailings material, and development of the site and regional seismotectonic sections of the Remedial Action Plan and Site Design for Stabilization of Moab Title I Uranium Mill Tailings at the Crescent Junction, Utah, Disposal Site (RAP) requires an estimation of the Maximum Credible Earthquake (MCE) and the attenuation of the peak horizontal acceleration (PHA) associated with this MCE to the site.

Method of Solution:

The estimation of MCE and the associated PHA are part of the seismotectonic calculation set to develop seismic design parameters for the disposal site. Following procedures outlined in the UMTRA–DOE Technical Approach Document (TAD) (DOE 1989), the calculation set includes an estimation of the floating earthquake (FE) associated with the Colorado Plateau province applied 15 kilometers (km) from the site, the MCE associated with all pertinent outlying provinces, and the MCE associated with all known or suspected Quaternary faults within the study region. For each of these identified earthquake events, the on-site PHA is assessed, and the design PHA is established.

Assumptions:

It is assumed that the literature sources are reliable and representative of the current understanding of the seismotectonic characteristics of the region.

Calculation:

MCE estimations are calculated using the formulas developed by Wells and Coppersmith (1994) as follows:

$$M_w = 5.08 + 1.16 \times \log(SRL) \quad \text{(Eq. 1)}$$

$$M_w = 4.07 + 0.98 \times \log(RA) \quad \text{(Eq. 2)}$$

where M_w is Moment Magnitude, SRL is surface rupture length (km), and RA is rupture area (km^2).

The coefficients in these equations are based on regression data developed for all slip types.

Attenuation to the site is calculated using the corrected peak ground acceleration, mean-plus-one standard deviation (84^{th} percentile) relationship developed by Campbell and Bozorgnia (2003) as follows:

$$\ln Y = c_1 + f_1(M_w) + c_4 * \ln\sqrt{f_2(M_w, r_{seis}, S)} + f_3(F) + f_4(S) + f_5(HW, F, M_w, r_{seis}) + \varepsilon \quad \text{(Eq. 3)}$$

where:

Y = peak horizontal ground acceleration,

c_1, c_4 = coefficients corresponding to corrected PHA regression analysis,

M_w =moment magnitude,

R_{seis} = closest distance from site to seismogenic rupture (km), where depth to seismogenic rupture is a minimum of 3 km (Campbell 1997),

S = local site condition factors (consistent with firm rock sites for Crescent Junction),

F = faulting mechanism factors (consistent with normal faulting for Crescent Junction),

HW = hanging-wall effect factor for faults with surface projection within 5 km of site and fault dip less than or equal to 70 degrees, and

ε = random error term equivalent to zero for mean and standard deviation equal to σ_{lny}, defined as a function of magnitude.

The Campbell and Bozorgnia (2003) relationship is an updated attenuation relationship to the Campbell (1981) relationship referenced in the TAD (DOE 1989).

Criteria and Definitions:

The following are the standards and definitions that are applied to the evaluation of the seismicity of the Crescent Junction Site as specified in the TAD (DOE 1989, p. 133).

Design life. As specified by the U.S. Environmental Protection Agency (EPA) Promulgated Standards for Remedial Actions at Inactive Uranium Processing Sites (40 CFR 192), the controls implemented at UMTRA Project Sites are to be effective for up to 1,000 years, to the extent reasonably achievable and, in any case, for at least 200 years. For the purpose of the seismic hazard evaluation, a 1,000-year design life is adopted.

Design earthquake. For UMTRA Project Sites, the magnitude(s) of the earthquake(s) that produces the largest on-site PHA and that produces the most severe effects upon the site is the design earthquake. This earthquake could be either a floating earthquake or an earthquake whose magnitude is derived from a relationship between fault length and maximum magnitude. The latter case is applied for a verified or assumed capable fault of known rupture length.

Floating earthquake. An FE is an earthquake within a specific seismotectonic province that is not associated with a known tectonic structure. Before assigning the FE magnitude, the earthquake history and tectonic character of the province are analyzed.

Capable fault. A capable fault is a fault that has exhibited one or more of the following characteristics:

- Movement at or near the ground surface at least once within the past 35,000 years, or movement of a recurring nature within the past 500,000 years.
- Macroseismicity (magnitude 3.5 or greater) determined with instruments of sufficient precision to demonstrate a direct relationship with the fault.
- A structural relationship to a capable fault such that movement on one fault could be reasonably expected to cause movement on the other.

Acceleration. Acceleration, or PHA, is the mean of the peaks of the two orthogonal horizontal components of an accelerogram record. The accelerations are determined from the corrected peak horizontal ground acceleration attenuation relationship based on distance and magnitude as developed by Campbell and Bozorgnia (2003). The mean-plus-one standard deviation (84th percentile) value is adopted. This relationship is an update to the Campbell (1981) relationship referenced in the TAD (DOE 1989).

Surface acceleration. Surface acceleration is the site acceleration adjusted for the site soil attenuation or amplification effects.

Magnitude and intensity. Magnitude is the base-10 logarithm of amplitude of the largest deflection observed on a torsion seismograph 100 km from the epicenter (Richter 1958). This local magnitude value may not be the same as the body-wave and surface-wave magnitudes derived from measurements at teleseismic distances. Unless specified otherwise, Richter magnitudes for values less than 6.5 are used in UMTRA Project seismic hazard evaluations. Intensity is the index of the effects of any earthquake on the human population and structures. The most commonly applied scale is the 1931 Modified Mercalli (MM) Intensity Scale, which will be used in this study.

Maximum earthquake. The term "Maximum Earthquake" (ME) was defined by Krinitzsy and Chang (1977) as the largest earthquake that is reasonably expected on a given structure or within a given area. No recurrence interval is specified for such an event.

Local regional study area. The regional study area is selected by calculating the distance at which the largest magnitude earthquake possible for a region, as determined by Algermissen et al. (1982), produces the minimum accepted on-site design acceleration (0.10g). All further characterization work is then limited to this region. Using this definition, the ME for the region as determined by Algermissen et al.

(1982) is magnitude 6.1. Using Campbell and Bozorgnia (2003) attenuation relations for corrected peak ground accelerations, 84th-percentile values, distances within 30 km of the site are considered within the local regional study area.

Expanded regional study area. Although UMTRA defines the study area as discussed above, the U.S. Nuclear Regulatory Commission (NRC), per *Code of Federal Regulations* Title 10, Part 100 (10 CFR 100), Appendix A, requires an investigation within 200 miles of the site. For purposes of this seismotectonic evaluation, capable faults, historical earthquakes, and floating earthquakes associated with neighboring tectonic provinces that lie within 200 miles of the site and are capable of producing a minimum on-site acceleration of 0.10 g or greater will be evaluated in the expanded regional study area.

Discussion:

Floating Earthquake

The purpose of the FE evaluation is to estimate a "background" level of seismicity within a tectonic province. The FE evaluation allows for potential low to moderate earthquakes not associated with tectonic structures to contribute to the seismic hazard of the site. Because these events are not associated with a known structure, the location of these events is assumed to occur randomly. The maximum magnitude for these background events within the Intermountain U.S. ranges between local magnitude (M_L) 6.0 and 6.5 (Woodward-Clyde 1996). Larger earthquakes would be expected to leave a detectable surface expression, especially in arid to semiarid climates, with slow erosion rates and limited vegetation. In seismically less active areas such as the Colorado Plateau, the maximum magnitude associated with an FE event is assumed to be 6.2, consistent with that used in the Green River RAP (DOE 1991a, pg. 26), Grand Junction RAP (DOE 1991b, pg. 71), and the seismic evaluation performed for the tailings site in Moab (Woodward-Clyde 1996, pg. 4–19).

Historical earthquake data for the area within a 200-mile radius of the Crescent Junction Site were obtained for the initial phase of this study. The complete data file was included in Appendix B of the *Site and Regional Seismicity – Results of Literature Research* calculation set (RAP Attachment 2, Appendix E). To assess the FE magnitude and recurrence interval associated with the Colorado Plateau, a second historical earthquake search was conducted to limit events to those occurring within the boundaries of the Colorado Plateau (NEIC 2005). A rectangular search was conducted initially, with the latitudes constrained to between 34.5 and 40.75 degrees north, and the longitude between 106.5 and 112.5 degrees west. After the initial search, events with epicenters lying outside the boundaries of the Colorado Plateau (as shown in Figure 1) were deleted. For consistency, moment magnitude (M_w) was used where possible. Consistent with Campbell (1981) attenuation equations, M_w was considered approximately equal to surface wave magnitudes (M_s) for events greater than 6.0, and approximately equal to local magnitude (M_L) for events smaller than 6.0. Modified Mercalli Intensity (MMI) values were converted to Richter scale using the following equation:

$$M = 1 + \frac{2}{3} * I_o \qquad \text{(Eq. 4)}$$

where M = magnitude on the Richter scale, and I_o is the MMI in the epicentral area.

Magnitudes were used in this order of preference: M_w, M_s if >6.0, M_L if ≤ 6.0, other reported magnitudes, and MMI values converted to magnitude.

Events were filtered to include only events with magnitudes equal or greater than 3.0. Events that are thought to be non-tectonic in origin or induced by non-natural causes are not considered further in the evaluation. One cluster of such events is described by Smith and Sbar (1974) to include a swarm of events at approximately latitude 39.5 N and longitude 110.5 W located along the Book Cliffs in the coal-mining district of eastern Utah. These earthquakes, the largest having a compressional body wave magnitude (M_b) of 4.5, are thought to be indirectly triggered by subsurface coal mining in an area of high regional stress. Other clusters of events include those associated with fluid injection at the Rangely oil

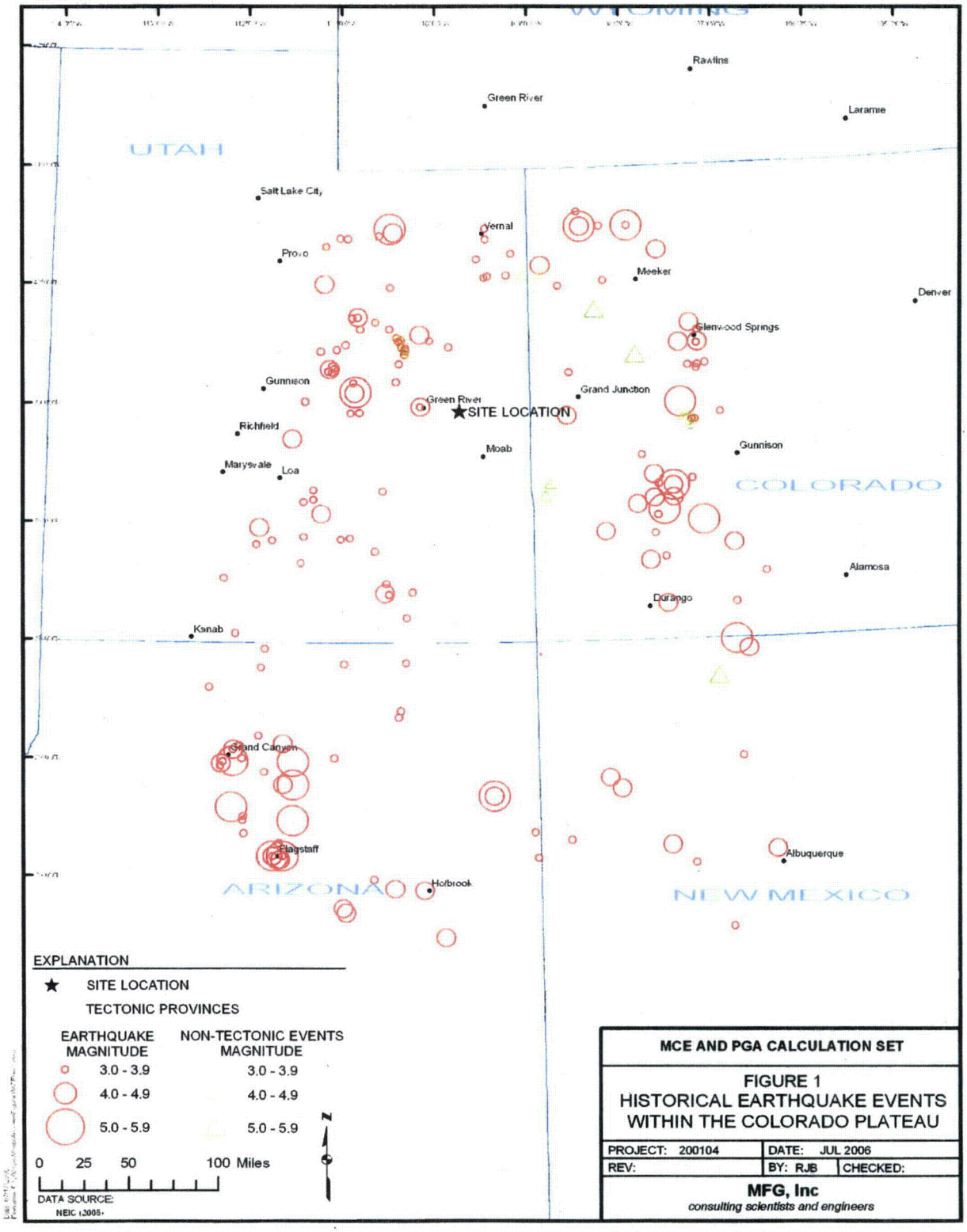

Figure 1. Historical Earthquake Events within the Colorado Plateau

field along the border between northeastern Utah and northwestern Colorado, and a series of events associated with the Paradox Valley desalinization project that included deep water injections beginning in 1995 (Colorado Geological Survey 2002). In addition, the earthquake data was declustered to remove aftershocks and foreshocks. The events considered in the evaluation of the Colorado Plateau FE are shown in Appendix A.

As shown in Figure 1, there is more activity on the borders of the Colorado Plateau than within the interior portions. This increased activity is associated with the transitional area of crustal thinning (30 to 35 km along the perimeter area) associated with extension. The interior of the Plateau has a crustal thickness of approximately 45 km (Keller et al. 1979). For the FE evaluation, a conservative recurrence of events was evaluated for the entire Colorado Plateau; the interior and perimeter portions were not evaluated separately.

The regional study area is located in an area with a relatively quiet recorded earthquake history. The first recorded earthquake in the state of Utah was estimated to have an MMI of IV, and occurred near Salt Lake City in 1850 (Arabasz et al. 1979). The earliest recorded earthquake event in Colorado had an MMI of VI, and occurred near Pueblo in 1870 (Kirkham and Rogers 1981). Since this time, only approximately 15 events have been recorded within the Colorado Plateau with an intensity greater than VI or a magnitude greater than 5. Most of these early events were recorded in populated areas. This short recorded history can be misleading when attempting to predict future events, especially in sparsely populated areas such as the Colorado Plateau, and should be used with caution (Kirkham and Rogers 1981).

The historical completeness record was estimated by examining the data set of events and the frequency of recorded occurrence as grouped by magnitude. By examining the frequency distribution with time, the completeness record can be estimated, as shown in Figures 2, 3, and 4. For this report, it is estimated that the historical record is complete since approximately 1890 for events with a magnitude 5.0 or greater, approximately 1960 for events with a magnitude of 4.0 or greater, and approximately 1970 for events with a magnitude of 3.0 or greater. This is in general agreement with the completeness record assumed for the Cheney disposal cell in Grand Junction, Colorado (DOE 1991b, p. 68).

A log-frequency versus magnitude plot was generated for the Colorado Plateau, and a straight line fit to the data. The estimated recurrence interval for the Colorado Plateau was estimated to be represented by the equation:

$$M = 4.35 - 0.82 * \log(\frac{1}{y}) \qquad \text{(Eq. 5)}$$

where y is the recurrence interval.

The graphical representation is shown in Figure 5. The frequency-magnitude data can also be normalized with area to be of the form:

$$M = 4.35 - 0.82 * \log\frac{A_p}{y * a}, \qquad \text{(Eq. 6)}$$

where:

Ap= area of the Colorado Plateau Province (approximately 117,000 square miles or 303,000 square km),
y = recurrence interval, and
a = area of interest.

When normalized to 1 square km, the recurrence interval is represented by

$$M = -0.14 - 0.82 * \log(\frac{1}{y}). \qquad \text{(Eq. 6)}$$

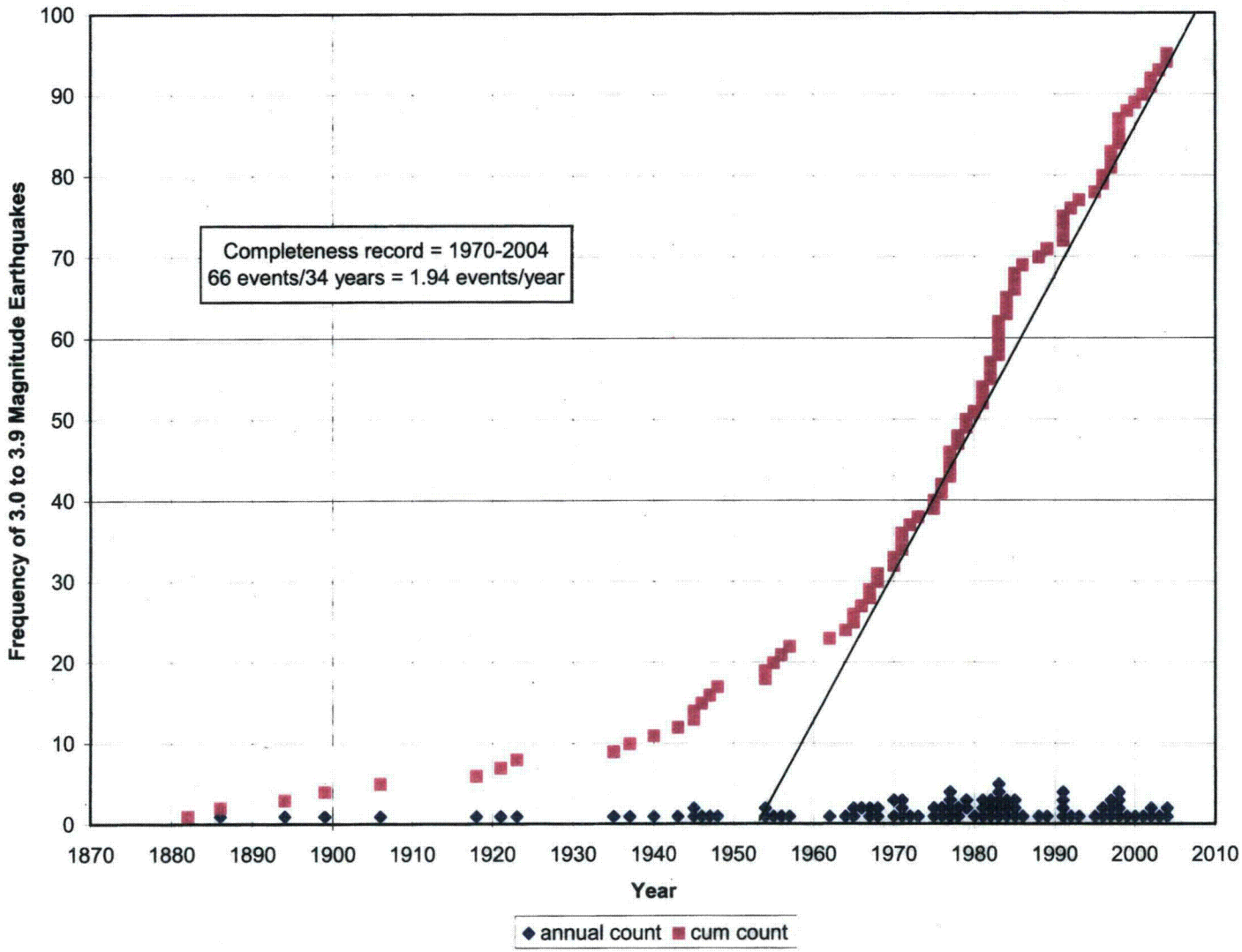

Figure 2. Magnitude 3.0 to 3.9 Earthquake Frequency—Colorado Plateau

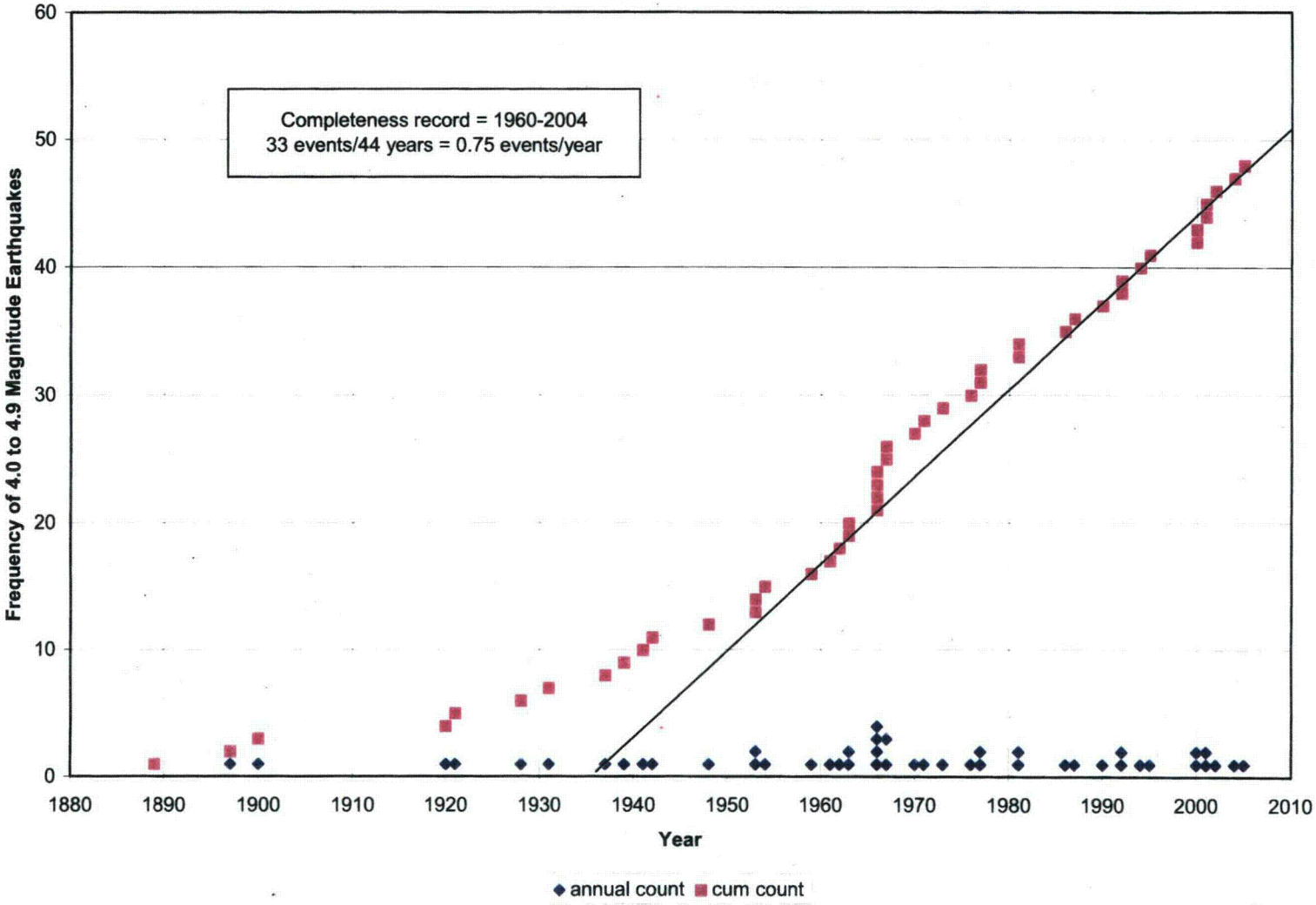

Figure 3. Magnitude 4.0 to 4.9 Earthquake Frequency—Colorado Plateau

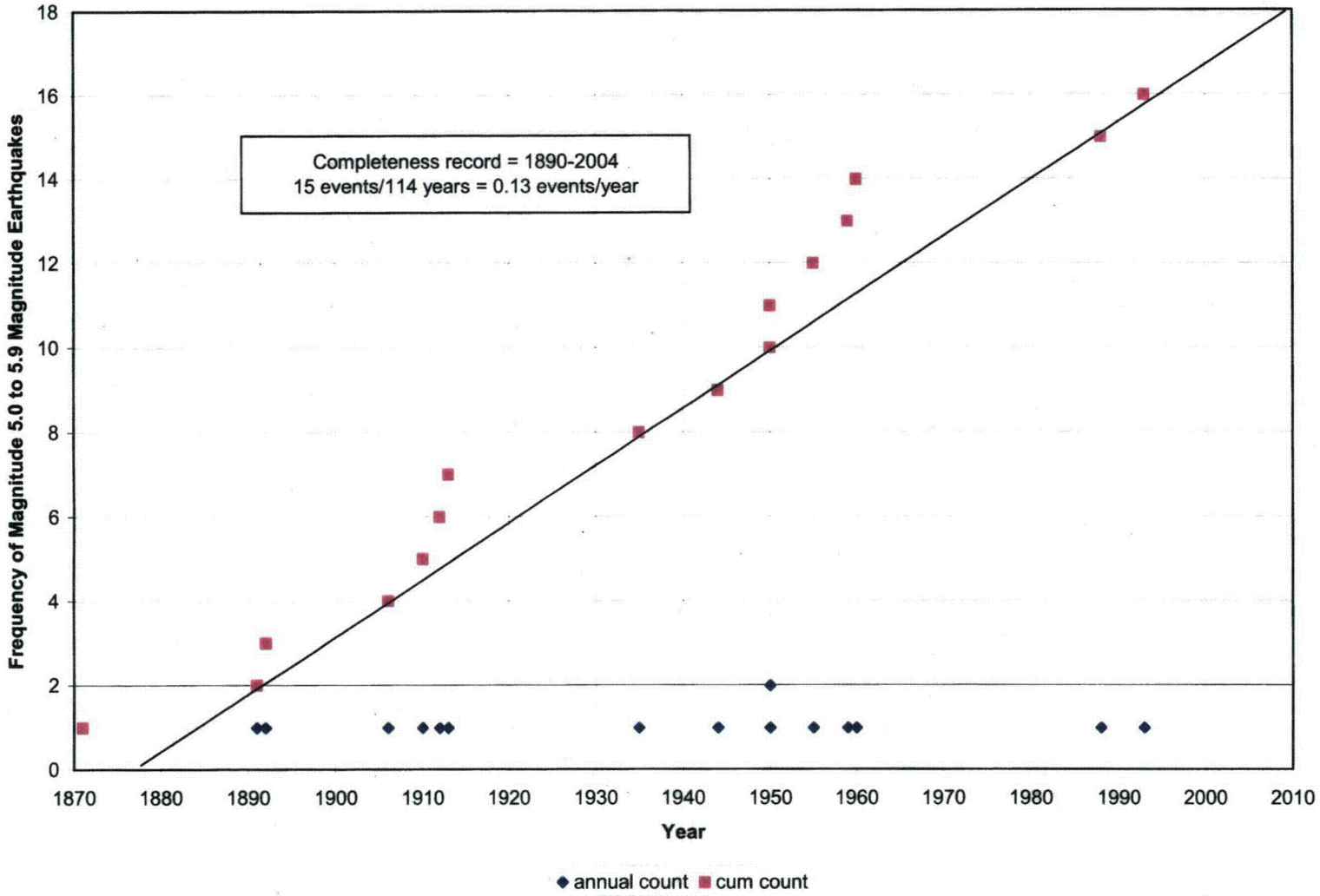

Figure 4. Magnitude 5.0 to 5.9 Earthquake Frequency—Colorado Plateau

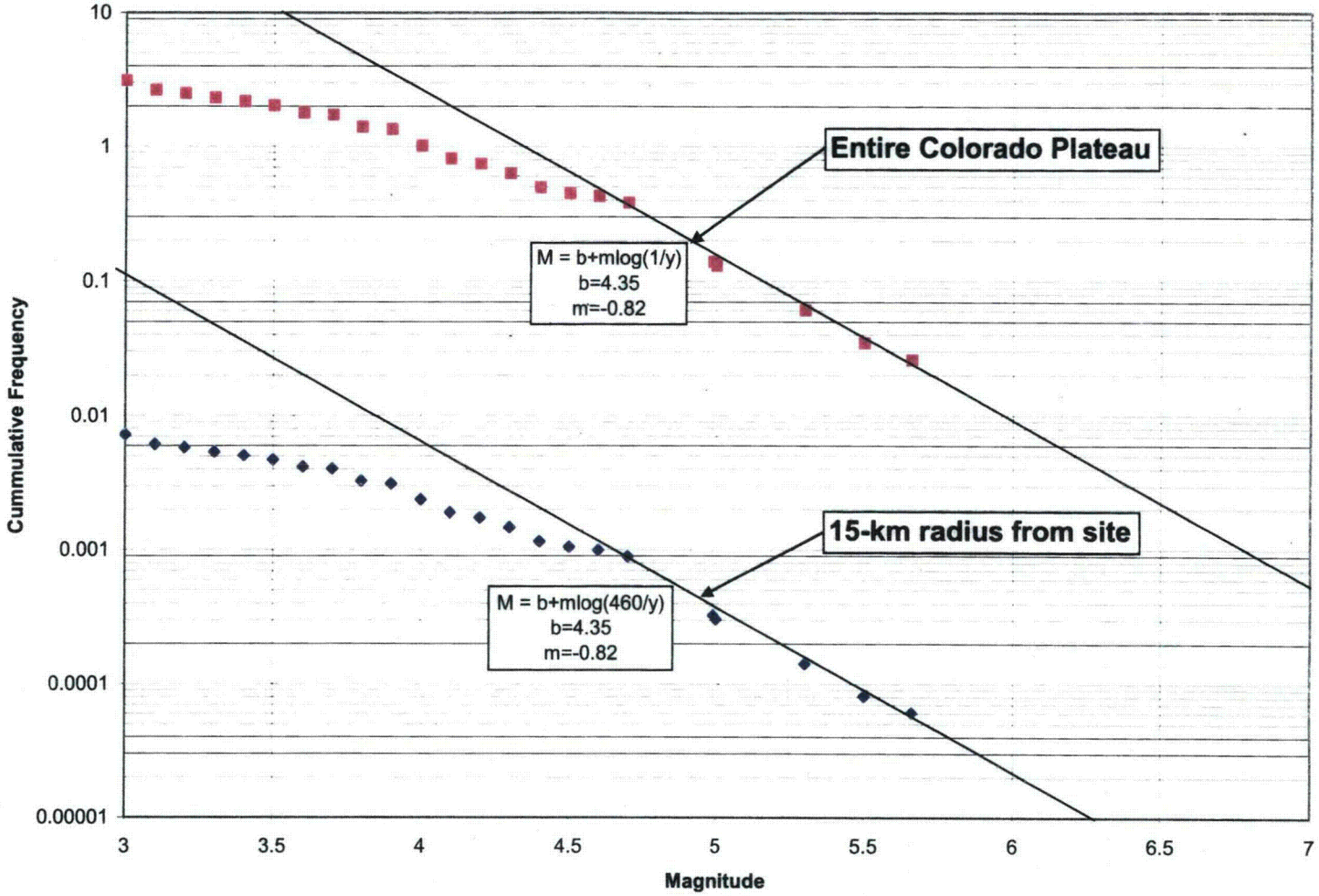

Figure 5. Magnitude Versus Earthquake Frequency—Colorado Plateau

Limiting the FE event to magnitude 6.2, and assuming this event occurs at a radial distance of 15 km (9 miles) from the site, results in a PHA of 0.22 g (using Campbell and Bozorgnia 2003 corrected peak horizontal ground acceleration, 84th percentile relationship). It should be noted that the largest historical event within the Colorado Plateau had a magnitude of 5.7 (1912 Lockett Tanks, Arizona earthquake, reported MMI of 7). The use of a magnitude 6.2 for evaluation of the FE is based on extrapolation of the log-frequency plot, limited, as discussed previously, to a practical maximum event that could result in an undetected tectonic structure. Based on Equation 5, above, the recurrence interval of a magnitude-6.2 event occurring within 15 km of the site is 77,000 years. The probability of this event being exceeded within the assumed design life of 1,000 years is 1 percent.

MCE Associated with Outlying Tectonic Provinces

The MCE values for remote seismotectonic provinces, such as the Intermountain Seismic Belt, Rio Grande Rift, Wyoming Basin, and Southern Rocky Mountains, were taken from published studies (Kirkham and Rogers 1981, DOE 1991b). The MCE from each event is attenuated to the site assuming that the event occurs at the point within the outlying province that is closest to the site. The PHA calculated for each event is shown in Table 1.

Table 1. PHA Associated with MCE Event in Outlying Tectonic Provinces

Tectonic Province	MCE	Closest Point to Site (miles)	PHA (g)
Rio Grande Rift	7.5	180	0.02
Intermountain Seismic Zone	7.9	65	0.08
Eastern Mountain	6.75	200	0.01
Western Mountain	6.5	140	0.02
Wyoming Basin	6.5	140	0.02

As shown in the above table, the greatest PHA associated with an outlying province is a 7.9-magnitude event occurring within the Intermountain Seismic Zone, resulting in a PHA of 0.08 g.

MCE associated with known or suspected Quaternary faults

Quaternary faults were identified using the USGS and Utah Geological Survey Quaternary Fault and Fold databases (Black et al. 2003, USGS 2002). An initial search for critical Quaternary faults was conducted using the minimum fault lengths given in NRC document 10 CFR 100, Appendix A, as shown in Table 2. The complete list of faults meeting these minimum length requirements is included in the "Site and Regional Seismicity–Results of Literature Research" calculation (RAP Attachment 2, Appendix E).

Table 2. Minimum Length of Fault to Be Considered in Establishing MCE

Distance from Site		Minimum Length	
Miles	Kilometers	Miles	Kilometers
0 to 20	0 to 32	1	1.6
Greater than 20 to 50	Greater than 32 to 80	5	8
Greater than 50 to 100	Greater than 80 to 161	10	16
Greater than 100 to 150	Greater than 160 to 240	20	32
Greater than 150 to 200	Greater than 240 to 320	40	64

In addition to faults included in the Quaternary Fault and Fold database, faults of undetermined age that are shown on geologic maps in the area (Williams 1964, Gaultieri 1988, Witkind 1995, Williams and Hackman 1971), were considered if the PHA associated with these structures (if considered Quaternary) is greater than 0.1 g. The faults considered in this study are shown in Figure 6. In addition, a tabular form of the data is shown in the current calculation set as Appendix B.

Figure 7 shows the considered faults overlain by historical earthquakes in the area. Two historic earthquakes appear close to the Little Grand Wash Fault (Fault No. 9). The two events in question are a July 30, 1953 event with an estimated intensity of 5, and a March 31, 1954 event with an estimated intensity of 4. Both events are cataloged in Eastern, Central, and Mountain States of the United States, 1534-1986 (SRA) as non-instrumental events. Epicenter accuracy for both events is estimated in SRA to be within 0.5 to 1 degrees, or approximately 30 to 60 miles. The source for the catalog comes from the University of Utah Seismograph Station (Arabasz et. al, 1979). In this earthquake listing, non-instrumental epicenters are assigned coordinates corresponding to the location of the town or city where the felt effects were strongest. In this case, the coordinates were assigned to the location of the town of Green River. Therefore, the earthquake location is fairy uncertain, and in actuality could have occurred at any location within 30 to 60 miles of Green River. Due to the low magnitude of the events (estimated by converting intensity to Richter magnitude) of 4.3 and 3.7, respectively, it is unlikely that either of these events would result in a surface rupture. Therefore, it is unlikely that the true location of these events could be better estimated by field evidence.

The capability of the Little Grand Wash Fault, more recently known as the Little Grand Fault, was evaluated during the seismotectonic study performed for the Green River site, as discussed in the "Site and Regional Seismicity–Results of Literature Research" calculation (RAP Attachment 2, Appendix E). Based on the lack of offset in the alluvial, colluvial, and talus materials overlying the fault, it was concluded during that study that the fault is not capable.

Later field mapping of the fault (Chitwood 1994, Doelling 2001) also did not observe any offset of Quaternary deposits. Further capability of the Little Grand Fault was also evaluated in April 2007 to specifically examine the eastern portion of this fault that is closest to the site. South of the Green River, Utah, Site, displacement on the Little Grand Fault is more than 500 feet. Displacement on this easterly-striking normal fault (down to the south) decreases eastward. The fault was checked for evidence of Quaternary movement for approximately 6.5 miles along its eastern part (using mapping mainly by Doelling [2001] and Chitwood [1994]), starting where the fault passes under old U.S. Highway 50 in the SE¼ Section 27, T.21S., R.17E. The fault becomes less distinct eastward through Green River Gap (where displacement is only a few tens of feet) and to the easternmost place where it is recognized by Chitwood (1994) along the left fork (or west branch) of Floy Wash in the SE1/4 Section 22, T.21S., R.18E. In places along the fault where it is overlain by Quaternary pediment-mantling material or terrace gravels, no displacement of these units was seen. Based on this traverse of the eastern part of the Little Grand Fault, it is concluded from the lack of Quaternary displacement that the fault is not capable.

No other historical earthquake events (above magnitude 3.0) are associated with any of the considered faults that could impact the site.

The MCE associated with each fault was calculated using Wells and Coppersmith (1994) relationships. PHA was calculated using Campbell and Bozorgnia (2003) attenuation equations. Using these relationships, 14 faults were initially identified as potentially capable of producing site PHA of 0.10 g or greater, and are summarized in Table 3.

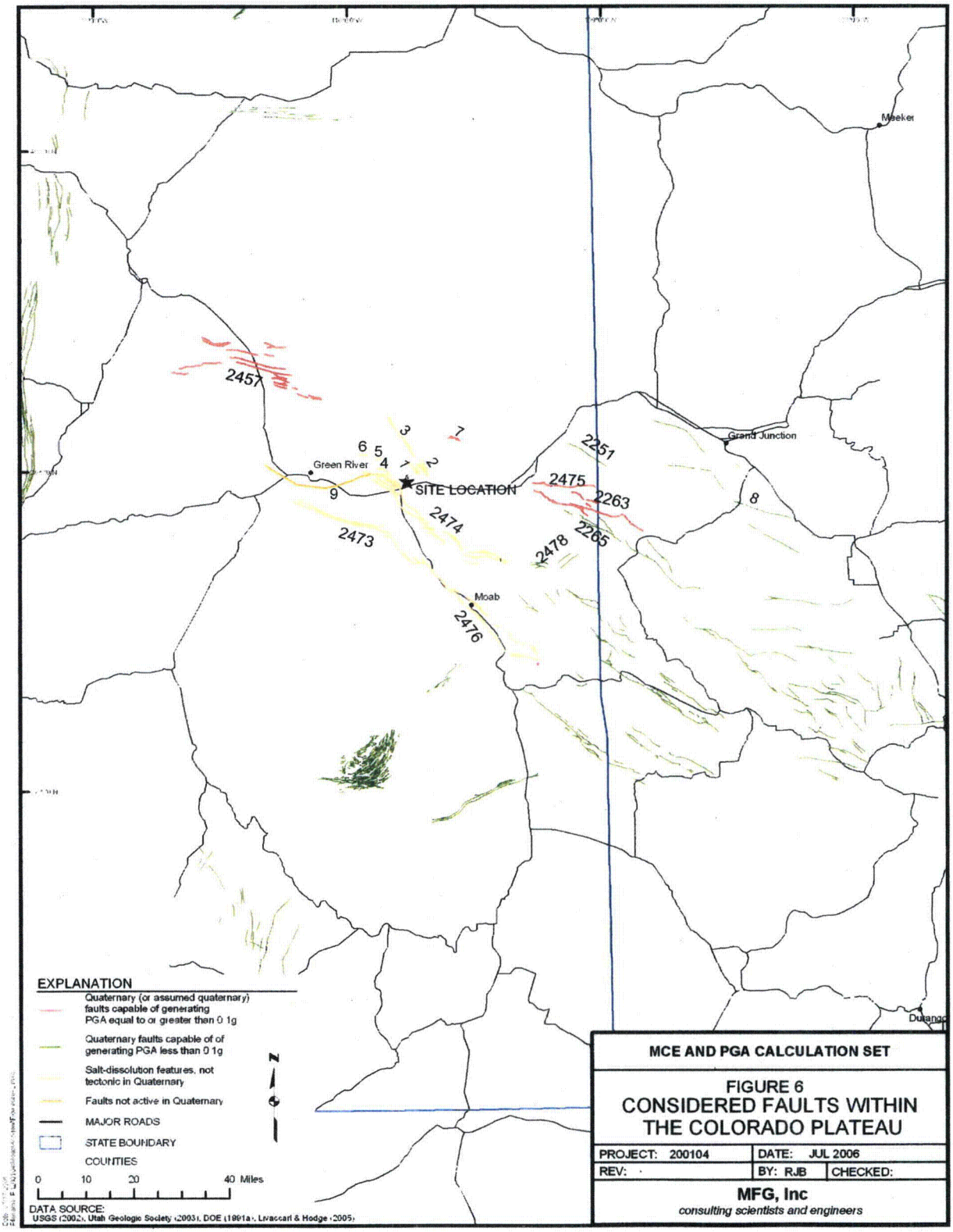

Figure 6. Considered Faults within the Colorado Plateau

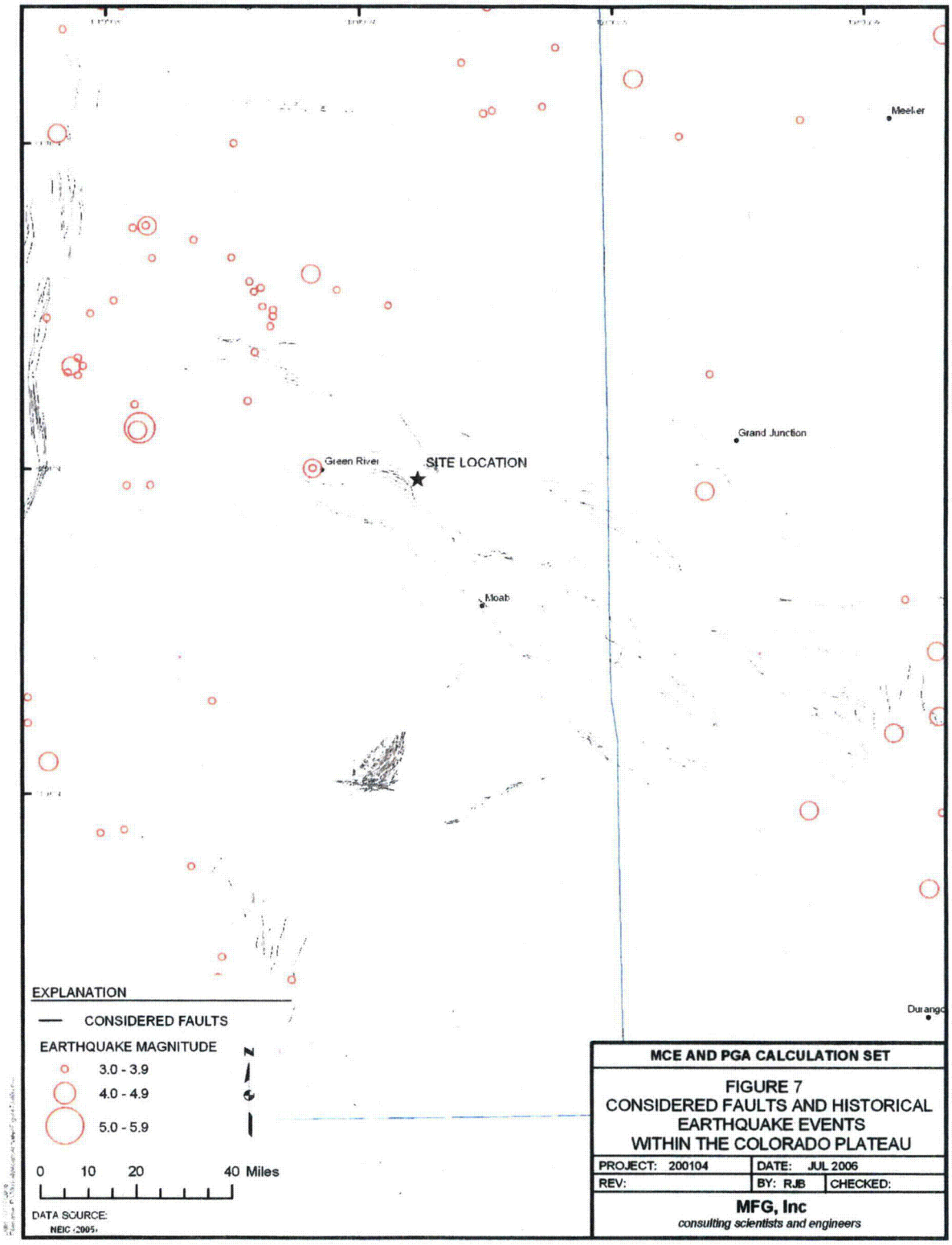

Figure 7. Considered Faults and Historical Earthquake Events within the Colorado Plateau

Table 3. Preliminary MCE Associated with Quaternary Faults and Faults of Unknown Age

Fault Name	Fault Number[a]	Length (km)	Depth of Rupture (km)	Rupture Area (km^2)	Distance From Site (mi)	MCE (M_w)[b]	PHA (g) Campbell and Bozorgnia (2003)	Comments
Salt and Cache Valley faults	2474	57.9	<2	115.8	1.8	6.09	0.67	Fault determined to not be active in Quaternary based on field evidence and lack of microearthquake activity (Wong et al. 1996, Woodward-Clyde 1984). Not potential design fault.
Tenmile Graben Faults	2473	34.6	<2	69.2	10.5	5.87	0.16	Fault likely not active in Quaternary (Woodward-Clyde 1996). Shallow structure not likely capable of large events (Olig et al. 1996). Not potential design fault.
Moab Fault and Spanish Valley Faults	2476	72.4	<2	114.8	12.5	6.19	0.16	Fault likely not active in Quaternary (Olig et al. 1996). Shallow structure likely not capable of large events (Olig et al. 1996). Not potential design fault.
Price River area faults	2457	50.9			24.8	7.06	0.13	Potential design fault.
Ryan Creek Fault zone	2263	39.5			26.6	6.93	0.11	Potential design fault.
Sand Flat Graben Faults	2475	23.1			26.4	6.66	0.10	Potential design fault.
Unnamed fault in Westwater Quad, R19E, T21S	1	8.0			2.4	6.13	0.60	Associated with Thompson Anticline. Subsidence features. Not potential design fault.
Unnamed parallel faults in Westwater Quad, R20E, T21S	2	6.4			3.1	6.02	0.49	Associated with Thompson Anticline. Subsidence features. Not potential design fault.

Table 3 (continued). Preliminary MCE Associated with Quaternary Faults and Faults of Unknown Age

Fault Name	Fault Number[a]	Length (km)	Depth of Rupture (km)	Rupture Area (km^2)	Distance From Site (mi)	MCE (M_w)[b]	PHA (g) Campbell and Bozorgnia (2003)	Comments
Unnamed fault in Westwater Quad, R19E, T19S	3	15.7			5.3	6.47	0.42	Associated with Thompson Anticline. Subsidence features. Not potential design fault.
Unnamed fault in Westwater Quad, R18E, T21S	4	2.9			4.9	5.62	0.29	Associated with Salt Valley Anticline. No evidence of Quaternary faulting. Not potential design fault.
Unnamed fault in Westwater Quad, R18E, T20S	5	1.9			7.0	5.40	0.19	Associated with Salt Valley Anticline. No evidence of Quaternary faulting. Not potential design fault.
Unnamed fault in Westwater Quad, R17E, T20S	6	3.3			9.6	5.68	0.16	Associated with Salt Valley Anticline. No evidence of Quaternary faulting. Not potential design fault.
Unnamed fault in Westwater Quad, R21E, T20S	7	4.4			12.4	5.83	0.13	No evidence of Quaternary faulting. Potential design fault.
Cactus Park-Bridgeport Fault	8	22.5			70	6.65	0.02	Design fault for Grand Junction Site (1991b). Potential design fault.
Little Grand Fault	9	47.0			6.5	7.02	0.47	Fault determined not to be active in Quaternary based on field evidence (DOE 1991a). Not potential design fault.

[a]Fault number identical to UGS Quaternary Fault and Fold Database if fault is included in database, otherwise assigned number 1 – 7 unique to this report.
[b]MCE based on rupture area, where data available, otherwise based on rupture length.

As discussed in the "Site and Regional Seismicity–Results of Literature Research" calculation (RAP Attachment 2, Appendix E), the Salt and Cache Valley faults, Tenmile Graben, and the Moab and Spanish Valley faults are all associated with the salt structures within the Paradox Basin. Reports by Olig et al. (1996), Woodward-Clyde (1996), and Woodward-Clyde (1984) found no evidence of Quaternary tectonic deformation of these structures. Based on detailed mapping, structural evidence, and geophysical data, Olig et al (1996) determined that the faults within the Moab and Spanish Valley areas are most likely related to salt dissolution. They concluded that the primary movement on the Moab Fault is tectonic and occurred during a period of Tertiary extension. They also concluded that most, if not all, of the slip on the Moab Fault is pre-Quaternary, and that the Moab Fault is a shallow structure that probably soles into the Moab salt-cored anticline within 2-km depth along much of its length. Therefore, it is not likely to be capable of producing significant earthquakes.

In addition, geomorphic expression of the fault indicates very low rates of activity. The report also indicates that the earthquake potential of the other salt structures within the Paradox Basin may also be similarly low. From these discussions, the MCE associated with these structures was calculated using Wells and Coppersmith (1994) relationships based on rupture area, assuming that the rupture depth is 2 km.

Of the faults listed in Table 3, only the Salt and Cache Valley faults, Little Grand Wash Fault, and faults No. 2, 3, and 4 would generate PHA values greater than those estimated by the FE (0.22 g). As discussed in the literature review, these five faults have been determined to not be capable faults. Of the faults whose capability is still undetermined or proven capable, the Price River Area faults have the potential of creating the largest PHA at the site, at 0.13 g.

Conclusion and Recommendations:

Of the faults that are suspected of being active in the Quaternary, none are expected to have an impact on the site greater than that calculated for an FE event occurring 15 km from the site. Therefore, the design PHA is estimated to be 0.22 g. Features such as the Salt and Cache Valley faults, Tenmile Graben, Moab Fault, Little Grand Fault, and the faults associated with the Thompson Anticline have been investigated and determined to not be seismogenic.

Amplification

Amplification of horizontal accelerations due to specific site conditions must be considered. Geotechnical investigations at the site, as noted in the *Borehole Logs* calculation (RAP Attachment 5, Appendix B), indicate alluvial and eolian soils overlying the withdrawal area range in depth from approximately 2 to 23 feet (ft). In the proposed area of the disposal cell, refusal (standard penetration tests [SPT] greater than 50 blows per 6 inches) was typically encountered between 5 and 15 ft below ground surface. Correlations between SPT and shear wave velocities (Sykora 1987) estimate the range of shear wave velocities at a blow count of 100 blows per foot to be between approximately 600 and 1,850 ft per second (fps).

The TAD (DOE 1989) states in Section 5.4.4 that for shallow soil sites with less than 30 ft of overburden above bedrock, the site surface acceleration is considered to be the same as the acceleration derived from the seismic study. In Campbell and Bozorgnia (2003) attenuation relations, the PHA equations account for local site conditions of the upper 30 meters of rock or soil. As defined in their paper, the site is categorized as a firm rock site, based on underlying geologic unit consisting of pre-Tertiary sedimentary rock (Late Cretaceous Mancos Shale). This category assignment is supported by the SPT data, which place the less-weathered Mancos Shale as a BC soil class as defined by the National Earthquake Hazard Reduction Program.

A geophysical investigation at the Crescent Junction Site was done specifically to access rippability of the Mancos Shale during construction of the disposal cell (see the "Seismic Rippability" calculation in RAP Attachment 5, Appendix G). As such, the investigation consisted of determining the seismic velocities of the weathered and unweathered shale deposits using compression wave data. Shear wave velocities and shear modulus are typically the parameters used to evaluate the stiffness of the foundational materials to evaluate whether amplification of ground motions would be expected. However, on a qualitative basis, the seismic velocity data is discussed here as further evidence the site is founded on firm rock. The

investigation summarized the three main geologic layers. The upper layer (alluvium and eolian deposits) ranged in depths from 4.5 to 18 ft, with seismic velocities ranging from approximately 1,160 to 1,330 fps, typical for unsaturated alluvial overburden soils. The base of the second layer (weathered Mancos Shale) was interpreted to vary between approximately 24 and 60 ft, with seismic velocities ranging from about 4,060 to 5,220 fps. Velocities for the unweathered Mancos Shale ranged from about 9,000 to 10,000 fps. The apparent discrepancy between the depth to unweathered Mancos Shale from the borehole data (5 to 15 ft) versus the geophysical data (24 to 60 ft) is due to differences between definitions of weathered shale. From a geologic standpoint, the shale contains fractures to a significant depth. The grading from weathered to unweathered is gradual and somewhat arbitrary. However, as indicated by SPT data, at a depth of 15 ft, the shale is sufficiently stiff to classify as a firm rock.

Based on the above data, the PHA of 0.22 g should be used in slope stability and liquefaction analyses. Amplification of site accelerations due to soil conditions is not warranted.

Comparison to Other Sites

As discussed in the "Site and Regional Seismicity–Results of Literature Research" calculation (RAP Attachment 2, Appendix E), several other studies have estimated PHAs for nearby sites. Specifically, the study done by Utah Geological Survey, and the Green River, Grand Junction, and Moab Sites are addressed here.

Halling et al. (2002) developed peak acceleration maps for the state of Utah. A statewide map was published in the document that shows peak horizontal ground acceleration for the Crescent Junction Site to be approximately 0.5 g. These ground accelerations were entirely influenced by predicted ground motion from the Tenmile Graben Fault. Substantial studies have been done (Woodward-Clyde 1996, Olig et al. 1996) that indicate this structure is not capable. It is unclear why the Tenmile Graben was included in this map while similar salt-related features, such as Salt and Cache Valley faults, Moab Fault, and Fisher Valley faults, were not included. Documentation regarding these faults reads "A number of faults identified in Hecker's (1993) report were cited as having questionable seismogenic potential. The majority of these faults are located in eastern Utah, where the faults are attributed to salt diapers or salt dissolution and flow instead of actual tectonic faulting. These faults were not included in the peak bedrock acceleration calculations" (Halling et al. 2002).

In addition, several conservative assumptions resulted in the ground accelerations at the Crescent Junction Site as calculated by Halling et al. (0.5 g) to be substantially higher than those values calculated in this study (0.16 g). First, PHAs generated for the map were estimated using relationships developed by Abrahamson and Silva (1997). Comparisons done by Halling et al. (2002) show that of the three attenuation relations considered (Abrahamson and Silva 1997, Campbell 1997, and Spudich et al. 1997), the Abrahamson and Silva relationship is the most conservative of the three for the magnitude and distance considered for the Tenmile Graben. The Campbell relationship yielded a middle value between the three and is thought to be appropriate for this study. In addition, Halling et al. (2002) conservatively modeled the Tenmile Graben to dip at 60 degrees on both sides of the fault, to a depth of 15 km. The effect of this assumption is to decrease the distance from the site to the fault rupture plane from 17.1 km to 14.6 km. However, because the graben scarps define the extent of the rupture plane, it seems reasonable to define the distance from the site to the rupture plane as the distance from the site to the nearest surface expression of the structure. These two main differences account for the variability in site acceleration determined by the two studies.

For comparison purposes only, the peak ground accelerations determined for the UMTRA Project Sites at Green River and Grand Junction/Cheney Disposal Site were investigated. The seismotectonic stability study performed for the Green River Disposal Site recommended the design acceleration based on a floating earthquake of 6.2 M_L occurring 15 km (9.5 miles) from the site, resulting in a peak ground acceleration of 0.21 g. This recommendation is essentially the same as the recommendation for this study.

Seismotectonic stability studies done for the Grand Junction mill tailings/Cheney Disposal Site identified a fault (Fault 8) with a length of 11.0 km at a distance of 9.0 km from the site. Although no evidence of Quaternary displacement was proven, it was considered to be capable on the basis of its apparent association with a possibly active regional structure, the Uncompahgre Uplift. This fault was adopted as

the design fault for the Cheney Disposal Site, resulting in a recommended design acceleration of 0.42 g. The capability of this fault and other faults related to the Uncompahgre Uplift has negligible impact on the Crescent Junction Site because of the distance of these faults to the Crescent Junction Site.

Woodward-Clyde (1996) performed a probabilistic seismic hazard analysis for the uranium mill tailings site in Moab, Utah. In their study, seismic sources included 11 faults, an area of seismicity along the Colorado River, and the random seismic events within the Colorado Plateau. At a return period of 10,000 years, they estimated a mean PHA of 0.18 g. The dominant contributor to the PHA is the random event, or FE, within the Colorado Plateau.

Computer Source:

Not applicable.

References:

10 CFR 100. U.S. Nuclear Regulatory Commission (NRC), "Reactor Site Criteria," *Code of Federal Regulations*, Title 10, Part 100, Appendix A.

40 CFR 192. U.S. Environmental Protection Agency (EPA), "Promulgated Standards for Remedial Actions at Inactive Uranium Processing Sites," *Code of Federal Regulations,* Title 40, Part 192.

Abrahamson, N.A., and W.J. Silva, 1997. "Empirical Response Spectral Attenuation Relationships for Shallow Crustal Earthquakes," Seismological Research Letters, 68(1), pp. 94–127.

Algermissen, S.T., D.M. Perkins, P.C. Thenhaus, S.L. Benson, and S.L Bender, 1982. *Probabilistic Estimates of Maximum Acceleration and Velocity in Rock in the Contiguous United States,* U.S. Geological Survey Open-File Report 82-1033.

Arabasz, W.J., R.B. Smith, and W.D. Richins, 1979. *Earthquake Studies in Utah, 1850 to 1978,* University of Utah Seismograph Stations, Department of Geology and Geophysics, University of Utah Special Publication 5527.

Black, B., S. Hecker, M. Hylland, G. Christenson, and G. McDonald, 2003. *Quaternary Fault and Fold Database and Map of Utah*, Utah Geological Survey Map 193DM, CD-ROM, scale 1:500,000.

Campbell, K.W., 1981. *Near-Source Attenuation of Peak Horizontal Acceleration,* Bulletin of the Seismological Society of America, 71(6), pp. 2039–2070, December.

Campbell, K.W., 1997. *Empirical Near-Source Attenuation Relationships for Horizontal and Vertical Components of Peak Ground Acceleration, Peak Ground Velocity, and Pseudo-Absolute Acceleration Response Spectra,* Seismological Research Letters, 68(1), pp. 154–179.

Campbell, K.W., and Y. Bozorgnia, 2003. *Updated Near-Source Ground-Motion (Attenuation) Relations for the Horizontal and Vertical Components of Peak Ground Acceleration and Acceleration Response Spectra,* Bulletin of the Seismological Society of America, 93(1), pp. 314–331, February.

Chitwood, J.P., 1994. *Provisional Geologic Map of the Hatch Mesa Quadrangle, Grand County, Utah,* Utah Geological Survey Map 152, scale 1:24,000.

Colorado Geological Survey, 2002. *Earthquakes Caused by Humans in Colorado,* RockTalk, 5(2), April.

DOE (U.S. Department of Energy), 1989. *Technical Approach Document,* Revision II, AL 050425.0002, United States Department of Energy, Uranium Mill Tailings Remedial Action Project, December.

DOE (U.S. Department of Energy), 1991a. *Remedial Action Plan and Final Design for Stabilization of the Inactive Uranium Mill Tailings at Green River, Utah.*

DOE (U.S. Department of Energy), 1991b. *Remedial Action Plan and Site Design for Stabilization of the Inactive Uranium Mill Tailings Site at Grand Junction, Colorado.*

Doelling, H.H., 2001. *Geologic Map of the Moab and Eastern Part of the San Rafael Desert 30' × 60' Quadrangles, Grand and Emery Counties, Utah, and Mesa County, Colorado,* Utah Geological Survey Map 180, scale 1:100,000.

Gaultieri, J.L, 1988. *Geologic Map of the Westwater 30' × 60' Quadrangle, Grand and Uintah Counties, Utah, and Garfield and Mesa Counties, Colorado,* U.S. Geological Survey Miscellaneous Investigations Series Map I-1765, scale: 1:100,000.

Halling, M.W., J.R. Keaton, L.R. Anderson, and W. Kohler, 2002. *Deterministic Maximum Peak Bedrock Acceleration Maps for Utah,* Utah Geological Survey Miscellaneous Publication 02-11, July.

Hecker, S., 1993. *Quaternary Tectonics of Utah with Emphasis on Earthquake-Hazard Characterization,* Utah Geological Survey Bulletin 127.

Keller, G., L. Braile, and P. Morgan, 1979. *Crustal Structure, Geophysical Models and Contemporary Tectonism of the Colorado Plateau,* Tectonophysics, Vol. 61, pp. 131–147.

Kirkham, R., and W. Rogers, 1981. *Earthquake Potential in Colorado, a Preliminary Evaluation,* Colorado Geological Survey Bulletin 43.

Krinitzsky, E.L., and F.K. Chang, 1977. *State-of-the-Art for Assessing Earthquake Hazards in the United States, Report 7, Specifying Peak Motions for Design Earthquakes,* U.S. Army Engineer Waterways Experiment Station, Miscellaneous Paper S-74-1, Vicksburg, Mississippi.

NEIC (National Earthquake Information Center), 2005. *Circular and Rectangular Searches of Historical Earthquakes,* http://neic.usgs.gov/neis/epic/.

Olig, S.S., C.H. Fenton, J. McCleary, and I.G. Wong, 1996. "The Earthquake Potential of the Moab Fault and Its Relation to Salt Tectonics in the Paradox Basin, Utah," in Huffman, A.C. Jr., W.R. Lund, and L.H. Godwin, editors, *Geology and Resources of the Paradox Basin,* Utah Geological Association Guidebook 25, pp. 251–264.

Richter, C.F., 1958. *Elementary Seismology,* W.H. Freeman and Company, San Francisco, California.

Smith, R. and M. Sbar, 1974. *Contemporary Tectonics and Seismicity of the Western United States with Emphasis on the Intermountain Seismic Belt,* Geological Society of America Bulletin, Vol. 85, pp. 1205–1218.

Spudich, P., J. Fletcher, M. Hellweg, J. Boatwright, C. Sullivan, W. Joyner, T. Hanks, D. Boore, A. McGarr, L. Baker, and A. Lindh, 1997. *SEA96, A New Predictive Relationship for Earthquake Ground Motions in Extensional Tectonic Regimes,* Seismological Research Letters, 68(1), pp. 190–198.

Sykora, D.W., 1987. *Examination of Existing Shear Wave Velocity and Shear Modulus Correlations in Soils,* U.S. Army Engineer Waterway Experiment Station, Miscellaneous Paper GL-87-22, Vicksburg, Mississippi.

USGS (U.S. Geological Survey) 2002. *Quaternary Fault and Fold Database,* http: //Qfaults.cr.usgs.gov/.

Wells, D.L., and K.J. Coppersmith, 1994. *New Empirical Relationships among Magnitude, Rupture Length, Rupture Width, Rupture Area, and Surface Displacement,* Bulletin of the Seismological Society of America, 84(4), pp. 974–1002, August.

Williams, P., compiler, 1964. *Geology, Structure, and Uranium Deposits of the Moab Quadrangle, Colorado and Utah,* U.S. Geological Survey Miscellaneous Geologic Investigations Map I-360, scale 1:250,000.

Williams, P., and R. Hackman, 1971. *Geology of the Salina Quadrangle, Utah*, U.S. Geological Survey Miscellaneous Geologic Investigations Map I-591, scale 1:250,000.

Willis, G.C., 1986. *Provisional Geologic Map of the Sego Canyon Quadrangle, Grand County, Utah*, Utah Geological Survey Map 89, scale 1:24,000.

Witkind, I.J., 1995. *Geologic Map of the Price 1° x 2° Quadrangle, Utah*, U.S. Geological Survey Miscellaneous Geologic Investigations Map I-2462, scale 1:250,000, USGS.

Wong, I.G., S.S Olig, and J.D.J. Bott, 1996. "Earthquake Potential and Seismic Hazards in the Paradox Basin, Southeastern Utah," in Huffman, A. C., Jr., W. R. Lund, and L. H. Godwin, editors, *Geology and Resources of the Paradox Basin*, Utah Geological Association Guidebook 25, pp. 241–250.

Woodward-Clyde Consultants, 1984. *Geologic Characterization Report for the Paradox Basin Study Region, Utah Study Areas, Volume VI, Salt Valley*, Walnut Creek, California, unpublished consultant's report for Battelle Memorial Institute, Office of Nuclear Waste Isolation, ONWI-290, scale 1:62,500.

Woodward-Clyde Consultants, 1996. *Evaluation and Potential Seismic and Salt Dissolution Hazards at the Atlas Uranium Mill Tailings Site, Moab, Utah*, Oakland, California, unpublished Consultant's report for Smith Environmental Technologies and Atlas Corporation, SK9407.

Appendix A

National Earthquake Information Center (NEIC): Earthquake Search Results

Site and Regional Seismicity - Results of MCE and PHA
APPENDIX A
NEIC: Earthquake Search Results

UNITED STATES GEOLOGICAL SURVEY

EARTHQUAKE DATA BASE

FILE CREATED: Mon Aug 15 14:28:55 2005
Geographic Grid Search Earthquakes= 549
Latitude: 40.750N - 34.500N
Longitude: 106.500W - 112.500W
Catalog Used: PDE
Data Selection: Historical & Preliminary Data

FILE CREATED: Mon Aug 15 14:31:32 2005
Geographic Grid Search Earthquakes= 991
Latitude: 40.750N - 34.500N
Longitude: 106.500W - 112.500W
Catalog Used: SRA
Data Selection: Eastern, Central and Mountain States of U.S. (SRA)

FILE CREATED: Mon Aug 15 14:30:22 2005
Geographic Grid Search Earthquakes= 64
Latitude: 40.750N - 34.500N
Longitude: 106.500W - 112.500W
Catalog Used: USHIS
Data Selection: Significant U.S. Earthquakes (USHIS)

The above searches have been filtered to include only events occuring within the Colorado Plateau
Only events with magnitudes 3.0 or greater or Intensities of 4 or greater are considered further.
Data has been declustered to remove aftershocks and foreshocks.
BOLD EVENTS ARE EVENTS CONSIDERED NON-TECTONIC IN ORIGIN AND ARE NOT INCLUDED IN RECURRENCE CALCULATIONS

	Date			ORIGIN	COORDINATES		DEPTH	MAGNITUDES				INFORMATION (see below for explanation of symbols)																	Converted Magnitude	Comments
										Other																				
CATALOG SOURCE	YEAR	MO	DA	TIME	LAT	LONG	km	mb	Ms	Value	Scale	INT	EFF	MAP	FPS	MO	DEP	IDE	PFD	FLG	D	T	S	V	N	W	G		
SRA	1871	10	0	0	40.5	-108.5						6																5.0	
SRA	1882	2	11	830	37.3	-107						4																3.7	
SRA	1889	1	15	22	39.5	-107.3						5																4.3	
SRA	1891	12	0	21	40.5	-108						6																5.0	
SRA	1892	2	2	830	35.2	-111.6						6																5.0	
SRA	1894	1	1	10	37.9	-107.8						4																3.7	
SRA	1897	8	3	7	38.2	-107.8						5																4.3	
SRA	1899	0	0	230	40.5	-108						4																3.7	
SRA	1900	5	0	0	36.9	-106.9						5																4.3	
SRA	1906	1	25	213230	35.2	-111.7						7																5.7	
SRA	1906	4	0	0	40.5	-108.3						4																3.7	
SRA	1910	9	24	405	35.8	-111.5						7																5.7	
SRA	1912	8	18	2112	36	-111.5						7																5.7	
SRA	1913	11	11	2155	38.1	-107.7						6																5.0	
SRA	1918	4	28	1258	35.2	-111.6						4																3.7	
SRA	1920	12	29	250	39.5	-107.5						5																4.3	
SRA	1921	4	6	2107	34.9	-110.2						5																4.3	
SRA	1921	7	31	355	36	-107						4																3.7	
SRA	1923	9	28	0	35.2	-111.7						4																3.7	
SRA	1928	4	30	1550	37.8	-107						5																4.3	
SRA	1931	4	17	1238	34.5	-110						5																4.3	
SRA	1935	1	10	810	36	-112.1						6																5.0	
SRA	1935	10	6	3	37.9	-111.4						4																3.7	
SRA	1937	4	8	12	35.7	-109.5						5																4.3	
SRA	1937	12	17	2330	35.2	-111.7						4																3.7	
SRA	1939	3	9	1330	36.1	-112.1						5																4.3	
SRA	1940	10	16	1325	35.2	-111.7						4																3.7	
SRA	1941	8	29	1134	37.3	-107.7						5																4.3	
SRA	1942	7	23	1940	40.5	-108.5						5																4.3	
SRA	1943	8	14	540	38.2	-111.4						4																3.7	
SRA	1944	9	9	41220	39	-107.5						6																5.0	
SRA	1945	4	29	1708	37.7	-107.7						4																3.7	
SRA	1945	7	0	1155	36.1	-112.1						4																3.7	
SRA	1946	1	31	2245	39.6	-107.3						4																3.7	
SRA	1947	10	27	41540	35.5	-112						4																3.7	
SRA	1948	8	8	2320	36.1	-112.1						5																4.3	
SRA	1948	12	3	1845	35	-110.7						4																3.7	
SRA	1950	1	17	51	35.7	-109.5						6																5.0	
SRA	1950	1	18	15551	40.5	-110.5				5.3	UK	5																5.3	
SRA	1953	7	30	545	39	-110.2						5																4.3	
SRA	1953	10	8	201946	34.75	-111						5																4.3	
SRA	1954	2	21	202051	40	-108.75						4																3.7	
SRA	1954	3	31	14	39	-110.2						4																3.7	
SRA	1954	11	3	2039	35.2	-106.7						5																4.3	
SRA	1955	3	27	1213	38.3	-111.3						4																3.7	
SRA	1955	8	3	63942	38	-107.3						6																5.0	

CATALOG SOURCE	Date YEAR	MO	DA	ORIGIN TIME	COORDINATES LAT	LONG	DEPTH km	MAGNITUDES mb	Ms	Other Value	Other Scale	INFORMATION (see below for explanation of symbols) INT	E FF	MAP S	FPS	MOO	DEP E	IDE	PFD	FLG	D	T	S	V	N	W	G	Converted Magnitude	Comments
SRA	1956	2	12	3	40.5	-109.5						4																3.7	
SRA	1957	7	18	152420	40	-110.5						4																3.7	
SRA	1959	2	11	1401	35.2	-111.7						5																4.3	
SRA	1959	10	13	815	35.5	-111.5		5		5	ML	5																5.0	
SRA	1960	10	11	80530	38.3	-107.6	49			5.5	mb	6																5.5	
SRA	1961	5	6	161220	39.6	-110.2	25					5																4.3	
SRA	1962	1	13	1333	38.4	-107.8				4.4	ML	4																4.4	
SRA	1962	2	5	144551	38.2	-107.6	25			4.7	ML	5																4.7	
SRA	1962	9	7	165023.8	39.2	-110.89	7			3.1	ML																	3.1	
SRA	1962	12	11	102813	39.36	-110.42	7			3.4	ML																	3.4	
SRA	**1963**	**4**	**15**	**221824.6**	**39.59**	**-110.35**	**7**	**4.2**		**3.4**	**ML**														**N**			**3.4**	**Related to coal mining (Smith and Sbar)**
SRA	**1963**	**4**	**24**	**133303.3**	**39.44**	**-110.33**	**7**	**4.6**		**3.3**	**ML**														**N**			**3.3**	**Related to coal mining (Smith and Sbar)**
SRA	1963	7	9	202525	40.03	-111.19	7	4.1		4	ML		F															4.0	
SRA	1963	9	30	91739	38.1	-111.22	7	4.5		4.3	ML																	4.3	
SRA	**1963**	**12**	**24**	**145108.8**	**39.56**	**-110.32**	**7**	**4.1**		**3**	**ML**														**N**			**3.0**	**Related to coal mining (Smith and Sbar)**
SRA	1964	8	5	151756	38.95	-110.92	7			3	ML																	3.0	
SRA	**1965**	**1**	**14**	**123010.8**	**39.44**	**-110.35**	**7**	**4.5**		**3.3**	**ML**														**N**			**3.3**	**Related to coal mining (Smith and Sbar)**
SRA	1965	6	7	142801	36	-112.2	33			3.5	mb																	3.5	
SRA	**1965**	**6**	**27**	**192408.7**	**39.51**	**-110.38**	**7**	**4**		**3.1**	**ML**																	**3.1**	**Related to coal mining (Smith and Sbar)**
SRA	**1965**	**6**	**29**	**74628**	**39.5**	**-110.39**	**7**	**4.3**		**3.2**	**ML**																	**3.2**	**Related to coal mining (Smith and Sbar)**
SRA	1965	7	18	35551.4	39.5	-109.9	33	3.1																				3.1	
USHIS	1966	1	23	15638	36.98	-107.02	3	5.1		4.99	Mw	7	F															5.0	
SRA	1966	5	20	134047	37.98	-111.85	7	4.3		4.1	ML																	4.1	
SRA	**1966**	**7**	**6**	**54708**	**40.1**	**-109**	**7**	**4.1**		**3.7**	**ML**																	**3.7**	**Rangley Oil Field gas oil and gas withdrawl**
SRA	**1966**	**7**	**30**	**32531**	**39.44**	**-110.36**	**7**	**4.1**		**3.1**	**ML**																	**3.1**	**Related to coal mining (Smith and Sbar)**
SRA	1966	9	4	95234	38.3	-107.6	33	4.2																				4.2	
SRA	1966	10	3	160350	35.8	-111.6	34	4.4																				4.4	
SRA	**1966**	**11**	**11**	**164534.6**	**39.6**	**-110.5**	**15**	**3.2**																	**N**			**3.2**	**Non-tectonic**
SRA	1967	1	16	92245	37.67	-107.86	33	4.1																				4.1	
SRA	1967	2	5	100716.6	39.55	-110.1	33	3																				3.0	
SRA	**1967**	**2**	**15**	**32803**	**40.1**	**-109.1**	**7**	**4.5**		**4**	**ML**	**5**																**4.0**	**Rangley Oil Field gas oil and gas withdrawl**
SRA	1967	4	4	225339	38.32	-107.75	33	4.5		3	ML																	3.0	
SRA	1967	9	4	232746	36.15	-111.6	33			4.2	ML																	4.2	
SRA	**1967**	**10**	**25**	**24134**	**39.47**	**-110.35**	**0**	**4**		**3.2**	**ML**																	**3.2**	**Related to coal mining (Smith and Sbar)**
SRA	**1967**	**12**	**10**	**193000.1**	**36.68**	**-107.21**	**0**	**5.1**																	**N**			**5.1**	**Non-tectonic**
SRA	1968	6	2	185923.2	39.21	-110.45	7	3.8		3.3	ML																	3.3	
SRA	1968	6	23	201613	39.31	-107.41	33	3.8																				3.8	
SRA	1968	11	17	143338	39.52	-110.97	7	4.6		3.5	ML																	3.5	
SRA	**1969**	**9**	**10**	**210000.1**	**39.41**	**-107.95**	**0**	**5.3**				**5**													**N**			**5.3**	**Non-tectonic**
SRA	1970	2	3	55935	37.92	-108.31	33	4																				4.0	
SRA	**1970**	**2**	**21**	**61348**	**39.49**	**-110.35**	**7**	**4.1**		**3.1**	**ML**																	**3.1**	**Related to coal mining (Smith and Sbar)**
SRA	1970	4	18	104211	37.87	-111.72	7	4.4		3.7	ML																	3.7	
SRA	1970	4	14	104054.1	39.65	-110.82	7	4.2		3	ML																	3.0	
SRA	**1970**	**4**	**21**	**85352**	**40.1**	**-108.9**	**4**	**4.3**		**3.9**	**ML**	**5**																**3.9**	**Rangley Oil Field gas oil and gas withdrawl**
SRA	1971	1	7	203952	39.49	-107.31	33	4.3		3.8	ML	5																3.8	
SRA	1971	7	10	172236	40.24	-109.6	7	3.8		3.7	ML																	3.7	
SRA	1971	11	12	93044	38.91	-108.68	5			4	ML	3																4.0	
SRA	1971	12	15	125814	36.791	-111.824	5			3	ML																	3.0	
SRA	1972	4	20	132816	35.311	-111.64	5	3.7				4																3.7	
SRA	1972	10	16	214931.2	40.42	-111.02	7	4.1		3.4	ML	4																3.4	
SRA	1973	2	9	173837	36.43	-110.425	5			3.2	ML																	3.2	
PDE	**1973**	**5**	**17**	**16**	**39.793**	**-108.366**	**0**	**5.4**	**4.1**	**5.7**	**UK**						**3**	**P**							**E**			**5.7**	**Explosion**
SRA	1973	12	24	22014	35.26	-107.74	18	4.4		4.1	ML	6																4.1	
SRA	1975	1	30	144840	39.27	-108.65	5	4.4		3.7	ML	5																3.7	
SRA	1975	3	7	31613	34.55	-107.16				3	ML																	3.0	
SRA	1976	1	5	62332	35.84	-108.34	25	5		4.6	ML	6																4.6	
SRA	1976	2	28	205358	35.91	-111.788	5			3	ML																	3.0	
SRA	**1976**	**4**	**19**	**233545**	**35.39**	**-109.1**	**5**			**3.5**	**ML**	**5**													**?**			**3.5**	**Classified as an earthquake, but a non-tectonic origin cannot be ruled out**
SRA	1977	2	9	4216	39.29	-111.11	7			3.2	ML	6																3.2	

CATALOG SOURCE	Date YEAR	MO	DA	ORIGIN TIME	COORDINATES LAT	LONG	DEPTH km	MAGNITUDES mb	Ms	Other Value	Other Scale	INFORMATION (see below for explanation of symbols) INT	EFF	MAP	FPS	MO	DEP	IDE	PFD	FLG	D	T	S	V	N	W	G	Converted Magnitude	Comments
USHIS	1977	3	5	30055	35.748	-108.222	44	4.6		4.2	ML	6	F															4.2	
SRA	1977	6	3	13722	39.65	-110.51	7			3.2	MD																	3.2	
SRA	1977	9	24	111648	39.31	-107.31	5	4		3	ML																	3.0	
SRA	1977	9	30	101920	40.47	-110.47	6	5		4.5	ML	6																4.5	
SRA	1977	11	29	213123	36.82	-110.99	7			3	MD																	3.0	
SRA	1978	5	29	164518	39.28	-107.32	5			3	ML																	3.0	
SRA	1978	9	23	82006	39.32	-111.09	2			3	ML																	3.0	
SRA	**1979**	**3**	**19**	**145929**	**40.2**	**-108.9**	**2**			**3.1**	**ML**	**4**																**3.1**	**Rangley Oil Field gas oil and gas withdrawl**
SRA	1979	4	30	20710	37.88	-111.02	7			3.8	ML	3																3.8	
SRA	1979	10	23	41719	37.89	-110.93	7			3.5	ML		F															3.5	
SRA	1980	6	1	84027	35.391	-111.986	5			3.6	ML	2																3.6	
PDE	1981	5	14	51104.1	39.481	-111.06	1	4.5		3.5	ML	5	F				4		P									3.5	
SRA	1981	5	29	30902	36.83	-110.37	1			3	MD																	3.0	
SRA	1981	9	10	75509	37.5	-110.56	2			3.1	MD																	3.1	
PDE	**1981**	**9**	**21**	**80133**	**39.578**	**-110.44**	**7**			**3.5**	**ML**	**3**	**F**				**3**		**P**									**3.5**	**Related to coal mining (Smith and Sbar)**
SRA	1981	12	6	90920	35.17	-111.62						5																	
SRA	1982	4	17	60012	38.22	-111.3	9			3	ML																	3.0	
SRA	1982	11	3	175411	35.32	-108.74	5			3	ML																	3.0	
SRA	1982	11	19	205734	36.03	-112.01	5			3	ML		F															3.0	
SRA	1983	1	27	233711	37.778	-110.674	7			3.3	MD																	3.3	
SRA	**1983**	**3**	**22**	**111235**	**39.546**	**-110.422**	**2**			**3.1**	**MD**		**F**															**3.1**	**Related to coal mining (Smith and Sbar)**
PDE	1983	5	3	124338	38.288	-110.592	7			3.2	ML						3		P									3.2	
SRA	1983	8	14	190830	38.359	-107.402	5			3.4	ML	2																3.4	
SRA	1983	8	31	81008	36.135	-112.037	5			3.3	ML		F															3.3	
SRA	1984	3	21	111930	39.344	-111.109	0			3.5	ML		F															3.5	
SRA	1984	5	14	101417	39.322	-107.228	5			3.2	ML	4																3.2	
SRA	1984	7	18	142931	36.216	-111.844	5			3	ML																	3.0	
SRA	1985	4	14	214800	35.174	-109.071	5			3.3	ML	3																3.3	
SRA	**1985**	**6**	**27**	**103629**	**39.558**	**-110.396**	**1**			**3**	**MD**																	**3.0**	**Related to coal mining (Smith and Sbar)**
SRA	1985	10	7	203340	40.407	-109.498	21			3	MD																	3.0	
SRA	1986	8	22	132633	37.42	-110.574	5			4	ML	5																4.0	
SRA	1986	9	3	62050	38.912	-107.09	5			3.5	ML	5																3.5	
SRA	1986	11	7	13153.7	37.43	-110.297	1			3	MD																	3.0	
PDE	1987	3	5	30250.49	40.442	-110.616	1	4		3.7	ML	4	F				4		P									3.7	
PDE	1988	1	15	73329.2	37.515	-106.684	5			3.1	ML		F				4		P									3.1	
PDE	1988	2	14	183240	40.626	-108.532	5					4	F				4		P									3.7	
PDE	1988	7	15	3809.59	36.374	-110.448	5			3.3	ML						4		P									3.3	
USHIS	1988	8	14	200303	39.128	-110.869	10	5.5		5.3	ML	6	F															5.3	
PDE	1989	2	3	180821	39.744	-110.897	0					4	F				4		P									3.7	
PDE	1989	4	9	112419.39	40.419	-110.942	9			3.2	ML	2	F				4		P									3.2	
PDE	**1989**	**5**	**13**	**210148.82**	**38.473**	**-108.924**	**7**			**3.1**	**MD**						4		**P**									**3.1**	**Paradox Valley salt-water injection**
PDE	1989	11	19	32113.61	38.055	-107.767	5			3	ML		F				4		P									3.0	
PDE	1990	4	7	153754.86	40.082	-109.519	3			3.5	ML						4		P									3.5	
PDE	1990	6	25	171533.54	38.952	-110.828	11			3	MD						4		P									3.0	
PDE	1990	10	21	43119	38.908	-108.355	10					5	F				4		P									4.3	
PDE	1991	1	26	214938	37.681	-111.429	9			3.5	ML	3	F				3		P									3.5	
PDE	1991	3	2	84137.49	40.091	-109.483	1	3		3.3	ML						4		P									3.3	
PDE	1991	4	26	130820	36.627	-112.345	10	3.3				4	F				4		P									3.3	
PDE	1991	6	25	210213.63	37.209	-110.358	1			3	MD						4		P									3.0	
PDE	1991	5	23	73840	39.298	-111.149	12	3.5		3.6	ML	3	F				3		P									3.6	
PDE	1991	11	8	131505	40.1	-109.286	2	3.4				3	F				4		P									3.4	
PDE	1992	5	15	213624	38.563	-107.914	5					4	F				4		P									3.7	
PDE	1992	7	5	181729	35.982	-112.219	5	4					F				4		P									4.0	
PDE	1992	7	5	122223	39.318	-111.134	5	4				3	F				1		P									4.0	
PDE	**1993**	**1**	**21**	**90120.4**	**39.712**	**-110.622**	**1**	**3.4**					**D**				**4**		**P**						**C**			**3.4**	**Coal bump or Rockburst in a coal mine**
PDE	1993	4	29	82100	35.611	-112.112	10	5.5	5	5.3	Mw	5	D	U		M	3		P									5.3	
PDE	1993	5	27	62153	37.084	-112.089	10	3.3		3.5	MD	3	F				3		P									3.5	
PDE	1994	9	13	60123	38.151	-107.976	10	4.4				6	D				4		P									4.4	
PDE	1994	11	3	114010.14	40.04	-108.269	5			3.4	ML						4		P									3.4	
PDE	1995	3	20	124616	40.179	-108.925	5	4.2				5	F				4		P									4.2	
PDE	1995	4	17	82346	35.964	-112.223	5	3.7				5	D				4		P									3.7	
PDE	1996	1	6	125558.62	39.12	-110.878	0	4.3		4.2	MD	5	F				4		P									4.2	
PDE	1996	2	2	21114	39.467	-111.23	1			3.2	ML						4		P									3.2	
PDE	1996	12	6	135314	39.706	-110.658	3			3.4	ML						3		P									3.4	
PDE	1997	3	31	73448	35.534	-111.993	5			3.7	ML		F				3		P									3.7	
PDE	1997	4	14	93048	39.048	-111.389	5			3.1	MD						3		P									3.1	
PDE	1997	10	20	70220	37.834	-111.879	10			3.1	ML						3		P									3.1	
PDE	1998	1	6	83646	34.916	-110.495	5			3.9	ML		D				3		P									3.9	
PDE	1998	2	5	51956	39.751	-110.846	1	3.6		3.7	ML		F				3		P									3.7	
PDE	**1998**	**4**	**10**	**65216**	**38.3**	**-108.8**	**5**			**3**	**ML**		**F**				**3**		**P**									**3.0**	**Paradox Valley salt-water injection**
PDE	1998	10	18	71310	36.033	-111.091	5			3.4	ML		F				3		P									3.4	

CATALOG SOURCE	Date YEAR	MO	DA	ORIGIN TIME	COORDINATES LAT	LONG	DEPTH km	MAGNITUDES mb	Ms	Other Value	Other Scale	INFORMATION (see below for explanation of symbols) I NT	E FF	MAP S	FPS MO	DEP	IDE	PFD	FLG	D	T	S	V	N	W	G	Converted Magnitude	Comments
PDE	1999	1	30	90547	37.55	-112.21	1	3.2		3	ML					3		P									3.0	
PDE	**1999**	**6**	**3**	**153534**	**38.3**	**-108.9**	**4**			**3.6**	**ML**		**F**			**3**		**P**									**3.6**	**Paradox Valley salt-water injection**
PDE	**1999**	**7**	**6**	**220545.19**	**38.319**	**-108.859**	**5**			**3.5**	**ML**		**F**			**3**		**P**									**3.5**	**Paradox Valley salt-water injection**
PDE	2000	3	7	21604	39.75	-110.84	1	4.3		4.2	ML		F			3		P								S	4.2	
PDE	**2000**	**3**	**15**	**121427.5**	**38.367**	**-108.867**	**5**			**3.3**	**ML**																**3.3**	**Paradox Valley salt-water injection**
PDE	**2000**	**5**	**27**	**215818**	**38.3**	**-108.9**	**5**			**4.3**	**ML**		**F**			**3**		**P**									**4.3**	**Paradox Valley salt-water injection**
PDE	2000	11	11	211753	40.28	-109.23	5			3.7	ML					3		P									3.7	
PDE	2001	7	19	201534	38.731	-111.521	3	4.5		4.3	ML		F			3		P									4.3	
PDE	2001	8	9	223854	39.66	-107.378	5			4	ML	4	F			3		P									4.0	
PDE	2001	11	5	83423	38.851	-107.384	1			3.4	ML		F			3		P									3.4	
PDE	2002	1	31	181745	40.287	-107.693	5			4.3	ML	3	F			3		P									4.3	
PDE	**2002**	**3**	**30**	**213843.9**	**38.853**	**-107.386**	**1**			**3.1**	**ML**		**F**			**3**		**P**						**C**			**3.1**	**Coal bump or Rockburst in a coal mine**
PDE	**2002**	**6**	**3**	**32523.98**	**38.907**	**-107.418**	**1**			**3.3**	**ML**		**F**			**3**		**P**						**C**			**3.3**	**Coal bump or Rockburst in a coal mine**
PDE	**2002**	**6**	**6**	**122910**	**38.3**	**-108.9**	**1**			**3.2**	**ML**					**3**		**P**									**3.2**	**Paradox Valley salt-water injection**
PDE	**2002**	**6**	**20**	**221704.8**	**38.908**	**-107.416**	**1**			**3.6**	**ML**		**F**			**3**		**P**						**C**			**3.6**	**Coal bump or Rockburst in a coal mine**
PDE	**2002**	**8**	**24**	**153719.7**	**38.92**	**-107.481**	**1**			**3.2**	**ML**		**F**			**3**		**P**						**C**			**3.2**	**Coal bump or Rockburst in a coal mine**
PDE	**2002**	**9**	**10**	**161811.4**	**38.789**	**-107.412**	**1**			**3.3**	**ML**		**F**			**3**		**P**						**C**			**3.3**	**Coal bump or Rockburst in a coal mine**
PDE	2002	9	26	103210	37.41	-110.53	3			3	ML					3		P									3.0	
PDE	**2002**	**11**	**26**	**54616.37**	**38.904**	**-107.448**	**1**			**3.1**	**ML**					**3**		**P**						**C**			**3.1**	**Coal bump or Rockburst in a coal mine**
PDE	2003	7	8	22033	36.95	-111.79	6			3.3	ML					3		P									3.3	
PDE	**2003**	**8**	**8**	**61105.19**	**38.907**	**-107.458**	**1**			**3.4**	**ML**					**3**		**P**						**C**			**3.4**	**Coal bump or Rockburst in a coal mine**
PDE	2003	11	17	231852	40.35	-111.17	12			3	ML																3.0	
PDE	**2004**	**4**	**15**	**45359.34**	**38.87**	**-107.35**	**1**			**3.1**	**ML**					**3**		**P**						**C**			**3.1**	**Coal bump or Rockburst in a coal mine**
PDE-W	2004	9	19	60943	38.853	-107.358	1			3.5	ML					3		P									3.5	
PDE	**2004**	**10**	**11**	**5841.02**	**38.825**	**-107.425**	**1**			**3.3**	**ML**					**3**		**P**						**C**			**3.3**	**Coal bump or Rockburst in a coal mine**
PDE-W	**2004**	**11**	**7**	**65459**	**38.2**	**-108.9**	**0**			**4.1**	**ML**	**4**	**F**			**3**		**P**									**4.1**	**Paradox Valley salt-water injection**
PDE	**2004**	**11**	**13**	**182830.4**	**38.875**	**-107.497**	**1**			**3.2**	**ML**		**F**			**3**		**P**						**C**			**3.2**	**Coal bump or Rockburst in a coal mine**
PDE-W	2004	11	24	101638	35.105	-107.51	5			3	ML					3		P									3.0	
PDE-W	2005	3	2	111257	34.715	-110.97	5	5.1		4.6	ML	3	F			1		P									4.6	
PDE	**2005**	**4**	**30**	**45704.76**	**38.918**	**-107.393**	**1**			**3.1**	**ML**					**3**		**P**						**C**			**3.1**	**Coal bump or Rockburst in a coal mine**
PDE-W	**2005**	**5**	**2**	**172955.8**	**38.795**	**-107.393**	**1**			**3.2**	**ML**		**F**			**3**		**P**						**C**			**3.2**	**Coal bump or Rockburst in a coal mine**
PDE-W	**2005**	**5**	**13**	**142604.3**	**38.835**	**-107.372**	**1**			**3.3**	**ML**		**F**			**3**		**P**						**C**			**3.3**	**Coal bump or Rockburst in a coal mine**
PDE-W	**2005**	**5**	**30**	**14921.14**	**38.889**	**-107.474**	**1**			**3.3**	**ML**					**3**		**P**						**C**			**3.3**	**Coal bump or Rockburst in a coal mine**
PDE-W	**2005**	**6**	**8**	**84600.4**	**38.953**	**-107.527**	**1**			**3.5**	**ML**					**3**		**P**						**C**			**3.5**	**Coal bump or Rockburst in a coal mine**
PDE-W	**2005**	**7**	**25**	**115128.3**	**38.831**	**-107.415**	**1**			**3.1**	**ML**					**3**		**P**						**C**			**3.1**	**Coal bump or Rockburst in a coal mine**

INFORMATION

INFORMATION (IEFM DTSVNWG on Screen Search): Dots are used in place of blanks to aid in the distinction between the columns. Read the sub-headers vertically.

Intensity (sub-header INT):
Maximum intensity on the Modified Mercalli Intensity Scale of 1931 (Wood and Neumann, 1931) or any similar 12-point intensity scale. It may also be an MMI value approximated from other intensity scales such as Ross-Forel or Japan Meteorological Agency. Possible intensity values are 1 - 9; X = 10; E = 11; T = 12.

Cultural Effects (sub-header EFF):
The most severe effect is listed (C = Casualities; D = Damage; F = Felt; H = Heard).
Note that casualties includes human deaths or injuries. Domestic animal casualties are considered to be damage.

Isoseismal Map (sub-header MAP): (Expanded Format only)
Indicates the publication where an isoseismal map for this event has been published.
U = United States Earthquakes.
E = Earthquake Notes. (Now Seismological Research Letters)
P = Preliminary Determination of Epicenters.
W = Wellington (New Zealand Seismology Reports, Wellington, N.Z.).
N = Nature Magazine.
S = Bulletin of the Seismological Society of America.

Fault Plane Solution (sub-header FPS):
Coded as an "F" to indicate the availability of a fault plane solution in the publication, "Preliminary Determination of Epicenters, Monthly Listing".

Moment Tensor Solution (sub-header MO):
Coded as an "G" to indicate the availability of a moment tensor solution in the publication "Preliminary Determination of Epicenters, Monthly Listing" (Sipkin, 1982; Dziewonski, 1980; and Hanks and others, 1979).

ISC Alternate Depth Indicator (sub-header DEP):
A "D" in this column indicates that a pP depth is given, but the pP depth is not the adopted depth in the hypocenter solution.

International Data Exchange (sub-header IDE):
An "X" in this column identifies the event as a "IDE" earthquake.

Preferred Solution (sub-header PFD):
A "P" in this column designates a preferred solution. Earthquake hypocenters which are located within a seismic network, such as Pasadena or Berkeley, or seismic catalogs which have undergone critical review during their compilation will be designated as a preferred solution.

Flag (sub-header FLG): Currently not used.

PHENOMENA

Diastrophism: (sub-header D)
F = Faulting.
U = Uplift.
S = Subsidence.
3 = Uplift and Subsidence.
4 = Uplift and Faulting.
5 = Faulting and Subsidence.
6 = Faulting with Uplift and Subsidence.
7 = Uplift or Subsidence.
8 = Faulting and Uplift or Subsidence.

Tsunami: (sub-header T)
T = Tsunami generated.
Q = Questionable Tsunami.

Seiche: (sub-header S)
S = Seiche.
Q = Questionable Seiche.

Volcanism: (sub-header V)
V = Earthquake associated with volcanism.

Non-Tectonic: (sub-header N)
E = Explosion.
I = Collapse.
C = Coal bump or Rockburst in a coal mine.
R = Rockburst.
M = Meteoritic.
N = Either known to be or likely to be of non-tectonic origin.
? = Classified as an earthquake, but a non-tectonic origin cannot be ruled out.
V = Reservoir induced earthquake.

Guided Waves in Atmospheric And/Or Ocean: (sub-header W)
T = T-wave.
A = Acoustic wave.
G = Gravity wave.
B = Both A and G.
M = T-wave plus and A or G.

Miscellaneous Phenomena: (sub-header G)
L = Liquefaction.
G = Geyser.
S = Landslides and/or Avalanches.
B = Sandblows.
C = Ground cracks not known to be an expression of faulting.
V = Lights or other visual phenomena seen.
O = Olfactory (Unusual odors noted).
M = More than one of these phenomena observed.

Appendix B

Quaternary and Undated Faults within Expanded Site Region

SITE AND REGIONAL SEISMICITY - RESULTS OF MCE AND PHA
APPENDIX B:
QUATERNARY AND UNDATED FAULTS WITHIN EXPANDED SITE REGION

Name	Number	Age of Most Recent Prehistoric Deformation (ya)	Slip-rate (mm/yr)	Fault Length (km)	Fault Type	Distance from site (miles)[1]	Distance from site (km)	Depth to seismo-genic rupture (km)	r_{seis} (km)	MCE (Based on fault length, all slip types, Wells and Coppersmith, 1994)	Rupture depth (km)	Rupture area (km^2)	MCE (based on fracture area, Wells and Coppersmith, 1994)	PHA (Campbell-Bozorgnia 2003) corrected, plus 1SD (based on Mw)
Salt and Cache Valleys faults (Class B)	2474	Class B	<0.2	57.9	N	1.8	2.9	3	4.2	7.12	2.00	115.80	6.09	0.67
unnamed fault in Westwater Quad, R19E, T21S (no. 1)	1			8.0		2.4	3.8	3	4.8	6.13				0.60
unnamed fault in Westwater Quad, R20E, T21S (no. 2)	2			6.4		3.1	5.1	3	5.9	6.02				0.49
Little Grand fault	9			47.0	N	6.5	10.5	3	10.9	7.02				0.47
unnamed fault in Westwater Quad, R19E, T19S (no. 3)	3			15.7		5.3	8.5	3	9.0	6.47				0.42
unnamed fault in Westwater Quad, R18E, T21S (no. 4)	4			2.9		4.9	7.9	3	8.4	5.62				0.29
unnamed fault in Westwater Quad, R18E, T20S (no. 5)	5			1.9		7.0	11.3	3	11.7	5.40				0.19
Ten Mile graben faults (Class B)[2]	2473	Class B	<0.2	34.6	N	10.5	16.8	3	17.1	6.87	2.00	69.20	5.87	0.16
Ten Mile graben faults (Class B)[3]	2473	Class B	<0.2	34.6	N	10.5	16.8	3	17.1	6.87	2.00	69.20	5.87	0.31
Ten Mile graben faults (Class B)[4]	2473	Class B	<0.2	34.6	N	10.5	16.8	3	14.6	7.15	2.00	69.20	5.87	0.45
Moab fault and Spanish Valley faults (Class B)	2476	Class B	<0.2	72.4	N	12.5	20.1	3	20.3	7.24	2.00	144.80	6.19	0.16
unnamed fault in Westwater Quad, R17E, T20S (no. 6)	6			3.3		9.6	15.5	3	15.7	5.68				0.16
Price River area faults (Class B)	2457	<1,600,000	<0.2	50.9	N	24.8	39.9	3	40.0	7.06				0.13
unnamed fault in Westwater Quad, R21E, T0S (no. 7)	7			4.4		12.4	19.9	3	20.1	5.83				0.13
Ryan Creek fault zone	2263	<1,600,000	<0.2	39.5	N	26.6	42.8	3	42.9	6.93				0.11
Sand Flat graben faults	2475	<1,600,000	<0.2	23.1	N	26.4	42.5	3	42.6	6.66				0.10
Granite Creek fault zone	2265	<1,600,000	<0.2	22.7	N	33.4	53.8	3	53.8	6.65				0.08
Fisher Valley faults (Class B)	2478	Class B	<0.2	15.9		31.0	49.8	3	49.9	6.47				0.07
Sinbad Valley graben (Class B)	2285	<1,600,000	<0.2	31.8		39.3	63.2	3	63.3	6.82				0.07
unnamed fault in Salina Quad, R13E, T24S				19.6		36.0	57.9	3	57.9	6.58				0.07
Paradox Valley graben (Class B)	2286	<1,600,000	<0.2	56.4	N	49.6	79.9	3	79.9	7.11				0.07
Little Doloras River fault	2251	<1,600,000	<0.2	15.7	R	34.5	55.5	3	55.6	6.47				0.07
Castle Valley faults (Class B)	2477	Class B	<0.2	12.4		34.2	54.9	3	55.0	6.35				0.06
unnamed fault in Salina Quad, R11E, T22S				22.7		41.6	66.9	3	67.0	6.65				0.06
unnamed fault in Salina Quad, R11E, T23S				25.8		44.7	72.0	3	72.0	6.72				0.06
Unnamed fault near Pine Mountain	2267	<1,600,000	<0.2	30.7		47.2	75.9	3	75.9	6.81				0.06
Lisbon Valley fault zone (Class B)	2511	<1,600,000	<0.2	37.5		50.9	81.9	3	82.0	6.91				0.06
Lockhart fault (Class B)	2510	Class B	<0.2	15.7		40.8	65.6	3	65.7	6.47				0.06
unnamed fault in Salina Quad, R11E, T21S				14.0		42.1	67.7	3	67.8	6.41				0.05
unnamed fault in Price Quad, R12E, T19S				13.7		42.4	68.2	3	68.3	6.40				0.05
Needles fault zone (Class B)	2507	Class B	<0.2	28.5		53.9	86.6	3	86.7	6.77				0.05
unnamed fault in Salina Quad, R12E, T24S				10.1		42.6	68.6	3	68.7	6.25				0.05
Redlands fault complex	2252	<1,600,000	<0.2	21.1	N,R	53.1	85.4	3	85.4	6.62				0.05
Unnamed fault of Lost Horse Basin	2264	<1,600,000	<0.2	8.1		40.8	65.6	3	65.7	6.13				0.05
unnamed fault in Salina Quad, R12E, T23S				9.0		43.5	70.0	3	70.1	6.19				0.04
Bright Angel fault system (Class B)	2514	<1,600,000	<0.2	102.3		89.6	144.1	3	144.1	7.41				0.04
unnamed fault in Salina Quad, R16E, T28S				9.0		43.9	70.6	3	70.6	6.19				0.04
Wasatch monocline (Class B)	2450	<1,600,000	<0.2	103.5	?	90.3	145.3	3	145.3	7.42				0.04

Name	Number	Age of Most Recent Prehistoric Deformation (ya)	Slip-rate (mm/yr)	Fault Length (km)	Fault Type	Distance from site (miles)[1]	Distance from site (km)	Depth to seismo-genic rupture (km)	r_{seis} (km)	MCE (Based on fault length, all slip types, Wells and Coppersmith, 1994)	Rupture depth (km)	Rupture area (km^2)	MCE (based on fracture area, Wells and Coppersmith, 1994)	PHA (Campbell-Bozorgnia 2003) corrected, plus 1SD (based on Mw)
Shay graben faults (Class B)	2513	Class B	<0.2	39.5		68.1	109.5	3	109.6	6.93				0.04
unnamed fault in Salina Quad, R11E, T24S				9.8		47.0	75.7	3	75.7	6.23				0.04
Joes Valley fault zone, east fault	2455	<15,000	0.2-1	56.6		79.0	127.0	3	127.1	7.11				0.04
Joes Valley fault zone, west fault	2453	<15,000	0.2-1	57.2		81.1	130.4	3	130.4	7.12				0.04
unnamed fault in Price Quad, R16E, T13S				9.5		48.6	78.2	3	78.2	6.22				0.04
Southern Joes Valley fault zone	2456	<750,000	<0.2	47.2		77.2	124.2	3	124.3	7.02				0.04
Big Gypsum Valley graben (Class B)	2288	Class B	<0.2	33.1		70.9	114.0	3	114.0	6.84				0.04
Duchesne-Pleasant Valley fault system (Class B)	2414	<1,600,000	<0.2	45.3	N	79.1	127.2	3	127.3	7.00				0.04
Monitor Creek fault	2268	<1,600,000	<0.2	30.1		79.1	127.3	3	127.3	6.80				0.03
Joes Valley fault zone, intragraben faults	2454	<15,000	<0.2	34.0		82.9	133.3	3	133.4	6.86				0.03
Thousand Lake fault	2506	<750,000	<0.2	48.3		97.2	156.4	3	156.5	7.03				0.03
Pleasant Valley fault zone, unnamed faults	2425	<1,600,000	<0.2	31.0	N	86.1	138.5	3	138.5	6.81				0.03
Unnamed faults of Pinto Mesa	2277	<1,600,000	<0.2	19.7		78.4	126.1	3	126.1	6.58				0.03
Unnamed faults south of Love Mesa	2271	<1,600,000	<0.2	17.6		78.8	126.8	3	126.8	6.52				0.03
Unnamed faults near San Miguel Canyon (Class B)	2284	Class B	<0.2	32.1		94.5	152.1	3	152.1	6.83				0.03
Snow Lake graben	2452	<15,000	<0.2	25.4		89.7	144.3	3	144.4	6.71				0.03
Gunnison fault	2445	<15,000	<0.2	42.0	N	104.3	167.8	3	167.9	6.96				0.03
Unnamed fault at Red Canyon	2279	<1,600,000	<0.2	24.2		90.9	146.3	3	146.4	6.69				0.03
Roubideau Creek fault	2270	<15,000	<0.2	20.5		88.7	142.7	3	142.7	6.60				0.03
Wasatch fault zone, Provo section	2351g	<15,000	1-5	58.8		122.2	196.6	3	196.6	7.13				0.03
Gooseberry graben faults	2424	<750,000	<0.2	22.6		93.1	149.8	3	149.8	6.65				0.03
Pleasant Valley fault zone, graben	2426	<750,000	<0.2	17.6		88.3	142.1	3	142.2	6.52				0.03
Aquarius and Awapa Plateaus faults	2505	<1,600,000	<0.2	35.7		108.6	174.8	3	174.8	6.88				0.03
Red Rocks fault	2291	<1,600,000	<0.2	38.3		111.8	179.9	3	179.9	6.92				0.02
Valley Mountains monocline (Class B)	2449	<1,600,000	<0.2	38.6		112.9	181.7	3	181.7	6.92				0.02
Paunsaugunt fault	2504	<1,600,000	<0.2	44.1		118.0	189.8	3	189.8	6.99				0.02
Wasatch fault zone, Nephi section	2351h	<15,000	1-5	43.1		119.9	192.9	3	193.0	6.98				0.02
White Mountain area faults	2451	<1,600,000	<0.2	16.4		90.5	145.6	3	145.6	6.49				0.02
Sevier/Toroweap fault zone, Sevier section	997a	<130,000	0.2-1	88.7		155.4	250.0	3	250.1	7.34				0.02
Sevier fault	2355	<1,600,000	<0.2	41.3	N	126.4	203.4	3	203.4	6.95				0.02
Unnamed fault at Hanks Creek	2281	<1,600,000	<0.2	17.5		99.0	159.2	3	159.3	6.52				0.02
Cactus Park-Bridgeport fault	8			22.5		70.0	112.6	3	112.7	6.65				0.02
East Tintic Mountains (west side) faults	2420	<750,000	<0.2	33.1		129.6	208.6	3	208.6	6.84				0.02
Sevier Valley-Marysvale-Circleville area faults	2500	<750,000	<0.2	34.9		133.7	215.2	3	215.2	6.87				0.02
Cannibal fault	2337	<130,000	<0.2	49.3		148.9	239.6	3	239.6	7.04				0.02
Hogsback fault, southern section	732b	<130,000	1-5	38.3		144.3	232.1	3	232.1	6.92				0.02
Bear River fault zone	730	<15,000	0.2-1	33.2		140.4	225.8	3	225.9	6.84				0.02
West Kaibab fault system	994	<1,600,000	<0.2	82.9	N	187.7	301.9	3	302.0	7.31				0.02
Frontal fault	2302	<130,000	0.2-1	75.0	N,R	190.1	305.8	3	305.9	7.26				0.02
Sevier/Toroweap fault zone, northern Toroweap section	997b	<130,000	<0.2	80.9		198.5	319.4	3	319.4	7.29				0.02
Central Kaibab fault system	993	<1,600,000	<0.2	71.5	N	192.3	309.5	3	309.5	7.23				0.02
Almy fault zone	742	<1,600,000	<0.2	10.7				3		6.27				

Name	Number	Age of Most Recent Prehistoric Deformation (ya)	Slip-rate (mm/yr)	Fault Length (km)	Fault Type	Distance from site (miles)[1]	Distance from site (km)	Depth to seismo-genic rupture (km)	r_{seis} (km)	MCE (Based on fault length, all slip types, Wells and Coppersmith, 1994)	Rupture depth (km)	Rupture area (km^2)	MCE (based on fracture area, Wells and Coppersmith, 1994)	PHA (Campbell-Bozorgnia 2003) corrected, plus 1SD (based on Mw)
Andrus Canyon fault	1013	<1,600,000	<0.2	5.6				3		5.95				
Annabella graben faults	2472	<15,000	<0.2	12.5				3		6.35				
Antelope Range fault	2517	<750,000	<0.2	24.5				3		6.69				
Arrowhead fault zone	953	<130,000	<0.2	5.2				3		5.91				
Aubrey fault zone	995	<130,000	<0.2	53.1				3		7.08				
Babbitt Lake fault zone	954	<750,000	<0.2	7.6				3		6.10				
Bald Mountain fault	2390	<1,600,000	<0.2	2.3				3		5.50				
Bangs Canyon fault	2256	<1,600,000	<0.2	6.3				3		6.01				
Basalt Mountain fault (Class B)	2299	Class B	<0.2	7.0				3		6.06				
Bear Lake (west side) fault (Class B)	2531	<1,600,000	<0.2	5.5				3		5.94				
Bear River Range faults	2410	<1,600,000	<0.2	62.9	N, Dextral			3		7.17				
Beaver Basin faults, eastern margin faults	2492a	<15,000	<0.2	34.2				3		6.86				
Beaver Basin faults, intrabasin faults	2492b	<15,000	<0.2	38.9				3		6.92				
Beaver Ridge faults	2464	<130,000	<0.2	14.2				3		6.42				
Big Pass faults	2366	<1,600,000	<0.2	17.3				3		6.52				
Black Mesa fault zone	2006	<1,600,000	<0.2	18.5				3		6.55				
Black Mountains faults	2487	<750,000	<0.2	25.9				3		6.72				
Black Point/Doney Mountain fault zone	957	<750,000	<0.2	23.8	N			3		6.68				
Black Rock area faults	2461	<130,000	<0.2	8.2				3		6.14				
Blue Springs Hills faults	2363	<750,000	<0.2	2.5				3		5.54				
Bright Angel fault zone	991	<1,600,000	<0.2	66.0	N			3		7.19				
Broadmouth Canyon faults	2377	<130,000	<0.2	3.4				3		5.70				
Buckskin Valley faults (Class B)	2499	Class B	<0.2	3.5				3		5.71				
Busted Boiler fault	2274	<130,000	<0.2	18.0				3		6.54				
Cactus Park fault	2258	<1,600,000	<0.2	1.9				3		5.40				
Calabacillas fault	2035	<750,000	<0.2	31.3				3		6.81				
Cameron graben and faults	988	<750,000	<0.2	10.8				3		6.28				
Campbell Francis fault zone	959	<750,000	<0.2	10.1				3		6.25				
Canones fault (Class B)	2003	<1,600,000	<0.2	29.4				3		6.78				
Cataract Creek fault zone	990	<1,600,000	<0.2	51.1	N			3		7.06				
Cattle Creek anticline (Class B)	2293	Class B	<0.2	8.6				3		6.16				
Cedar City-Parowan monocline (and faults)	2530	<15,000	<0.2	24.8				3		6.70				
Cedar Ranch fault zone	961	<750,000	<0.2	10.2				3		6.25				
Cedar Valley (north end) faults	2529	<130,000	<0.2	15.5				3		6.46				
Cedar Valley (south side) fault	2408	<750,000	<0.2	2.8				3		5.60				
Cedar Valley (west side) faults	2527	<750,000	<0.2	12.8				3		6.36				
Cedar Wash fault zone	962	<750,000	<0.2	11.6				3		6.31				
Chicken Springs faults	780	<15,000	<0.2	13.7				3		6.40				
Cimmarron fault, Blue Mesa section	2290c	<1,600,000	<0.2	22.5				3		6.65				
Cimmarron fault, Bostwick Park section (Class B)	2290a	Class B	<0.2	11.2				3		6.30				
Cimmarron fault, Poverty Mesa section (Class B)	2290b	Class B	<0.2	24.1				3		6.68				
Citadel Ruins fault zone	963	<1,600,000	<0.2	4.5				3		5.84				

Name	Number	Age of Most Recent Prehistoric Deformation (ya)	Slip-rate (mm/yr)	Fault Length (km)	Fault Type	Distance from site (miles)[1]	Distance from site (km)	Depth to seismo-genic rupture (km)	r_{seis} (km)	MCE (Based on fault length, all slip types, Wells and Coppersmith, 1994)	Rupture depth (km)	Rupture area (km^2)	MCE (based on fracture area, Wells and Coppersmith, 1994)	PHA (Campbell-Bozorgnia 2003) corrected, plus 1SD (based on Mw)
Clear Lake fault zone (Class B)	2436	<15,000	<0.2	35.5				3		6.88				
Clover fault zone	2396	<130,000	<0.2	4.0				3		5.78				
County Dump fault	2038	<1,600,000	<0.2	35.3				3		6.88				
Cove Fort fault zone (Class B)	2491	Class B	<0.2	22.2				3		6.64				
Crater Bench faults	2433	<15,000	<0.2	15.9				3		6.47				
Crawford Mountains (west side) fault	2346	<130,000	<0.2	25.3				3		6.71				
Cricket Mountains (north end) faults	2434	<750,000	<0.2	2.8				3		5.60				
Cricket Mountains (west side) fault	2460	<15,000	<0.2	41.0				3		6.95				
Cross Hollow Hills faults	2524	<1,600,000	<0.2	5.3				3		5.92				
Curlew Valley faults	3504	<15,000	<0.2	20.0				3		6.59				
Dayton fault (Class B)	2370	Class B	<0.2	16.3				3		6.49				
Deadman Wash faults	964	<1,600,000	<0.2	1.8				3		5.38				
Deep Creek Range (east side) faults	2416	<750,000	<0.2	20.7				3		6.61				
Deep Creek Range (northwest side) fault zone	2403	<130,000	<0.2	10.7				3		6.27				
Deseret faults	2435	<750,000	<0.2	7.1				3		6.07				
Diamond Gulch faults	2393	<1,600,000	<0.2	20.2				3		6.59				
Doloras fault zone (Class B)	2289	Class B	<0.2	15.2				3		6.45				
Dolphin Island fracture zone	2367	<750,000	<0.2	19.2				3		6.57				
Double Knobs fault	966	<1,600,000	<0.2	6.0				3		5.98				
Double Top fault zone	965	<1,600,000	<0.2	6.1				3		5.99				
Drum Mountains fault zone	2432	<15,000	<0.2	51.5	N			3		7.07				
Dry Wash fault and syncline	2496	<130,000	<0.2	18.6				3		6.55				
Duncomb Hollow fault	743	<1,600,000	<0.2	2.4				3		5.52				
Dutchman Draw fault	1003	<130,000	<0.2	16.3	N			3		6.49				
East Cache fault zone, central section	2352b	<15,000	0.2-1	16.5				3		6.49				
East Cache fault zone, northern section	2352a	<750,000	<0.2	25.7				3		6.72				
East Cache fault zone, southern section	2352c	<130,000	<0.2	22.1				3		6.64				
East Canyon (east side) fault (Class B)	2350	<1,600,000	<0.2	28.9				3		6.77				
East Canyon fault, Northern East Canyon section (Class B)	2354a	Class B	<0.2	22.5				3		6.65				
East Canyon fault, Southern East Canyon section	2354b	<750,000	<0.2	8.4				3		6.15				
East Dayton-oxford fault	3509	<130,000	<0.2	23.2	N			3		6.66				
East Great Salt Lake fault zone, Antelope Island section	2369c	<15,000	0.2-1	35.1				3		6.87				
East Great Salt Lake fault zone, Fremont Island section	2369b	<15,000	0.2-1	30.1				3		6.80				
East Great Salt Lake fault zone, Promontory section	2369a	<15,000	0.2-1	49.2	N			3		7.04				
East Kamas fault	2391	<1,600,000	<0.2	14.6				3		6.43				
East Lakeside Mountains fault zone	2368	<1,600,000	<0.2	36.0				3		6.89				
East Pocatello valley faults	3507	<15,000	<0.2	6.8				3		6.05				
Eastern Bear Lake fault, central section	2364b	<15,000	<0.2	23.8				3		6.68				
Eastern Bear Lake fault, southern section	2364c	<15,000	0.2-1	34.8				3		6.87				
Eastern Bear Valley fault (Class B)	734	Class B	<0.2	47.2				3		7.02				
Eastern Pilot Range fault	2371	<1,600,000	<0.2	10.6				3		6.27				
East-Side Chase Gulch fault	2317	<130,000	<0.2	30.7				3		6.81				

Name	Number	Age of Most Recent Prehistoric Deformation (ya)	Slip-rate (mm/yr)	Fault Length (km)	Fault Type	Distance from site (miles)[1]	Distance from site (km)	Depth to seismo-genic rupture (km)	r_{seis} (km)	MCE (Based on fault length, all slip types, Wells and Coppersmith, 1994)	Rupture depth (km)	Rupture area (km^2)	MCE (based on fracture area, Wells and Coppersmith, 1994)	PHA (Campbell-Bozorgnia 2003) corrected, plus 1SD (based on Mw)
Ebert Tank fault zone	967	<750,000	<0.2	3.1				3		5.65				
Eleven Mile fault	2318	<130,000	<0.2	4.7				3		5.86				
Elk Mountain fault	736	<1,600,000	<0.2	7.8				3		6.11				
Ellison Gulch scarp (Class B)	2304	Class B	<0.2	1.2				3		5.17				
Elsinore fault (fold)	2470	<1,600,000	<0.2	28.1				3		6.76				
Embudo fault, Hernandez section	2007b	<1,600,000	<0.2	31.6				3		6.82				
Embudo fault, Pilar section	2007a	<130,000	<0.2	38.7				3		6.92				
Eminence fault zone	992	<1,600,000	<0.2	36.0				3		6.89				
Enoch graben faults	2528	<15,000	<0.2	17.2				3		6.51				
Enterprise faults	2516	<750,000	<0.2	8.4				3		6.15				
Escalante Desert (east side) faults	2526	<15,000	<0.2	6.4				3		6.02				
Escalante Desert faults (Class B)	2488	Class B	<0.2	6.6				3		6.03				
Escalante Desert faults near Zane	2518	<130,000	<0.2	3.9				3		5.77				
Faults in Raft River Valley	3503	<750,000	<0.2	35.2				3		6.87				
Faults near Garcia	2323	<130,000	<0.2	3.4				3		5.70				
Faults near Monte Vista	2315	<1,600,000	<0.2	16.2				3		6.48				
Faults near of Cochiti Pueblo	2142	<1,600,000	<0.2	32.2				3		6.83				
Faults north of Placitas	2043	<750,000	<0.2	10.5				3		6.26				
Faults of Cove Creek Dome	2462	<1,600,000	<0.2	18.8				3		6.56				
Faults of the northern Basaltic Hills	2322	<1,600,000	<0.2	12.6				3		6.36				
Faults on north flank of Phil Pico Mountains	744	<130,000	<0.2	4.4				3		5.83				
Fish Springs fault	2417	<15,000	<0.2	29.7				3		6.79				
Foote Range fault	2429	<750,000	<0.2	3.1				3		5.65				
Fremont Wash faults	2495	<750,000	<0.2	7.2				3		6.07				
Frog Valley fault	2389	<1,600,000	<0.2	4.6				3		5.85				
Gallina fault	2001	<1,600,000	<0.2	39.3				3		6.93				
Glade Park fault	2254	<1,600,000	<0.2	9.4	R			3		6.21				
Goose Creek Mountains faults (Class B)	2356	Class B	<0.2	4.0				3		5.78				
Grand Hogback monocline (Class B)	2331	Class B	<0.2	22.0				3		6.64				
Grand Wash fault zone	1005	<130,000	<0.2	34.9	N			3		6.87				
Gray Mountain faults	1018	<1,600,000	<0.2	23.6				3		6.67				
Greenhorn Mountain fault (Class B)	2297	Class B	<0.2	21.5				3		6.63				
Grouse Creek and Dove Creek Mountains faults	2357	<750,000	<0.2	47.7				3		7.03				
Guaje Mountain fault	2027	<15,000	<0.2	10.7				3		6.27				
Gunlock fault (Class B)	2515	Class B	<0.2	7.5				3		6.10				
Gyp Pocket graben and faults	1001	<130,000	<0.2	11.8	N			3		6.32				
Hansel Mountains (east side) faults	2359	<750,000	<0.2	14.7				3		6.43				
Hansel Valley (valley floor) faults	2360	<750,000	<0.2	19.5				3		6.58				
Hansel Valley fault	2358	<150	<0.2	13.0				3		6.37				
Hidden Tank fault zone	970	<750,000	<0.2	10.2				3		6.25				
Hogsback fault, northern section	732a	<750,000	0.2-1	22.4				3		6.65				
House Range (west side) fault	2430	<15,000	<0.2	45.5	N			3		7.00				

Name	Number	Age of Most Recent Prehistoric Deformation (ya)	Slip-rate (mm/yr)	Fault Length (km)	Fault Type	Distance from site (miles)[1]	Distance from site (km)	Depth to seismo-genic rupture (km)	r_{seis} (km)	MCE (Based on fault length, all slip types, Wells and Coppersmith, 1994)	Rupture depth (km)	Rupture area (km^2)	MCE (based on fracture area, Wells and Coppersmith, 1994)	PHA (Campbell-Bozorgnia 2003) corrected, plus 1SD (based on Mw)
Hurricane fault zone, Anderson Junction section	998c	<15,000	0.2-1	42.2				3		6.97				
Hurricane fault zone, Ash Creek section	998b	<15,000	<0.2	32.0				3		6.83				
Hurricane fault zone, Cedar City section	998a	<15,000	<0.2	13.2				3		6.38				
Hurricane fault zone, Shivwitz section	998d	<130,000	<0.2	56.5	N			3		7.11				
Hurricane fault zone, southern section	998f	<1,600,000	<0.2	66.6	N			3		7.20				
Hurricane fault zone, Whitmore Canyon section	998e	<15,000	<0.2	28.5				3		6.77				
Hyrum fault	2374	<1,600,000	<0.2	3.1				3		5.65				
James Peak fault	2378	<130,000	<0.2	6.3				3		6.01				
Japanese and Cal Valleys faults	2447	<750,000	<0.2	30.1				3		6.80				
Jemez-San Ysidro fault, Jemez section	2029a	<1,600,000	<0.2	24.1				3		6.68				
Jemez-San Ysidro fault, San Ysidro section	2029b	<1,600,000	<0.2	30.1				3		6.80				
Johns Valley fault (Class B)	2539	Class B	<0.2	2.1				3		5.45				
Joseph Flats area faults and syncline (Class B)	2468	Class B	<0.2	3.2				3		5.67				
Juab Valley (west side) faults (Class B)	2423	<750,000	<0.2	13.2				3		6.38				
Judd Mountain fault	1597	<1,600,000	<0.2	20.4				3		6.60				
Killarney faults	2336	<1,600,000	<0.2	5.6				3		5.95				
Kolob Terrace faults	2525	<750,000	<0.2	12.1				3		6.34				
Koosharem fault	2503	<1,600,000	<0.2	2.2				3		5.48				
La Bajada fault	2032	<1,600,000	<0.2	40.3				3		6.94				
La Canada del Amagre fault zone	2005	<1,600,000	<0.2	17.2				3		6.51				
Ladder Creek fault	2255	<1,600,000	<0.2	6.2				3		6.00				
Lakeside Mountains (west side) fault (Class B)	2384	Class B	<0.2	4.7				3		5.86				
Large Whiskers fault zone	972	<1,600,000	<0.2	11.6				3		6.31				
Las Tablas fault	2020	<1,600,000	<0.2	14.8				3		6.44				
Lee Dam faults	973	<1,600,000	<0.2	7.6				3		6.10				
Leupp faults	1017	<750,000	<0.2	32.2				3		6.83				
Lime Mountain fault	2415	<1,600,000	<0.2	10.6				3		6.27				
Little Diamond Creek fault	2411	<750,000	<0.2	20.0				3		6.59				
Little Rough Range faults	2458	<750,000	<0.2	3.2				3		5.67				
Little Valley faults	2439	<15,000	<0.2	19.2				3		6.57				
Littlefield Mesa faults	1008	<750,000	<0.2	21.2				3		6.62				
Lobato Mesa fault zone	2004	<1,600,000	<0.2	21.3				3		6.62				
Lockwood Canyon fault zone	974	<1,600,000	<0.2	20.8				3		6.61				
Log Hill Mesa graben	2275	<130,000	<0.2	9.5				3		6.21				
Long Ridge (northwest side) fault	2422	<1,600,000	<0.2	20.8				3		6.61				
Long Ridge (west side) faults	2421	<750,000	<0.2	15.2				3		6.45				
Lookout Pass fault	2404	<1,600,000	<0.2	3.9				3		5.77				
Los Cordovas faults	2022	<1,600,000	<0.2	12.2				3		6.34				
Lucky Boy fault	2314	<1,600,000	<0.2	11.1				3		6.29				
Main Street fault zone	1002	<130,000	<0.2	87.3	N			3		7.33				
Malpais Tank faults	975	<750,000	<0.2	4.6				3		5.85				
Mantua area faults	2373	<750,000	<0.2	21.1				3		6.62				

Name	Number	Age of Most Recent Prehistoric Deformation (ya)	Slip-rate (mm/yr)	Fault Length (km)	Fault Type	Distance from site (miles)[1]	Distance from site (km)	Depth to seismo-genic rupture (km)	r_{seis} (km)	MCE (Based on fault length, all slip types, Wells and Coppersmith, 1994)	Rupture depth (km)	Rupture area (km^2)	MCE (based on fracture area, Wells and Coppersmith, 1994)	PHA (Campbell-Bozorgnia 2003) corrected, plus 1SD (based on Mw)
Maple Grove faults	2443	<15,000	<0.2	12.8				3		6.36				
Markagunt Plateau faults (Class B)	2535	<750,000	<0.2	56.4				3		7.11				
Martin Ranch fault	731	<15,000	0.2-1	3.7				3		5.74				
Maverick Butte faults	976	<750,000	<0.2	3.7				3		5.74				
Meadow-Hatton area faults	2466	<15,000	<0.2	4.0				3		5.78				
Mesa Butte North fault zone	987	<1,600,000	<0.2	22.6				3		6.65				
Mesita fault	2015	<130,000	<0.2	27.9				3		6.76				
Mesquite fault	1007	<130,000	<0.2	36.2				3		6.89				
Michelbach Tank faults	978	<750,000	<0.2	13.4				3		6.39				
Mineral Hot Springs fault	2320	<130,000	<0.2	7.8				3		6.11				
Mineral Mountains (northeast side) fault (Class B)	2490	Class B	<0.2	14.2				3		6.42				
Mineral Mountains (west side) faults	2489	<15,000	<0.2	36.6				3		6.89				
Morgan fault, central section	2353b	<15,000	<0.2	4.9				3		5.88				
Morgan fault, northern section	2353a	<750,000	<0.2	7.9				3		6.12				
Morgan fault, southern section	2353c	<750,000	<0.2	2.3				3		5.50				
Mosquito fault	2303	<130,000	<0.2	51.5				3		7.07				
Mountain Home Range (west side) faults	2480	<1,600,000	<0.2	26.4				3		6.73				
Nacimiento fault, northern section	2002a	<1,600,000	<0.2	35.9				3		6.88				
Nacimiento fault, southern section	2002b	<1,600,000	<0.2	45.2				3		7.00				
Nambe fault	2024	<1,600,000	<0.2	47.8				3		7.03				
North Bridger Creek fault	737	<1,600,000	<0.2	4.2				3		5.80				
North Hills faults	2522	<750,000	<0.2	5.0				3		5.89				
North of Wah Wah Mountains faults	2459	<750,000	<0.2	12.5				3		6.35				
North Promontory fault	2361	<15,000	<0.2	25.8				3		6.72				
North Promontory Mountains fault	2362	<1,600,000	<0.2	6.3				3		6.01				
Northern Boundary fault system	2309	<750,000	<0.2	49.0				3		7.04				
Northern Sangre de Cristo fault, Blanca section	2321c	<15,000	<0.2	6.7				3		6.04				
Northern Sangre de Cristo fault, Crestone section	2321a	<15,000	<0.2	79.1	N			3		7.28				
Northern Sangre de Cristo fault, San Luis section	2321d	<15,000	<0.2	59.1	N			3		7.14				
Northern Sangre de Cristo fault, Zapata section	2321b	<15,000	<0.2	25.8				3		6.72				
Ogden Valley North Fork fault	2376	<750,000	<0.2	26.1				3		6.72				
Ogden Valley northeastern margin fault	2379	<1,600,000	<0.2	12.8				3		6.36				
Ogden Valley southwestern margin faults	2375	<750,000	<0.2	17.8				3		6.53				
Oquirrh fault zone	2398	<15,000	<0.2	21.1				3		6.62				
Overton Arm faults	1119	<130,000	<0.2	50.9				3		7.06				
Pajarito fault	2008	<130,000	<0.2	49.4				3		7.04				
Paragonah fault	2534	<130,000	0.2-1	27.2				3		6.74				
Parleys Park faults (Class B)	2388	Class B	<0.2	3.4				3		5.70				
Parowan Valley faults	2533	<15,000	<0.2	16.3				3		6.49				
Pavant faults	2438	<15,000	<0.2	30.1				3		6.80				
Pavant Range fault	2442	<15,000	<0.2	14.2				3		6.42				
Pearl Harbor fault zone	981	<1,600,000	<0.2	15.3				3		6.45				

Name	Number	Age of Most Recent Prehistoric Deformation (ya)	Slip-rate (mm/yr)	Fault Length (km)	Fault Type	Distance from site (miles)[1]	Distance from site (km)	Depth to seismo-genic rupture (km)	r_{seis} (km)	MCE (Based on fault length, all slip types, Wells and Coppersmith, 1994)	Rupture depth (km)	Rupture area (km^2)	MCE (based on fracture area, Wells and Coppersmith, 1994)	PHA (Campbell-Bozorgnia 2003) corrected, plus 1SD (based on Mw)
Picuris-Pecos fault	2023	<1,600,000	<0.2	98.2	N			3		7.39				
Pilot Range faults	1599	<1,600,000	<0.2	40.2				3		6.94				
Pine Ridge faults (Class B)	2512	Class B	<0.2	5.5				3		5.94				
Pine Valley (south end) faults	2482	<1,600,000	<0.2	10.7				3		6.27				
Pine Valley faults	2481	<750,000	<0.2	3.7				3		5.74				
Pleasant Valley fault zone, Dry Valley graben	2427	<750,000	<0.2	12.4				3		6.35				
Pojoaque fault zone	2010	<1,600,000	<0.2	46.5				3		7.01				
Porcupine Mountain faults	2380	<130,000	<0.2	34.6	N			3		6.87				
Pot Creek faults	2394	<1,600,000	<0.2	13.4				3		6.39				
Puddle Valley fault zone	2383	<15,000	<0.2	6.5				3		6.02				
Puye fault	2009	<130,000	<0.2	16.7				3		6.50				
Raft River Mountains fault	2448	<750,000	<0.2	1.5				3		5.28				
Red Canyon fault scarps	2471	<15,000	<0.2	9.4				3		6.21				
Red Hills fault	2532	<130,000	<0.2	13.8				3		6.40				
Red House faults	983	<750,000	<0.2	3.4				3		5.70				
Red River fault zone	2019	<1,600,000	<0.2	10.0				3		6.24				
Rendija Canyon fault	2026	<130,000	<0.2	11.1				3		6.29				
Ridgway fault	2276	<1,600,000	<0.2	23.8				3		6.68				
Rimmy Jim fault zone	984	<1,600,000	<0.2	8.2				3		6.14				
Rock Creek fault	729	<15,000	0.2-1	40.5	N			3		6.94				
Round Valley faults	2400	<750,000	<0.2	12.8	N			3		6.36				
Ryckman Creek fault	740	<1,600,000	<0.2	5.3				3		5.92				
Sage Valley fault	2444	<1,600,000	<0.2	10.5				3		6.26				
Saint John Station fault zone	2397	<130,000	<0.2	5.2				3		5.91				
Saleratus Creek fault	2365	<750,000	<0.2	37.6				3		6.91				
San Felipe fault, Algodones section	2030b	<1,600,000	<0.2	15.9				3		6.47				
San Felipe fault, Santa Ana section	2030a	<1,600,000	<0.2	43.8				3		6.98				
San Francisco fault	2031	<1,600,000	<0.2	25.7				3		6.72				
San Francisco Mountains (west side) fault	2486	<750,000	<0.2	41.4				3		6.96				
Sand Hill fault zone	2039	<1,600,000	<0.2	35.6				3		6.88				
Sawatch fault, northern section	2308a	<130,000	<0.2	34.0				3		6.86				
Sawatch fault, southern section	2308b	<15,000	<0.2	41.1				3		6.95				
Sawyer Canyon fault	2028	<130,000	<0.2	8.4				3		6.15				
Scipio fault zone	2441	<15,000	<0.2	12.5				3		6.35				
Scipio Valley faults	2440	<15,000	<0.2	7.3				3		6.08				
Sevier Valley fault	2502	<1,600,000	<0.2	7.4				3		6.09				
Sevier Valley faults and folds (Class B)	2537	<130,000	<0.2	23.6				3		6.67				
Sevier Valley faults north of Panguitch	2536	<130,000	<0.2	6.2				3		6.00				
Sevier/Toroweap fault zone, central Toroweap section	997c	<15,000	<0.2	60.4	N			3		7.15				
Sevier/Toroweap fault zone, southern Toroweap section	997d	<750,000	<0.2	18.8				3		6.56				
Shadow Mountain grabens	989	<750,000	<0.2	10.4				3		6.26				
Sheeprock fault zone	2405	<130,000	<0.2	11.7				3		6.32				

Name	Number	Age of Most Recent Prehistoric Deformation (ya)	Slip-rate (mm/yr)	Fault Length (km)	Fault Type	Distance from site (miles)[1]	Distance from site (km)	Depth to seismo-genic rupture (km)	r_{seis} (km)	MCE (Based on fault length, all slip types, Wells and Coppersmith, 1994)	Rupture depth (km)	Rupture area (km^2)	MCE (based on fracture area, Wells and Coppersmith, 1994)	PHA (Campbell-Bozorgnia 2003) corrected, plus 1SD (based on Mw)
Sheeprock Mountains fault	2419	<1,600,000	<0.2	6.7				3		6.04				
Silver Island Mountains (southeast side) fault	2382	<15,000	<0.2	1.8				3		5.38				
Silver Island Mountains (west side) fault	2381	<1,600,000	<0.2	6.4				3		6.02				
Simpson Mountains faults	2418	<750,000	<0.2	10.8				3		6.28				
Sinagua faults	986	<130,000	<0.2	4.9				3		5.88				
Sinbad Valley graben (Class B)	2385	<1,600,000	<0.2	9.9				3		6.23				
Skull Valley (mid-valley) faults	2387	<15,000	<0.2	54.8	N			3		7.10				
Snake Valley fault	1246	<15,000	<0.2	41.1				3		6.95				
Snake Valley faults	2428	<15,000	<0.2	45.3	N			3		7.00				
South Granite Mountains fault system, Seminoe Mountains section (Class B)	779e	Class B	<0.2	35.0				3		6.87				
Southern Oquirrh Mountains fault zone	2399	<130,000	<0.2	24.1				3		6.68				
Southern Sangre de Cristo fault zone, San Pedro section	2017a	<130,000	<0.2	24.4				3		6.69				
Southern Sangre de Cristo fault, Cañon section	2017e	<15,000	<0.2	15.2				3		6.45				
Southern Sangre de Cristo fault, Hondo section	2017d	<15,000	<0.2	22.2				3		6.64				
Southern Sangre de Cristo fault, Questa section	2017c	<15,000	<0.2	17.8				3		6.53				
Southern Sangre de Cristo fault, Urraca section	2017b	<15,000	<0.2	21.9				3		6.63				
Southern Snake Range fault zone	1433	<130,000	<0.2	27.5	N			3		6.75				
SP fault zone	958	<130,000	<0.2	12.5				3		6.35				
Spring Creek fault	738	<1,600,000	<0.2	2.3				3		5.50				
Spry area faults	2498	<750,000	<0.2	5.1				3		5.90				
Stansbury fault zone	2395	<15,000	<0.2	49.8	N			3		7.05				
Stinking Springs fault	2413	<130,000	0.2-1	10.0				3		6.24				
Strawberry fault	2412	<15,000	<0.2	31.9				3		6.82				
Strong fault	2021	<1,600,000	<0.2	8.1				3		6.13				
Sublette Flat fault	733	<750,000	<0.2	36.0				3		6.89				
Sugarville area faults	2437	<15,000	<0.2	4.3				3		5.81				
Sunshine faults	1000	<130,000	<0.2	29.2	N			3		6.78				
Sunshine Trail graben and faults	999	<130,000	<0.2	17.0	N			3		6.51				
Sunshine Valley faults	2016	<130,000	<0.2	14.1				3		6.41				
Swasey Mountain (east side) faults	2431	<750,000	<0.2	3.8				3		5.75				
Tabernacle faults	2465	<15,000	<0.2	7.9				3		6.12				
The Pinnacle fault	739	<1,600,000	<0.2	2.3				3		5.50				
Tijeras-Cañoncito fault system, Galisteo section	2033a	<1,600,000	<0.2	37.1				3		6.90				
Topliff Hill fault zone	2407	<130,000	<0.2	19.9				3		6.59				
Towanta Flat graben (Class B)	2401	<750,000	<0.2	5.2				3		5.91				
Tushar Mountains (east side) fault	2501	<1,600,000	<0.2	18.5				3		6.55				
Uinkaret Volcanic field faults	1012	<1,600,000	<0.2	18.5				3		6.55				
Unnamed fault along Grand Hogback monocline (Class B)	2292	Class B	<0.2	2.4				3		5.52				
Unnamed fault at Big Dominquez Creek	2260	<1,600,000	<0.2	3.9				3		5.77				
Unnamed fault at Little Dominquez Creek	2261	<1,600,000	<0.2	14.2				3		6.42				
Unnamed fault at northwest end of Paradox Valley (Class B)	2287	Class B	<0.2	5.1				3		5.90				

Name	Number	Age of Most Recent Prehistoric Deformation (ya)	Slip-rate (mm/yr)	Fault Length (km)	Fault Type	Distance from site (miles)[1]	Distance from site (km)	Depth to seismo-genic rupture (km)	r_{seis} (km)	MCE (Based on fault length, all slip types, Wells and Coppersmith, 1994)	Rupture depth (km)	Rupture area (km^2)	MCE (based on fracture area, Wells and Coppersmith, 1994)	PHA (Campbell-Bozorgnia 2003) corrected, plus 1SD (based on Mw)
Unnamed fault east of Whitewater	2257	<1,600,000	<0.2	1.9				3		5.40				
Unnamed fault near Bridgeport	2259	<1,600,000	<0.2	11.0				3		6.29				
Unnamed fault near Escalante	2262	<1,600,000	<0.2	1.6				3		5.32				
Unnamed fault near Johnson Spring	2282	<1,600,000	<0.2	7.1				3		6.07				
Unnamed fault near Wolf Hill	2266	<1,600,000	<0.2	15.2				3		6.45				
Unnamed fault north of Horsefly Creek	2280	<1,600,000	<0.2	8.1				3		6.13				
Unnamed fault of Missouri Peak	2312	<130,000	<0.2	5.9				3		5.97				
Unnamed fault south of Shavano Peak	2311	<1,600,000	<0.2	5.8				3		5.97				
Unnamed fault southeast of China Mountain	1598	<1,600,000	<0.2	2.9				3		5.62				
Unnamed fault west of Buena Vista	2310	<1,600,000	<0.2	2.7				3		5.58				
Unnamed fault west of White Rock Mountains	1437	<1,600,000	<0.2	27.7				3		6.75				
Unnamed fault zone in Ferber Hills	1721	<1,600,000	<0.2	37.3				3		6.90				
Creek (Class B)	2294	Class B	<0.2	2.5				3		5.54				
Creek (Class B)	2295	Class B	<0.2	5.7				3		5.96				
Unnamed faults at Clay Creek	2283	<1,600,000	<0.2	9.2				3		6.20				
Unnamed faults east of Atkinson Masa	2269	<1,600,000	<0.2	41.1	N			3		6.95				
Unnamed faults east of Roubideau Creek (Class B)	2272	Class B	<0.2	11.7				3		6.32				
Unnamed faults in Williams Fork Valley	2300	<750,000	<0.2	18.4				3		6.55				
Unnamed faults near Burns (Class B)	2296	Class B	<0.2	13.3				3		6.38				
Unnamed faults near Cottonwood Creek	2278	<1,600,000	<0.2	10.8				3		6.28				
Unnamed faults near Loma Barbon	2045	<1,600,000	<0.2	1.2				3		5.17				
Unnamed faults near Picuda Peak	2041	<1,600,000	<0.2	10.6				3		6.27				
Unnamed faults near Twin Lakes Reservoir	2307	<1,600,000	<0.2	14.0				3		6.41				
Unnamed faults northwest of Leadville	2306	<1,600,000	<0.2	18.8				3		6.56				
Unnamed faults of Jemez Mountains, caldera margin section (Class B)	2143c	<750,000	<0.2	20.3				3		6.60				
Unnamed faults of Jemez Mountains, intracaldera section (Class B)	2143d	<1,600,000	<0.2	11.3	N			3		6.30				
Unnamed faults of Jemez Mountains, Toledo caldera section (Class B)	2143b	<1,600,000	<0.2	10.9				3		6.28				
Unnamed faults of Jemez Mountains, Valles caldera section (Class B)	2143a	<1,600,000	<0.2	16.7				3		6.50				
Unnamed faults of Red Hill (Class B)	2298	Class B	<0.2	6.1				3		5.99				
Unnamed faults on southeast side of Kern Mountains	1256	<1,600,000	<0.2	11.4	N			3		6.31				
Unnamed faults south of Leadville	2305	<1,600,000	<0.2	12.8				3		6.36				
Unnamed faults southeast of Montrose (Class B)	2273	Class B	<0.2	9.2				3		6.20				
Unnamed syncline northeast of Carbondale (Class B)	2333	Class B	<0.2	1.5				3		5.28				
Unnamed syncline northwest of Carbondale (Class B)	2334	Class B	<0.2	1.9				3		5.40				
Unnamed syncline southwest of Carbondale (Class B)	2332	Class B	<0.2	3.0				3		5.63				
Unnamed syncline west of Carbondale (Class B)	2335	Class B	<0.2	0.6				3		4.82				
Utah Lake faults	2409	<15,000	<0.2	30.8				3		6.81				
Vernon Hills fault zone	2406	<130,000	<0.2	3.7				3		5.74				

Name	Number	Age of Most Recent Prehistoric Deformation (ya)	Slip-rate (mm/yr)	Fault Length (km)	Fault Type	Distance from site (miles)[1]	Distance from site (km)	Depth to seismo-genic rupture (km)	r_{seis} (km)	MCE (Based on fault length, all slip types, Wells and Coppersmith, 1994)	Rupture depth (km)	Rupture area (km^2)	MCE (based on fracture area, Wells and Coppersmith, 1994)	PHA (Campbell-Bozorgnia 2003) corrected, plus 1SD (based on Mw)
Villa Grove fault zone	2319	<15,000	<0.2	19.0				3		6.56				
Volcano Mountain faults	2520	<750,000	<0.2	2.9				3		5.62				
Wah Wah Mountains (south end near Lund) fault	2485	<130,000	<0.2	40.2				3		6.94				
Wah Wah Mountains faults	2483	<1,600,000	<0.2	53.6				3		7.09				
Wah Wah Valley (west side) faults (Class B)	2484	Class B	<0.2	2.1				3		5.45				
Wasatch fault zone, Brigham City section	2351d	<15,000	0.2-1	37.3				3		6.90				
Wasatch fault zone, City section	2351a	<130,000	<0.2	39.6				3		6.93				
Wasatch fault zone, Clarkston Mountain section	2351b	<130,000	<0.2	10.4				3		6.26				
Wasatch fault zone, Collinston section	2351c	<15,000	<0.2	29.7				3		6.79				
Wasatch fault zone, Fayette section	2351j	<15,000	<0.2	15.6				3		6.46				
Wasatch fault zone, Levan section	2351i	<15,000	<0.2	30.1				3		6.80				
Wasatch fault zone, Salt Lake City section	2351f	<15,000	1-5	42.5				3		6.97				
Wasatch fault zone, Weber section	2351e	<15,000	1-5	56.2				3		7.11				
Washington fault zone, Mokaac section	1004b	<130,000	<0.2	11.2	N			3		6.30				
Washington fault zone, northern section	1004a	<15,000	<0.2	36.2	N			3		6.89				
Washington fault zone, Sullivan Draw section	1004c	<130,000	<0.2	34.5	N			3		6.86				
West Cache fault zone, Clarkston fault	2521a	<15,000	0.2-1	13.0				3		6.37				
West Cache fault zone, Junction Hills fault	2521b	<15,000	<0.2	24.3				3		6.69				
West Cache fault zone, Wellsville fault	2521c	<15,000	<0.2	19.9				3		6.59				
West Pocatello Valley faults	3506	<1,600,000	<0.2	7.7				3		6.11				
West Valley fault zone, Granger fault	2386b	<15,000	0.2-1	16.0	N			3		6.48				
West Valley fault zone, Taylorsville fault	2386a	<15,000	<0.2	15.1	N			3		6.45				
Western Bear Lake fault	622	<15,000	<0.2	58.2				3		7.13				
Western Bear Valley faults	735	<1,600,000	<0.2	12.4				3		6.35				
Western Boundary fault	2313	<1,600,000	<0.2	20.1				3		6.59				
West-Side Chase Gulch fault	2316	<130,000	<0.2	2.7				3		5.58				
Wheeler fault zone and graben	1006	<750,000	<0.2	45.3				3		7.00				
White Sage Flat faults	2467	<130,000	<0.2	11.8				3		6.32				
Whitney Canyon fault	741	<15,000	<0.2	5.5				3		5.94				
Williams Fork Mountains fault	2301	<15,000	0.2-1	37.7				3		6.91				
Woodruff fault	3508	<1,600,000	<0.2	12.5				3		6.35				
Yampai graben	996	<1,600,000	<0.2	6.9				3		6.05				
Zia fault	2046	<750,000	<0.2	32.4				3		6.83				

Class B=Geologic evidence demonstrates the existence of Quaternary deformation, but either (1) the fault might not extend deeply enough to be a potential source of significant earthquakes, or (2) the currently available geologic evidence is too strong to confidently assign the feature to Class C but not strong enough to assign it to Class A.

Fault Type: N=normal, R=reverse, D=Dextral

r_{seis}=distance from site to fault plane

[1]Distance from site only measured for those faults meeting the minimum length requirements as given in NRC 10 CFR part 100, Appendix A. Other faults have minimal impact on site.

[2]Attenuation calculated using mean MCE value based on rupture area, distance to site based on vertical projection of fault

[3]Attenuation calculation using mean MCE value based on rupture length, distance to site based on vertical projection of fault

[4]Attenuation calculation using mean plus one standard deviation MCE value based on rupture length, distance to site based on projecting fault dip at 60 degrees to NE

U.S. Department of Energy—Grand Junction, Colorado

Calculation Cover Sheet

Calc. No.: MOA-02-04-2007-1-02-01 **Doc. No.:** X0136100	**Discipline:** Geologic and Geophysical Properties	**No. of Sheets:** 12

Location: Attachment 2, Appendix G

Project: Moab UMTRA Project

Site: Crescent Junction, Utah

Feature: Photogeologic Interpretation

Sources of Data:

Aero-graphics, Inc., 2005. *Crescent Junction Photography,* one set of twelve 10" x 10" color contact prints of the high-altitude flight, Transmittal No. 13224 for S.M. Stoller Corporation, August 1.

Aero-graphics, Inc., 2005. *Crescent Junction Photography,* two sets of ten 10" x 10" color contact prints of the low-sun-angle flight, Transmittal No. 13330 for S.M. Stoller Corporation, October 3.

Historical black-and-white, high-altitude aerial photographs of the Crescent Junction, Utah, Site and surrounding area from August 31, 1944, and June 11, 1974.

Remedial Action Plan (RAP) calculations as referenced in text.

Purpose of Revision:

Revision is being issued to include results of additional field investigations to determine significance of features seen in aerial photographs. Also, U.S. Nuclear Regulatory Commission questions on several features were addressed, and historical aerial photographs were used in the interpretation of features.

Sources of Formulae and References:

N/A.

Preliminary Calc. ☐ **Final Calc.** ☒ **Supersedes Calc. No. MOA-02-11-2005-1-02-00**

Author:	Craig Goodknight	31 May 07	**Checked by:**		31 May 07
	Name	Date		Name	Date
				Mark Kautsky	5-31-07
Approved by:		5/31/07		Name	Date
	Name	Date			
				Name	Date
				Name	Date

No text for this page

Problem Statement:

Preliminary site selection performed jointly by the U.S. Department of Energy (DOE) and the Contractor has identified a 2,300-acre withdrawal area in the Crescent Flat area just northeast of Crescent Junction, Utah, as a possible site for final disposal of the Moab uranium mill tailings. The proposed disposal cell would cover approximately 250 acres. Situated between the Union Pacific Railroad and the base of the Book Cliffs, the withdrawal area extends for about 3 miles (mi) in an east-west direction and is approximately 1 mi wide in a north-south direction (Plate 1). Based on the preliminary site-selection process, the suitability of the Crescent Junction Disposal Site is being evaluated from several technical aspects, including geomorphic, geologic, hydrologic, seismic, geochemical, and geotechnical. The objective of this calculation set is to interpret stereographic color aerial photographs made in summer 2005 (including High-Altitude Vertical [HAV] and Low Sun-Angle [LSA] photographs) of the area to analyze structural and geomorphic conditions that may affect the site. Historic black-and-white aerial photographs of the site area dating back to 1944 were also used in analysis of site conditions.

This calculation set was initially prepared in November 2005 and included structural and geomorphic features identified from examination of the HAV and LSA photographs that may affect the Crescent Junction Disposal Site. The significance of some of the features relative to site suitability was explained in that calculation set, but several of the features required additional field investigation to determine their significance and to address review questions by the U.S. Nuclear Regulatory Commission (NRC) about specific features. Additional information from historic aerial photos of the site from 1944 and 1974 also was used to evaluate the identified features.

Information from this revised calculation was incorporated into Attachment 2 (Geology) of the Remedial Action Plan and Site Design for Stabilization of Moab Title I Uranium Mill Tailings at the Crescent Junction, Utah, Disposal Site (RAP), and summarized in the appropriate sections of the Remedial Action Selection (RAS) report for the Moab Site.

Method of Solution:

Color aerial photographs of an area of approximately 25 square mi, which included the proposed disposal site, the withdrawal area, and surrounding area, were taken by Aero-graphics, Inc., in July 2005. Both HAV and LSA photographs of the area were made at a scale of 1:24,000. The HAV photographs were taken on July 8, and two sets of the LSA photographs were taken—one in the morning and one in the evening—on July 27. Both HAV and LSA aerial photographs were taken in two flight lines from west to east across the north and south parts of the site area. The photographic coverage extends approximately 2.5 mi outside of the site withdrawal area in all directions. These photographs were interpreted to provide an assessment of geologic structures and geomorphic conditions that may affect the disposal site.

Historic black-and-white aerial photographs of the withdrawal area and surrounding area from 1944 and 1974 were acquired to investigate the rate of recent erosion by advance of headcutting incision in drainages and how this could affect the disposal cell over time. Standard procedures and techniques were used to perform these analyses. Field inspections of several of the features identified from the aerial photographs were necessary to substantiate the significance of the feature. The details of any field inspections are included in the narrative for each identified feature in the Discussion section of this calculation set.

Assumptions:

Not applicable.

Calculation:

None required.

Discussion:

Results of these interpretations are used to assess structural and geomorphic conditions that may affect the Crescent Junction Disposal Site. These results are also used to confirm and supplement other field observations associated with site geologic mapping and with fault investigation for the "Site and Regional Seismicity–Results of Literature Research" calculation (RAP Attachment 2, Appendix E). These interpretations are part of the comprehensive evaluation of the area relative to its suitability for location of the disposal facility. Features are grouped into those noted from inspection of the HAV and LSA photographs, and they are described in the following subsections along with an explanation of their significance. The features are further segregated by location: those which are in or adjacent to the withdrawal area (numbered 1 through 6), and those which are outside the withdrawal area (a through i). Each feature was assigned a relative importance in relation to the disposal cell by their number and letter order. All features are shown in relation to the withdrawal area in Plate 1.

High-Altitude Vertical Photographs

1. Paths of active sheet wash flow are shown in the color HAV photographs from the base of the Book Cliffs south to south-southeast across parts of the site withdrawal area. Water flowing in this sheet wash drains across the site to the West and East Branches of Kendall Wash. These sheet wash deposits are evident on the ground by their gray color (similar to Mancos Shale) and are mapped in Plate 1 of the "Surficial and Bedrock Geology of the Crescent Junction Disposal Site" calculation (RAP Attachment 2, Appendix B). The active sheet wash areas are an expression of the continuing process of deposition of alluvial and colluvial mud, which may be as much as 25 feet (ft) thick, covering the Mancos Shale bedrock over most of the site.

2. An east-trending discontinuous line of low mounds that appear as a lineament are mainly in the S½ of Sections 22 and 23. These mounds are as much as 15 ft high and are capped by a calcareous, dolomitic concretionary layer that marks the top of the Prairie Canyon Member of the Mancos Shale in this area, as described by Cole et al. (1997) and Hampson et al. (1999). The straight line of these mounds follows the strike direction of the Mancos Shale in this area and indicates that this stratigraphic horizon in the Mancos Shale is not displaced by faults.

3. The incised course of the N45W-trending West Branch of Kendall Wash is well exposed in the southwest part of the withdrawal area in the south-central part of Section 27. Bedrock is not exposed in the wash bottom upstream from the Union Pacific Railroad bridge although the wash there has been incised to depths of as much as 8 ft (for one of the wash tributaries, see Figure 1 in the "Site and Regional Geomorphology–Results of Site Investigations" calculation in RAP Attachment 2, Appendix D). Incision of the wash is apparently actively advancing to the northwest.

   Historic aerial photographs of the West Branch of Kendall Wash were examined to determine if the progress of headward incision could be seen over a period of 60 years. Three reference points were selected on the 2005 color aerial photograph at abrupt head-of-incision points (typically about 3 to 4 ft deep) in the tributaries to the West Branch. These same head-of-incision points were found in the tributary drainages in the black-and-white 1944 and 1974 aerial photographs. These head-of-incision points and their migration distances headward from 1944 to 2005 are shown in Plate 2. Distances of head-of-incision advance for the three tributaries range from 81 to 139 ft for the past 60 years, or approximately 1.3 to 2.3 ft per year. Northward advance of headward incision of these tributaries could reach the site access road (600 ft away) in as soon as 250 years. Continued northward incision advance of the easternmost tributary (Plate 2) north of the site access road could reach just west of the southwest corner of the disposal cell footprint in another 250 years.

   Crescent Wash is about 3,600 ft northwest of the incision heads of the two western tributaries of the West Branch. If the head of incision advanced at the faster of the two rates (139 ft per 60 years) for the western tributaries, incision would reach Crescent Wash at the meander bend near the northwest corner of Section 27 in approximately 1,600 years. At that time, a capture of Crescent Wash by the head of the West Branch of Kendall Wash would be possible. This capture would bring the course of a larger, high-energy drainage to within about 1,000 ft of the west side of the disposal cell.

4. In the west parts of Sections 22 and 15, the west end of the Book Cliffs terminates abruptly along a linear feature that trends several degrees east of north. This feature continues northward across Crescent Canyon into the west part of Section 10. Mapped from Landsat images of the northern Paradox Basin as a lineament by Friedman and Simpson (1980), this feature is also shown in Friedman et al. (1994). The feature does not coincide with any faults mapped for the area by Doelling (2001) or Gualtieri (1988), but the trend is similar to a joint system measured in the withdrawal area in the SW¼ of Section 22. This topographic lineament or feature is likely an expression of a prominent joint system in the area striking several degrees east of north. This feature may have had influence on the alignment of Crescent Wash, just west of the withdrawal area.

5. An abandoned wash course in SE¼ of Section 24 trends south for nearly 0.5 mi in the east end of the withdrawal area. From the aerial photographs, the north end of the abandoned wash appears to intersect the incised present course of the southwest-draining East Branch of Kendall Wash. Surface investigations of the abandoned drainage were made in January and October 2006 to determine if the abandonment was natural or human caused, and, if human caused, to evaluate the implications to the disposal cell area. It was found that the drainage was abandoned naturally, owing to capture by northwest headcutting of the present East Branch of Kendall Wash. The abandoned ancestral drainage of the East Branch is about 40 ft wide and as much as 8 ft deep at the north end (Figure 1), gradually decreasing in depth to only a foot or two at its south end near the Union Pacific Railroad. The abandoned wash bottom is flat to slightly concave and has been filled mostly with fine-grained material since abandonment. Large sandstone boulders (from the Mesaverde Group capping the Book Cliffs) as much as 5 ft in diameter are scattered along the sides and top of the drainage. A fan of these large boulders, 2 to 5 ft in diameter, extends for several hundred feet along the west side of the drainage near its south end.

Figure 1. View northeast of the north end of the ancestral drainage of the East Branch of Kendall Wash; Little Blaze Canyon is the reentrant to the Book Cliffs at the left.

The north end of the ancestral drainage has no connection with the present East Branch, which is incised to a depth of about 15 ft. At the point of capture, the bottom of the present East Branch drainage appears to be in unconsolidated Quaternary alluvial mud material. Several hundred feet downstream from the capture point, the present East Branch has incised about 3 ft into weathered Mancos Shale bedrock. At the capture point, considering the several feet of material filling the bottom of the ancestral East Branch drainage, the depth of the incision of the present East Branch is estimated at 3 ft below the base of the ancestral East Branch. From this difference in incised depths, a rough estimate of the time of abandonment can be made by comparison to a regional incision rate of 10 to 15 centimeters (or 4 to 6 inches) per 1,000 years, given by Dethier (2001). Application of this incision rate to the depth estimated gives a time range for the abandonment at 6,000 to 9,000 years ago.

Tributaries of the East Branch of Kendall Wash head in the reentrants, Little Blaze Canyon and an unnamed canyon, into the Book Cliffs escarpment (Plate 1) about 1 mi north of the capture point of the present East Branch. Evidence of high-energy flows along the ancestral course of the East Branch indicates that this drainage transported much of the material eroded from the reentrants. Accelerated erosion that formed these reentrants apparently was during wetter climatic episodes during the Pleistocene. Northwest-striking faults and joints are responsible for the location of the reentrants along the Book Cliffs escarpment. The absence of these structures is expressed by the unbroken, more than 2-mi-long escarpment immediately north of the disposal cell footprint. Because these structures are absent, significant fluvial erosion processes of stream abandonment and capture will more likely occur east and west of the disposal site where drainages such as the East Branch of Kendall Wash and Crescent Wash transport material eroded from reentrant canyons.

6. Several slump blocks containing sandstone of the Blackhawk Formation are along the south face of the Book Cliffs, immediately north of the site withdrawal area, mainly in Section 22. These slump blocks are lighter colored (tan to yellowish brown) than the typical gray Mancos Shale in the lower badland slopes of the Book Cliffs and apparently represent erosional remnants of larger slumps that slid down from the Book Cliffs in wetter Pleistocene times.

   Two larger areas of slump features are just outside the withdrawal area. One is north of the withdrawal area in the south part of Horse Heaven, just north of the western point of the Book Cliffs (elevation point 5,870 ft). The other is northeast of the withdrawal area just north of the detached block of the Book Cliffs (elevation point 5,903 ft) in the south-central part of Section 13. Both of these are shown in the landslide map by Harty (1993), and the slides were apparently initiated in wetter, colder climatic episodes associated with times of glaciation during the Pleistocene (Shroder 1971).

The following features outside of the withdrawal area are designated by lowercase letters:

a. The head of south-draining Crooked Wash, about 0.5 mi northwest of the northwest end of the withdrawal area, bends abruptly to trend N45W and forms an embayment in the Book Cliffs in the NW¼ of Section 16. This trend extends farther to the northwest and influences topography, forming an elongated cliff face just southwest of elevation point 5,882 ft. Southeastward along this trend, at the northwest end of the withdrawal area, is the abrupt west end of a section of the Book Cliffs in the NW¼ of Section 22. No fault coincides with this feature from mapping by Doelling (2001) for this area. The N45W trend is a common joint strike in the area, and this major joint likely imparts some topographic control on the shape of the front of the Book Cliffs.

b. A linear feature that trends approximately N50W appears to control the shape of the front of the Book Cliffs in the NE¼ of Section 13 approximately 1 mi north of the northeast end of the withdrawal area. This feature appears to extend northwestward for at least 0.5 mi into the SW¼ of Section 12 where it forms a low saddle on the ridge northwest of elevation point 6,545 ft. No fault corresponds to this feature from mapping of the Moab 30-minute × 60-minute quadrangle by Doelling (2001) and mapping of the adjacent Westwater 30-minute × 60-minute quadrangle to the north by Gualtieri (1988). The nearest fault to this feature is about 0.5 mi to the northeast in Little Blaze Canyon and it strikes almost parallel at N40W (Doelling 2001). Prominent vertical joints that strike N40W were measured along the top of the Book Cliffs about 1.5 mi to the southwest of this feature at elevation point 5,932 ft. From the orientation of this joint system and faults of similar orientation to the

northeast of this feature, it is concluded that this feature is a major joint that imparts some topographic control on the shape and location of a reentrant (unnamed canyon in Plate 1) on the face of the Book Cliffs and on drainages/ridges to the north.

c. Approximately 20 small pits are spaced about 200 ft apart in an area mainly north of old U.S. Highway 50, south of the Union Pacific Railroad, and just east of the East Branch of Kendall Wash. Field examination of the pits indicates that they are about 60 ft long, 25 ft wide, and 5 ft deep. Several 4-inch x 4-inch wooden posts were also found scattered on the ground through this area. Earlier, it was thought that these pits were likely dug as part of assessment work for mining claims staked for gold in the late 1970s and early 1980s. This area was part of a larger area (Floy to Cisco) sampled in a study by Marlatt (1991) for analysis of gold content in Mancos Shale. He found the gold content ranged from 30 to 100 parts per billion (ppb), which is about 10 times the background level, but much too low for economic extraction.

Further investigation of the pits found that they are much older and not related to gold exploration/speculation. Historic aerial photos from 1944 and 1974 show the pits, which were probably dug in exploration for gravel (road metal) associated with construction of old U.S. Highway 50 in the 1930s.

d. Green vegetation just north of old U.S. Highway 50 is in washes from the area of the East Branch of Kendall Wash westward to the West Branch of Kendall Wash. These vegetation areas coincide with and verify the location of the buried water line (which leaked before it was replaced by a new line in 2006) from Thompson Springs to Crescent Junction.

Low Sun-Angle Photographs

The LSA photographs covering the withdrawal area show that no terraces or mantled pediment surfaces are displaced and no scarps or linear features are present that would suggest the presence of faulting.

e. Best-shown of all the structural features in the LSA photographic coverage area are the bounding normal faults of the graben that strikes N20W along the axis of the Thompson Anticline. This graben is about 2 mi northeast of the northeast end of the withdrawal area. The southwest-bounding fault of the graben has the greater displacement (as much as 90 ft) of the two bounding faults (Willis 1986) and is well shown in the evening LSA photographs. The faults displace resistant sandstone beds of the Blackhawk Formation and Castlegate Sandstone, both of which cap the Book Cliffs. Displacement on these faults cannot be seen below the cliffs where they contact the underlying soft and mostly talus-covered Mancos Shale on the badland slopes of the Book Cliffs.

f. A prominent vertical joint system that strikes N55W is in sandstone of the Blackhawk Formation exposed on a point on the Book Cliffs in Horse Heaven in the east-central part of Section 15 approximately 1 mi north of the withdrawal area. No displacement occurs along this joint and it is a common joint orientation exposed elsewhere in the surrounding area.

g. The terrace surface just north of Interstate 70 (I-70), across from the highway Rest Area about 0.5 mi west of Crescent Junction, abruptly drops down to the northwest to a lower surface. Mapping by Doelling (2001) indicates that both surfaces are covered by pediment-mantling material. From the aerial photographs and mapping information, it is uncertain whether the two surfaces represent two terrace (or pediment) levels or if they are the same surface that has been displaced by a fault.

A surface investigation of this area was made in May 2006 to check for evidence of fault displacement of the surfaces. Results of the investigation were that the upper surface north of I-70 is a continuation of the terrace surface known as Crescent Bench south of I-70, and that no evidence for faulting was seen to the north to explain the lower surface. The upper surface, at an elevation of approximately 5,000 ft, is mantled by pedogenically cemented gravel and cobbles, whereas the lower (by about 40 ft) surface is a Mancos Shale pediment not mantled by cemented gravel. No evidence for faulting (i.e., drag on dipping shale beds, slickensides, anomalous color indicating alteration) was seen between the surfaces, and it is concluded that the lower surface is an erosional pediment surface that was not covered by alluvial material from the ancestral Crescent Wash

drainage. The higher surface was preserved and stands at a higher elevation because it was mantled by ancestral Crescent Wash drainage material that was later pedogenically cemented to form a resistant cap.

h. Aerial photographs show a pediment mantled by surficial material (mapped by Doelling [2001]) crossed by a faint northwest trending linear feature about 0.5 mi southeast of Thompson Pass in the SE¼ SW¼ of Section 17. From the photograph, the mantled pediment surface appears slightly higher north of the linear feature, and it is uncertain if the linear feature is a fault.

A surface investigation of this area, about 1.5 mi west of the west edge of the withdrawal area, was made in November 2006 to check for evidence of fault displacement. Results of the investigation were that no displacement occurs along the pediment surface where it is crossed by the linear feature, which is the eroded trace of a straight, geophysical seismic exploration line road cut by a dozer probably in the 1960s. This faint road trace trends northwest and goes about 2 mi from the west edge of the withdrawal area to Thompson Pass. The west half of the road trace, west of Crescent Wash, is shown in Figure 2.

i. A prominent vertical joint system that strikes approximately N70E is in sandstone of the Blackhawk Formation exposed on the narrow west point of the Book Cliffs just west of elevation 5,870 feet, just north of the withdrawal area, in the north-central part of Section 22. No displacement is apparent along this joint, and it is parallel to the south edge of the large landslide in Horse Heaven just to the north (feature 6, above).

A surface investigation of this west point of the Book Cliffs and the landslide area in the south part of Horse Heaven, immediately to the north, was made in March 2007. This investigation was in response to an NRC request that a linear feature visible on Plate 1 and discussed during a site visit in December 2006 be further investigated to determine if it is a fault, and if so, if it is capable. The linear feature trends approximately N70E and extends from the Crescent Wash area, north-northeast up the slopes of the Book Cliffs to the south edge of Horse Heaven.

No evidence for faulting was found along the linear feature. As noted during the December 2006 NRC site visit, no evidence for faulting was seen in the abrupt bend of the course of Crescent Wash (about where the linear feature would cross the wash) in the NE¼ of Section 21, where the wash is incised into Quaternary alluvial material. Northeastward along the feature as it crosses the slope of the Book Cliffs, prominent northeast-striking (vertical) joints were seen in the siltstone of the lower part of the Blackhawk Formation. At the top of the Book Cliffs along the trend of the linear feature in the NE¼ NW¼ of Section 22, several rotational slump blocks are aligned parallel along a trend of approximately N70E across the south part of the Horse Heaven landslide area (Figure 3).

From the strike of the prominent joint system on the west point of the Book Cliffs and its coincidence with the trend of rotational slump blocks just to the north in the Horse Heaven landslide area, and the lack of any characteristics of faulting along the linear feature, it is concluded that the linear feature is an expression of a prominent joint system in the area. This joint system will not affect the disposal site area, but it will continue to provide a passageway for water—important in the landslide/slump block erosion of the north side of the Book Cliffs.

Figure 2. View northwest of the trace of the straight seismic line road cut in the 1960s; Crooked Wash is in the foreground, and Thompson Pass is in the background.

Figure 3. View east-northeast along the south side of Horse Heaven where the deep-seated landslide area is shown with several parallel (trending approximately N70E) rotational slump blocks; sandstone cliffs of the Blackhawk Formation to the right (south) border the landslide area.

Conclusions:

Examination of HAV and LSA color aerial photographs and black-and-white historical aerial photographs of the withdrawal area found no faults or erosional features that would adversely affect the geologic suitability of the disposal site. Historical aerial photographs back to 1944 show that the headward incision of tributaries of the West Branch of Kendall Wash is advancing to the north and northwest at 1.3 to 2.3 ft per year. This erosion could reach the site access road in about 250 years and the area just west of the southwest corner of the disposal cell footprint after another 250 years. About 1,600 years of headward erosion would place the drainage near Crescent Wash, which could then possibly be captured by the West Branch of Kendall Wash.

A south-draining ancestral drainage course of the East Branch of Kendall Wash is in the east end of the withdrawal area, about 1.5 mi east of the disposal cell. This drainage was captured by northeastward incision advance of the present East Branch at a time roughly estimated as 6,000 to 9,000 years ago. Large boulders along the abandoned course of the ancestral East Branch are evidence for occasional extremely high flows associated with erosion of two reentrants to the Book Cliff escarpment at the head of the wash (Little Blaze Canyon and an unnamed canyon about 0.5 mi to the southwest of it).

Several areas near but outside the withdrawal area were identified from aerial photographs where Quaternary pediment-mantling material appeared to be displaced, possibly by faults. Field investigation of these areas found the displacements (if they occurred) were not because of faults. No structural features outside of the withdrawal area were identified that are of such significance to be addressed further in the "Site and Regional Seismicity–Results of Maximum Credible Earthquake Estimation and Peak Horizontal Acceleration" calculation (RAP Attachment 2, Appendix F).

Computer Source:

Not applicable.

References:

Cole, R.D., R.G. Young, and G.C. Willis, 1997. *The Prairie Canyon Member, a New Unit of the Upper Cretaceous Mancos Shale, West-Central Colorado and East-Central Utah*, Utah Geological Survey Miscellaneous Publication 97-4.

Dethier, D.P., 2001. "Pleistocene Incision Rates in the Western United States Calibrated Using Lava Creek B Tephra," Geological Society of America, *Geology*, 29(9), pp. 783–786.

Doelling, H.H., 2001. *Geologic Map of the Moab and Eastern Part of the San Rafael Desert 30' x 60' Quadrangles, Grand and Emery Counties, Utah, and Mesa County, Colorado,* Utah Geological Survey Map 180, scale 1:100,000.

Friedman, J.D., J.E. Case, and S.L. Simpson, 1994. "Tectonic Trends of the Northern Part of the Paradox Basin, Southeastern Utah, and Southwestern Colorado," as derived from *Landsat Multispectral Scanner Imaging and Geophysical and Geologic Mapping,* U.S. Geological Survey Bulletin 2000-C.

Friedman, J.D., and S.L Simpson, 1980. *Lineaments and Geologic Structure of the Northern Paradox Basin, Colorado and Utah,* U.S. Geological Survey Miscellaneous Field Studies Map MF–1221, scale 1:250,000.

Gualtieri, J.L., 1988. *Geologic Map of the Westwater 30' x 60' Quadrangle, Grand and Uintah Counties, Utah, and Garfield and Mesa Counties, Colorado*, U.S. Geological Survey Miscellaneous Investigations Series Map I–1765, scale 1:100,000.

Hampson, G.J., J.A. Howell, and S.S. Flint, 1999. "A Sedimentological and Sequence Stratigraphic Re-interpretation of the Upper Cretaceous Prairie Canyon Member ('Mancos B') and Associated Strata, Book Cliffs Area, Utah, U.S.A.," *Journal of Sedimentary Research*, 69(2), pp. 414–433.

Harty, K.M., 1993. *Landslide Map of the Moab 30' x 60' Quadrangle, Utah,* Utah Geological Survey Open File Report 276, scale 1:100,000.

Marlatt, Gordon, 1991. *Gold Occurrence in the Cretaceous Mancos Shale, Eastern Utah,* Utah Geological and Mineral Survey Contract Report 91-5.

Shroder, J.F., Jr., 1971. *Landslides of Utah*, Utah Geological and Mineral Survey Bulletin 90.

Willis, G.C., 1986. *Provisional Geologic Map of the Sego Canyon Quadrangle, Grand County, Utah*, Utah Geological and Mineral Survey Map 89, scale 1:24,000.

End of current text

THIS PAGE IS AN OVERSIZED DRAWING OR FIGURE,

THAT CAN BE VIEWED AT THE RECORD TITLED:

DRAWING NO.: X0136200, "PLATE 1 - AERIAL PHOTOGRAPHY INTERPRETATION FOR CRESCENT JUNCTION WITHDRAWAL AREA AND NEARBY SURROUNDING AREA"

WITHIN THIS PACKAGE... OR, BY SEARCHING USING THE DOCUMENT/REPORT DRAWING NO. X0136200

D-05

THIS PAGE IS AN OVERSIZED DRAWING OR FIGURE,

THAT CAN BE VIEWED AT THE RECORD TITLED:

DRAWING NO.: X0211800, "PLATE 2 - HEAD OF EROSION INCISION FROM 1944 TO 2005 AT WEST BRANCH OF KENDALL WASH, CRESCENT JUNCTION, UT, SITE"

WITHIN THIS PACKAGE... OR, BY SEARCHING USING THE DOCUMENT/REPORT DRAWING NO. X0211800

D-06